Metathesis Catalysts in Tandem Catalysis: Methods and Mechanisms for Transformation

Nicholas James Beach

Thesis submitted to the
Faculty of Graduate and Postdoctoral Studies
University of Ottawa
in partial fulfillment of the requirements for the degree of
Doctor of Philosophy

Ottawa-Carleton Chemistry Institute
Faculty of Science
University of Ottawa

Table of Contents

List of Figures

List of Schemes

List of Tables

List of Charts

Abstract

The ever-worsening environmental crisis has stimulated development of less wasteful "green" technologies. To this end, tandem catalysis enables multiple catalytic cycles to be performed within a single reaction vessel, thereby eliminating intermediate processing steps and reducing solvent waste. Assisted tandem catalysis employs suitable chemical triggers to transform the initial catalyst into new species, thereby providing a mechanism for "switching on" secondary catalytic activity.

This thesis demonstrates the importance of highly productive secondary catalysts through a comparative hydrogenation study involving prominent hydrogenation catalysts of tandem ring-opening metathesis polymerization (ROMP)-hydrogenation, of which hydridocarbonyl species were proved superior. This thesis illuminates optimal routes to hydridocarbonyls under conditions relevant to our ROMP-hydrogenation protocol, using Grubbs benzylidenes as isolable proxies for ROMP-propagating alkylidene species. Analogous studies of ruthenium methylidenes and ethoxylidenes illuminate optimal routes to hydridocarbonyls following ring-closing metathesis (RCM) and metathesis quenching, respectively. The formation of unexpected side products using aggressive chemical triggers is also discussed, and emphasizes the need for cautious design of the post-metathesis trigger phase.

Acknowledgements

First and foremost, thank you Deryn for teaching me to see the forest for the trees, and to be mindful of where the forest stands. Your constant guidance and contagious enthusiasm have transformed the way I view chemistry, and science in general. Greg, the skills I acquired during my Honours and Masters gave me the confidence to pursue this degree, and for that I thank you.

Ken, thanks for schooling me in the art of "bombcraft"; our day-long hydrogenolysis experiments were the most fun I've had in the lab. Jo, our many discussions never failed to provide new and exciting approaches to complicated problems. Cheers to Lummiss for always asking "what's the point?", and for maintaining a light atmosphere regardless of the chemistry. Jennifer and Carolyn, I greatly enjoyed the work we did together, however brief. To Seb, Heather, Titel, Adrien, Josh, Debbie, and Matt(s): thank you for the insightful discussions and the fun times.

Many thanks go to Glenn Facey for his seemingly limitless NMR knowledge (and patience), and to Roxanne Clement for her generous instruction on the use of the various high-throughput instruments. I must also thank the University of Ottawa, NSERC, and OGS for supporting me financially, thus enabling me to pursue this degree.

To Mom, Dad, Mikey and Miss, and to Paul and all my aunts, uncles, and cousins, thanks for all your support and encouragement through yet another degree, and for making it easy to come home.

Lastly, but mostly, thank you Mel for being my companion during this terrifying, yet wonderful, chapter in my life. You pulled me back from the brink of despair more times than I can count, and I simply would not be writing these words were it not for your constant love and support.

Abbreviations

Ac	Acetyl, -C(O)CH_3
ADMET	Acyclic diene metathesis
atm	Atmosphere (1 atm = 14.7 psi)
Ar	Aryl
ATRP	Atom transfer radical polymerization
Bn	Benzyl, -CH_2Ph
BOC	-C(O)O^{t}Bu
Cat.	Catalyst
CM	Cross metathesis
COD	1,5-cyclooctadiene, C_8H_{12}
Conv.	Conversion
Cy	Cyclohexyl, - C_6H_{11}
DEPT	Distortionless enhancement by polarization transfer
DFT	Density functional theory
DMB	2,4-dimethoxybenzyl
EPR	Electron paramagnetic resonance
equiv	Equivalents
Et	Ethyl, -C_2H_5
EVE	Ethyl vinyl ether, CH_2=CHOEt
GC-FID	Gas chromatography flame ionization detection
GC-MS	Gas chromatography mass spectrometry
H_2IMes	*N*,*N*'-bis-(2,4,6-trimethylphenyl)imidazolin-2-ylidene
H_2IPr	*N*,*N*'-bis-(2,6-diisopropylphenyl)imidazolin-2-ylidene
H_2ITol	*N*,*N*'-bis-(2-methylphenyl)imidazolin-2-ylidene
HMBC	Heteronuclear multiple-bond correlation
HMQC	Heteronuclear multiple-quantum coherence
Hz	Hertz (s^{-1})
IMes	*N*,*N*'-bis-(2,4,6-trimethylphenyl)imidazol-2-ylidene
^{i}Pr	Isopropyl, -$CH(CH_3)_2$

IR	Infrared
KA	Kharasch addition
Me	Methyl, -CH_3
Mes	Mesityl, 2,4,6-trimethylphenyl
MMA	Methylmethacrylate, CH_2=CH(Me)C(O)(OMe)
NBR	Nitrile-butadiene rubber
n.d.	Not determined
NHC	*N*-heterocyclic carbene
NMR	Nuclear magnetic resonance
NOESY	Nuclear Overhauser effect spectroscopy
Ns	Nosyl, -SO_2(*p*-NO_2-C_6H_4)
OTf	Triflate, -OSO_2CF_3
OTMS	Trimethylsiloxy, -$OSiMe_3$
Oxone®	$KHSO_5$
PDI	Polydispersity index
Ph	Phenyl, -C_6H_5
ppm	Parts per million
py	Pyridine, C_5H_5N
RCEYM	Ring-closing enyne metathesis
ROMP	Ring-opening metathesis polymerization
RCM	Ring-closing metathesis
$T_{1(min)}$	Minimum temperature-dependent spin-lattice relaxation time
^{t}Bu	Tert-butyl, -CMe_3
THF	Tetrahydrofuran, C_4H_8O
THN	1,2,3,4-tetrahydronaphthalene
TMB	1,3,5-trimethoxybenzene
TMS	Tetramethylsilane, $SiMe_4$
-TMS	Trimethylsilyl, -$SiMe_3$
TOF	Turnover frequency
TON	Turnover number
Ts	Tosyl, -SO_2(*p*-CH_3-C_6H_4)

TS	Transition state
UHP	Ultra High Purity
xs	Excess

List of Compounds

Ruthenium complexes

	L	L'
a	PCy_3	PCy_3
b	IMes	PCy_3
b'	H_2IMes	PCy_3
c	IMes	IMes
d	IMes	$(py)_2$
e'	H_2Itol	-
f'	H_2IPr	-

No.	Structure	No.	Structure
Ru-1	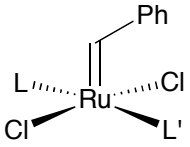	**Ru-1a'**	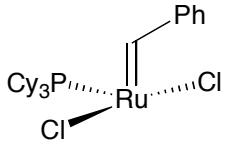
Ru-1a^{Br}	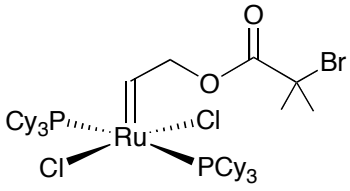	**Ru-1a^{Ph2}**	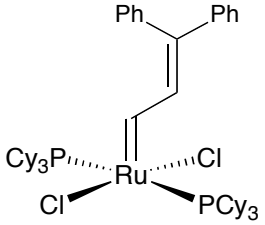
Ru-2	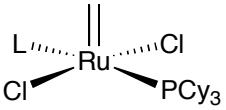	**Ru-3**	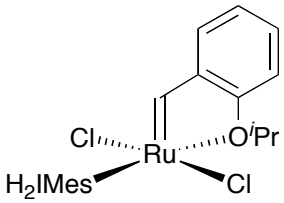
Ru-4	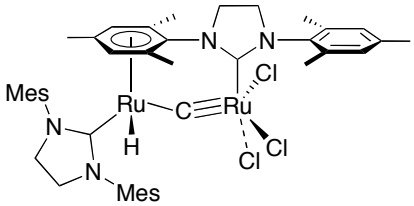	**Ru-5**	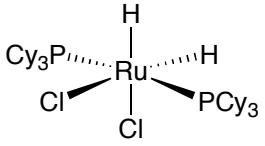
Ru-5'	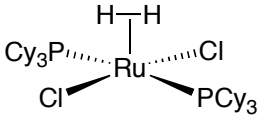	**Ru-6**	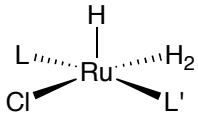
Ru-7	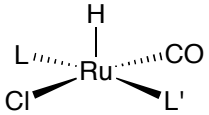	**Ru-7'**	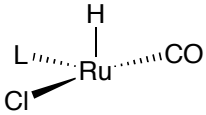
Ru-8	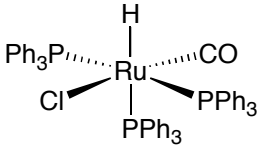	**Ru-9**	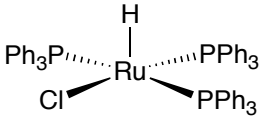

Ru-10

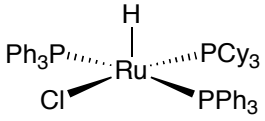

Ru-11

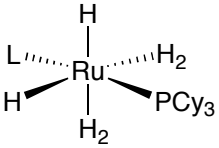

Ru-12

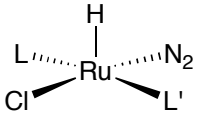

Ru-13

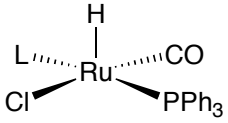

Ru-14

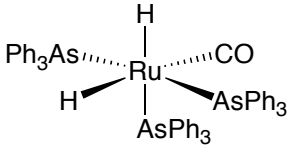

Ru-15

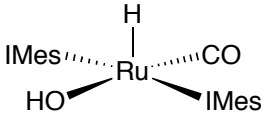

Ru-16

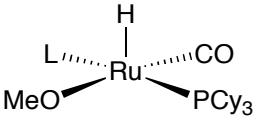

Ru-17

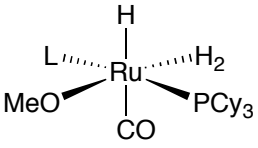

Ru-18

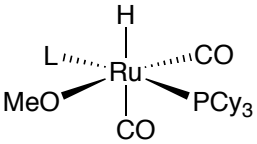

Ru-19

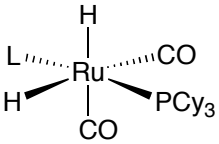

Ru-20

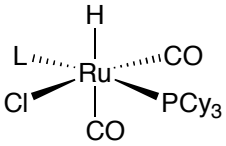

Ru-21

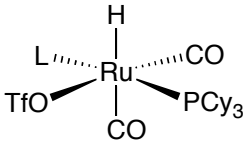

Ru-22

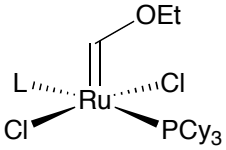

Ru-23

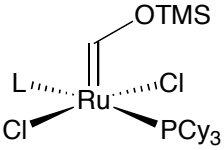

Ru-24

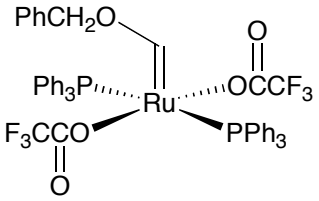

Ru-25

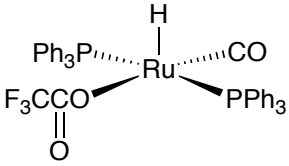

Ru-26

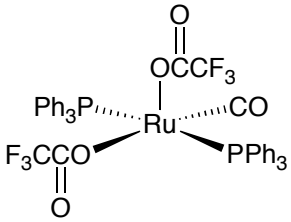

Ru-27

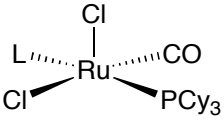

Ru-28

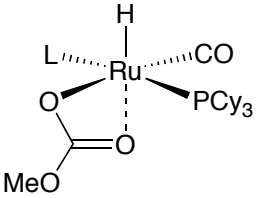

Ru-29

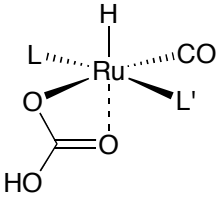

Ru-30	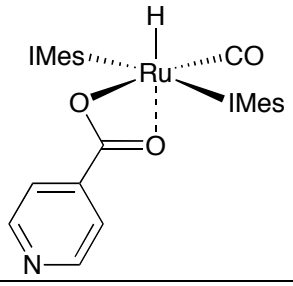

Substrates

No.	Structure
S1	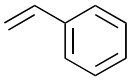
S2	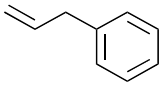
S3	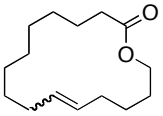
S4	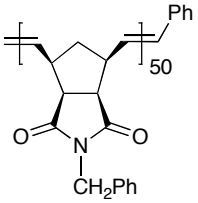
S5	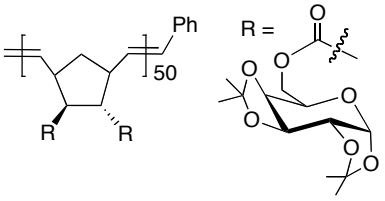

N-heterocyclic carbenes

No.	Structure
IMes	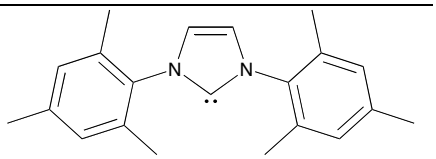
H_2IMes	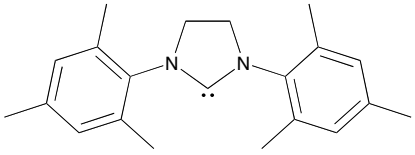
H_2IPr	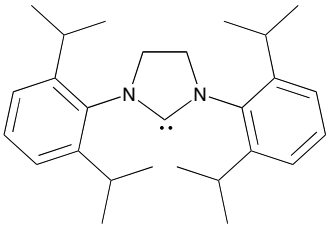
H_2ITol	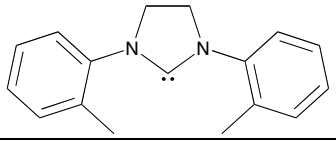

List of Contributions

1) **Beach, N. J.**; Lummiss, J.A.M.; Bates, J.M.; Fogg, D.E. *Reaction of the Grubbs Catalysts with Excess Methoxide: Formation of Novel Methoxyhydride Complexes*. *Organometallics* **2012**, *31*, 2349-2356.

2) Blacquiere, J.M.; Higman, C.S.; Gorelsky, S.I.; **Beach, N.J**.; Fogg, D.E. *Unprecedentedly Strong Binding of Dinitrogen by a Ruthenium–N-Heterocyclic Carbene Complex*. *Angew*. *Chem*. *Int*. *Ed*. **2011**, *50*, 916-919.

3) **Beach, N.J.**; Camm, K.D.; Fogg, D.E. *Hydrogenolysis versus Methanolysis of First-and Second-Generation Grubbs Catalysts: Rates, Speciation and Implications for Tandem Catalysis*. *Organometallics* **2010**, *29*, 5450-5455.

4) **Beach, N.J.**; Blacquiere, J.M.; Drouin, S.D.; Fogg, D.E. *Carbonyl-Amplified Catalyst Performance: Balancing Stability against Activity for Five-Coordinate Ruthenium Hydride and Hydridocarbonyl Catalysts*. *Organometallics* **2009**, *28(2)*, 441-447.

5) **Beach, N.J.**; Dharmasena, U.L.; Drouin, S.D.; Fogg, D.E. *Improved Synthesis of Versatile Ruthenium Hydridocarbonyl Catalysts Containing Electron-Rich Ancillary Ligands, Adv*. *Synth*. *Catal*. **2008**, *350*, 773-777.

6) Monfette, S.; Blacquiere, J.M.; Conrad, J.C.; **Beach, N.J.**; Fogg, D.E. *Ruthenium-Aryloxide Catalysts for Olefin Metathesis*. *Metathesis Chemistry: From Nanostructure Design to Synthesis of Advanced Materials*, NATO Science Series II, Vol 243, Y. Imamoglu, V. Dragutan, Eds. Springer Verlag, Berlin, **2007**, p. 79-89.

Chapter 1: Introduction

1.1 Tandem Catalysis

The improved quality of life enabled by industrialized societies has exacted an environmental price. Balancing the two constitutes a major challenge for our own and future generations. "Green Chemistry" seeks to address this challenge by fostering the development of energy- and resource-efficient technologies designed to reduce environmental impact. As a blueprint for the development of improved industrial practices, Anastas and Warner put forward "Twelve Principles of Green Chemistry",[1,2] a core objective of which is the replacement of wasteful stoichiometric processes by catalytic methodologies.

Catalysis reduces the energy demands of chemical reactions by decreasing the barrier to activation (E_a; Figure 1.1a). In a simplified catalytic cycle, a reactant (e.g. **A**, Figure 1.1b) combines with the catalyst **C** to form intermediate **CA**, which reacts with another reactant **B** to yield product **AB** and regenerate **C**. This process constitutes a single "turnover" of the catalytic cycle. A kinetic benefit results from the decreased energy barrier, but the net thermodynamics of the system are unchanged.

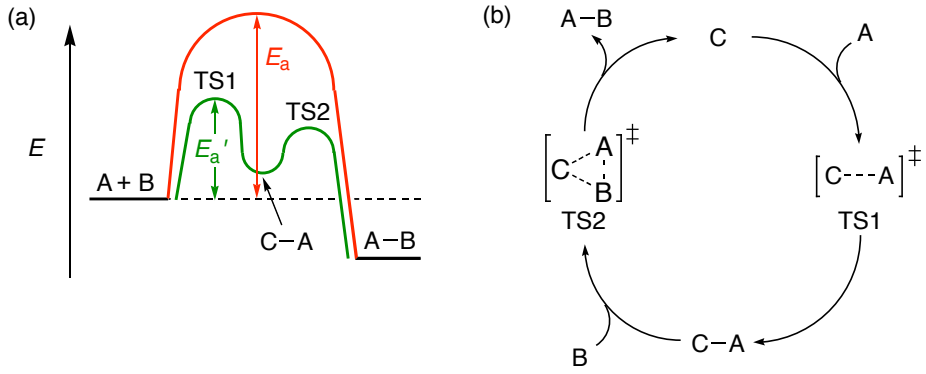

Figure 1.1. (a) Potential energy diagram for reaction of **A** and **B** in the presence (green) or absence (red) of catalyst **C**. (b) A simple model in which reaction of **A** with **B** is catalyzed by **C**.

In most catalytic processes, the active species is generated via *initiation* of a *precatalyst*, while *termination* involves catalyst deactivation, whether incidental (e.g. decomposition) or deliberately induced (e.g. quenching). Catalyst activity is often expressed in terms of the *turnover number* (TON): that is, the number of catalytic cycles completed by each molecule of catalyst prior to termination. The TON is thus readily determined from the molar ratio of product vs. precatalyst. Also important is the *turnover frequency* (TOF), or the number of turnovers per unit time. To maximize catalyst efficiency, the lifetime of the active catalyst must be long relative to the timescale of catalyst decomposition. For less active or chemically sensitive catalysts, high loadings are often required to attain useful TOFs. This can drastically increase process costs where expensive precious metal catalysts are used.

The efficiency of chemical reactions is often described in terms of *atom economy*, or the molecular weight ratio of the desired product relative to all reactants. The term was coined by Trost in 1995 to aid synthetic organic chemists in recognizing more materials-efficient transformations.[3] However, atom economy does not take into account materials expenditures arising from (e.g.) unused reactants, side-products, or solvents required for reaction or work-up. A broader metric for efficiency is the *E factor* (or *Environmental factor*) introduced by Sheldon, which reports on the kilograms of waste generated for each kilogram of isolated product. Process *sustainability*, as gauged by the E-factor, ranges from ca. 0.1 for the petroleum industry to >100 for pharmaceutical synthesis (Table 1.1). A major contributor to waste in the latter context is solvent use: a GlaxoSmithKline estimate puts solvent wastes at 85% of the total mass of chemical waste generated in pharma.[4] Eliminating unnecessary reaction steps, as well as solvent-intensive workup and purification stages, can greatly improve process efficiencies.

Table 1.1. Typical E-factors for various sectors of the chemical industry.

Sector	Production scale (t/y)	E-factor	Waste (t/y)
Petroleum industry	10^6-10^8	ca. 0.1	10^5-10^7
Commodity chemicals	10^4-10^6	≤5	10^4-5×10^6
Fine chemicals	10^2-10^4	5-50	5×10^2-5×10^5
Pharmaceuticals	10-10^3	25-100	2.5×10^2-10^5

Tandem catalysis offers a potentially important means of reducing the waste associated with operating sequential catalytic reactions as separate steps. Much recent attention has focused on use of this approach to couple such transformations, thus enabling two or more originally independent reactions to be carried out within a single reaction vessel.[5, 6] Fogg and dos Santos put forward a taxonomy (Figure 1.2) to aid in analyzing the opportunities and limitations offered by different types of tandem catalytic processes. Of particular interest is *assisted tandem catalysis* (described in more detail below), which offers the opportunity to independently optimize each of the catalytic processes involved.

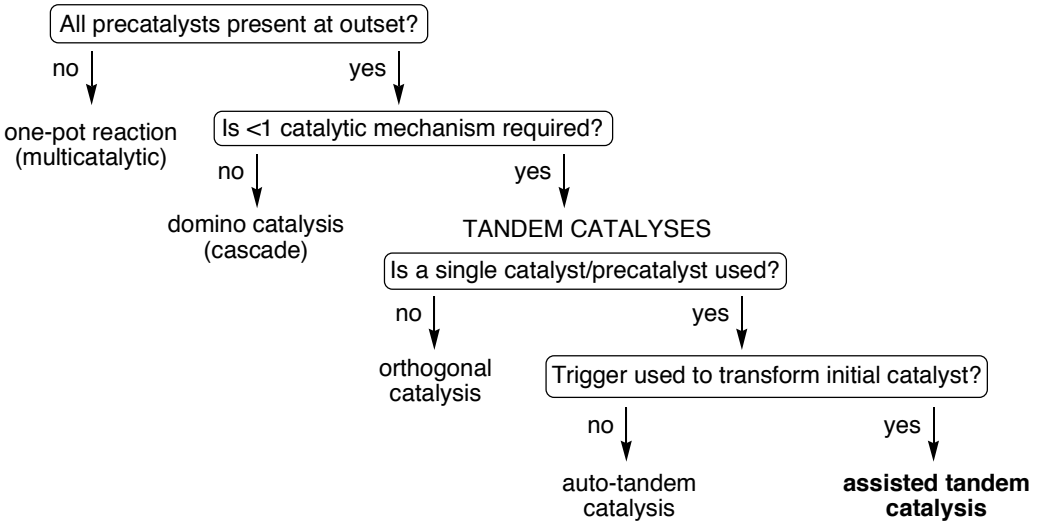

Figure 1.2. Flowchart for classification of one-pot processes in which an organic substrate is elaborated via multiple, sequential catalytic transformations.[5c]

Assisted tandem catalysis relies on use of a *trigger* reagent or condition, applied once the first cycle is complete, to switch between distinct modes of catalysis. As shown in Figure 1.3, the trigger converts **Catalyst A** into a new species (**Catalyst B**), and the latter drives transformation of organic **Product A** into **Product B**. Fast transformation of the catalyst is important to minimize the timescale of operations; efficient, high-yield transformation is essential to maximize capture of the initial catalyst charge. To date, however, few processes have attempted to optimize this step. The following sections describe progress in tandem metathesis-functionalization and metathesis-hydrogenation. Interest in such methodologies is high, due in part to the versatility of olefin metathesis (**Cycle A**) as a method for assembling new C=C bonds.[7,8]

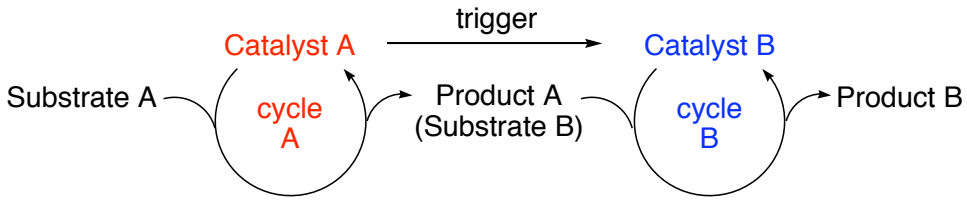

Figure 1.3. Schematic representation of assisted tandem catalysis.[5c]

1.2 Assisted tandem catalysis utilizing Grubbs metathesis catalysts

The Grubbs metathesis catalysts (Chart 1.1) have been harnessed in a range of tandem catalysis processes. Developments prior to 2006 have been reviewed,[5] and the majority of these will not be repeated here. The following section describes reports of tandem metathesis-functionalization that have emerged over the past five years, focusing in particular on *assisted* tandem catalysis[5c] via the Grubbs catalysts. This is followed by a more detailed review of tandem metathesis-hydrogenation, a transformation central to the work presented in this thesis.

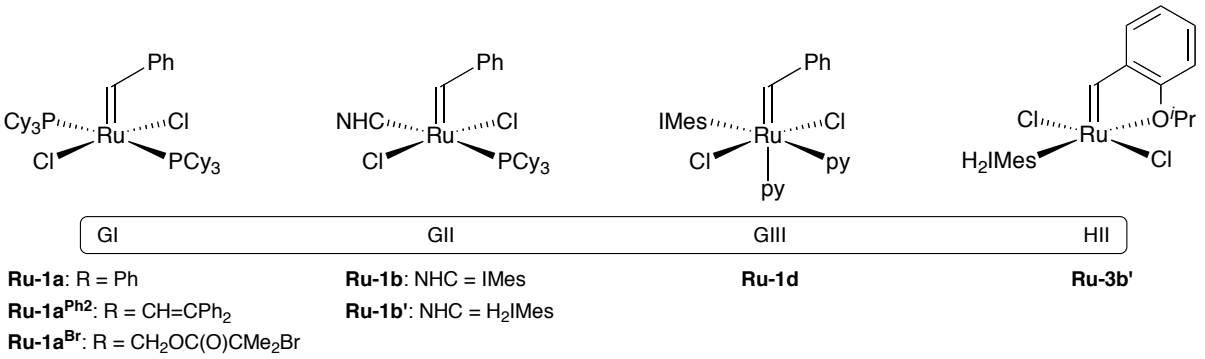

Chart 1.1. Grubbs and Hoveyda-Grubbs catalysts employed in assisted tandem catalysis.

1.2.1 Tandem metathesis-cyclopropanation

Snapper and coworkers used precatalyst **Ru-1a** to couple ring-closing enyne metathesis (RCEYM) with cyclopropanation.[9] The cyclopropanation step was initiated by purging the metathesis reaction with N_2 to remove the ethylene atmosphere, following which the diazo reagent was added dropwise (Scheme 1.1). In situ NMR studies did not aid in identifying the cyclopropanation catalyst. However, no metathesis activity was retained following cyclopropanation, tending to argue against involvement of an ester-alkylidene species, as such complexes are known to be metathesis active.[10]

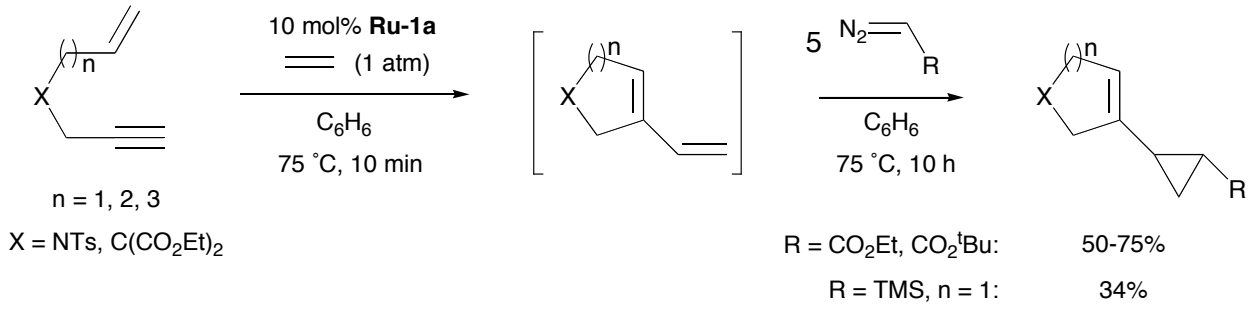

Scheme 1.1. Ru-1a-catalyzed tandem RCEYM-cyclopropanation.[9]

This methodology was later applied by Perez-Castells and coworkers in the RCM assembly and cyclopropanation of five- to seven-membered enamide rings (Scheme 1.2).[11]

Poor control over regioselectivity of cyclopropanation was found for the six- and seven-membered rings, implying isomerization prior to cyclopropanation. Adopting a suggestion by Fustero and coworkers,[12] the authors proposed that the isomerization catalyst could be dinuclear hydride **Ru-4** (earlier observed on thermolysis of the resting-state methylidene species **Ru-2b'**)[13]

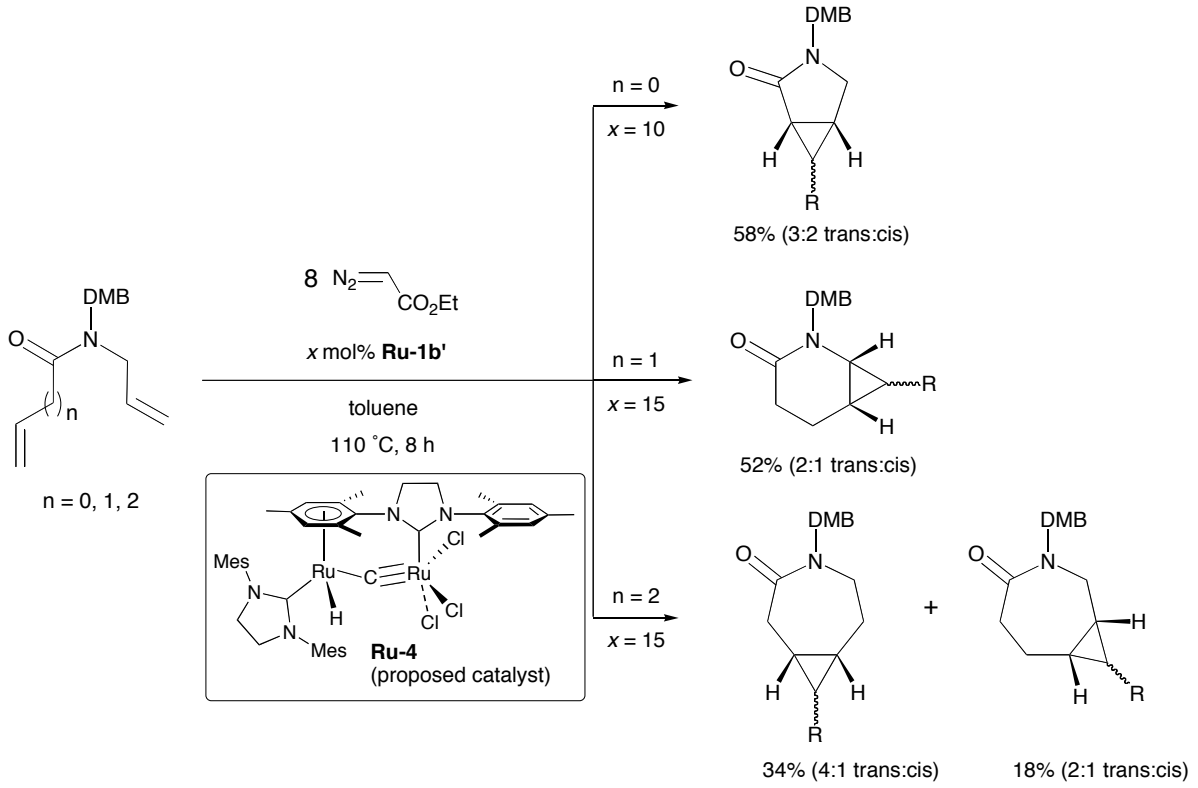

Scheme 1.2. Ru-1b'-catalyzed tandem RCM-isomerization-cyclopropanation.[11]

1.2.2 Tandem metathesis-Kharasch addition (KA)

Tandem metathesis-Kharasch addition (KA) involves the post-metathesis addition of a trihaloacetyl C-X bond across a newly-formed C=C bond. This addition may be intra- or intermolecular. For trichloroacetyl substrates, the metathesis and Kharasch cycles can be isolated by the elevated temperatures required for KA[14,15] (provided that metathesis is efficient at ambient temperature). This is important to ensure that KA modification does not

occur prematurely on the diene substrate. The first-generation Grubbs catalyst **Ru-1a**, which exhibits high initiation efficiency at room temperature, promoted efficient RCM-KA of trichloroacetamide-functionalized 1,6-, 1,7- and 1,8-dienes,[16] as well as trichloroacetate-functionalized 1,7-dienes (Scheme 1.3).[17]

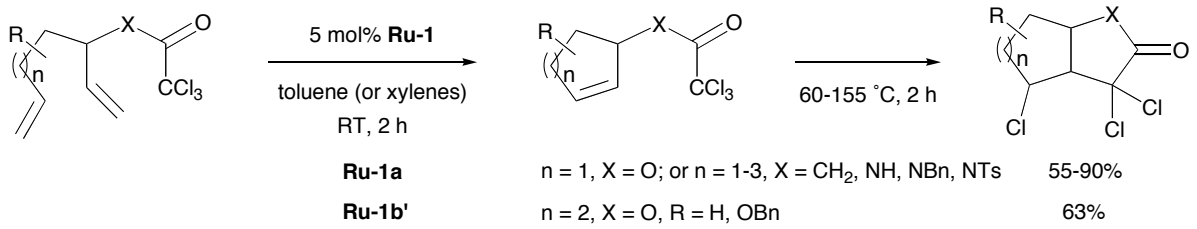

Scheme 1.3. Ru-1a/b'-catalyzed RCM-Kharasch addition.[16,17]

Thermal segregation of the metathesis and Kharasch steps also requires a relatively high C-X bond dissociation energy, a condition met by the C-Cl bond, but not by C-Br species.[18] Thus, attempted RCM-KA of tribromoacetamides at ambient temperature suffers from poor product selectivity, owing to competing KA of the starting diene.

This chemistry was incorporated into the extended sequence depicted in Scheme 1.4. Thus, a Pd-catalyzed Overman rearrangement of trichloroacetimidates was followed by tandem RCM-KA.[19] The bicyclic products were formed with excellent enantioselectivity (≤90% e.e.) during the process of Scheme 1.4b, in particular, although the Overman rearrangement was slow.

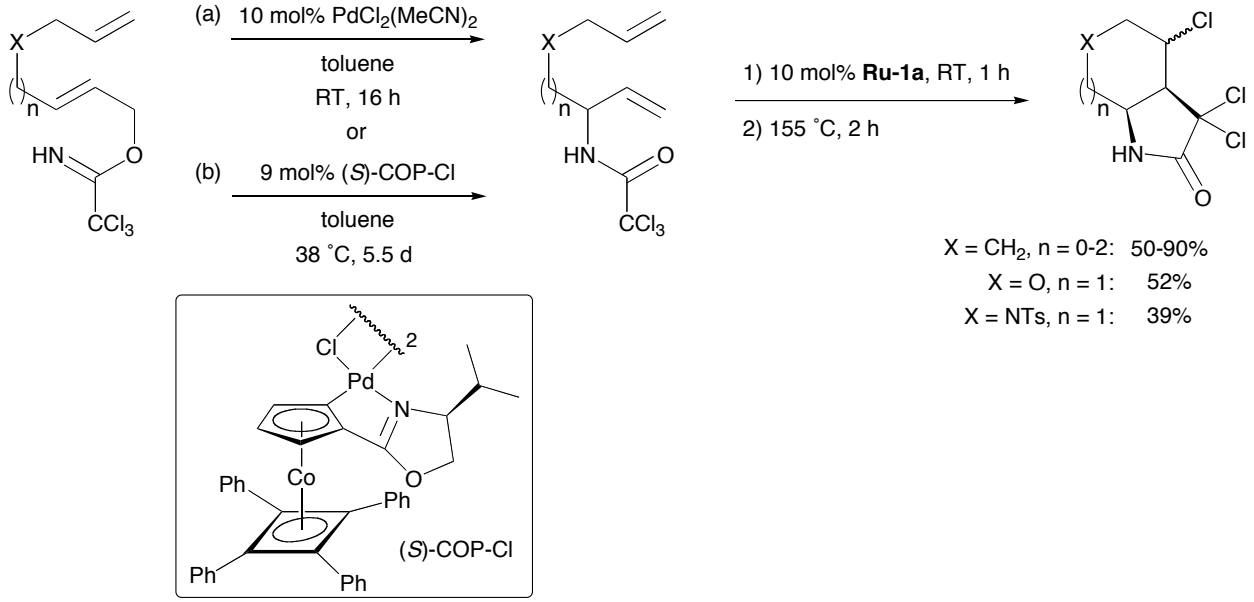

Scheme 1.4. Overman rearrangement in sequence with **Ru-1a**-catalyzed RCM-KA.[19]

The superior metathesis activity of the second-generation **Ru-1b'** enabled efficient RCM-KA of trichloroacetate-functionalized 1,6-dienes (Scheme 1.3).[17] Cross-metathesis (CM) of *N*-phenyl-trichloroacetamide with various styrenes, followed by KA, was also employed by Quayle and coworkers (Scheme 1.5). However, yields of the KA products were low.[20]

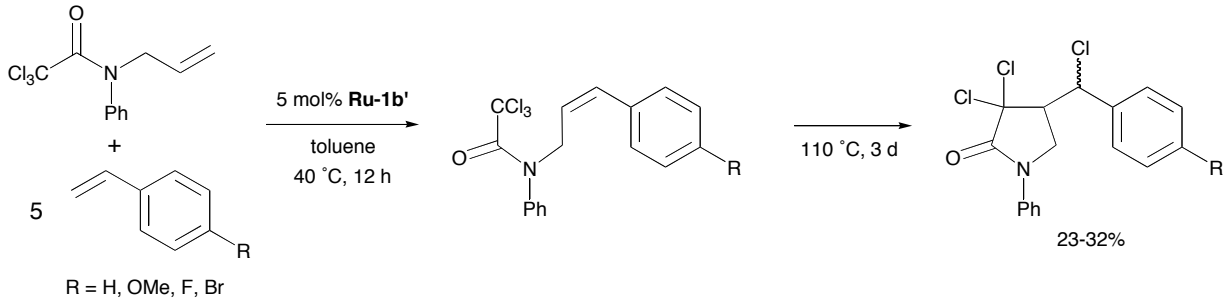

Scheme 1.5. Ru-1b'-catalyzed tandem CM-KA.[20]

While the Kharasch catalyst was not identified during any of the above studies, Schmidt suggested the potential involvement of paramagnetic ruthenium species, formation of which was inferred from the severe broadening of NMR signals for crude RCM-KA reaction

mixtures.[17] Chlorination of the metathesis catalyst to form Ru(III) products could account for the conversion of trichloroacetamides to their dichlorinated analogues during RCM-KA promoted by **Ru-1a**.[16]

1.2.3 Tandem metathesis-oxidation

Blechert and coworkers were the first to exploit the residual ruthenium present after olefin metathesis to carry out C=C oxidation (specifically dihydroxylation).[21] Their protocol began by stripping off the CH_2Cl_2 solvent used for metathesis, and suspending the residue in 3:3:1 MeCN/EtOAc/H_2O. The dihydroxylation stage was then initiated by cooling to 0 ˚C and adding the Lewis acid catalyst $YbCl_3$•6 H_2O, accompanied by excess $NaIO_4$ oxidant. A screening study revealed superior dihydroxylation activity for the first-generation Grubbs catalyst **Ru-1a** relative to second-generation **Ru-1b'** (though see later). Use of **Ru-1a** for RCM-dihydroxylation of various 1,7- and 1,8-dienes (Scheme 1.6) enabled rapid dihydroxylation (≤40 min) to afford exclusively *cis*-1,2-diols.

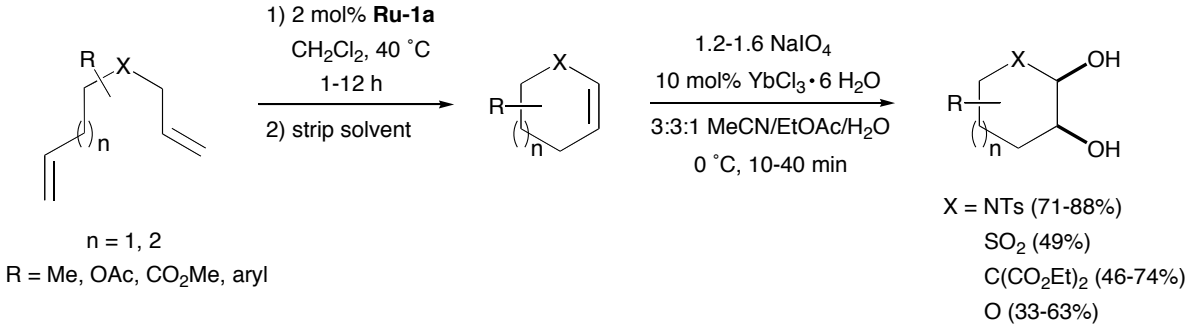

Scheme 1.6. Ru-1a-catalyzed RCM-dihydroxylation.[21]

Dihydroxylation of internal, electron-deficient olefins formed by CM was also examined. These experiments utilized the second-generation Hoveyda-Grubbs catalyst **Ru-3b'**. Dihydroxylation efficiency is lower than that found with **Ru-1a**. The nature of the olefin

substituent had a pronounced effect on diol geometry: acrylates led to *cis*-diols, and cyanide to *trans*-diols (Scheme 1.7).

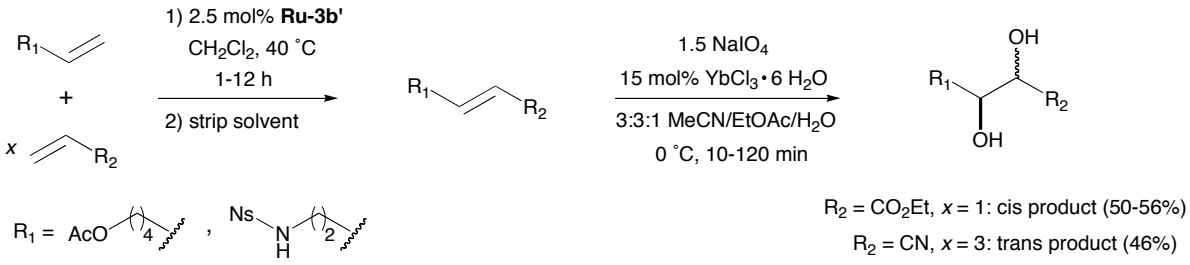

Scheme 1.7. Ru-3b'-catalyzed CM-dihydroxylation.[21]

A minor drawback to this protocol is the need to remove the metathesis solvent CH_2Cl_2 prior to dihydroxylation.[22,23] Snapper performed the metathesis reaction in EtOAc, and used $CeCl_3$•7 H_2O as the Lewis acid catalyst.[24] The latter is thought to generate RuO_4 (the putative olefin oxidation catalyst) more effectively than $YbCl_3$•6 H_2O.[25] Olefin oxidation was complete within 20 minutes at 0 °C. **Ru-1b'** was also employed as the metathesis catalyst, enabling efficient RCM-dihydroxylation of 1,6-dienes. Diol yields were comparable or higher than those found in the Blechert study of Scheme 1.6 above.[21]

Snapper also applied an oxidation protocol developed by Plietker, in which Oxone® (i.e. $KHSO_5$) and $NaHCO_3$[26,27] are added after metathesis to achieve tandem metathesis-ketohydroxylation. In contrast with the trends in dihydroxylation, in which **Ru-1a** showed higher activity, the second-generation **Ru-1b'** proved more effective for ketohydroxylation. Thus, RCM of disubstituted 1,6-, 1,7-, and 1,8-dienes and trisubstituted 1,6-dienes by **Ru-1b'** was followed by rapid ketohydroxylation to yield the desired α-hydroxyketones (Scheme 1.8).

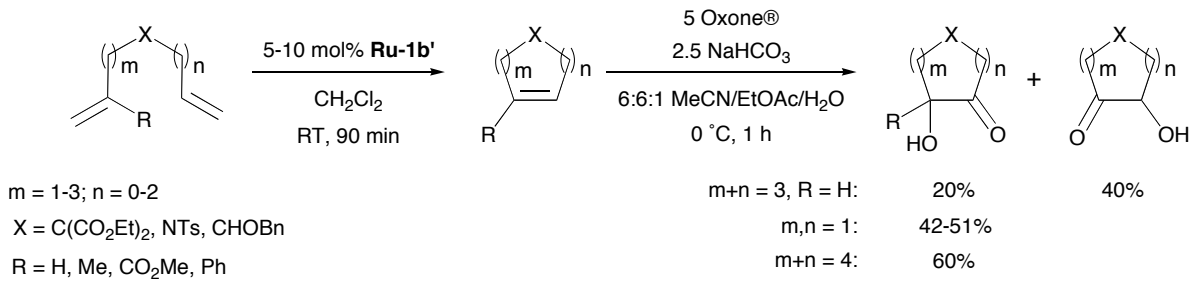

Scheme 1.8. Ru-1b'-catalyzed RCM-ketohydroxylation.[24]

This technique was also effective for tandem CM-ketohydroxylation of various olefins with methyl acrylate or methyl methacrylate (Scheme 1.9). However, CH_2Cl_2 was required as solvent for efficient CM.

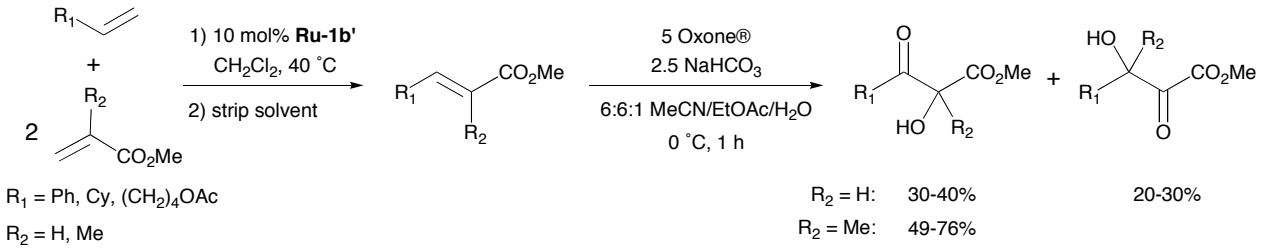

Scheme 1.9. Ru-1b'-catalyzed CM-ketohydroxylation.[24]

Plietker later modified Snapper's CM-dihydroxylation protocol to include chloride abstraction from **Ru-3b'** by Bu_4NIO_4, prior to addition of $NaIO_4$.[28] Stereoselective dihydroxylation following CM of vinylcyclohexane was achieved with chirally pure camphorsulfamidate and camphorsultame substrates. Two sea anemone alarm pheromones (anthopleurine and *ent*-anthopleurine)[29] were obtained with >99% e.e.

In the above examples of tandem metathesis-oxidation, the oxidation catalyst is believed to be RuO_4, a well-known olefin oxidant.[30] Pleitker has postulated that the reaction of $CeCl_3$•6 H_2O with $NaIO_4$ results in formation of Ce(IV)-periodato complexes,[25] which then

oxidize the metathesis catalysts to RuO_4. Differences in oxidation activity noted above may reflect variations in the efficiency with which RuO_4 is produced in situ. The efficiency of the oxidation step could potentially be improved further by a deeper mechanistic understanding of the processes involved.

1.2.4 Tandem metathesis-isomerization

In an early study of tandem RCM-isomerization promoted by **Ru-1b'**, Snapper and coworkers screened various agents (HCO_2H, $NaBH_3CN$, methanolic NaOMe and H_2) for their ability to promote isomerization.[31] Optimal isomerization activity was observed using H_2 diluted with N_2 (i.e. "regeneration gas"; 5% H_2) to suppress competing hydrogenation. α-Enol ethers were obtained from 1,7- and 1,8-dienes (Scheme 1.10), although small amounts (<10%) of saturated byproducts were also formed.

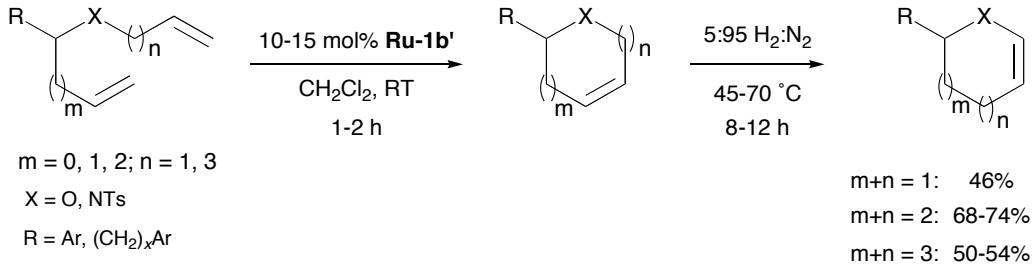

Scheme 1.10. Ru-1b'-catalyzed tandem RCM-isomerization.[31]

Schmidt later employed the inorganic hydrides NaH and $NaBH_4$ to promote similar reaction chemistry (Scheme 1.11). The precatalyst used was **Ru-1a**.[32] Isomerization yielded only minor amounts of trisubstituted olefin, despite Snapper's proposed 4 kcal/mol preference for this product.[31]

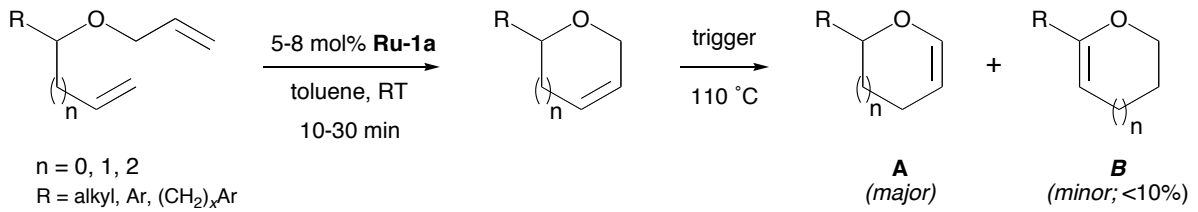

Scheme 1.11. Ru-1a-catalyzed RCM-isomerization.[33]

This study was followed by an assessment of the capacity of various bases to turn on isomerization (Table 1.2).[33] Isopropoxide (i.e. NaOH/^{i}PrOH) enabled much faster reaction. Unlike the hydride reagents, it also enabled isomerization even where an alcohol substituent was present (R = OH; Scheme 1.11). However, transfer hydrogenation was also observed.[34] In subsequent investigations, the isopropoxide system was used as the system of first resort, but NaH or $NaBH_4$ were used when transfer hydrogenation was found to compete.

Table 1.2. Dependence of isomerization yields on the trigger used to convert the metathesis catalyst into an isomerization catalyst in the reactions of Scheme 1.11.[33]

Trigger	Loading (mol%)[a]	Time (h)[b]	Ring size	Yield range (%)	**A** : **B**
CH_2=CHOEt	500	5-7	five	61-77	<8:1
NaH (or $NaBH_4$)	30-50	5-7	five	53-79	<8:1
			six	73-94	>19:1
			seven	44-82	>19:1
NaOH + ^{i}PrOH[c]	50	1-2	six	63-91	>19:1
			seven	51-74	>19:1
$HSiEt_3$	110	10-16	six	71-84	>19:1

[a] Catalyst loading refers to the amount of **Ru-1a** initially used for RCM. [b] Time is that required for complete consumption of the RCM product during isomerization. [c] Isoropanol was used as cosolvent (25% v/v).

The Schmidt group used these methodologies to establish high-yield routes to enantiopure spirocycles,[35] diastereopure dihydrofurans and dihydropyrans,[36] unsaturated six- and seven-membered glycals, and eight-membered oxacycles.[37] Various natural products were also prepared. These include L-rhodinal and L-amicetal,[38] oligosaccharide side-chains present in

naturally-occurring antibiotic and anticancer agents,[39] as well as the potent antibiotic centrolobine.[40]

Blechert and coworkers have reported the enantioselective preparation of (-)-centrolobine using their methodology for diastereoselective ring-rearrangement metathesis (dRRM) via **Ru-1b'**,[41] followed by Schmidt's isomerization protocol involving post-RCM addition of $NaBH_4$ (40 mol%).[42]

In all the above studies, the isomerization catalyst is reasonably presumed to be a ruthenium hydride. Such complexes can be highly active for olefin isomerization.[43] Schmidt and coworkers observed several hydride signals by in situ ^1H NMR analysis of crude RCM-isomerization reaction mixtures, although the chemical shifts ($-7 > \delta_H > -15$ ppm) suggested coordinative saturation. ^{31}P NMR analysis of CH_2=CHOEt-assisted reaction mixtures also revealed the presence of hydridocarbonyl complex **Ru-7a**, formed by thermolysis of ethoxylidene **Ru-22a**, as discussed in Section 1.4.[44]

1.2.5 Tandem enyne metathesis-hydrovinylation

Snapper and coworkers reported tandem RCEYM-hydrovinylation of 1,6- and 1,7-enynes using the first-generation catalyst **Ru-1a** (Scheme 1.12).[45] The hydrovinylation catalyst, hydride **Ru-7a**, was generated using the Mol strategy (see Section 1.4).[46] Thus, after synthesis of the conjugated 1,3-dienes by ethylene-assisted enyne metathesis, methanolic NaOMe was added to convert the metathesis catalyst into **Ru-7a**.[47-50] Reaction with ethylene yielded the 1,4-hydrovinylation products depicted. No 1,2-hydrovinylation was observed (cf. the behaviour of the **Ru-7a**-HBF_4 system; Figure 1.4). The preference for 1,4-addition was attributed to isomerization of the conjugated diene prior to hydrovinylation. The authors

suggested that this may be due to the ability of methanol to compete with ethylene for binding to Ru. Control experiments showed that hydrovinylation was faster for a 1:1 mixture of **Ru-1a** and **Ru-7a** than for **Ru-7a** alone. An unspecified cooperative interaction of the two catalysts was inferred. This implies that the reasonable yields seen in the tandem metathesis reactions rely upon incomplete conversion of **Ru-1a** into **Ru-7a**. In situ NMR analysis confirmed that this transformation is only ca. 50% over the 10 min period allowed.

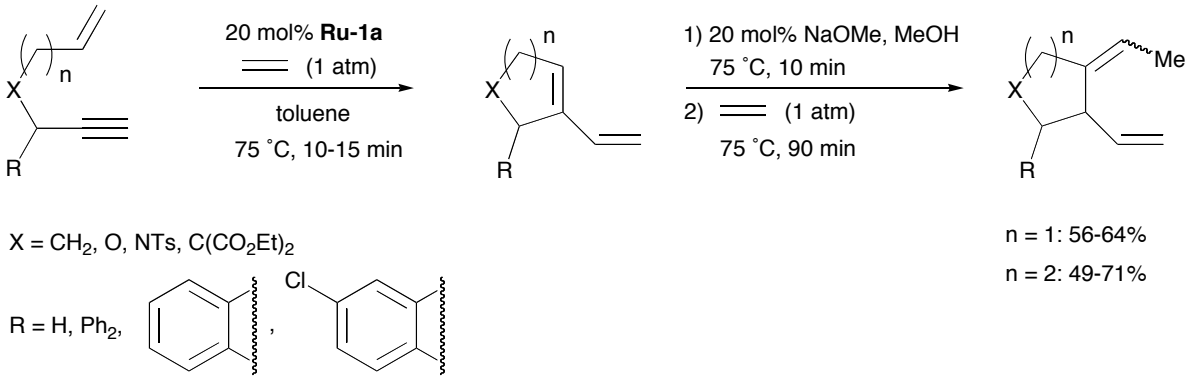

Scheme 1.12. Ru-1a-catalyzed RCEYM-isomerization.[45]

1.2.6 Tandem metathesis-hydrogenation

Saturation of metathesis polymers is key to preventing unwanted chemistry at the olefinic backbone, as discussed in more detail below. The simplest protocol entails exposure to H_2 after metathesis is complete. Grubbs extended this methodology to tandem RCM-hydrogenation, using **Ru-1a/b'** as the RCM catalyst. H_2-hydrogenation yielded saturated cyclic alkanes, ethers, ketones, lactones, and lactams (Scheme 1.13).[51] Yields of saturated products were lower for trisubstituted olefins than disubstituted olefins, owing to the steric encumbrance of the double bonds. This protocol was also applied to CM-hydrogenation of various olefins (Scheme 1.14).

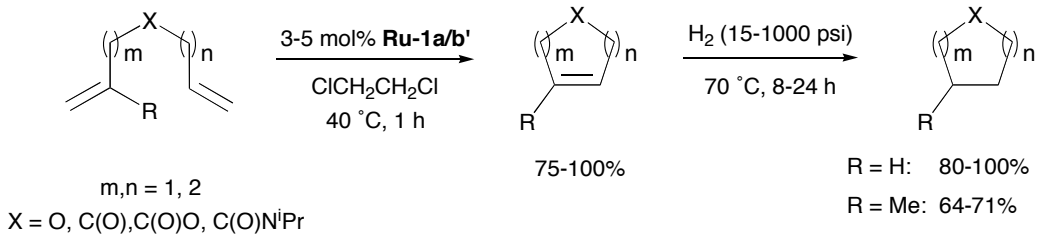

Scheme 1.13. Ru-1a/b'-catalyzed RCM-hydrogenation.[51]

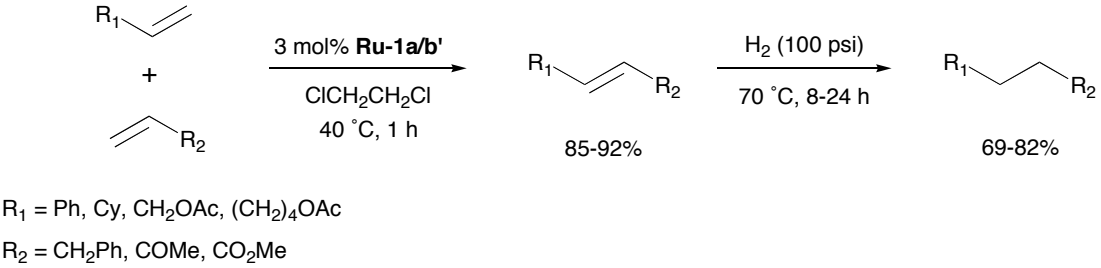

Scheme 1.14. Ru-1a/b'-catalyzed CM-hydrogenation.[51]

This report also demonstrated transfer dehydrogenation of an alcohol to a ketone following CM of 3-butene-2-ol with 5-acetoxy-1-hexene, using NaOH and 3-pentanone to trigger formation of the hydrogenation catalyst (Scheme 1.15). Tandem RCM-transfer dehydrogenation-hydrogenation was then used in a one-pot preparation of (R)-(-)-muscone (Scheme 1.16).

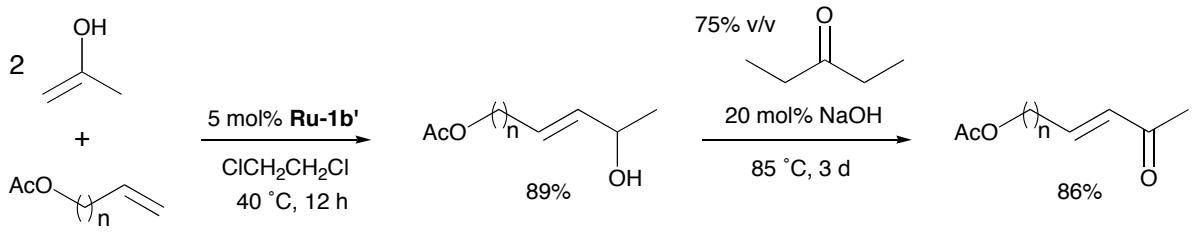

Scheme 1.15. Ru-1b'-catalyzed CM-transfer dehydrogenation.[51]

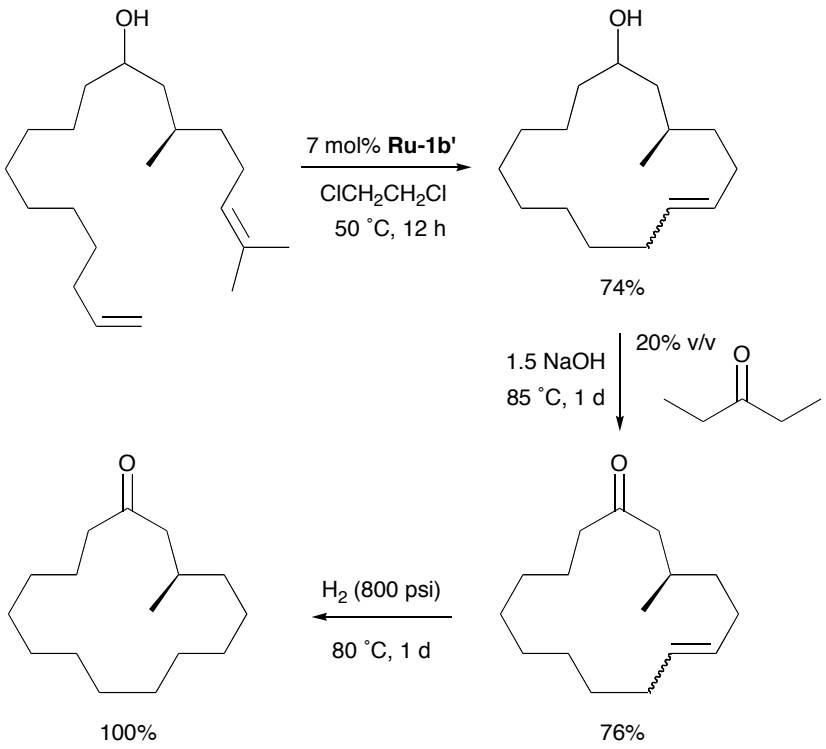

Scheme 1.16. Ru-1b'-catalyzed RCM-transfer dehydrogenation-hydrogenation.[51]

More recently, Yu and coworkers reported use of **Ru-1b** to promote tandem RCEYM-hydrogenation of chiral α,β-acetylenic esters (Scheme 1.17).[52]

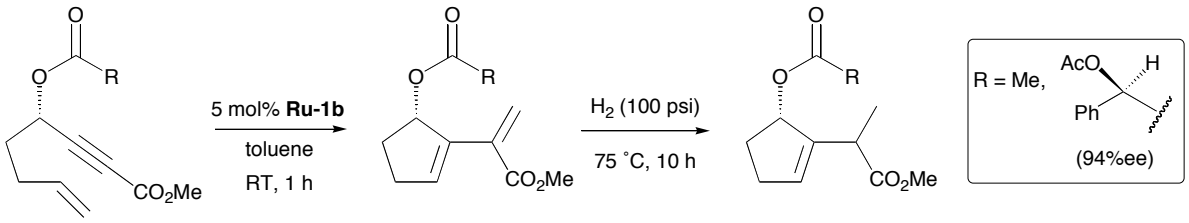

Scheme 1.17. Ru-1b-catalyzed RCEYM-hydrogenation.[52]

Ramharter and coworkers later employed the first-generation diphenylvinylylidene Grubbs catalyst **Ru-1a^{Ph2}** to prepare the polycyclic scaffold of (+)-lycoflexine, a potent acetylcholinesterase inhibitor (Scheme 1.18).[53]

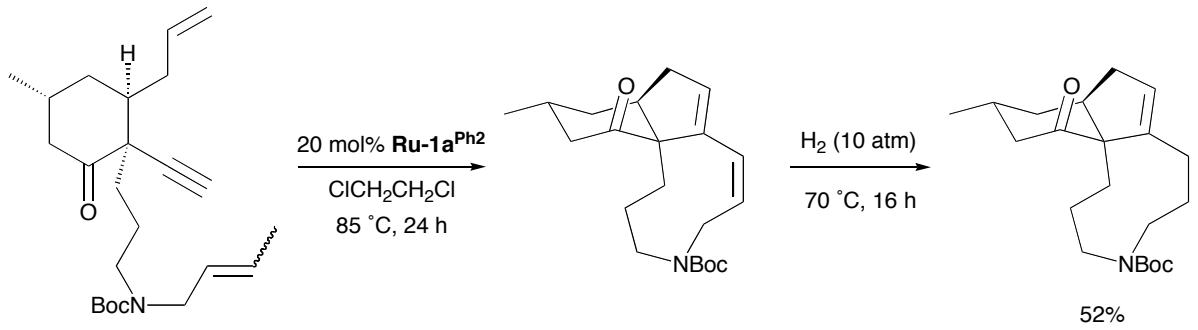

Scheme 1.18. Ru-1a^{Ph2}-catalyzed RCEYM-hydrogenation.[53]

Dixneuf and coworkers described tandem CM-hydrogenation using the Hoveyda-Grubbs isopropoxybenzylidene catalysts such as **Ru-3b'**. In an initial report, saturated nitrile-esters were prepared via CM-hydrogenation of acrylonitrile with unsaturated fatty esters (Scheme 1.19).[54]

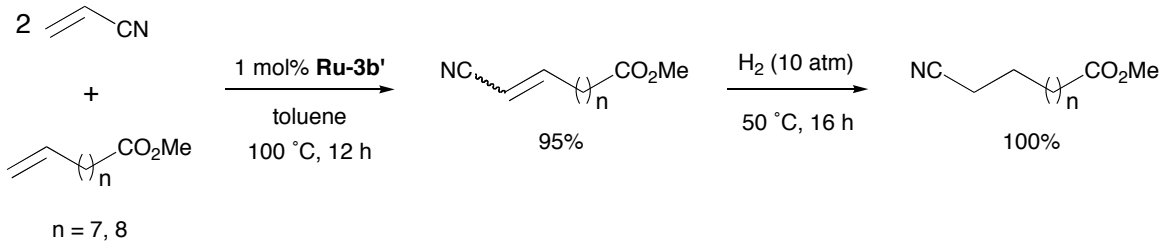

Scheme 1.19. Ru-3b'-catalyzed CM-hydrogenation.[54]

The Dixneuf group later employed **Ru-3e'** (in which the NHC ligand is H_2ITol; Scheme 1.20) for tandem self-CM-hydrogenation of ω-undecylenal.[55] This process is of interest in the context of renewable feedstocks, as the olefinic precursor is obtained by cracking castor oil. Tandem CM-hydrogenation of ω-undecylenal with acrolein was also investigated: yields of saturated α,ω-alcohols were on the order of 75%.

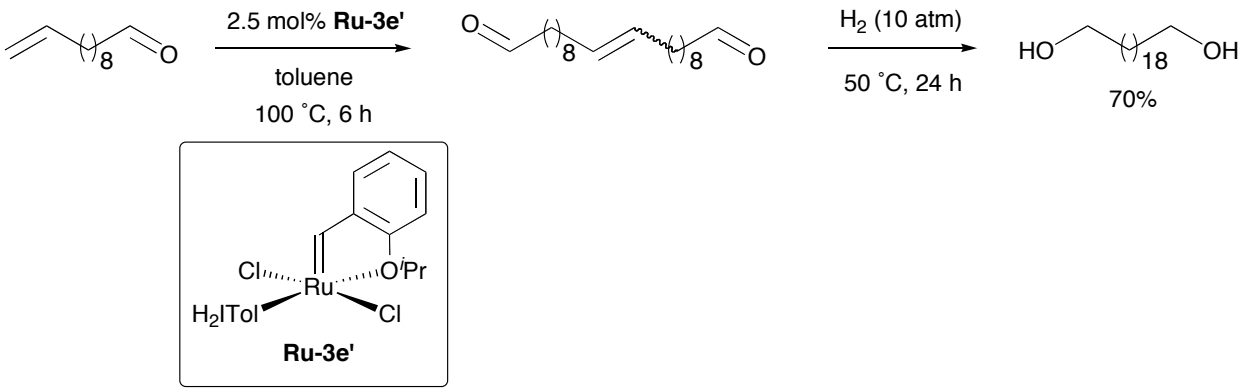

Scheme 1.20. Ru-3e'-catalyzed CM-hydrogenation.[55]

Tandem metathesis-hydrogenation has attracted most attention in the context of metathesis polymerization, as a means of reducing the polymers obtained via acyclic diene metathesis (ADMET) and ring-opening metathesis polymerization (ROMP). Reduction of ROMP materials is of particular importance in enhancing the stability of these designer materials toward thermal and oxidative degradation.[56] The following section describes in detail the developments in this area since the 1997 report by McLain, Brookhart and coworkers.

In this first, groundbreaking study, ROMP of a cyclooctene derivative was followed by hydrogenation at high temperatures and pressures to yield ester-functionalized polyethylene (Scheme 1.21).[57] The process was presumed to involve transformation of the metathesis catalyst **Ru-1a^{Ph2}** into a hydride species formulated as "$RuHCl(PCy_3)_2$". Saturation reached >99%, but forcing conditions were required (135 ˚C), which could promote competitive crosslinking.

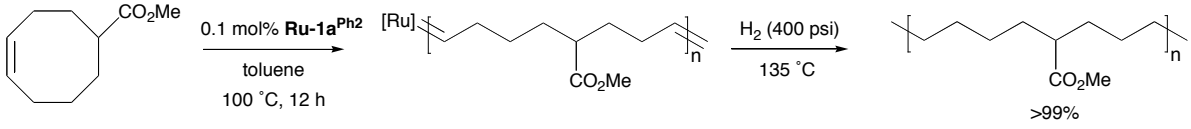

Scheme 1.21. Ru-1a^{Ph2}-catalyzed ROMP-hydrogenation of a cyclooctene substrate.[57]

Grubbs extended this approach to concurrent ROMP of cyclooctadiene (COD) and atom transfer radical polymerization (ATRP) of methylmethacrylate (MMA). This study used the first-generation initiator **Ru-1a^{Br}** (Scheme 1.22).[58] Hydride complex RuHCl(H_2)(PCy_3)$_2$ **Ru-6a** was presumed to be the hydrogenation catalyst.

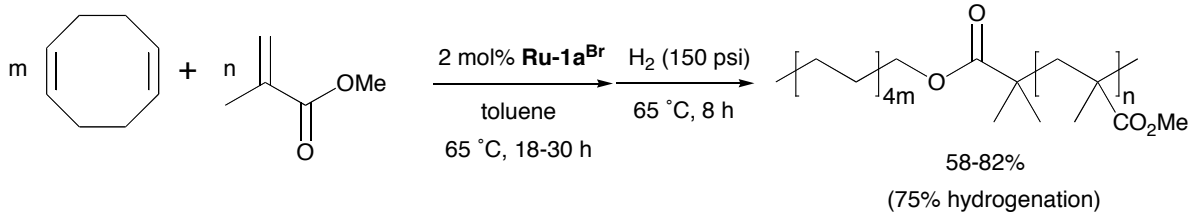

Scheme 1.22. Ru-1a^{Br}-catalyzed ROMP-hydrogenation of cyclooctadiene.[58]

Fogg and coworkers were able to reduce the hydrogen pressure required to 1 atm.[59] This advance rested on use of NEt_3 and MeOH as triggers to convert the ROMP catalyst **Ru-1a** into RuHCl(CO)(PCy_3)$_2$ **Ru-7a**, a key hydrogenation catalyst (Section 1.4). The latter was indeed observed via in situ NMR analysis of crude reaction mixtures (Scheme 1.23).

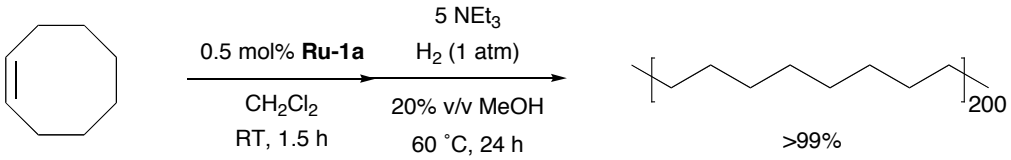

Scheme 1.23. Ru-1a-catalyzed ROMP-hydrogenation of cyclooctene.[59]

Subsequent studies by the Fogg group integrated the high ROMP activity and chain-length control of the third-generation Grubbs catalyst **Ru-1d** with the high hydrogenation efficiency of **Ru-1b**. This approach was used to prepare saturated neoglycopolymers, as well as other saturated polymers. The key to overcoming the poor hydrogenation activity of **Ru-1d** lay in adding PCy_3 post-ROMP, thus converting the Ru-alkylidene endgroup into that formed in ROMP via **Ru-1b**.[60] Subsequent addition of NEt_3 and MeOH enabled generation

of a more robust, PCy_3-stabilized hydrogenation catalyst. This methodology was used to prepare saturated neoglycopolymers which proved effective as collagen crosslinking agents for construction of artificial corneas (Scheme 1.24).[61] Nishihara and coworkers later used this protocol to prepare cyano- and ester-functionalized polynorbornanes.[62]

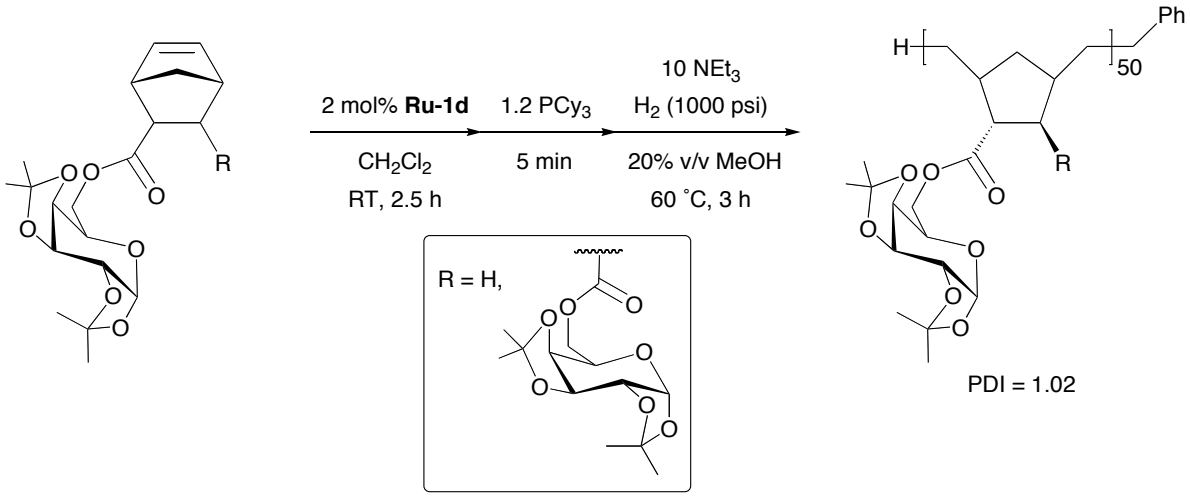

Scheme 1.24. Ru-1d-catalyzed ROMP-hydrogenation of galactose-functionalized norbornenes.[61]

The above studies demonstrate how understanding of the organometallic chemistry involved in "switching" the nature of the catalyst can aid in design of effective protocols for assisted tandem catalysis. It is noteworthy that the hydridocarbonyl complex $RuHCl(CO)(PCy_3)_2$ **Ru-7a** was implicated as "Catalyst B" during tandem metathesis-isomerization, RCEYM-hydrovinylation, and ROMP-hydrogenation. The diverse olefin functionalization activity of hydridocarbonyl complexes is illustrated further in the following section.

1.3 Olefin functionalization activity of RuHCl(CO)(L)(PCy_3) Ru-7

The hydridocarbonyl complexes RuHCl(CO)(L)(PCy_3) **Ru-7**, particularly bis-phosphine **Ru-7a**, promote many olefin transformations, ranging from simple hydrogenation and isomerization to coupling reactions (Figure 1.4).

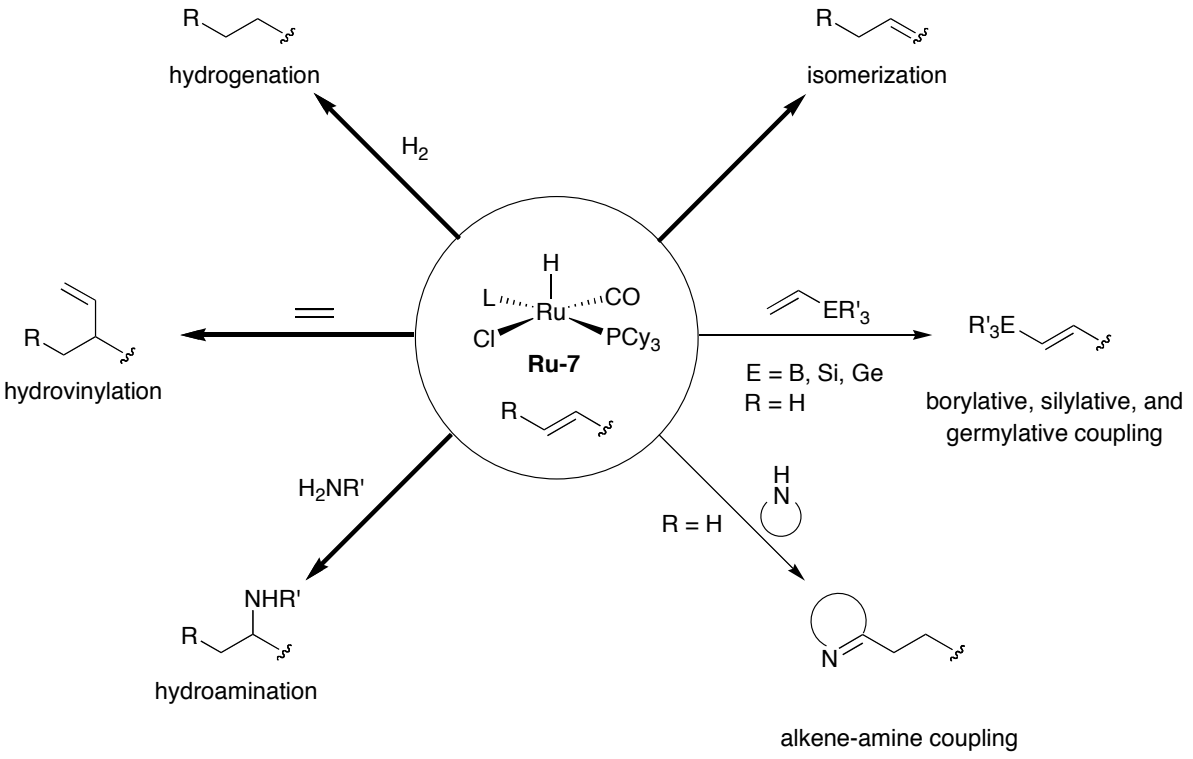

Figure 1.4. Olefin functionalization processes catalyzed by **Ru-7**. Bold arrows denote compatibility with internal olefins (i.e. potential relevance to tandem (R)CM-functionalization).

Rempel carried out pioneering work on **Ru-7a** as a hydrogenation catalyst, with a particular focus on reduction of the C=C bonds in nitrile-butadiene rubber (NBR).[63-64] Forcing conditions were required (40 atm H_2, 160 ˚C) for these challenging polymer substrates. More recent work by de Souza and coworkers showed that this transformation can be carried out in ionic liquids.[65] Yi and coworkers have reported that **Ru-7a** effects efficient hydrogenation of cis and trans olefins, as well as terminal olefins, in molecular

substrates.[66] This not surprising, given the much greater accessibility of the olefinic group in small molecules, relative to polymers. In subsequent work, Yi et al. included HBF_4 as a co-catalyst to sequester dissociated PCy_3 as $[HPCy_3]BF_4$ (and hence presumably to trap the catalyst as the four-coordinate active species $RuHCl(CO)(PCy_3)$ **Ru-7a'**).[67] Low pressures of H_2 (1-2 atm) could then be used, although the effect on catalyst lifetime (total TON) was not explored. Soon after, Yi and Nolan reported the related catalyst $RuHCl(CO)(IMes)(PCy_3)$ **Ru-7b**. This exhibits lower hydrogenation activity than **Ru-7a** at ambient temperatures (presumably due to the low lability of the PCy_3 ligand trans to an NHC), but superior activity at 100 °C.[68] In a comparative study of the hydrogenation activity of **Ru-7a/b** and the PPh_3-substituted analogues $RuHCl(CO)(NHC)(PPh_3)$ **Ru-14b/b'**, Fogg and coworkers correlated hydrogenation activity with phosphine lability.[69]

The olefin isomerization activity of **Ru-7a** was noted by Yi in studies originally directed at hydrogenation,[66] and similar behaviour was noted for **Ru-7b** and **Ru-14** by Fogg.[69] Since then, Arisawa explored isomerization of allyl amines to vinyl amines, using as a catalyst system **Ru-1b'** and vinyloxytrimethylsilane.[70,71] This system generates **Ru-7b'** in situ, as discussed in more detail below. The latter complex was observed by in situ NMR analysis. Likewise, **Ru-7a** was observed by NMR analysis on use of a **Ru-1a**-CH_2=CHOEt system used for tandem RCM-isomerization (Section 1.2.4).[33]

To the multitude of reports concerning catalysis by **Ru-7a**, Marciniec and coworkers have contributed a very large body of work on silylative,[72] borylative[73] and germylative[74] coupling of many terminal olefins with vinyl silanes, boronates and germanes, respectively.

Yi and coworkers reported that **Ru-7a** catalyzes the coupling of terminal olefins with secondary amines.[75] The **Ru-7a**/HBF_4 catalyst system was used for hydroamination of terminal olefins, including conjugated olefins, by primary arylamines and benzocyclic amines.[76] Hydrovinylation of vinylarenes and conjugated internal olefins,[48,49] as well as terminal and internal dienoates (typically at elevated temperatures),[50] was also reported. RajanBabu[77] and Connell[78] were able to use mild conditions by adding AgOTf or $AgSbF_5$ as cocatalysts (1:1 vs. Ru). The activity was attributed to generation of four-coordinate $[RuH(CO)(PCy_3)_2]X$ (X = OTf, SbF_5) by chloride abstraction from **Ru-7a**.

The loadings of **Ru-7** employed in many of these studies (<2 mol%) are low compared to those typical of olefin metathesis (1-20 mol%). This is an asset in terms of the efficiency with which post-metathesis catalysis can be carried out, as it can compensate for the inefficient formation of **Ru-7**. As the catalyst loadings used in olefin metathesis are forced to improve, however, this luxury will disappear. Even in the current state of the art, the long reaction times and forcing conditions often required for the "alkylidene-to-hydride" or other transformations described above underscore the need for greater efficiency. The following section summarizes the efficiency with which **Ru-7** could be generated from the Grubbs catalysts at the outset of this thesis work.

1.4 Transformation of Grubbs catalysts into hydridocarbonyls

In the first mechanistic investigation of the reaction of **Ru-1a** with H_2 ("hydrogenolysis"), Fogg and coworkers[79] reported that the benzylidene ligand of **Ru-1a** is evolved as toluene, with co-formation of $Ru(H_2)Cl_2(PCy_3)_2$ **Ru-5** and its dihydride tautomer $Ru(H)_2Cl_2(PCy_3)_2$ **Ru-5'**. Use of a base to abstract HCl yielded $RuHCl(H_2)(PCy_3)_2$ **Ru-6a** as the sole product.

Proton Sponge® (1,8-bis(dimethylamino)naphthalene) was used for convenience in NMR monitoring, but NEt_3 was also effective. A requirement for several equivalents of base was observed: this was attributed to rechlorination of the ruthenium species by the CH_2Cl_2 solvent. Subsequent catalytic studies showed that use of methanol as co-solvent greatly enhanced hydrogenation activity during ROMP-hydrogenation (Scheme 1.25).[59] In situ NMR analysis revealed the known, highly active hydrogenation catalyst $RuHCl(CO)(PCy_3)_2$ **Ru-7a**, which was presumed to form via decarbonylation of methanol by **Ru-6a** (a long-established process; see later).[80-82] Higher hydrogenation activity was inferred for **Ru-7a**, vs. **Ru-6a**, but was not directly examined. The question of the efficiency with which both complexes can be obtained from **Ru-1a**, or the important second- and third-generation Grubbs catalysts, was taken up in the present work.

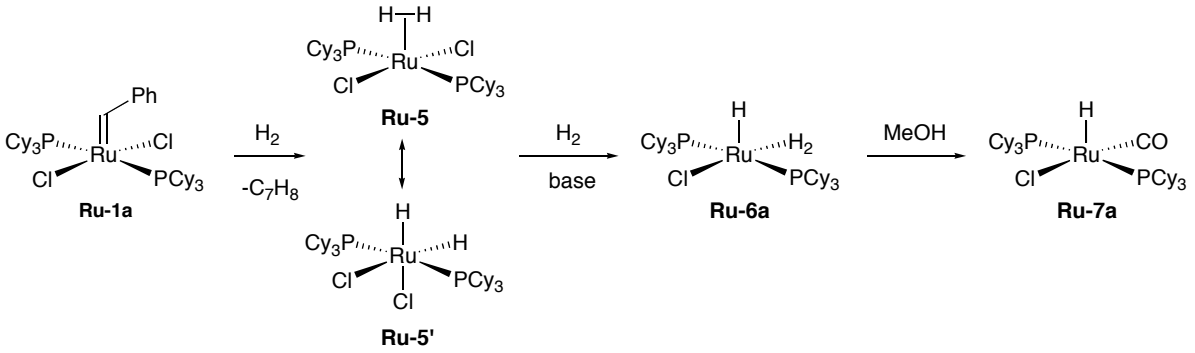

Scheme 1.25. Hydrogenolysis of **Ru-1a**.[59,79]

Subsequent work by Mol and coworkers reported that H_2 is not required in order to form the hydridocarbonyl complexes from **Ru-1** (**Ru-1a**: L = PCy_3;[46] **Ru-1b'**: L = H_2IMes;[83] **Ru-1f'**: L = H_2IPr).[84] Reaction of these benzylidene complexes with methanol in the presence of a base ("methanolysis", Scheme 1.26) likewise affords **Ru-7**, albeit in variable yields. The **Ru-1a** study employed the inorganic bases NaOH, NaOMe, and K_2CO_3 to effect rapid formation of **Ru-7a** in moderate yield. Methanolysis of second-generation **Ru-1b'** and **Ru-**

1f' in the presence of NEt_3 afforded the related complexes **Ru-7b'** and **Ru-7f'** and multiple unidentified side-products. Ligand disproportionation during methanolysis of **Ru-1b'** is indicated by the formation of bis(PCy_3) species **Ru-7a**.

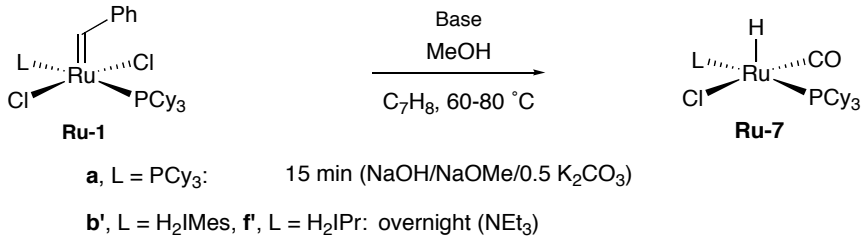

Scheme 1.26. Methanol-induced transformation of benzylidene complexes **Ru-1a/b'/f'** into carbonyl hydride **Ru-7**.[46,83,84]

A plausible mechanism for methanolysis of **Ru-1a** (Scheme 1.27) was proposed by Mol and coworkers.[46] Dehydrohalogenation of **Ru-1a** and methanol was suggested to form a methoxide complex, which undergoes proton transfer to the benzylidene C_α to form a benzyl intermediate and formaldehyde. Abstraction of a proton from formaldehyde would liberate the benzyl ligand as toluene, following which formyl deinsertion would yield **Ru-7a**.

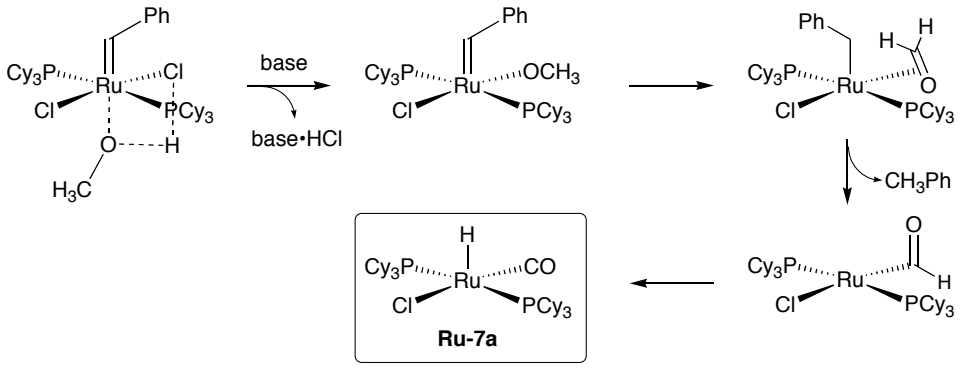

Scheme 1.27. Proposed mechanism for base-assisted methanolysis of **Ru-1a**.[46]

A Grubbs report described the formation of hydridocarbonyl $RuH(OC(O)CF_3)(CO)(PPh_3)_2$ **Ru-25** by decomposition of a Fischer carbene (Scheme 1.28).[85] A mechanism involving PPh_3

dissociation and formyl deinsertion was proposed. The resulting formyl intermediate may undergo reductive elimination of $PhCH_2OC(O)CF_3$ to form hydride **Ru-25** (Scheme 1.28, Path (a)) or of toluene to generate carbonyl **Ru-26** (Scheme 1.28, Path (b)). Both $PhCH_2OC(O)CF_3$ and $PhCH_2D$ were observed (GC-MS) following decomposition of $Ru(OC(O)CF_3)_2(PPh_3)_2(=CDOCH_2Ph)$ **α-*d*$_1$-Ru-24**. The 8.5:1 ratio indicated a strong preference for hydridocarbonyl formation.

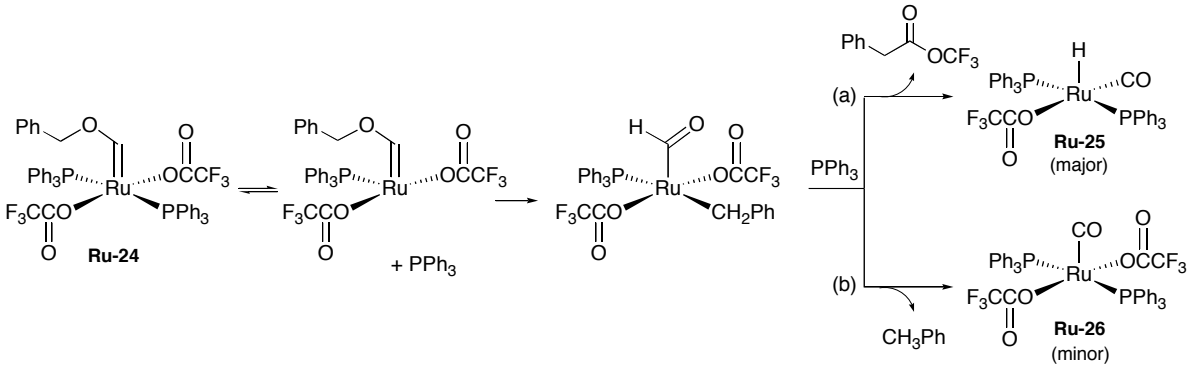

Scheme 1.28. Proposed pathways for decomposition of **Ru-24**.[85]

Grubbs suggested that such a mechanism could also account for generation of **Ru-7a** on thermolysis of the Fischer carbene $RuCl_2(PCy_3)_2(=CHOEt)$ **Ru-22a** (Scheme 1.29, Path (a)).[44] Arisawa later described a much more efficient process involving CM of **Ru-1b'** with CH_2=CHOTMS. This affords $RuHCl(CO)(H_2IMes)(PCy_3)$ **Ru-7b'** in quantitative yields within 1 hour at 50 °C (Scheme 1.29, Path (b)).[71] Reactivity studies with **Ru-22a/b** are confined to metathesis and thermolysis, and the potential for combining metathesis quenching with tandem catalysis has not been considered to date.

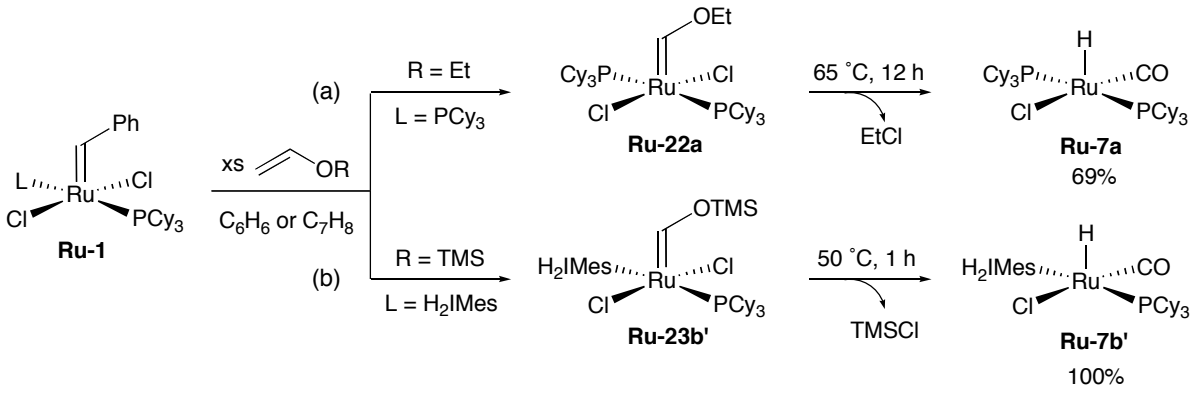

Scheme 1.29. Formation of **Ru-7** by thermolysis of Fischer carbenes.[44,71]

The organometallic chemistry of Grubbs methylidenes $RuCl_2(L)(PCy_3)(=CH_2)$ **Ru-2a/b** is even less studied, perhaps surprisingly given the importance of these species as catalyst resting states in Ru-catalyzed RCM[86] and CM.[87] A rare exception is a report by Caulton and coworkers, who described the clean hydrogenolysis of **Ru-2a** to **Ru-6a** (Scheme 1.30).[88]

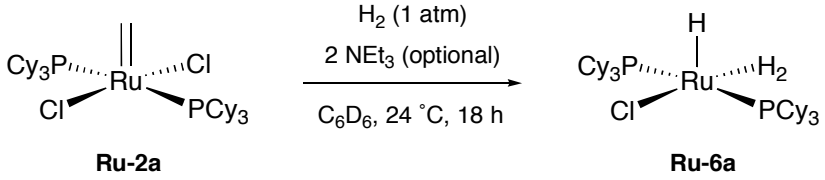

Scheme 1.30. Hydrogenolysis of **Ru-2a**.[88]

Assessment of the efficiency with which the Grubbs catalysts **Ru-1a/b** can be converted into their hydridocarbonyl analogues **Ru-7a/b**, using the methods summarized above, could improve existing methodologies in tandem ROMP-hydrogenation. Insight into methods suitable for the corresponding transformation of methylidenes **Ru-2a/b** would open up new opportunities for (R)CM-functionalization, while such studies of Fischer carbenes **Ru-22a/b** would enable introduction of an intervening quenching step.

1.5 Scope of Thesis Work

This work was aimed at establishing the efficiency with which the Grubbs catalysts are transformed into Ru-hydrides using state-of-the-art protocols for ROMP-hydrogenation. The relative hydrogenation activity of the ruthenium products is also examined. Transformation of the first- and second-generation Grubbs benzylidenes into hydridocarbonyl complexes using various chemical agents is examined. The corresponding behaviour of ruthenium methylidenes and ethoxylidenes is also evaluated, to assess the compatibility of these transformations with tandem (R)CM-functionalization and metathesis quenching, respectively. Particular care is taken to examine disproportionation of Ru-NHC-catalysts, a potential vector for catalyst decomposition. In studying second-generation Grubbs catalysts, we chose to focus on the chemistry of the IMes derivatives, because preliminary studies of H_2IMes complex **Ru-1b'** in ROMP-hydrogenation indicated much lower hydrogenation activity (work carried out by Dr. Debbie Mitra of the Fogg group). This may point toward a lower thermal stability of the H_2IMes complexes (perhaps a function of the higher lability of the phosphine ligand in **Ru-1b'** relative to IMes complex **Ru-1b**),[89] although this issue was not investigated.

1.6 References

1. Anastas, P.; Eghbali, N. *Chem. Soc. Rev.* **2010**, *39*, 301-312.
2. Sheldon, R. A., *Green Chemistry and Catalysis*. Wiley-VCH: Chichester, 2007.
3. Trost, B. M. *Science* **1991**, *254*, 1471-7.
4. Constable, D. J. C.; Jimenez-Gonzalez, C.; Henderson, R. K. *Org. Process Res. Dev.* **2007**, *11*, 133-137.
5. Recent reviews of tandem catalysis: (a) V. Dragutan, I. Dragutan, *J. Organomet. Chem.* **2006**, *691*, 5129-5147. (b) J.-C. Wasilke, S. J. Obrey, R. T. Baker, G. C. Bazan, *Chem. Rev.* **2005**, *105*, 1001-1020. (c) D. E. Fogg, E. N. dos Santos, *Coord. Chem. Rev.* **2004**, *248*, 2365-2379.
6. Shindoh, N.; Takemoto, Y.; Takasu, K. *Chem. Eur. J.* **2009**, *15*, 12168-12179.
7. Grubbs, R. H., *Handbook of Metathesis*. Wiley-VCH: Weinheim, 2003.
8. Fürstner, A. *Angew. Chem., Int. Ed.* **2000**, *39*, 3012-3043.
9. Kim, B. G.; Snapper, M. L. *J. Am. Chem. Soc.* **2006**, *128*, 52-53.
10. Ulman, M.; Belderrain, T. R.; Grubbs, R. H. *Tetrahedron Lett.* **2000**, *41*, 4689-4693.
11. Mallagaray, A.; Dominguez, G.; Gradillas, A.; Perez-Castells, J. *Org. Lett.* **2008**, *10*, 597-600.
12. Fustero, S.; Sanchez-Rosello, M.; Jimenez, D.; Sanz-Cervera, J. F.; Del Pozo, C.; Acena, J. L. *J. Org. Chem.* **2006**, *71*, 2706-2714.
13. Hong, S. H.; Day, M. W.; Grubbs, R. H. *J. Am. Chem. Soc.* **2004**, *126*, 7414-7415.
14. Tallarico, J. A.; Malnick, L. M.; Snapper, M. L. *J. Org. Chem.* **1999**, *64*, 344-345.
15. Quayle, P.; Fengas, D.; Richards, S. *Synlett* **2003**, 1797-1800.
16. Seigal, B. A.; Fajardo, C.; Snapper, M. L. *J. Am. Chem. Soc.* **2005**, *127*, 16329-16332.
17. Schmidt, B.; Pohler, M. *J. Organomet. Chem.* **2005**, *690*, 5552-5555.
18. Smith, M. B.; March, J., *March's Advanced Organic Chemistry*. 5th ed.; Wiley: New York, 1994; p 911.
19. McGonagle, F. I.; Brown, L.; Cooke, A.; Sutherland, A. *Org. Biomol. Chem.* **2010**, *8*, 3418-3425.
20. Edlin, C. D.; Faulkner, J.; Quayle, P. *Tetrahedron Lett.* **2006**, *47*, 1145-1151.
21.Beligny, S.; Eibauer, S.; Maechling, S.; Blechert, S. *Angew. Chem., Int. Ed.* **2006**, *45*, 1900-1903.
22. Low yields of dihydroxylated product are obtained when trace amounts of CH_2Cl_2 are present.
23. It is notable that post-metathesis solvent removal violates the waste-reduction objectives of green chemistry (Section 1.1).
24. Scholte, A. A.; An, M. H.; Snapper, M. L. *Org. Lett.* **2006**, *8*, 4759-4762.
25. Plietker, B.; Niggemann, M. *J. Org. Chem.* **2005**, *70*, 2402-2405.
26. Plietker, B. *Eur. J. Org. Chem.* **2005**, 1919-1929.
27. Plietker, B. *J. Org. Chem.* **2003**, *68*, 7123-7125.
28. Neisius, N. M.; Plietker, B. *J. Org. Chem.* **2008**, *73*, 3218-3227.
29. Howe, N. R.; Sheikh, Y. M. *Science* **1975**, *189*, 386-388.
30. W. P. Griffith, Ruthenium Oxidation Catalysts, Catalysis by Metal Complexes 34, © Springer Science+Business Media B.V. 2011.
31. Sutton, A. E.; Seigal, B. A.; Finnegan, D. F.; Snapper, M. L. *J. Am. Chem. Soc.* **2002**, *124*, 13390-13391.

32. Schmidt, B. *Eur. J. Org. Chem.* **2003**, 816-819.
33. Schmidt, B. *J. Org. Chem.* **2004**, *69*, 7672-7687.
34. The authors speculate that unprotected alcohol groups and exocyclic olefinic bonds aid in transfer hydrogenation by coordinating to the metal center.
35. Schmidt, B.; Staude, L. *J. Organomet. Chem.* **2006**, *691*, 5218-5221.
36. Schmidt, B.; Biernat, A. *Synlett* **2007**, 2375-2378.
37. Schmidt, B.; Biernat, A. *Org. Lett.* **2008**, *10*, 105-108.
38. Schmidt, B.; Biernat, A. *Chem. Eur. J.* **2008**, *14*, 6135-6141.
39. Gräfe, U., *Biochemie der Antibiotika*. Spektrum: Heidelberg, 1992.
40. Schmidt, B.; Hoelter, F. *Chem.-Eur. J.* **2009**, *15*, 11948-11953.
41. Boehrsch, V.; Neidhoefer, J.; Blechert, S. *Angew. Chem., Int. Ed.* **2006**, *45*, 1302-1305.
42. Boehrsch, V.; Blechert, S. *Chem. Commun.* **2006**, 1968-1970.
43. Tanaka, K., In *Comprehensive Organometallic Chemistry*, Crabtree, R. H.; Mingos, D. M. P., Eds. Elsevier: New York, 2007; Vol. 10, Chapter 2, and references therein.
44. Louie, J.; Grubbs, R. H. *Organometallics* **2002**, *21*, 2153-2164.
45. Gavenonis, J.; Arroyo, R. V.; Snapper, M. L. *Chem. Commun.* **2010**, *46*, 5692-5694.
46. Dinger, M. B.; Mol, J. C. *Organometallics* **2003**, *22*, 1089-1095.
47. Yi, C. S.; Lee, D. W.; Chen, Y. *Organometallics* **1999**, *18*, 2043-2045.
48. Yi, C. S.; He, Z.; Lee, D. W. *Organometallics* **2001**, *20*, 802-804.
49. He, Z.; Yi, C. S.; Donaldson, W. A. *Org. Lett.* **2003**, *5*, 1567-1569.
50. He, Z.; Yi, C. S.; Donaldson, W. A. *Synlett* **2004**, 1312-1314.
51. Louie, J.; Bielawski, C. W.; Grubbs, R. H. *J. Am. Chem. Soc.* **2001**, *123*, 11312-11313.
52. Yue, Y.; Turlington, M.; Yu, X.-Q.; Pu, L. *J. Org. Chem.* **2009**, *74*, 8681-8689.
53. Ramharter, J.; Weinstabl, H.; Mulzer, J. *J. Am. Chem. Soc.* **2010**, *132*, 14338-14339.
54. Malacea, R.; Fischmeister, C.; Bruneau, C.; Dubois, J.-L.; Couturier, J.-L.; Dixneuf, P. H. *Green Chem.* **2009**, *11*, 152-155.
55. Miao, X.; Fischmeister, C.; Bruneau, C.; Dixneuf, P. H. *ChemSusChem* **2009**, *2*, 542-545.
56. (a) McManus, N. T.; Rempel, G. L. J. *Macromol. Sci., Rev. Macromol. Chem. Phys.* **1995**, *C35*, 239. (b) Maréchal, E. In *Comprehensive Polymer Science*; Eastmond, G. C., Ledwith, A., Russo, S., Sigwalt, P., Eds.; Pergamon: Toronto, 1989; Vol. 6.
57. McLain, S. J.; McCord, E. F.; Arthur, S. D.; Hauptman, E.; Feldman, J.; Nugent, W. A.; Johnson, L. K.; Mecking, S.; Brookhart, M. *Polym. Mater. Sci. Eng.* **1997**, *76*, 246-247.
58. Bielawski, C. W.; Louie, J.; Grubbs, R. H. *J. Am. Chem. Soc.* **2000**, *122*, 12872-12873.
59. Drouin, S. D.; Zamanian, F.; Fogg, D. E. *Organometallics* **2001**, *20*, 5495-5497.
60. Camm, K. D.; Castro, N. M.; Liu, Y.; Czechura, P.; Snelgrove, J. L.; Fogg, D. E. *J. Am. Chem. Soc.* **2007**, *129*, 4168-4169.
61. Merrett, K.; Liu, W.; Mitra, D.; Camm, K. D.; McLaughlin, C. R.; Liu, Y.; Watsky, M. A.; Li, F.; Griffith, M.; Fogg, D. E. *Biomaterials* **2009**, *30*, 5403–5408.
62. Nishihara, Y.; Izawa, S.; Inoue, Y.; Nakayama, Y.; Shiono, T.; Takagi, K. *J. Polym. Sci., Part A* **2008**, *46*, 3314-3325.
63. Martin, P.; McManus, N. T.; Rempel, G. L. *Ibid.* **1992**, *73*, 161
64. Martin, P.; McManus, N. T.; Rempel, G. L. *J. Mol. Catal. A* **1997**, *126*, 115-131.
65. De Souza, R. F.; Rech, V.; Dupont, J. *Adv. Synth. Catal.* **2002**, *344*, 153-155.
66. Yi, C. S.; Lee, D. W. *Organometallics* **1999**, *18*, 5152-5156.

67. Yi, C. S.; Lee, D. W.; He, Z.; Rheingold, A. L.; Lam, K.-C.; Concolino, T. E. *Organometallics* **2000**, *19*, 2909-2915.
68. Lee, H. M.; Smith, D. C., Jr.; He, Z.; Stevens, E. D.; Yi, C. S.; Nolan, S. P. *Organometallics* **2001**, *20*, 794-797.
69. Dharmasena, U. L.; Foucault, H. M.; dos Santos, E. N.; Fogg, D. E.; Nolan, S. P. *Organometallics* **2005**, *24*, 1056-1058.
70. Arisawa, M.; Terada, Y.; Nakagawa, M.; Nishida, A. *Angew. Chem., Int. Ed.* **2002**, *41*, 4732-4734.
71. Arisawa, M.; Terada, Y.; Takahashi, K.; Nakagawa, M.; Nishida, A. *J. Org. Chem.* **2006**, *71*, 4255-4261.
72. Leading references: (a) Marciniec, B. *Coord. Chem. Rev.* **2005**, *249*, 2374-2390. (b) Marciniec, B.; Dudziec, B.; Kownacki, I. *Angew. Chem., Int. Ed.* **2006**, *45*, 8180-8184. (c) Majchrzak, M.; Marciniec, B.; Kubicki, M.; Pawelczyk, A. *Organometallics* **2005**, *24*, 3731-3736. (d) Pawluc, P.; Hreczycho, G.; Marciniec, B. *Synlett* **2005**, 1105-1108. (e) Marciniec, B.; Majchrzak, M.; Prukala, W.; Kubicki, M.; Chadyniak, D. *J. Org. Chem.* **2005**, *70*, 8550-8555. (f) Yi, C.S.; He, Z.; Lee, D.W.; Rheingold, A.L.; Lam, K.-C. *Organometallics* **2000**, *19*, 2036-2039. (g) Itami, Y.; Marciniec, B.; Kubicki, M. *Organometallics* **2003**, *22*, 3717-3722..
73. Marciniec, B.; Jankowska, M.; Pietraszuk, C. *Chem. Commun.* **2005**, 663-665.
74. Marciniec, B.; Lawicka, H.; Dudziec, B. *Organometallics* **2007**, *26*, 5188-5192.
75. Yi, C. S.; Yun, S. Y.; Guzei, I. A. *Organometallics* **2004**, *23*, 5392-5395.
76. Yi, C. S.; Yun, S. Y. *Org. Lett.* **2005**, *7*, 2181-2183.
77. RajanBabu, T. V.; Nomura, N.; Jin, J.; Nandi, M.; Park, H.; Sun, X. *J. Org. Chem.* **2003**, *68*, 8431-8446.
78. Sanchez, R. P.; Connell, B. T. *Organometallics* **2008**, *27*, 2902-2904.
79. Drouin, S. D.; Yap, G. P. A.; Fogg, D. E. *Inorg. Chem.* **2000**, *39*, 5412-5414.
80. Chaudret, B. N.; Cole-Hamilton, D. J.; Nohr, R. S.; Wilkinson, G. *J. Chem. Soc., Dalton Trans.* **1977**, 1546-1557.
81. Van der Sluys, L. S.; Kubas, G. J.; Caulton, K. G. *Organometallics* **1991**, *10*, 1033-1038.
82. Chen, Y.-Z.; Chan, W. C.; Lau, C. P.; Chu, H. S.; Lee, H. L.; Jia, G. *Organometallics* **1997**, *16*, 1241-1246.
83. Dinger, M. B.; Mol, J. C. *Eur. J. Inorg. Chem.* **2003**, 2827-2833.
84. Banti, D.; Mol, J. C. *J. Organomet. Chem.* **2004**, *689*, 3113-3116.
85. Wu, Z.; Nguyen, S. T.; Grubbs, R. H.; Ziller, J. W. *J. Am. Chem. Soc.* **1995**, *117*, 5503-5511.
86. Dias, E. L.; Nguyen, S. T.; Grubbs, R. H. *J. Am. Chem. Soc.* **1997**, *119*, 3887-3897.
87. Schwab, P.; Grubbs, R. H.; Ziller, J. W. *J. Am. Chem. Soc.* **1996**, *118*, 100-110.
88. Oliván, M.; Caulton, K. G. *Inorg. Chem.* **1999**, *38*, 566-570.
89. Sanford, M. S.; Love, J. A.; Grubbs, R. H. *J. Am. Chem. Soc.* **2001**, *123*, 6543-6554.

Chapter 2. Carbonyl-Amplified Catalyst Performance: Assessing the Balance Between Stability and Activity for $RuHCl(H_2)LL'$ and RuHCl(CO)LL' Catalysts.*

2.1 Introduction

The high volume of waste characteristic of fine chemicals and pharmaceutical manufacturing[1,2] was discussed in Chapter 1. Such issues are coming under increasing scrutiny in a stringent economic climate in which the contribution of waste to process costs is no longer regarded as insignificant. Tandem catalysis has attracted much interest[3-5] for the potential economic and environmental benefits that accrue from coupling multiple catalytic transformations in a single vessel. Particularly important is the potential to improve process efficiencies by eliminating unnecessary workup stages and solvent use, two major contributors to waste in pharmaceutical manufacturing.[1,6] Improved efficiencies in catalyst consumption confer added advantages in reducing direct catalyst costs, as well as indirect costs associated with purification of the organic products.

Within a program of study focusing on tandem catalysis, prior work in the Fogg group targeted development of efficient methodologies for tandem ROMP-hydrogenation (ROMP = ring-opening metathesis polymerization).[7-10] These and improved methodologies, which enable important routes to "designer materials", are described in detail in Chapter 3. In general, they rest on the accessibility of five-coordinate Ru hydrides from Grubbs catalysts of type **Ru-1** (Scheme 2.1). Earlier work by Samantha Drouin of this research group[9] showed that the

*This Chapter is adapted from: N.J. Beach, J.M. Blacquiere, S.D. Drouin, D.E. Fogg, *Organometallics*, **2009**, 28, 441-447.

hydrido-dihydrogen complex **Ru-6a** is formed cleanly by hydrogenolysis of **Ru-1a** in the presence of base: the corresponding hydridocarbonyl complexes **Ru-7** are formed from both **Ru-1**[11-13] and **Ru-6**[7] by reaction with methanol or other primary alcohols, via established alcohol decarbonylation pathways.[14-17] Small amounts of methanol cosolvent dramatically increased hydrogenation efficiency. Use of isopropanol led to smaller rate accelerations. An increase in the dielectric constant of the reaction medium almost certainly contributes to the beneficial effect. The higher activity in the presence of the primary alcohol, however, also correlates with formation of **Ru-7a** – by inference, a more reactive catalyst than **Ru-6a**.[7]

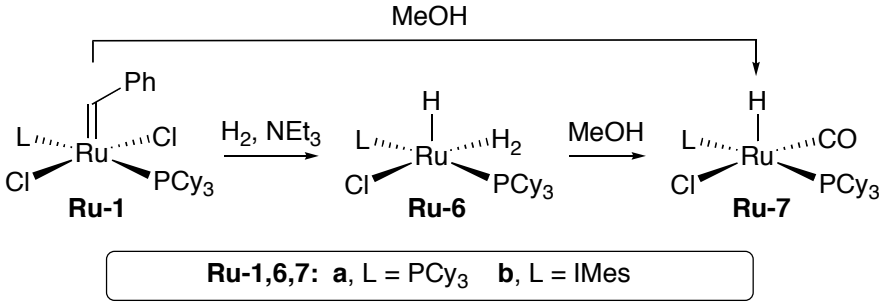

Scheme 2.1. Hydride complexes formed from first- and second-generation Grubbs metathesis catalysts. [7,9,11-13]

While ample precedents exist for hydrogenation via **Ru-7a**,[11,18-23] catalysis via **Ru-6a** has gone less studied,[24] and no direct comparison of the hydrogenation activity of the two complexes has been reported. The possibility that **Ru-7a** is more active is intriguing, given that much evidence correlates higher hydrogenation activity with a more electron-rich Ru center. Thus, Ru catalysts containing strongly σ-donating alkylphosphine ligands outperform those containing arylphosphines, and incorporation of a CO ligand is known to *decrease* hydrogenation activity in arylphosphine complexes of Ru, Rh, and Ir.[22,25-27] The latter behaviour is consistent with the inhibiting effect of the π-acid ligand on both phosphine loss

(a required step in olefin hydrogenation via **Ru-7a**[18,23] and related polyphosphine[27] catalysts), and oxidative addition of dihydrogen. Further, in a computational study designed to probe the effect of a σ-donor, vs. a π-acid, ancillary ligand in $RuHCl(L)(P^iPr_3)_2$ model systems (L = CO, PH_3), a systematically more stable reaction profile emerged for the PH_3 species.[28] That is, this study revealed no electronic basis for increased hydrogenation activity on the part of the CO complex.

Given the apparent contradiction between these findings and the tandem catalysis data in the presence of methanol, a systematic experimental study was undertaken to compare the hydrogenation activity of the isolated, well-defined dihydrogen and carbonyl complexes. The complexes examined are those accessible from the first- and second-generation Grubbs catalysts, viz. $RuHCl(H_2)(L)(PCy_3)$ (**Ru-6**) and $RuHCl(CO)(L)(PCy_3)$ (**Ru-7**). This Chapter describes the synthesis of the previously unreported **Ru-6b**, and the higher hydrogenation efficiency of the carbonyl catalysts relative to their dihydrogen analogues. Finally, it demonstrates that this effect originates in the longer lifetimes of the CO complexes, rather than their higher reactivity.

2.2 Results and Discussion

*2.2.1 Synthesis of $RuHCl(H_2)LL'$ complexes **Ru-6**.*

We recently reported a clean, high-yield route to the hydridocarbonyl complexes **Ru-7**, in which $RuHCl(CO)(PPh_3)_3$ **Ru-8** is warmed with PCy_3 in benzene.[29] The success of this approach led us to attempt synthesis of **Ru-6a** by the analogous reaction of $RuHCl(PPh_3)_3$ **Ru-9**. These efforts were thwarted, however, by the poor solubility of **Ru-9** in aromatic solvents, which resulted in only partial conversion to $RuHCl(PCy_3)(PPh_3)_2$ **Ru-10** (30% of

the soluble portion, and an undetermined amount of the suspended material; Scheme 2.2) over 24 h at room temperature. Complete conversion, moreover, was hindered by the onset of product decomposition on longer reaction, while use of methylene chloride, in which **Ru-9** is soluble, is precluded by the susceptibility of the basic alkylphosphine to chlorination by this solvent. We therefore prepared **Ru-6a** by existing methods, involving hydrogenolysis of **Ru-1a**[9] or ligand exchange[30] of $[RuCl_2(COD)]_n$ with PCy_3 (in the latter synthesis, we used isopropanol as a convenient alternative to the original *sec*-butanol solvent,[30] and higher pressures of H_2).

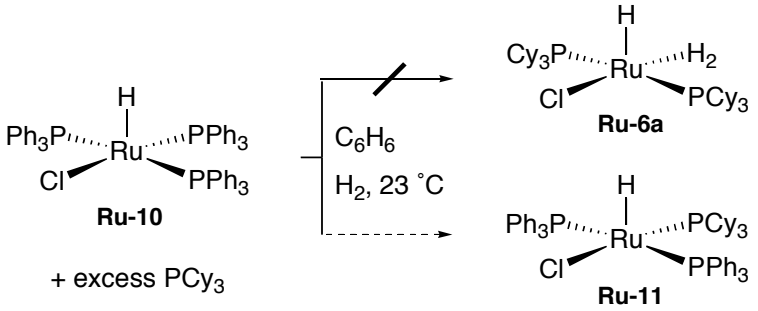

Scheme 2.2. Attempted synthesis of **Ru-6a**. Dashed arrow indicates incomplete reaction: for details, see text.

Leitner and coworkers prepared dihydride complex $Ru(H)_2(H_2)_2(IMes)(PCy_3)$ **Ru-11b** by ligand exchange of $Ru(H)_2(H_2)_2(PCy_3)_2$ **Ru-11a** with IMes at 55 ˚C under H_2.[31] The room-temperature reaction did not yield product. We obtained $RuHCl(H_2)(IMes)(PCy_3)$ **Ru-6b** by the corresponding reaction of **Ru-6a** under argon: in this case, reaction was complete within 2 h at 23 ˚C (Equation 2.1). No products other than **Ru-6b** and free PCy_3 were evident by NMR analysis, and the 1:1 ratio between the signals for free and bound PCy_3 confirmed clean formation of **Ru-6b** (i.e. free of paramagnetic byproducts; see below). Extraction of

the free phosphine with hexanes enabled isolation of clean **Ru-6b** in ca. 70% yield. Its identity is supported by spectroscopic and elemental analysis.

(2.1)

The NMR features for **Ru-6b** correspond well with those for **Ru-6a** (Table 2.1). Thus, a $^{31}P\{^{1}H\}$ NMR singlet appears at 56.4 ppm, and the broad singlet due to the hydride/dihydrogen ligands at –16.44 ppm. The $T_{1(min)}$ value for the latter signal, 36.6 ms in C_7D_8 (253K, 300 MHz), corresponds to a H-H distance of 1.03 Å, assuming a fast-spinning H_2 ligand.[32] Both the breadth of this signal, and its comparatively long relaxation time, are characteristic of η^2-H_2 perturbed by interaction with cis-hydride.[32] In comparison, a value of ca. 30 ms was reported for **Ru-6a** at 243 K and 250 MHz.[33] Exchange between classical and nonclassical hydrides occurs with a typical barrier of ca. 10-13 kcal/mol.[34] The averaged NMR signal for these ligands in **Ru-6b** appears ca. 11 ppm downfield from the -27.6 ppm location of the doublet due to the unperturbed hydride in dinitrogen analogue **Ru-12a** (the latter complex is discussed in greater detail below). Well-resolved singlets appear for the IMes methyl, aromatic, and =C*H*N groups for **Ru-6b**, integration of which against the H/H_2 singlet is consistent with the proposed structure.

Table 2.1. Key NMR data for Ru-hydride complexes relevant to this work (Ar, 298 K).

Complex	Solvent	δ_P (ppm)	δ_H (ppm)	Ref.
$RuHCl(H_2)(PCy_3)_2$ **Ru-6a**[a]	C_6D_6	54.2 (s)	–16.3 (br s)[b]	[9,33]
	CD_2Cl_2	52.8 (s)	–16.93 (br s)[b,c]	this work
$RuHCl(N_2)(PCy_3)_2$ **Ru-12a**	C_6D_6	43.7 (s)	–27.26 (t, $^2J_{HP}$ = 18 Hz)	[35]
$RuHCl(H_2)(IMes)(PCy_3)$ **Ru-6b**	C_6D_6	56.4 (s)	–16.44 (br s)[b]	this work
$RuHCl(N_2)(IMes)(PCy_3)$ **Ru-12b**	C_6D_6	45.1 (s)	–27.63 (d, $^2J_{HP}$ = 21 Hz)	this work
$RuHCl(CO)(PCy_3)_2$ **Ru-7a**[a]	C_6D_6	46.9 (s)	–24.21 (t, $^2J_{HP}$ = 18 Hz)	[29]
$RuHCl(CO)(IMes)(PCy_3)$ **Ru-7b**	C_6D_6	47.8 (s)	–24.82 (d, $^2J_{HP}$ = 21 Hz)	[29]
$Ru(H)_2Cl_2(PCy_3)_2$ **Ru-5**	C_6D_6[a]	91.3 (s)	–12.0 (t, $^2J_{HP}$ = 32 Hz)	[9]
	CD_2Cl_2	91.3 (s)	–12.39 (t, $^2J_{HP}$ = 32 Hz)	[9,36]

[a] In C_6D_6, the $^{31}P\{^1H\}$ NMR singlet for $Ru(H_2)Cl_2(PCy_3)_2$ **Ru-5'** is coincident with that for **Ru-6a**, but is accompanied by a singlet for the Ru(IV) tautomer **Ru-5** (ratio 1:2).[9] The corresponding hydride signals appear at –16.2 ppm (br s, **Ru-5'**) and –12.0 ppm (t, $^2J_{HP}$ = 32 Hz, **Ru-5**). In CD_2Cl_2, only **Ru-5** is present. [b] The hydride and dihydrogen signals for **Ru-6** appear as a single broad peak integrating to 3H. [c] A chemical shift of –16.8 (br t, $^2J_{HP}$ = 11 Hz) was originally reported for **Ru-6a** in CD_2Cl_2 (250 MHz).[33] The difference may reflect the presence of H_2 in the literature report.

*2.2.2 Catalytic Activity of **Ru-6** vs. **Ru-7**.*

Hydrogenation studies focused on the substrates shown in Chart 2.1. In a preliminary assessment of the relative hydrogenation activity of catalysts **Ru-6** and **Ru-7**, we established their baseline activity toward styrene (**S1**) at 23 °C. The duration of these experiments was normalized to that required for quantitative formation of ethylbenzene by the most reactive catalyst, **Ru-7a** (Figure 2.1a). The lower activity of the IMes derivative **Ru-7b** at room temperature, vs. its "first-generation" analogue **Ru-7a**, has precedent;[37] the data for **Ru-6** indicate that this trend is retained for the H_2 complexes. We attribute the drop in activity to the low lability of PR_3 trans to an NHC ligand,[38,39] originally described by the Grubbs group in a seminal paper on olefin metathesis.[38] Within both the bis(PCy_3) and the IMes-PCy_3 series, the activity of the CO complexes **Ru-7** is consistently greater than that of their dihydrogen analogues **Ru-6**. The implications in terms of process efficiency are manifested most explicitly in the time profile for complete hydrogenation of styrene at a catalyst

loading of 0.1 mol % (Figure 2.1b). Reduction by **Ru-7a** under the conditions specified is complete at 1.5 h, while quantitative reduction via **Ru-6a** requires 12 h.

We also evaluated the tendency of the more reactive catalysts **Ru-6a**/**Ru-7a** to promote competing isomerization, using allylbenzene **S2** as substrate. Hydridocarbonyl **Ru-7a** proves considerably more reactive than its H_2 analogue **Ru-6a** in both reduction and isomerization (Figure 2.1a). Of note, hydrogenation is ca. 30 times faster than isomerization for **Ru-6a**, but only 15 times faster for **Ru-7a**, suggesting that the higher activity of the latter may come at the price of reduced discrimination.

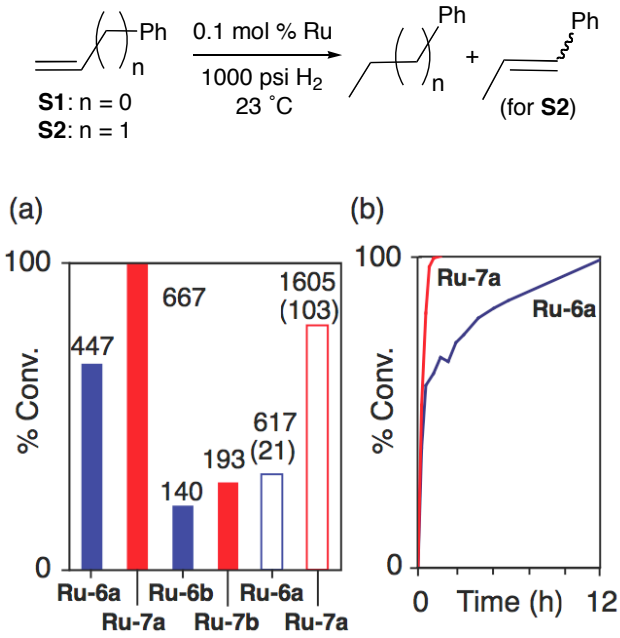

Figure 2.1. (a) Relative catalyst performance in hydrogenation of styrene (**S1**, 1.5 h, filled bars) and allylbenzene (**S2**, 0.5 h, unfilled), showing turnover frequencies (TOF; mol product • mol catalyst^{-1} h^{-1}), with isomerization TOF in parentheses. (b) Time for complete hydrogenation of styrene by **Ru-6a** vs. **Ru-7a**. All reactions carried out in benzene at 23 ˚C under 1000 psi H_2, using 0.1 mol% Ru and 1.0 M styrene or 0.7 M allylbenzene. Average of three trials (± 3%).

To assess the generality of the trends indicated in Figure 2.1, we turned to hydrogenation of several substrates of broader interest, which present successively greater challenges to reduction (Chart 2.1; Table 2.2).

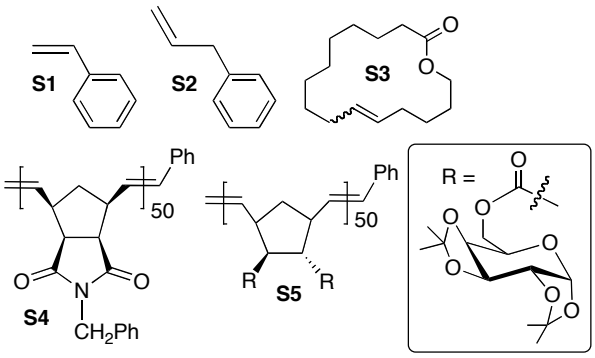

Chart 2.1. Substrates employed in hydrogenation studies.

Reduction of lactone **S3** affords the musk-odoured perfume Exaltolide, while the reduced ROMP polymers are of interest for their relevance to well-defined polymer platforms for further functionalization (**S4**),[40] or for tissue engineering (**S5**).[41] Other hydrogenated ROMP polynorbornenes find applications as engineering thermoplastics[42,43] and fluoropolymers,[44] as polymer supports in synthetic applications,[45,46] as nanoporous materials,[47] and as gradient polymers with potentially programmable thermal properties.[48] We recently described tandem ROMP-hydrogenation of **S5** via first, second, and third-generation Grubbs catalysts, using protocols that generate **Ru-6** and, in the presence of methanol, **Ru-7**.[8]

Reduction of these substrates in CH_2Cl_2 follows the trend established above, with the CO complexes **Ru-7** outperforming their H_2 analogues **Ru-6** in all cases. As well, the "first-generation" catalysts (series **a**) generally outperform the second-generation catalysts (series **b**) in reduction of all substrates, with the exception of neoglycopolymer **S5**. The challenging nature of **S5** is illustrated by the low turnover numbers found even at 0.5 mol % Ru. While

the CO catalysts remain more effective than their H_2 analogues for reduction of this substrate, maximum conversions are found for the IMes derivative **Ru-7b**, rather than the bis-PCy_3 complex **Ru-7a**. We attribute this to the significant steric bulk present in **S5**, arising from its polymeric nature, the *endo*/*exo* disubstitution of the repeat unit, the bulk of the galactose groups, and the additional steric pressure exerted by the acetal protecting groups. The unexpectedly higher activity of the IMes catalyst **Ru-6b** may reflect the essentially two-dimensional steric bulk of the *N*-heterocyclic carbene, relative to PCy_3; we presume that one phosphine ligand is replaced by olefin during the hydrogenation cycle as for **Ru-6a**; vide supra.

Table 2.2. Relative efficiency of dihydrogen and carbonyl catalysts in hydrogenation of various olefinic substrates.[a]

Substrate	mol % Ru	Time (h)	Cat.	TOF (h^{-1})	Conv. (%)
S1	0.1	0.5	**Ru-6a**	1260	63
			Ru-7a	1840	92
			Ru-6b	540	27
			Ru-7b	1520	76
S3	0.1	1	**Ru-6a**	830	83
			Ru-7a	960	96
			Ru-6b	530	53
			Ru-7b	810	81
S4	0.1	1	**Ru-6a**	310	31
			Ru-7a	660	66
			Ru-6b	310	31
			Ru-7b	510	51
S5	0.5[b]	6	**Ru-6a**	3	10
			Ru-7a	7	21
			Ru-6b	7	20
			Ru-7b	17	50

[a] Conditions: 1000 psi H_2, refluxing CH_2Cl_2 (except for **S1**: 23 °C); conversions measured by GC-FID or ^1H NMR analysis; data represent average of two independent runs (±3%). [b] Conversions <10% at 0.1 mol % Ru.

A more detailed study focused on the effect of solvent and additives on hydrogenation of lactone **S3** (Figure 2.2). Consistently higher conversions are found for reduction in methylene chloride, relative to benzene: the reactivity trends in both solvents follow the norm established above. Addition of base to the reactions in CH_2Cl_2 improves activity slightly, particularly for the IMes derivatives, suggesting some competing chlorination of the hydride catalyst by the chlorocarbon solvent (see later). Finally, the difference in activity between the H_2 and CO series of catalysts is minimized in the presence of MeOH, in which the dihydrogen catalysts undergo carbonylation, as discussed above.

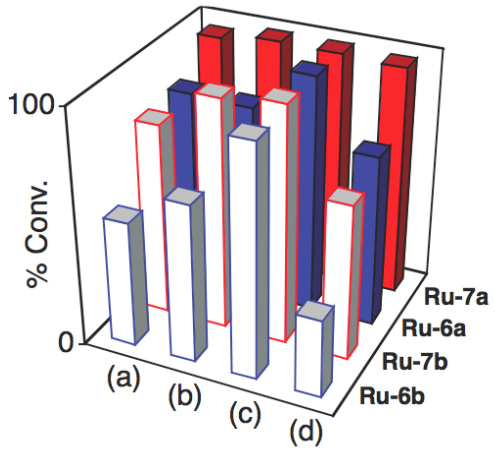

Figure 2.2. Effect of solvent and additives on hydrogenation of lactone **S3** via catalysts **Ru-6** and **Ru-7**: (a) CH_2Cl_2 solvent without additives (Table 2.2); (b) CH_2Cl_2, 3 equiv NEt_3; (c) 20 MeOH : 80 CH_2Cl_2, 3 equiv NEt_3; (d) C_6H_6 without additives. Conditions: 1000 psi H_2, 0.1 mol% Ru, bath temperature 55 °C, 1 h reaction time. Data represent average of two independent runs (±3%).

*2.2.3 Relative stability of **Ru-6** and **Ru-7**.*

The data above demonstrate that the carbonyl complexes **Ru-7** are more effective hydrogenation catalysts than their dihydrogen analogues **Ru-6**. Given the similarly low bulk of the CO and H_2 ligands, we discount a steric origin for this higher activity. However, the

DFT study described in Section 2.1, which predicts a higher-energy reaction profile for hydrogenation via $RuHCl(L)(PR_3)_2$ species in which L is CO, vs. the σ-donor PH_3, implies that the π-acidity of the CO ligand should be detrimental to hydrogenation activity.[28] We speculated that the higher hydrogenation efficiency of **Ru-7** might be due to an improved stability relative to **Ru-6**, and hence longer catalyst lifetime. This would translate into higher catalyst concentrations over the timescale of hydrogenation.

This hypothesis stemmed in part from the high reactivity characteristic of the related, classic H_2 complex $Ru(H)_2(H_2)_2(PCy_3)_2$ **Ru-11a**, a function of the electron-rich character of the metal and the lability of the dihydrogen ligand(s).[49] In **Ru-11a** and cyclohexylphosphine complexes, this reactivity is manifested in C-H bond activation even at ambient temperatures.[49-52] Of interest, Leitner and coworkers have reported that $Ru(H)_2(H_2)_2(IMes)(PCy_3)$ is more reactive than **Ru-11a** in C-H activation chemistry.[31] While this was of value in enabling intermolecular C-H bond activation at room temperature, it may also signify a greater susceptibility to deactivation via *intra*molecular bond activation.

The ease of H_2-N_2 exchange can afford a preliminary indicator of such lability.[32a] The relative robustness of the Ru-H_2 interaction in **Ru-6a** is suggested by the early comment that this complex resists exchange with 1 atm N_2 at room temperature.[33] We find that exchange does occur to afford **Ru-12a**, but slowly (5-15% after 24 h; **Ru-12a** identified on the basis of the reported chemical shifts[35] of –27.26 and 43.7 ppm for the hydride and ^{31}P nuclei, respectively; Table 2.1). The higher lability of the dihydrogen ligand in **Ru-6b** is suggested by observation of ca. 70% conversion to $RuHCl(N_2)(IMes)(PCy_3)$ **Ru-12b** after 24 h under N_2. Complex **Ru-12b** is identified from its well-resolved hydride doublet at –27.63 ppm (ca.

11 ppm upfield of the averaged hydride/dihydrogen signal for **Ru-6b**), which correlates in HMBC experiments with a new $^{31}P\{^{1}H\}$ NMR singlet at 45.1 ppm. These chemical shifts agree well with the values for **Ru-12a** above.

In related cyclohexylphosphine complexes, loss of a stabilizing H_2 or N_2 ligand is often the entry-point to extensive intramolecular bond activation, as noted above.[49-53] Under argon at 23 ˚C, neither **Ru-6** or **Ru-7** shows evidence of bond activation in C_6D_6 after 24 h, as judged by integration of their $^{31}P\{^{1}H\}$ NMR signals against an internal standard. (Use of an internal standard in these experiments is important, as the potential paramagnetism of the product(s), and the consequent absence of an NMR "marker", means that losses can otherwise easily go unnoticed). In CH_2Cl_2, however, **Ru-6a** undergoes partial conversion to the known[37] Ru(IV) complex $Ru(H)_2Cl_2(PCy_3)_2$ **Ru-5**, with a ca. 1:1 ratio of **Ru-6a**: **Ru-5** after 16 h. We earlier described the low catalytic activity of **Ru-5**.[7] Its identity was confirmed in the present experiment by HMBC correlation of the $^{31}P\{^{1}H\}$ NMR singlet at 91.3 ppm with the expected hydride triplet for **Ru-5** at –12.39 (t, $^{2}J_{HP}$ = 32 Hz; CD_2Cl_2). Chlorination of **Ru-6a** is consistent with earlier findings from the Toulouse group, which described the successive conversion of $Ru(H)_2(H_2)_2(PCy_3)_2$ **Ru-11a** to **Ru-6a** and **Ru-5** in Freons (mixtures of $CDCl_3$, $CDFCl_2$, and CDF_2Cl) and in neat $CDCl_3$.[36] In sharp contrast, **Ru-6b** undergoes complete decomposition to paramagnetic products in CH_2Cl_2 over 16 h, while **Ru-7** is stable.

In a more direct probe of the relative susceptibility of **Ru-6** and **Ru-7** to decomposition under conditions related to catalysis, we subjected all four complexes to thermolysis in benzene and methylene chloride under 1 atm H_2 (Figure 2.3). Again, the high stability of the carbonyl complexes is notable, little or no decomposition being evident in either solvent.

The dihydrogen complexes are less robust: after just one hour at 55 ˚C in benzene, the integration due to **Ru-6a** decreases by ca. 30% (Figure 2.3a). New $^{31}P\{^{1}H\}$ NMR signals are present for free PCy_3 and an unidentified species at ca. 63 ppm (6%), but the balance of material is either paramagnetic or devoid of ^{31}P nuclei. For **Ru-6b**, ca. 60% decomposition occurs over this time, and no new $^{31}P\{^{1}H\}$ NMR signals are apparent (Figure 2.4).

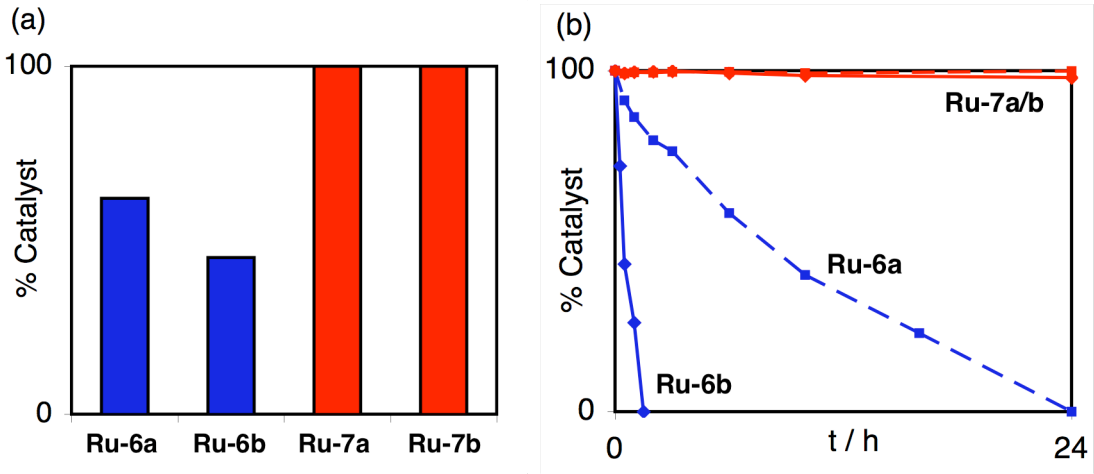

Figure 2.3. Thermolytic stability of **Ru-6** and **Ru-7** under 1 atm H_2, as indicated by $^{31}P\{^{1}H\}$ NMR integration vs. $Ph_3P{=}O$ as internal standard. (a) After 1 h in C_6D_6 at 55 ˚C. (b) In refluxing CH_2Cl_2. Dashed lines, L = PCy_3; solid lines, L = IMes. Data represent average of two independent runs (±3%).

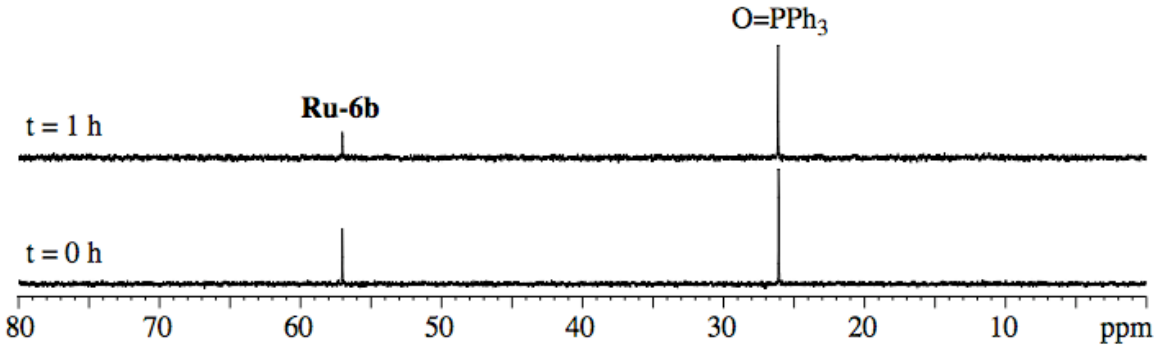

Figure 2.4. $^{31}P\{^{1}H\}$ NMR spectra for thermolysis of $RuHCl(H_2)(IMes)(PCy_3)$ **Ru-6b**. Conditions: C_6D_6, 55 ˚C.

In refluxing CH_2Cl_2, **Ru-6a** is completely consumed after 24 h (Figure 2.3b), and **Ru-5** is the only ^{31}P-containing product observed (70%). The coordinative saturation of **Ru-5** appears to confer some protection against more extensive decomposition. When formation of **Ru-5** is suppressed by repeating this reaction in the presence of NEt_3, the only species observed by $^{31}P\{^1H\}$ NMR is an unidentified product of singlet multiplicity at 36 ppm, which integrates to ca. 40%. Consistent with the generally greater vulnerability described above, **Ru-6b** undergoes near-total conversion to paramagnetic species within 2.5 h in refluxing CH_2Cl_2 (Figure 2.3b). Unexpectedly, however, a small signal for **Ru-6a** is observed within 15 min, which disappears over the next 2 h. A very small signal at 91 ppm (<5% integration, **Ru-5**) is also observable. Formation of **Ru-6a** signifies that **Ru-6b** undergoes some disproportionation under these conditions, as also reported by Mol for thermolysis of related benzylidene in MeOH at 80 °C.[12] Thermolysis of **Ru-6a** shows good first-order kinetics (Figure 2.5); fewer data-points are obtained for **Ru-6b** (k = 0.089 s^{-1} and 1.4 s^{-1}, respectively).

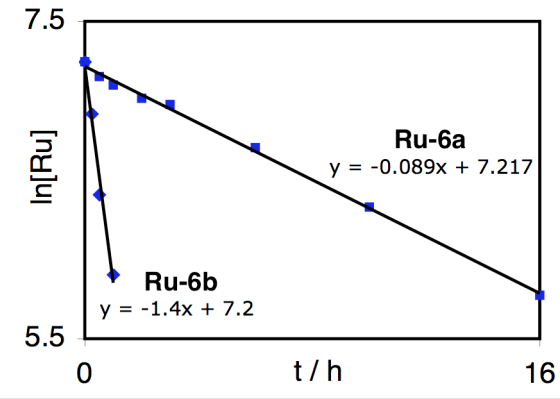

Figure 2.5. First-order plot for thermolysis of **Ru-6a/b**.

2.3 Conclusions

The foregoing describes a clean, high-yield synthetic route to $RuHCl(H_2)(IMes)(PCy_3)$ **Ru-6b** by ligand exchange reactions of $RuHCl(H_2)(PCy_3)_2$ **Ru-6a**, though attempts to develop a route to **Ru-6a** itself from $RuHCl(PPh_3)_3$ **Ru-9** were unsuccessful. Comparison of the olefin hydrogenation activity of **Ru-6** with the corresponding carbonyl complexes **Ru-7** demonstrates that replacing the H_2 ligand by CO improves hydrogenation efficiency. Thermolysis experiments suggest that this reflects a positive influence on catalyst lifetime associated with the low lability of the CO ligand, as complexes **Ru-7** are much more stable than their dihydrogen analogues **Ru-6**. The π-acidity of the carbonyl group may also play a part: while this will hamper catalyst initiation via ligand loss, as well as oxidative addition of H_2, it will also decrease the susceptibility of the complex to nucleophilic attack. The significantly greater robustness of the CO complexes appears to compensate for their lower activity, by maintaining higher concentrations of active catalyst over the timescale of hydrogenation.

2.4 Experimental

2.4.1 General Procedures.

Reactions were carried out at room temperature (23 ˚C) under argon, using standard Schlenk or glovebox techniques, unless otherwise stated. Dry, oxygen-free solvents were obtained using a Glass Contour solvent purification system, and stored over Linde 4Å molecular sieves. $CDCl_3$ and C_6D_6 were degassed by consecutive freeze/pump/thaw cycles and dried over activated sieves (Linde 4Å). $[RuCl_2(COD)]_n$,[54] $RuHCl(PPh_3)_3$ **Ru-9**,[55] $RuHCl(CO)(PCy_3)_2$ **Ru-7a**,[29] $RuHCl(CO)(IMes)(PCy_3)$ **Ru-7b**,[29] IMes,[56] and substrates **S3**,[57] **S4**,[8] and **S5**[8] were prepared according to literature methods. H_2 (UHP grade) was obtained

from BOC Gases and used as received. Styrene and allylbenzene (Aldrich) were distilled from CaH_2 under vacuum, and stored at -35 ˚C under Ar in the dark. Tetrahydronaphthalene was distilled from Na metal, freeze-pump-thaw degassed, and stored over Linde 4Å molecular sieves under Ar. Ethylbenzene (Aldrich) and PCy_3 (Strem) were used as received. NMR spectra were recorded on a Bruker Avance 300 or Avance 500 spectrometer at 298 K, unless otherwise specified. ^1H and ^{13}C NMR spectra were referenced to the residual proton and carbon signals of the deuterated solvent. Peaks are reported in ppm, relative to TMS (^1H, ^{13}C) or 85% H_3PO_4 (^{31}P) at 0 ppm. IR spectra were measured on a Bomem MB100 IR spectrometer. Microanalysis was carried out by Guelph Chemical Laboratories Ltd., Guelph, Ontario.

2.4.2 Synthesis of $RuHCl(H_2)(PCy_3)_2$ ***Ru-6a***.

In a modification of a literature method,[30] a suspension consisting of $[RuCl_2(COD)]_n$ (400 mg, 1.43 mmol), PCy_3 (850 mg, 3.0 mmol), NEt_3 (199 mL, 1.43 mmol) and 2-propanol (20 mL) was stirred at 200 psi H_2 and 80 ˚C for 40 h. The resulting orange precipitate was filtered off, washed with EtOH (3 × 3 mL) then cold hexanes (5 × 4 mL), and dissolved in 15 mL CH_2Cl_2 under H_2. A bright orange solid was obtained by filtering through Celite to remove a dark, insoluble impurity, concentrating to 0.2 mL and adding 5 mL cold hexanes under 1 atm H_2. The precipitate was filtered off, washed with hexanes (3 × 3 mL), and reprecipitated from a minimum volume of toluene by adding hexanes under H_2 and chilling at –35 ˚C for an hour, then dried under vacuum. Yield: 0.511 g (73%). $^{31}P\{^1H\}$ NMR (C_6D_6, Ar): δ 54.2 (s). ^1H NMR (C_6D_6, Ar): δ 2.3–0.9 (m, 66 H, Cy), –16.3 (br s, 3H, Ru*H*(H_2). Under N_2, ca. 10% $RuHCl(N_2)(PCy_3)_2$ **Ru-12a** is observed: δ_P 43.7 (s).[35] δ_H –27.26 (t, 1H, Ru*H*, $^2J_{HP}$ = 18.3 Hz).

2.4.3 Synthesis of RuHCl(H_2)(IMes)(PCy_3) ***Ru-6b***.

Solid IMes (46 mg, 0.15 mmol) was added to orange RuHCl(H_2)(PCy_3)$_2$ **Ru-6a** (100 mg, 0.142 mmol) in 5 mL benzene. No color change is apparent, but $^{31}P\{^1H\}$ NMR monitoring indicated complete reaction at 1.5 h at 23 ˚C: only signals for free phosphine and **Ru-6b** (integration 1:1) were observed in an aliquot removed at this time. The solvent was stripped off, and hexanes (2 mL) added. An orange powder was obtained on cooling to –35 ˚C overnight. This was filtered off, washed with cold hexanes (3 × 3 mL) and dried under vacuum. Yield 73 mg (71%; limited by partial solubility in hexanes). $^{31}P\{^1H\}$ NMR (C_6D_6, Ar): 56.4 (s, PCy_3). ^1H NMR: 6.82 (s, 4H, Mes *m*-C*H*), 6.16 (s, 2H, NC*H*=C*H*N), 2.37 (s, 12H, *o*-CH_3), 2.14 (s, 6H, *p*-CH_3), 1.88-1.10 (m, 33H, PCy_3), –16.44 (s, 3H, Ru*H*(*H_2*)). Hydride $T_{1(min)}$: 36.6 ms (C_7D_8, 253 K, 300 MHz; corresponds to a H-H distance of 1.03 Å). $^{13}C\{^1H\}$ NMR: 196.0 (d, $^2J_{CP}$ = 100 Hz, N*C*N), 138.1 (s, Mes *p*-*C*), 137.1 (s, Mes *i*-*C*), 136.5 (s, Mes *o*-*C*), 129.1 (s, Mes *m*-*C*), 121.4 (s, N*C*=*C*N), 35.3 (d, $^2J_{CP}$ = 17 Hz, Cy), 30.6 (d, $^2J_{CP}$ = 2 Hz, Cy), 28.0 (d, $^2J_{CP}$ = 10 Hz, Cy), 26.9 (s, Cy), 21.1 (s, *p*-*C*H_3), 19.0 (s, *o*-*C*H_3). IR (Nujol): ν(Ru-H) 2047 cm^{-1}. Anal. Calcd. for $C_{39}H_{60}ClN_2PRu$: C, 64.66 %; H, 8.35 %; N, 3.87 %. Found: C, 64.63 %; H, 7.98 %; N, 3.70 %. NMR spectra under N_2 (24 h) show ca. 70% RuHCl(N_2)(IMes)(PCy_3) **Ru-12b**: δ_P 45.1 (s, PCy_3). δ_H –27.63 ppm (d, Ru*H*, $^2J_{HP}$ = 21.4 Hz).

2.4.4 Attempted Synthesis of RuHCl(H_2)(PCy_3)$_2$ ***Ru-6a*** *from RuHCl(PPh_3)$_3$* ***Ru-9****: partial formation of RuHCl(PCy_3)(PPh_3)$_2$* ***Ru-10***.

Solid PCy_3 (31 mg, 0.11 mmol) was added to purple **Ru-9** (50 mg, 0.054 mmol) in 10 mL C_6H_6, and H_2 was bubbled through the suspension. No color change was observed after 3 h, but integration of the ^1H NMR signals against the quartet for **Ru-9** at –17.5 ppm indicates

70% unreacted **Ru-9** in the soluble portion. Complete conversion was hampered by competing decomposition of the product over a further 20 h reaction. $^{31}P\{^{1}H\}$ NMR for **Ru-10** (C_6D_6): 74.0 (d, $^{2}J_{PP}$ = 118 Hz, 2P, PPh_3), 28.9 (t, $^{2}J_{PP}$ = 118 Hz, 1P, PCy_3). Key ^{1}H NMR for **Ru-10** (C_6D_6): –18.1 (td, $^{2}J_{HP}$ = 29 and 18 Hz). ^{1}H-^{31}P HMBC correlations between the $^{31}P\{^{1}H\}$ NMR doublet at 74.0 ppm and the aromatic ^{1}H NMR signals support identification of **Ru-10** as a bis(PPh_3) complex.

2.4.5 Hydrogenation Reactions.

(a) Representative procedure for hydrogenation of molecular substrates. Solid $RuHCl(H_2)(PCy_3)_2$ **Ru-6a** (14 mg, 0.0198 mmol) was added to a glass-lined Parr autoclave containing a solution of styrene (2.083 g, 0.020 mol, 1.0 M) with 1,2,3,4-tetrahydronaphthalene (THN) as internal standard (1.322 g, 0.010 mol) in 20 mL C_6H_6 in the glovebox. The autoclave was sealed, removed from the drybox, purged with H_2, and pressurized to 1000 psi H_2 at 23 °C. Samples were analyzed by GC-FID. Kinetic runs on **S1** were monitored by removing 1 mL samples at set time intervals using the sampler tube. The first 0.5 mL was discarded; from the second half, a 5 mL aliquot was removed, diluted to 1.00 mL with CH_2Cl_2 and analyzed (GC-FID). Reactions of other substrates were carried out at a bath temperature of 55 °C. Reactions of **S3** were analyzed by GC-FID; of **S2**, by ^{1}H NMR.

(b) Representative procedure for hydrogenation of polymer substrates. A solution of **S4** (183 mg, 0.722 mmol, 1.0 M in CH_2Cl_2) with 1,3,5-trimethoxybenzene (51 mg, 0.30 mmol, 0.2 M in CH_2Cl_2) as internal standard was subjected to hydrogenation as above (1000 psi H_2, 55 °C). Following reaction, volatiles were removed under reduced pressure and the residues were dissolved in $CDCl_3$ for ^{1}H NMR analysis. Conversions were determined through

comparison of integrals between olefinic signals (**S4:** br m, 5.58 ppm) and the methoxy singlet of trimethoxybenzene (3.77 ppm). For **S5**, conversions were quantified by comparing the integrated intensity of the olefinic + galactopyranose C*H* signals at 5.60-5.30 ppm with the galactopyranose C^5 C*H* multiplet at 4.59 ppm.

*2.4.6 Thermolysis of **Ru-6** and **Ru-7**.*

In a representative procedure, a solution of **Ru-6a** (8 mg, 0.011 mmol) and $Ph_3P{=}O$ (4 mg, 0.014 mmol) was dissolved in CH_2Cl_2 (0.75 mL, with a 50 μL spike of C_6D_6 as deuterium lock for shimming) in a J. Young NMR tube. An initial $^{31}P\{^1H\}$ NMR spectrum was measured to establish the **Ru-6a**: $Ph_3P{=}O$ integration ratio at t_o. The NMR sample was then freeze-pump-thaw degassed, backfilled with H_2 (1 atm), and heated to 55 ˚C in an oil bath.

2.5 References.

(1) (a) Sheldon, R. A. *Green Chem. and Catalysis;* Wiley-VCH: Chichester, 2007. (b) Sheldon, R. A. *Green Chem.* **2007**, *9*, 1273-1283.
(2) Constable, D. J. C.; Dunn, P. J.; Hayler, J. D.; Humphrey, G. R.; Leazer, J. L., Jr.; Linderman, R. J.; Lorenz, K.; Manley, J.; Pearlman, B. A.; Wells, A.; Zaks, A.; Zhang, T. Y. *Green Chem.* **2007**, *9*, 411-420.
(3) Tandem catalysis originating in the Grubbs complexes has been reviewed: (a) Shindoh, N.; Takemoto, Y.; Takasu, K. *Chem. Eur. J.* **2009**, *15*, 12168-12179. (b) Wasilke, J.-C.; Obrey, S. J.; Baker, R. T.; Bazan, G. C. *Chem. Rev.* **2005**, *105*, 1001-1020. (c) Fogg, D. E.; dos Santos, E. N. *Coord. Chem. Rev.* **2004**, *248*, 2365-2379.
(4) Dragutan, V.; Dragutan, I.; Delaude, L.; Demonceau, A. *Coord. Chem. Rev.* **2007**, *251*, 765-794.
(5) (a) Schmidt, B. *Pure Appl. Chem.* **2006**, *78*, 469-476. (b) Schmidt, B. *Eur. J. Org. Chem.* **2004**, 1865-1880.
(6) Constable, D. J. C.; Jimenez-Gonzalez, C.; Henderson, R. K. *Org. Process Res. Dev.* **2007**, *11*, 133-137.
(7) Drouin, S. D.; Zamanian, F.; Fogg, D. E. *Organometallics* **2001**, *20*, 5495-5497.
(8) Camm, K. D.; Castro, N. M.; Liu, Y.; Czechura, P.; Snelgrove, J. L.; Fogg, D. E. *J. Am. Chem. Soc.* **2007**, *129*, 4168-4169.
(9) Drouin, S. D.; Yap, G. P. A.; Fogg, D. E. *Inorg. Chem.* **2000**, *39*, 5412-5414.
(10) Related advances in methodology by others: (a) McLain, S. J.; McCord, E. F.; Arthur, S. D.; Hauptman, E.; Feldman, J.; Nugent, W. A.; Johnson, L. K.; Mecking, S.; Brookhart, M. *Proc. PMSE* **1997**, *76*, 246. (b) Watson, M. D.; Wagener, K. B. *Macromolecules* **2000**, *33*, 3196-3201. (c) Bielawski, C. W.; Louie, J.; Grubbs, R. H. *J. Am. Chem. Soc.*, **2000**, *122*, 12872-12873. (d) Schmidt, B. *Chem. Commun.* **2004**, 742-743.
(11) Dinger, M. B.; Mol, J. C. *Organometallics* **2003**, *22*, 1089-1095.
(12) Dinger, M. B.; Mol, J. C. *Eur. J. Inorg. Chem.* **2003**, 2827-2833.
(13) Trnka, T. M.; Morgan, J. P.; Sanford, M. S.; Wilhelm, T. E.; Scholl, M.; Choi, T.-L.; Ding, S.; Day, M. W.; Grubbs, R. H. *J. Am. Chem. Soc.* **2003**, *125*, 2546-2558.
(14) Chaudret, B. N.; Cole-Hamilton, D. J.; Nohr, R. S.; Wilkinson, G. *J. Chem. Soc., Dalton Trans.* **1977**, 1546-1557.
(15) Jung, C. W.; Garrou, P. E. *Organometallics* **1982**, *1*, 658-666.
(16) Van der Sluys, L. S.; Kubas, G. J.; Caulton, K. G. *Organometallics* **1991**, *10*, 1033-1038.
(17) Chen, Y.-Z.; Chan, W. C.; Lau, C. P.; Chu, H. S.; Lee, H. L.; Jia, G. *Organometallics* **1997**, *16*, 1241-1246.
(18) Yi, C. S.; Lee, D. W.; He, Z.; Rheingold, A. L.; Lam, K.-C.; Concolino, T. E. *Organometallics* **2000**, *19*, 2909-2915.
(19) Yi, C. S.; Lee, D. W. *Organometallics* **1999**, *18*, 5152-5156.
(20) Mueller, L. A.; Dupont, J.; De Souza, R. F. *Macromol. Rapid Commun.* **1998**, *19*, 409-411.
(21) De Souza, R. F.; Rech, V.; Dupont, J. *Adv. Synth. Catal.* **2002**, *344*, 153-155.
(22) Martin, P.; McManus, N. T.; Rempel, G. L. *J. Mol. Catal. A* **1997**, *126*, 115-131.
(23) McManus, N. T.; Rempel, G. L. *J. Macromolecul. Sci. Rev. Macromol. Chem. Phys.* **1995**, *C35*, 239-285.

(24) For a study of **Ru-6a** in olefin silylation, see: (a) Lachaize, S.; Sabo-Etienne, S.; Donnadieu, B.; Chaudret, B. *Chem. Commun.* **2003**, 214-215; in dehydrogenative coupling of cyclic amines and alkenes, see: (b) Yi, C.S.; Yun, S.Y.; Guzei, I.A. *Organometallics* **2004**, *23*, 5392-5395. A DuPont patent also records its use in hydrogenation catalysis: (c) Beatty, R.P.; Paciello, R.A. U.S. Pat. 5,554,778, 1996.
(25) Clapham, S. E.; Hadzovic, A.; Morris, R. H. *Coord. Chem. Rev.* **2004**, *248*, 2201-2237.
(26) Burk, M. J. *Acc. Chem. Res.* **2000**, *33*, 363-372.
(27) (a) James, B.R. in *Comprehensive Organometallic Chemistry,* Wilkinson, G., Ed. Pergamon: New York, 1982; Vol. 8, Chapter 51, and references therein. (b) James, B.R., *Homogeneous Hydrogenation*. Wiley: Toronto, 1973.
(28) Rowley, C. N.; Foucault, H. M.; Woo, T. K.; Fogg, D. E. *Organometallics* **2008**, *27*, 1661-1663.
(29) Beach, N. J.; Dharmasena, U. L.; Drouin, S. D.; Fogg, D. E. *Adv. Synth. Catal.* **2008**, *350*, 773-777.
(30) Wilhelm, T. E.; Belderrain, T. R.; Brown, S. N.; Grubbs, R. H. *Organometallics* **1997**, *16*, 3867-3869.
(31) Giunta, D.; Hoelscher, M.; Lehmann, C. W.; Mynott, R.; Wirtz, C.; Leitner, W. *Adv. Synth. Catal.* **2003**, *345*, 1139-1145.
(32) (a) Jessop, P.G.; Morris, R.H. *Coord. Chem. Rev.* **1992**, *121*, 155-284. (b) Kubas, G.J., *Metal Dihydrogen and σ-Bond Complexes*. Kluwer/Plenum: Dordrecht, 2001.
(33) Christ, M. L.; Sabo-Etienne, S.; Chaudret, B. *Organometallics* **1994**, *13*, 3800-3804.
(34) Heinekey, D. M.; Mellows, H.; Pratum, T. *J. Am. Chem. Soc.* **1990**, *112*, 920-929.
(35) Oliván, M.; Caulton, K. G. *Inorg. Chem.* **1999**, *38*, 566-570.
(36) Rodriguez, V.; Sabo-Etienne, S.; Chaudret, B.; Thoburn, J.; Ulrich, S.; Limbach, H.-H.; Eckert, J.; Barthelat, J.-C.; Hussein, K.; Marsden, C. J. *Inorg. Chem.* **1998**, *37*, 3475-3485.
(37) Lee, H. M.; Smith, D. C., Jr.; He, Z.; Stevens, E. D.; Yi, C. S.; Nolan, S. P. *Organometallics* **2001**, *20*, 794-797.
(38) Sanford, M. S.; Love, J. A.; Grubbs, R. H. *J. Am. Chem. Soc.* **2001**, *123*, 6543-6554.
(39) Getty, K.; Delgado-Jaime, M. U.; Kennepohl, P. *J. Am. Chem. Soc.* **2007**, *129*, 15774-15776.
(40) Strong, L. E.; Kiessling, L. L. *J. Am. Chem. Soc.* **1999**, *121*, 6193-6196.
(41) Liu, Y.; Fogg, D.; Griffith, M. US Pat. 11/442,755, 2006.
(42) Mulhaupt, R. *Macromol. Chem. Phys.* **2003**, *204*, 289-327.
(43) Hatjopoulos, J. D.; Register, R. A. *Macromolecules* **2005**, *38*, 10320-10322.
(44) Feast, W. J.; Gimeno, M.; Khosravi, E. *J. Mol. Catal. A* **2004**, *213*, 9-14.
(45) Lee, B. S.; Mahajan, S.; Clapham, B.; Janda, K. D. *J. Org. Chem.* **2004**, *69*, 3319-3329.
(46) Barrett, A. G. M.; Hopkins, B. T.; Koebberling, J. *Chem. Rev.* **2002**, *102*, 3301-3323.
(47) Connor, E. F.; Sundberg, L. K.; Kim, H.-C.; Cornelissen, J. J.; Magbitang, T.; Rice, P. M.; Lee, V. Y.; Hawker, C. J.; Volksen, W.; Hedrick, J. L.; Miller, R. D. *Angew. Chem., Int. Ed.* **2003**, *42*, 3785-3788.
(48) Dettmer, C. M.; Gray, M. K.; Torkelson, J. M.; Nguyen, S. T. *Macromolecules* **2004**, *37*, 5504-5512.
(49) Sabo-Etienne, S.; Chaudret, B. *Coord. Chem. Rev.* **1998**, *178-180*, 381-407.
(50) Borowski, A. F.; Sabo-Etienne, S.; Christ, M. L.; Donnadieu, B.; Chaudret, B. *Organometallics* **1996**, *15*, 1427-1434.
(51) Christ, M. L.; Sabo-Etienne, S.; Chaudret, B. *Organometallics* **1995**, *14*, 1082-1084.

(52) Leitner, W.; Six, C. *Chem. Ber.* **1997**, *130*, 555-558.
(53) Amoroso, D.; Yap, G. P. A.; Fogg, D. E. *Can. J. Chem.* **2001**, *79*, 958-963.
(54) Genet, J. P.; Pinel, C.; Ratovelomanana-Vidal, V.; Mallart, S.; Pfister, X.; Cano De Andrade, M. C.; Laffitte, J. A. *Tetrahedron: Asymm.* **1994**, *5*, 665-674.
(55) Schunn, R. A.; Wonchoba, E. R.; Wilkinson, G. *Inorg. Synth.* **1971**, *13*, 131-134.
(56) Arduengo, A. J.; Krafczyk, R.; Schmutzler, R.; Craig, H. A.; Goerlich, J. R.; Marshall, W. J.; Unverzagt, M. *Tetrahedron* **1999**, *55*, 14523-14534.
(57) Fürstner, A.; Langemann, K. *Synthesis* **1997**, 792-803.

Chapter 3. Hydrogenolysis versus Methanolysis as a Means of Effecting Transformation of Grubbs Metathesis Catalysts into Ru Hydrides.*

3.1 Introduction.

Tandem ROMP-hydrogenation (ROMP = ring-opening metathesis polymerization) offers powerful routes to functionalized polyolefins inaccessible by direct polymerization of α-olefins.[1] Hydrogenation extends the range of applications for unsaturated ROMP polymers, reducing their susceptibility to oxidative, thermal, and chemical degradation.[2] The reduced materials are used in demanding applications ranging from tissue engineering[3] to separations science,[4-6] on-bead chemical synthesis,[7] and electronic and optical contexts,[8] among others; they also form the basis of specialty polymer products such as "perfect polyethylene",[9,10] alternating copolymers of ethylene with CO_2 or polar vinyl monomers,[11,12] and polymeric antioxidants.[13]

Hydrogenation of unsaturated polymers is much more challenging than hydrogenation of structurally similar molecular olefins, and the forcing conditions commonly required sets a high bar for catalyst lifetime and/or loadings, resulting in poor performance for highly active but fragile catalysts. Thus, limited efficiency has been reported in reduction of ROMP polymers via classical hydrogenation catalysts such as the Wilkinson or Crabtree catalysts ($RhCl(PPh_3)_3$ or $[Ir(COD)(PCy_3)(py)]PF_6$, respectively), or using supported palladium catalysts, despite their often outstanding performance in reduction of molecular olefins at relatively low H_2 pressures.[14] The best results to date are achieved via tandem ROMP-hydrogenation, which enables efficient reduction of ROMP polyoctenes at 50-60 °C and as

*This Chapter is adapted from: N.J. Beach, K.D. Camm, D.E. Fogg, *Organometallics*, **2010**, 28, 5450-5455.

little as 1 atm of H_2.[15] Hydrogenation of polynorbornenes, particularly those bearing bulky substituents, is considerably more demanding. Hydrogen pressures of up to 1000 psi can be required for efficient reduction at these moderate temperatures (high pressures are preferable to use of higher temperatures, which can trigger competitive thermal cross-linking of the unsaturated polymers).[15] Our group recently reported an advanced methodology for tandem ROMP-hydrogenation, which integrates the high activity and molecular weight precision of the "third-generation" Grubbs catalyst $RuCl_2(IMes)(py)_2(=CHPh)$ **Ru-1d** with the robust hydrogenation activity of $RuHCl(CO)(IMes)(PCy_3)$ **Ru-7b**.[3,16]

A number of methods have been successfully used to transform metathesis-active Ru-alkylidene complexes into hydrogenation catalysts.[12,15-25] In tandem ROMP-hydrogenation, the efficiency of the hydrogenation step depends both on the catalytic activity of the Ru-hydride species generated (see Chapter 2), and on the rate, selectivity, and efficiency of the alkylidene-to-hydride transformation (examined in this Chapter). Two protocols are compared. The first adopts the most recent methodologies developed by our group, and builds on the inorganic chemistry already established: that is, the early observation that reaction of the Grubbs catalyst **Ru-1a** with H_2 in CH_2Cl_2 affords solely dihydride $Ru(H)_2Cl_2(PCy_3)_2$ **Ru-5** (a feeble hydrogenation catalyst);[15] that addition of base enables clean conversion to $RuHCl(H_2)(L)(PCy_3)$ (L = PCy_3, **Ru-6a**; see Scheme 3.1);[17] and finally, that use of methanol as co-solvent affords $RuHCl(CO)(PCy_3)_2$ **Ru-7a**[17] (a more robust, productive hydrogenation catalyst; see Chapter 2).[26,27] The second method draws on subsequent work from the Mol and Grubbs groups, which described direct formation of complexes of type **Ru-7** (L = PCy_3, H_2IMes, H_2IPr; H_2IMes = *N*,*N*'-bis-(2,4,6-trimethylphenyl)imidazolin-2-ylidene, H_2IPr = *N*,*N*'-bis-(2,6-diisopropylphenyl)imidazolin-

2-ylidene) on treatment of the corresponding benzylidene catalysts with base and alcohol in the *absence* of H_2.[22,28-30] These and other[20,31-33] direct, H_2-free routes from **Ru-1** to **Ru-7** could be of keen interest for tandem metathesis-functionalization, as they would eliminate the risk of competing olefin hydrogenation.

The present study was thus aimed at improving our fundamental understanding of the non-metathetical reactivity of the Grubbs catalysts, by establishing the relative kinetics of hydrogenolysis vs. methanolysis. As well, motivated by the potential to further enhance efficiency in tandem catalysis reactions mediated by **Ru-1** and **Ru-7**, we wished to establish whether the **Ru-1→Ru-7** transformation is induced more efficiently by the two-step process – that is, by hydrogenolysis of the alkylidene **Ru-1**, followed by carbonylation of the hydrogenolysis product **Ru-6** (Scheme 3.1, paths (a) + (b)) – or by direct methanolysis of **Ru-1** (Scheme 3.1, path (c)). This Chapter presents a systematic comparison of rates, speciation, and efficiency for each of these reaction manifolds, utilizing both first-generation and second-generation Grubbs catalysts **Ru-1a/b** (L = PCy_3, IMes), and their hydride derivatives **Ru-6a/b**. Unanticipated differences in behaviour emerge, which highlight the need for "generation-specific" protocols for transforming **Ru-1**. It should be noted that this study excluded the commercially available H_2IMes complex **1b'**, because the latter was found to exhibit unexpectedly low activity in tandem ROMP-hydrogenation by Dr. Debbie Mitra of the Fogg group. The origins of this difference are not yet clear, and have not been systematically studied.

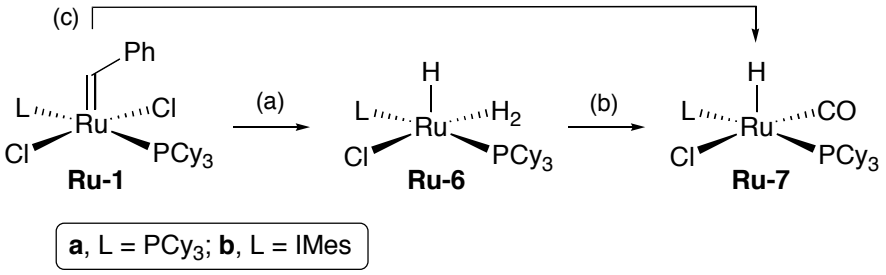

Scheme 3.1. Reaction manifolds targeted. (a) Hydrogenolysis of **Ru-1** (1000 psi H_2, 3 NEt_3, CH_2Cl_2). (b) Carbonylation of **Ru-6** (Ar, 3 NEt_3, 4:1 CH_2Cl_2-MeOH). (c) Methanolysis of **Ru-1** (conditions as in (b)). For byproducts, see text and Table 3.1. All reactions carried out at a bath temperature of 60 ˚C and a ruthenium concentration of 15 mM.

3.2 Results and Discussion.

In all experiments, reaction rates were assessed from the rate of disappearance of the $^{31}P\{^1H\}$ NMR signal for the ruthenium precursor relative to $Ph_3P{=}O$ as internal standard. Excellent agreement was found for yields determined in situ, vs. samples stripped and redissolved in C_6D_6. ^1H NMR analysis of the latter was used to quantify phosphine-free products, again by integration against an internal standard added prior to reaction. 1,3,5-Trimethoxybenzene (TMB) was chosen as the internal standard for its low volatility (b.p. 255 ˚C), which aids in reproducibility, and for the convenient location of its ^1H NMR singlets in regions rarely populated by other groups (CH_3: 3.30 ppm; C*H*: 6.25 ppm). Table 3.1 summarizes in situ yields of complexes **Ru-6** and **Ru-7** observed under the reaction conditions of Scheme 3.1. Chemical shifts of key complexes appear in Table 3.2.

Table 3.1. In situ distribution of products observed in reactions of Scheme 3.1.[a]

Entry	Reaction	time (h)	**Ru-6** (%)			**Ru-7** (%)	
			a	**b**	**c**	**a**	**b**
1a	**Ru-1a** + H_2, NEt_3	0.5	75	–	–	–	–
1b	**Ru-1b** + H_2, NEt_3	1	10	61	7	–	–
2a	**Ru-6a** + MeOH, NEt_3	2	–	–	–	96	–
2b	**Ru-6b** + MeOH, NEt_3	2.5	2	–	7	14	65
3a	**Ru-1a** + MeOH, NEt_3	8	–	–	–	58	–
3b	**Ru-1b** + MeOH, NEt_3	4	–	–	–		83

[a] Entry numbers correspond to the reactions of Scheme 3.1. Time corresponds to that required for consumption of the starting Ru species. NMR yields; agreement <±3% in replicate runs. Structures for all complexes are shown in Scheme 3.1, with the exception of **Ru-6c**, $RuHCl(H_2)(IMes)_2$.

Table 3.2. NMR chemical shifts for key complexes described in this Chapter.[a]

Complex	4:1 CH_2Cl_2-MeOH	C_6D_6	
	$^{31}P\{^1H\}$	$^{31}P\{^1H\}$	^1H[b]
$RuCl_2(PCy_3)_2$(=CHPh) **Ru-1a**	37.2	36.9	20.61
$RuCl_2$(IMes)(PCy_3)(=CHPh) **Ru-1b**	32.3	32.1	19.93
$RuHCl(H_2)(PCy_3)_2$ **Ru-6a**	53.4	54.2	-16.45
$RuHCl(H_2)$(IMes)(PCy_3) **Ru-6b**	55.4	56.3	-16.44
$RuHCl(H_2)(IMes)_2$ **Ru-6c**	–	–	-16.58
$RuHCl(CO)(PCy_3)_2$ **Ru-7a**	46.2	46.9	-24.21
$RuHCl(CO)$(IMes)(PCy_3) **Ru-7b**	47.7	47.8	-24.83
$RuHCl(CO)(IMes)_2$ **Ru-7c**	–	–	-25.39

[a] Values at 298 K, 300 or 500 MHz. [b] Position of Ru=C*H* (**Ru-1**) or Ru-*H* (**Ru-6**, **Ru-7**) signal. IMes = *N*,*N*'-bis-(2,4,6-trimethylphenyl)imidazol-2-ylidene.

*3.2.1 Two-step hydridocarbonylation, Step 1: hydrogenolysis of **Ru-1**.*

In a preliminary assay of the minimum conditions required for hydrogenolysis, consumption of **Ru-1a** was found to proceed very slowly (2.5 d) at 1 atm H_2 and room temperature (ca. 23 ˚C). At 1000 psi H_2, the required reaction time decreased to 6 h. In comparison, hydrogenolysis of **Ru-1b** was incomplete even after 1 week at 1 atm H_2, or after 24 h at 1000 psi H_2. Hydrogenolysis of the "third-generation" Grubbs catalyst $RuCl_2$(IMes)$(py)_2$(=CHPh) **Ru-1d** under the same conditions is complete within 2 h, but affords negligible amounts of hydride species (4% vs internal standard), consistent with the

poor performance of this catalyst in ROMP-hydrogenation.[16] In the case of **Ru-1a**, added PCy_3 inhibits reaction, indicating that hydrogenolysis (like metathesis reactions promoted by these alkylidene complexes) proceeds via a dissociative pathway. In the present case, incoming dihydrogen presumably replaces a phosphine ligand.[34]

The slower reaction of **Ru-1b** relative to **Ru-1a** is thus consistent with the lower lability of the phosphine ligand in the "second-generation" NHC catalysts.[34d,35] This difference in activity is amplified at ambient temperatures, elevated temperatures being required to gain access to the highly reactive 14-electron intermediate $RuCl_2$(IMes)(=CHPh).

The reactivity above sheds light on the efficiency of **Ru-1a** in effecting hydrogenation of polyoctenes under as little as 1 atm H_2, where elevated temperatures (50-60 °C) are used.[17] Functionalized polynorbornenes are more challenging, as noted above, and require use of higher hydrogen pressures. The experiments below were designed to probe efficiency and selectivity under conditions that reflect the current state of the art in tandem ROMP-hydrogenation of sterically encumbered polynorbornenes: thus, in CH_2Cl_2 (required to maintain solubility of the saturated polymers) with 3 equiv NEt_3, at 60 °C under 1000 psi H_2.[16]

Under these conditions, disappearance of **Ru-1a** was complete within 30 min (Figure 3.1a). Selectivity for **Ru-6a** was high, if less so than under our original[15] conditions: integration relative to internal standards indicated that 75% **Ru-6a** was formed from **Ru-1a** (Table 3.1, Entry 1a). Minor amounts of two unidentified phosphine-containing species were evident (<5% each). We assign one of these as a coordinatively saturated mono-phosphine complex, $RuHCl(PCy_3)L_3$, on the basis of the upfield location and multiplicity of the hydride

signal (-7.45 ppm; d, $^{2}J_{HP}$ = 51.3 Hz; correlates (HMBC) with a $^{31}P\{^{1}H\}$ NMR singlet at 62.9 ppm). Free PCy_3 was observed in similar amounts. No other phosphorus-containing species were apparent. A 20% decrease in total $^{31}P\{^{1}H\}$ NMR integration is thus evident, suggesting formation of paramagnetic Ru(III) species (possibly via solvent-induced chlorination). The paramagnetic nature of the byproducts was confirmed by EPR analysis; see below.

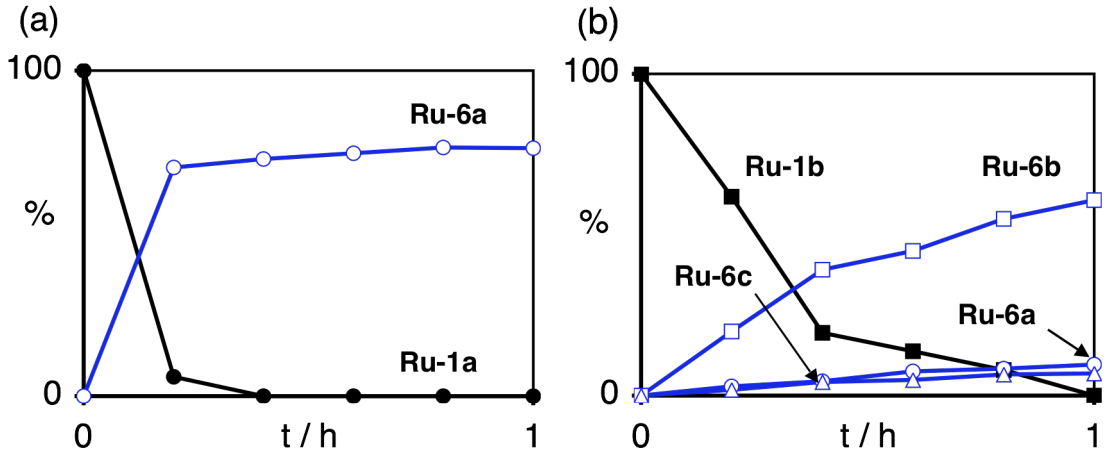

Figure 3.1. Rates of hydrogenolysis of first- and second-generation Grubbs catalysts under 1000 psi H_2 (CH_2Cl_2, 60 °C; 3 equiv NEt_3, [Ru]= 15 mM). (a) Transformation of **Ru-1a** into **Ru-6a**. (b) Transformation of **Ru-1b** into **Ru-6b** and (via disproportionation) **Ru-6a** and **Ru-6c**. Agreement between replicate runs ±3%.

Hydrogenolysis of **Ru-1b** was slower, as expected, requiring 1 h for complete reaction (Figure 3.1b). Good first-order kinetics are evident from the plot of Figure 3.2, with a first-order rate constant of k = 3.3 s^{-1}. (The corresponding analysis was not undertaken for Ru-1a because the much faster reaction limited the number of data points; see Figure 3.1a). Of note, $^{31}P\{^{1}H\}$ NMR analysis in C_6D_6 showed a singlet for **Ru-6a** (10% based on mol Ru; 20% of total integration) accompanying that expected for **Ru-6b** (61%; see Table 3.1, Entry 1b). The implied disproportionation of **Ru-6b** (Scheme 3.2, top) is confirmed by observation of ^{1}H NMR signals for $RuHCl(H_2)(IMes)_2$ (**Ru-6c**, 7%), assignment of which was

established by independent synthesis as described below. Disproportionation of **Ru-6b** obviously necessitates loss and recoordination of both the PCy_3 and the IMes ligands in **Ru-6b**. The observation of near-equimolar amounts of **Ru-6a** and **Ru-6c** indicate minimal scavenging of free IMes, despite the established susceptibility of IMes to reaction with chlorinated solvents.[36] Disproportionation of **Ru-6b** occurs independent of the presence of methanol, although it is slow at room temperature (10% after 24 h in C_6D_6). A similar process of loss and re-uptake of PCy_3 presumably also occurs for **Ru-6a**, but goes undiagnosed in the absence of a mixed-ligand "marker" to reveal its operation.

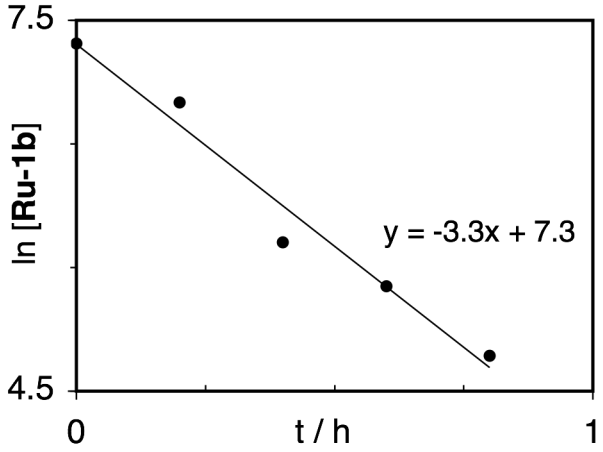

Figure 3.2. First-order log plot for hydrogenolysis of **Ru-1b**. $k = 3.3\ s^{-1}$.

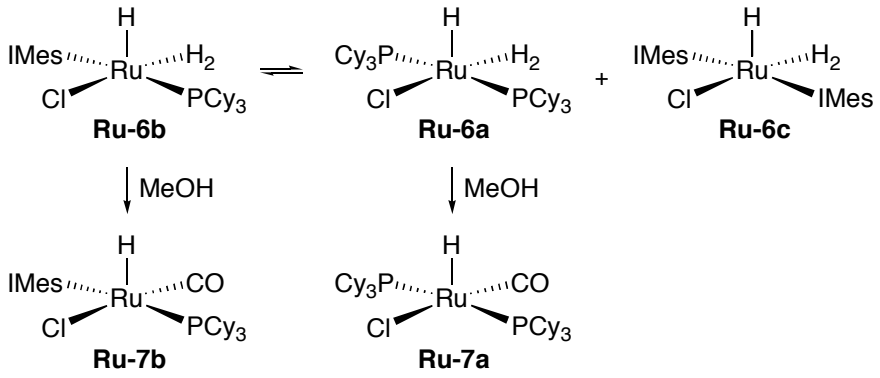

Scheme 3.2. Reactions of hydrogenolysis products **Ru-6** with methanol.

*3.2.2 Step 2: Carbonylation of dihydrogen complexes **Ru-6**.*

Figure 3.3a depicts the rate profile measured for the reaction of **Ru-6a** with methanol in the presence of base. Carbonylation is complete in 2 h at 60 ˚C, with near-quantitative selectivity for **Ru-7a** (Table 3.1, Entry 2a); no other products are observable by ^{1}H or $^{31}P\{^{1}H\}$ NMR analysis. The rate of reaction is essentially independent of added PCy_3, suggesting that the mechanism is not dissociative in phosphine. Good first-order dependence on [**Ru-6a**] is evident from Figure 3.4. Observation of extensive effervescence immediately on immersing the vessel in the preheated bath indicates loss of the dihydrogen ligand: given the absence of extensive C-H activation of the cyclohexyl rings,[37,38] methanol is presumed to rapidly take up the vacated site.

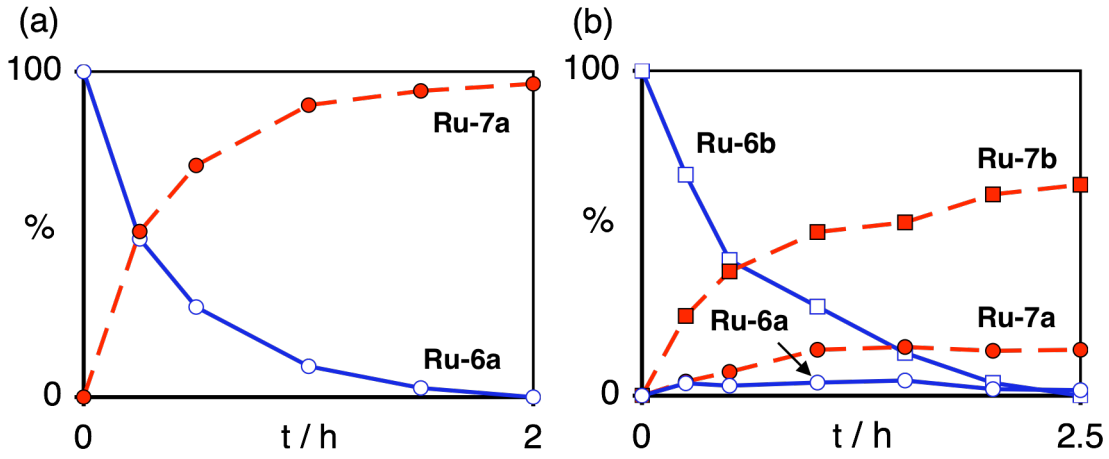

Figure 3.3. Rates of carbonylation of dihydrogen complexes by methanol (Ar, 3 NEt_3, 4:1 CH_2Cl_2-MeOH, 60 ˚C, [Ru] = 15 mM). (a) Transformation of **Ru-6a** into **Ru-7a**. (b) Transformation of **Ru-6b** into **Ru-7b** and **Ru-7a**, and disproportionation product **Ru-6a**. Agreement between replicate runs ±3%.

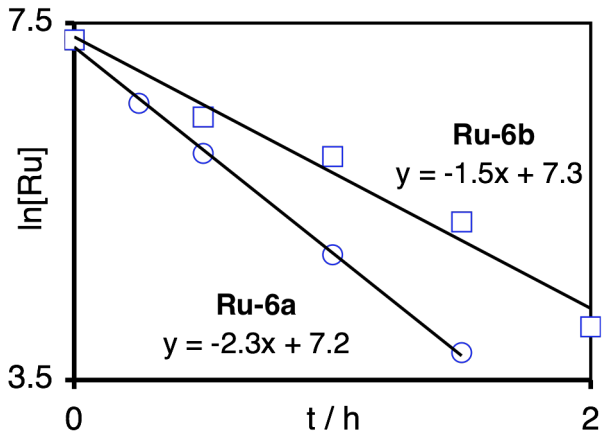

Figure 3.4. First-order log plot for carbonylation of **Ru-6**. **Ru-6a**: k = 1.5 s^{-1}; **Ru-6b**: k = 2.3 s^{-1}.

Consumption of **Ru-6b** occurs at a rate comparable to **Ru-6a** (Figure 3.3b), again in a process that appears to follow good first-order kinetics in terms of the loss of the starting complex (Figure 3.4). Yields of **Ru-7b** are considerably lower, however, at 65% (Table 3.1, Entry 2b). Complexes **Ru-6a** (2%) and **Ru-6c** (7%) are also generated, reflecting the susceptibility of the parent complex to disproportionation, as noted above. The bis-phosphine carbonyl complex **Ru-7a** is also observed (14%). We attribute formation of the latter to carbonylation of **Ru-6a** (Scheme 3.2, bottom), rather than disproportionation of the carbonyl complex **Ru-7b**, given that no disproportionation is observed on thermolysis of isolated **Ru-7b**.[27] The absence of **Ru-7c** is notable. It is unclear whether this reflects slower reaction of **Ru-6c** with methanol, or interception of the free carbene by CH_2Cl_2-induced decomposition. Relevant in the latter context is the longer timescale of carbonylation, relative to hydrogenolysis. Scavenging of free IMes by methanol[22] is probably less likely, given the general tolerance of these carbenes toward alcohols,[39] and the proposed reversibility with which their alcohol adducts are formed.[40,41] However, adduct formation could prolong the residence of the metal-free IMes species in solution, and thereby facilitate

its decomposition by CH_2Cl_2. Irrespective of the specific decomposition pathways involved, transformation of **Ru-6** into **Ru-7** is considerably less clean and efficient for **Ru-6b** than **Ru-6a**. This translates into a higher net yield for the **Ru-1a→Ru-6a→Ru-7a** transformation (ca. 75%, as compared to <40% for **Ru-1b→Ru-6b→Ru-7b**).

*3.2.3 One-step hydridocarbonylation: methanolysis of benzylidenes **Ru-1a/b**.*

Independent reports from the Mol and Grubbs groups have described the formation of products of type **Ru-7**, accompanied by varying amounts of decomposition, on reaction of Grubbs-class catalysts with primary alcohols.[22,28,30] Dinger and Mol noted that addition of base increased in situ yields for the **Ru-1a→Ru-7a** transformation to 85% over 24 h,[28] but that hydridocarbonylation of $RuCl_2(H_2IMes)(PCy_3)(=CHPh)$ **Ru-1b'** was limited to 30-40% yield by disproportionation and other side-reactions.[22] We find that methanolysis is much slower than hydrogenolysis for the benzylidene complexes **Ru-1a/b**, as evident from comparing Figures 3.1 and 3.5. Further, and consistent with the Mol report,[22] **Ru-1a** reacts more slowly than its NHC analogue (cf. Figures 3.5a and 3.5b).

In contrast with the behaviour reported for the H_2IMes complex **Ru-1b'**, however, we observe *no* disproportionation during methanolysis of **Ru-1b** (Table 3.1, Entry 3b), as indeed expected from the low lability of the PCy_3 ligand in both starting **Ru-1b**[42] and the carbonyl-containing product **Ru-7b** (vide supra). In consequence, the yield of **Ru-7b** (ca. 85%) is much improved in direct hydridocarbonylation of **Ru-1b**, relative to the two-step hydrogenolysis-carbonylation process, in which **Ru-6b** functioned as a vector for decomposition. The difference is unexpected, but may account for the poor performance observed on attempted use of **Ru-1b'** in tandem ROMP-hydrogenation noted above.

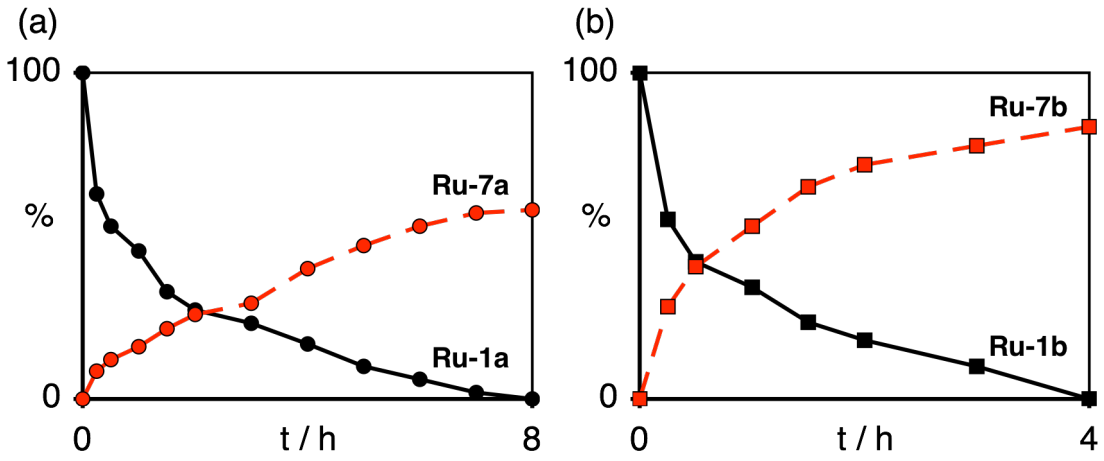

Figure 3.5. Methanolysis of the first- and second-generation Grubbs catalysts under the conditions of Scheme 3.1c (Ar, 3 equiv NEt_3, 4:1 CH_2Cl_2-MeOH, 60 °C, present, [Ru] = 15 mM). (a) Transformation of **Ru-1a** into **Ru-7a**. (b) Transformation of **Ru-1b** into **Ru-7b**. Agreement between replicate runs ±3%.

For **Ru-1a**, in comparison, methanolysis is less satisfactory as a route to **Ru-7a**, the latter being formed in only ca. 60% yield (Table 3.1, Entry 3a). Decomposition is unsurprising given the longer reaction time, the lability of the PCy_3 ligand in **Ru-1a**, relative to **Ru-1b**, and the susceptibility of this basic phosphine to reaction with the chlorinated solvent, which will impede its re-uptake. A $^{31}P\{^1H\}$ NMR signal is indeed observed in the region typical for phosphonium salts (34.7 ppm; cf. values of 34.5 ppm (C_6D_6)[43] for $MePCy_3$•Cl and of 33.8 ppm (CD_3OD)[44] for $HPCy_3$•Cl), which integrates to ca. 11% vs. the original proportion of **Ru-1a**. The importance of PCy_3 re-uptake in limiting decomposition of $RuCl_2(L)(=CHR)$ was demonstrated by our earlier study documenting the instability of the highly labile catalyst $RuCl_2(IMes)(py)_2(=CHPh)$ **Ru-1d**.[16] Finally, it should be noted that consumption of **Ru-1a/b** does not show a clean first-order dependence on ruthenium (Figure 3.6), suggesting that multiple competing pathways contribute. This contrasts sharply with the behaviour of the dihydrogen complexes **Ru-6a/b**, and may point toward a vulnerability specific to the

benzylidene moiety. We speculate that decomposition of **Ru-1** could occur via direct attack by methanol on the benzylidene functionality, as well as via a pathway dissociative in phosphine.

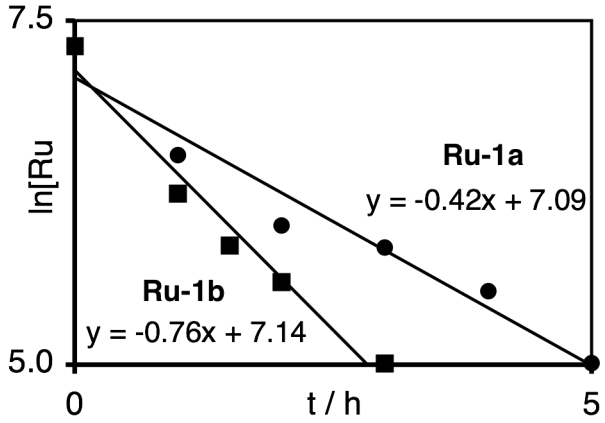

Figure 3.6. First-order plot for methanolysis of **Ru-1**. **Ru-1a**: $k = 0.42$ s^{-1}; **Ru-1b**: $k = 0.76$ s^{-1}.

EPR analysis of the crude products obtained following methanolysis of **Ru-1a** and **Ru-1b** confirmed the presence of paramagnetic species (Figure 3.7). In both cases, a signal is observed at a Landé *g* factor of ca. 2.07 (**Ru-1a**: 2.0704 ($\omega_{1/2}$ = 111 G); **Ru-1b**: g = 2.0779 ($\omega_{1/2}$ = 88 G)), suggesting formation of analogous products. The breadth of these signals is consistent with residence of an unpaired electron on a transition-metal center,[45] and the *g* factors are similar to that observed for $[Ru^{III}(C_9H_6NO)_3]$•MeOH (g = 2.074).[46] A second inorganic radical species is formed from **Ru-1a**, which gives rise to a higher-energy signal (g = 1.9630; $\omega_{1/2}$ = 38 G). An organic radical is also generated, as indicated by observation of a singlet at g = 1.9996, very near the organic-radical benchmark value of g = 2.000.[45]

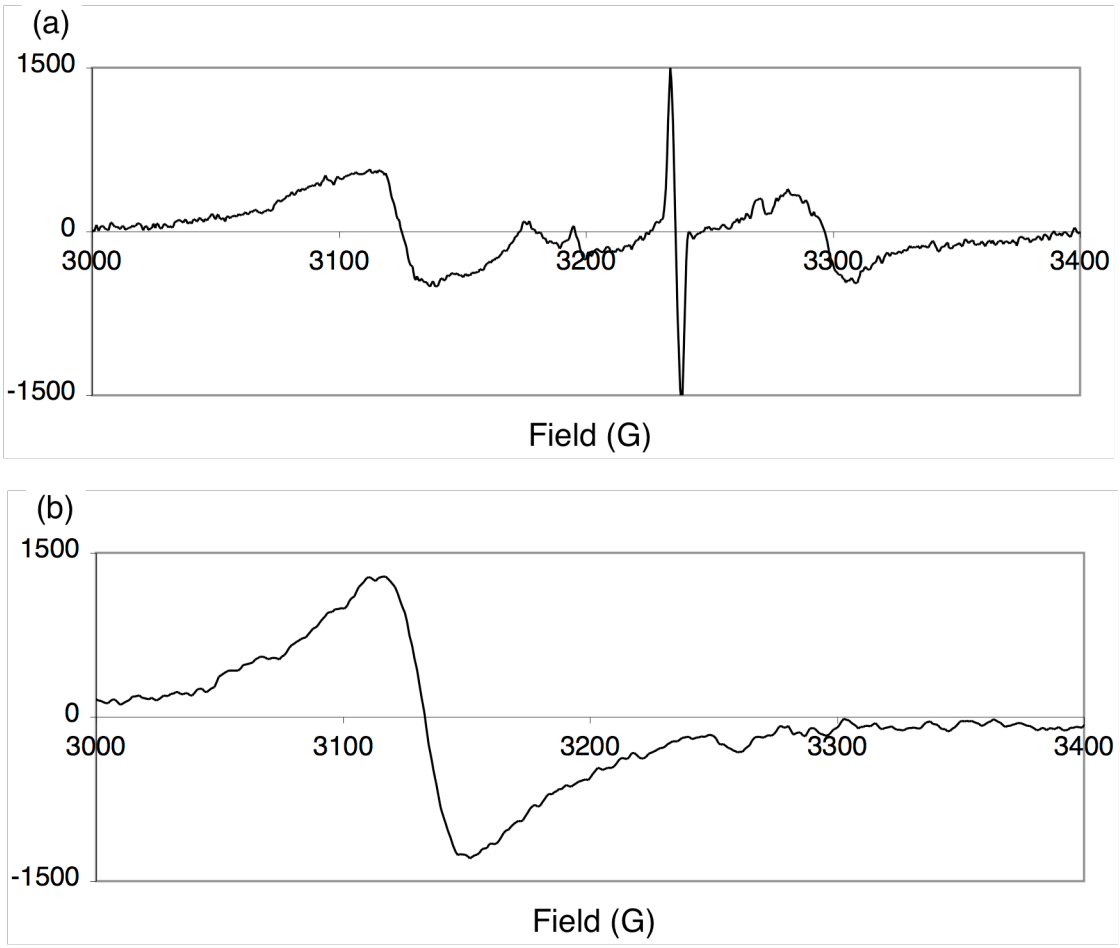

Figure 3.7. EPR spectra of products formed following methanolysis of (a) **Ru-1a** and (b) **Ru-1b**.

The much faster reaction of **Ru-1b**, vs. **Ru-1a**, is of interest. This may reflect the poor charge-donor capacity of the IMes ligand relative to PCy_3, which would render the Ru center in **Ru-1b** more electropositive, thus enhancing electrostatic attraction of the Lewis basic alcohol donor. In experimental and theoretical studies of the Grubbs catalysts **Ru-1a** and **Ru-1b'**, the Kennepohl group noted the poor charge-donor capacity of the related H_2IMes ligand.[47] This perspective was supported by a recent theoretical study by Carbo and Poblet utilizing extended charge decomposition analysis to quantify the donor-acceptor properties of the phosphine and NHC ligands in the same catalysts.[48]

The reason for the slower reaction of the benzylidene complexes with methanol, relative to hydrogen, is not obvious. We initially speculated that this behaviour might reflect the greater steric conflict incurred by approach of MeOH to five-coordinate **Ru-1** within an associative pathway. This would also account for the slower reaction of **Ru-1a**, relative to **Ru-1b**, access to the former being retarded by the three-dimensional bulk associated with the two PCy_3 ligands. However, we find that the rate of methanolysis is inhibited by added PCy_3, consistent with a mechanism that is *dissociative* in phosphine.[49] As the putative four-coordinate intermediate $RuCl_2(L)(=CHR)$ (L = PCy_3, IMes) is unlikely to exert significant steric discrimination in the approach of H_2, vs. MeOH, the slower reaction with methanol is presumably electronic in origin. Computational studies now under way are directed at clarifying the mechanisms of both reactions. Even at this stage, however, the trends in activity and the effect of added phosphine suggest very different pathways for the two reactions.

3.2.4 Synthesis of $RuHCl(H_2)(IMes)_2$ ***Ru-6c***.

Assignment of the NMR signals for **Ru-6c** was confirmed by independent synthesis of this complex via reaction of **Ru-6a** with IMes (Eqn 3.1). Use of hexanes as solvent limits solubility and hence disproportionation, this enabling clean conversion to **Ru-6c** over 4 days. The complex was isolated in >80% yield. Its identity was confirmed by NMR, infrared, and elemental analysis. IR analysis reveals a weak band, tentatively assigned to the ν(Ru-H) vibration, at 2037 cm^{-1}. The hydride and η^2-H_2 ligands appear as a broad ^1H singlet at -16.58 ppm in C_6D_6 (-16.63 ppm in C_7D_8), which did not decoalesce down to -90 ˚C. Integration against these signals indicates the presence of two IMes ligands. Efforts to

measure $^1J_{HD}$ values to obtain insight into the H-H bond distance were complicated by rapid exchange, as is also the case for **Ru-6a**, for which no H-D coupling was reportedly observable.[51] Of note is the long $T_{1(min)}$ value for the hydride signal (64.5 ms at 300 MHz, 250 K, C_7D_8), corresponding to an H-H distance of 1.13 Å for fast-spinning H_2.[50] While long relaxation times are characteristic of η^2-H_2 perturbed by interaction with cis-hydride,[50b] this value is significantly longer than those reported for **Ru-6a** (30 ms at 243 K, 250 MHz, CD_2Cl_2;[51] corrected to 36 ms at 300 MHz) or **Ru-6b** (36.6 ms at 300 MHz, 253 K, C_7D_8).[27] Elongation of the H-H distance may reflect increased donation from the H-H bond to the electropositive Ru center in this bis(NHC) complex. The poor charge-donor capacity of the NHC ligand, relative to PCy_3,[47,48] was noted above.

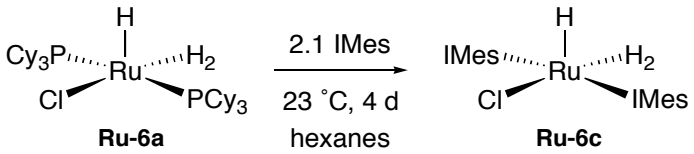

(3.1)

*3.2.5 Synthesis of RuHCl(CO)(IMes)$_2$ **Ru-7c**.*

Assignment of the NMR signals for **Ru-7c** was confirmed by independent synthesis of this complex via reaction of the known complex RuHCl(CO)(IMes)(PPh_3) **Ru-13b** with IMes (Eqn 3.2; 81% yield). While this work was in progress, synthesis of **Ru-7c** and related bis-NHC complexes was independently reported by the groups of Whittlesey[52] and Gunnoe.[53] The literature routes involved, respectively, thermolysis of $Ru(H)_2(CO)(AsPh_3)_3$ **Ru-14** with an excess of the NHC ligand, followed by addition of CH_2Cl_2 (yield reported as moderate to high), or thermolysis of $[RuCl_2(CO)_2]_n$ with excess IMes, followed by addition of methanol (32% yield). Alternatively, **Ru-7c** can be isolated in quantitative yields under very mild

conditions, by exposure of the hydroxy hydride complex RuH(OH)(CO)(IMes)$_2$ **Ru-15** to CH_2Cl_2 at ambient temperature.[52]

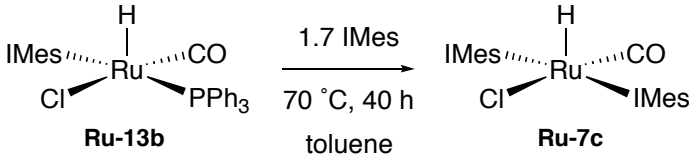

(3.2)

3.3 Conclusions.

The foregoing reveals unexpected reactivity differences between the first- and second-generation Grubbs complexes, which have striking implications for tandem catalysis processes mediated by these important metathesis catalysts. Direct interrogation of the inorganic transformations involved reveals that the protocols optimal for the **Ru-1a→Ru-6a** transformation are poorly suited to the **Ru-1b→Ru-7b** transformation. Thus, hydrogenolysis of **Ru-1a** is an efficient route to dihydrogen complex **Ru-6a**, which can in turn be converted into **Ru-7a** in high yields by reaction with methanol. Direct methanolysis of **Ru-1a**, however, occurs only over a timescale of hours, and decomposition therefore competes. Conversely, methanolysis is significantly more efficient than the hydrogenolysis-carbonylation sequence in converting **Ru-1b** to **Ru-7b**, with yields approaching 85%. The susceptibility of the dihydrogen complex **Ru-6b** to disproportionation is a major impediment to both hydrogenolysis of **Ru-1b** and carbonylation of **Ru-6b**. This difference in the behaviour of the first- and second-generation Grubbs catalysts indicates that surprisingly different experimental methodologies are required to attain maximum productivity in tandem ROMP-hydrogenation using either catalyst. Work currently under way is directed at elucidating whether similar behavioural differences exist for the corresponding methylidene complexes that represent the resting states in ring-closing metathesis (RCM) and cross-

metathesis (CM). This point is expected to be central to the development of efficient RCM-functionalization and CM-functionalization methodologies that exploit the catalytic versatility of complexes **Ru-7**.

3.4 Experimental.

3.4.1 General procedures.

Reactions were carried out at room temperature (23 °C) under argon, using standard Schlenk or glovebox techniques, unless otherwise stated. Dry, oxygen-free solvents were obtained using a Glass Contour solvent purification system, and stored over Linde 4Å molecular sieves. Methanol was distilled from $Mg(OCH_3)_2$ under argon and stored over molecular sieves (Linde 4Å). Triethylamine and C_6D_6 were distilled from CaH_2, degassed by consecutive freeze/pump/thaw cycles, and stored over molecular sieves (Linde 4Å). The Grubbs catalysts **Ru-1a**[54] and **Ru-1b**,[42c] and the dihydrogen complexes **Ru-6a**[15] and **Ru-6b**[27] were prepared according to literature procedures. Triphenylphosphine oxide and 1,3,5-trimethoxybenzene were purchased from Aldrich and used as received. Hydrogen (UHP Grade) was purchased from BOC Gases and used without purification. NMR spectra were recorded on a Bruker Avance 300 or Bruker AMX-500 spectrometer at 298 K. ^1H and $^{13}C\{^1H\}$ NMR spectra were referenced to the residual proton and carbon signals of the deuterated solvent. Peaks are reported in ppm, relative to TMS (^1H, ^{13}C) or external 85% H_3PO_4 (^{31}P) at 0 ppm. EPR spectra were acquired on a JEOL FA-100 X-band EPR spectrometer equipped with a JEOL ES-UCX2 cylindrical cavity. These spectra were kindly run by Mr. Paul Billone of the Scaiano group; spectrometer access provided by Prof. J .C. Scaiano. IR spectra were measured on a Bomem MB100 IR spectrometer. Microanalysis was carried out by Guelph Chemical Laboratories Ltd., Guelph, Ontario.

3.4.2 Synthesis of RuHCl(H_2)(IMes)$_2$ ***Ru-6c***.

Solid IMes (179 mg, 0.588 mmol) was added to an orange suspension of RuHCl(H_2)(PCy_3)$_2$ **Ru-6a** (200 mg, 0.283 mmol) in hexanes (10 mL). The reaction mixture was stirred for 4 d at 23 ˚C, concentrated to ~2 mL, and cooled to -35˚C for 2 h. The precipitate was filtered off, washed with cold hexanes (3 × 3 mL), and dried under vacuum to yield **Ru-6c** as an orange powder. Yield: 187 mg (88%). ^{1}H (300 MHz, C_6D_6): δ 6.80 (s, 8H, Mes *m*-C*H*), 6.09 (s, 4H, NC*H*=C*H*N), 2.34 (s, 12H, *p*-C*H*$_3$), 2.07 (s, 24H, *o*-C*H*$_3$), -16.58 (br s, 3H, Ru*H*Cl(*H*$_2$)). ^{13}C{^{1}H} NMR (75.5 MHz, C_6D_6): δ 199.6 (s, N*C*N), 137.8 (s, Mes *p-C*), 136.7 (s, Mes *i-C*), 136.4 (s, Mes *o-C*), 128.8 (s, Mes *m-C*), 120.7 (s, N*C*=*C*N), 21.3 (s, *p-C*H_3), 18.8 (s, *o-C*H_3). IR (Nujol, cm^{-1}): ν(Ru-H) 2037 (w). Anal. Calcd. for $C_{42}H_{51}ClN_4Ru$: C, 67.40 %; H, 6.87 %; N, 7.49 %. Found: C, 67.16 %; H, 7.04 %; N, 7.39 %.

3.4.3 Synthesis of RuHCl(CO)(IMes)$_2$ ***Ru-7c***.

Solid IMes (83 mg, 0.27 mmol) was added to a solution of RuHCl(CO)(IMes)(PPh_3) **Ru-13b** (100 mg, 0.14 mmol) in 3 mL toluene. The yellow solution was heated at 70 ˚C for 40 h, over which time conversions were monitored by NMR analysis. Once reaction was complete, the solution was concentrated, treated with hexanes, and chilled to –35 ˚C to precipitate a yellow-orange microcrystalline product. The solid was filtered off, washed with hexane (3 x 3 mL), and dried under vacuum. Yield: 85 mg (81%). Spectroscopic data are in good agreement with the values reported.[52,53] ^{1}H NMR (C_6D_6): δ 6.82 (s, 4H, Mes *m*-C*H*), 6.78 (s, 4H, Mes *m*-C*H*), 6.16 (s, 4H, NC*H*=C*H*N), 2.32 (s, 12H, *p*-C*H*$_3$), 2.17 (s, 12H, *o*-C*H*$_3$), 2.05 (br s, 12H, *o*-C*H*$_3$), -25.39 (s, 1H, Ru*H*). ^{13}C{^{1}H} NMR (C_6D_6): δ 202.1 (s, *C*O), 195.2 (s, N*C*N), 137.3 (br s, Mes *m-C*), 137.0 (s, Mes *p-C*), 136.3 (br s, Mes *o-C*), 129.0 (s,

Mes *m-C*), 121.6 (s, N*C*=*C*N), 21.3 (s, Mes *p-C*H_3), 19.0 (br s, Mes *o-C*H_3) 18.9 (br s, Mes *o-C*H_3). IR (Nujol, cm^{-1}): ν(CO) 1883 (s), ν(Ru-H) 1839 (w).

3.4.4 Representative procedure for hydrogenolysis of benzylidene complexes ***Ru-1***.

To a solution of **Ru-1a** or **Ru-1b** (100 mg, 0.12 mmol) was added NEt_3 (50 μL, 0.36 mmol; 3 equiv), 1,3,5-trimethoxybenzene (TMB; 20 mg, 0.12 mmol, 1 equiv) and Ph_3P=O (34 mg, 0.12 mmol, 1 equiv) in CH_2Cl_2 (20 mL). Aliquots of this stock solution (2.0 mL each) were distributed to five glass-lined autoclaves. These were purged with H_2 (3 × 250 psi), pressurized to 1000 psi and stirred at 60 ˚C (oil bath; 10 min allowed to reach temperature). At appropriate times, the autoclaves were vented to 50 psi, cooled for 10 min (ice bath), purged with Ar (250 psi), dried externally (acetone, CH_2Cl_2), and returned to the glovebox. The contents of each autoclave were evaporated to dryness and taken up in C_6D_6 for NMR analysis. Conversions were determined by monitoring the decrease in the integration of the ^{1}H NMR singlet for **Ru-1a** (20.6 ppm) or **Ru-1b** (19.9 ppm), and the increase in integration of a broad singlet for **Ru-6a**, or for **Ru-6a/b** (-16.45 ppm, 3H), relative to the methyl proton singlet for TMB (3.3 ppm, 9H). These conversions were confirmed by ^{31}P{^{1}H} NMR analysis, by integrating the singlets for **Ru-1a** (36.9 ppm) or **Ru-1b** (32.1 ppm) and **Ru-6a** (54.2 ppm) or **Ru-6b** (56.3 ppm) relative to that of Ph_3P=O (25.5 ppm).

For reactions at room temperature, aliquots were removed at regular intervals inside a glovebox, stripped, and redissolved in C_6D_6 for NMR analysis. Hydrogenolysis of **Ru-1b** was very slow: at 24 h, 35% unreacted **Ru-1b**, 8% **Ru-6b**, and 7% **Ru-6a**.

*3.4.5 Representative procedure for methanolysis of benzylidene complexes **Ru-1**.*

To a solution of **Ru-1a** or **Ru-1b** (10 mg, 0.012 mmol) and $Ph_3P{=}O$ (6 mg, 0.02 mmol) in CH_2Cl_2 (0.59 mL) in a thick-walled J. Young NMR tube was added MeOH (0.16 mL). C_6D_6 (50 μL) was added as deuterium lock, and a zero-time (t_0) $^{31}P\{^1H\}$ NMR spectrum was acquired. Addition of NEt_3 (5.0 μL, 0.036 mmol) and subsequent heating (oil bath, 60 ˚C) initiated the reaction, which was monitored by $^{31}P\{^1H\}$ NMR analysis. Conversions were determined by measuring the integration of the singlets due to **Ru-1a** (37.2 ppm) or **Ru-1b** (32.3 ppm) and **Ru-7a** (46.2 ppm) or **Ru-7b** (47.7 ppm) relative to that for $Ph_3P{=}O$ (32.8 ppm). The chemical shift for **Ru-1a** is shifted slightly downfield from its value in neat CD_2Cl_2 (36.6 ppm; cf. 36.9 in C_6D_6).

3.5 References.

(1) Fogg, D. E.; Foucault, H. M., Ring-Opening Metathesis Polymerization. In *Comprehensive Organometallic Chemistry III*, Crabtree, R. H.; Mingos, D. M. P., Eds. Elsevier: Oxford, 2007; Vol. 11, pp 623-652.
(2) Mulhaupt, R. *Macromol. Chem. Phys.* **2003**, *204*, 289-327.
(3) Merrett, K.; Liu, W.; Mitra, D.; Camm, K. D.; McLaughlin, C. R.; Liu, Y.; Watsky, M. A.; Li, F.; Griffith, M.; Fogg, D. E. *Biomaterials* **2009**, *30*, 5403–5408.
(4) Katsumata, T.; Shiotsuki, M.; Sanda, F.; Masuda, T. *Polymer* **2009**, *50*, 1389-1394.
(5) Vargas, J.; Santiago, A. A.; Tlenkopatchev, M. A.; Gavino, R.; Laguna, M. F.; Lopez-Gonzalez, M.; Riande, E. *Macromolecules* **2007**, *40*, 563-570.
(6) Wang, Y.-C.; Li, C.-L.; Lee, K.-R.; Liaw, D.-J. *J. Membrane Sci.* **2005**, *246*, 59-65.
(7) Arnauld, T.; Barrett, A. G.; Hopkins, B. T. *Tetrahedron Lett.* **2002**, *43*, 1081-1083.
(8) Kang, H. A.; Bronstein, H. E.; Swager, T. M. *Macromolecules* **2008**, *41*, 5540-5547.
(9) Myers, S. B.; Register, R. A. *Polymer* **2008**, *49*, 877-882.
(10) Trzaska, S. T.; Lee, L.-B. W.; Register, R. A. *Macromolecules* **2000**, *33*, 9215-9221.
(11) Lehman, S. E., Jr.; Wagener, K. B.; Baugh, L. S.; Rucker, S. P.; Schulz, D. N.; Varma-Nair, M.; Berluche, E. *Macromolecules* **2007**, *40*, 2643-2656.
(12) Watson, M. D.; Wagener, K. B. *Macromolecules* **2000**, *33*, 3196-3201.
(13) Xue, B.; Ogata, K.; Toyota, A. *Polym. Degrad. Stab.* **2008**, *93*, 347-352.
(14) See, for example: (a) Lee, L.-B. W.; Register, R. A. *Macromolecules* **2005**, *38*, 1216–1222. (b) Dettmer, C. M.; Gray, M. K.; Torkelson, J. M.; Nguyen, S. T. *Macromolecules* **2004**, *37*, 5504–5512. (c) Lee, B. S.; Mahajan, S.; Clapham, B.; Janda, K. D. *J. Org. Chem.* **2004**, *69*, 3319–3329. (d) Sohn, B. H.; Gratt, J. A.; Lee, J. K.; Cohen, R. E. *J. Appl. Polym. Sci.* **1995**, *58*, 1041. (e) Vargas, J.; Santiago, A. A.; Tlenkopatchev, M. A.; Gavino, R.; Laguna, M. F.; Lopez-Gonzalez, M.; Riande, E. *Macromolecules* **2007**, *40*, 563–570.
(15) Drouin, S. D.; Yap, G. P. A.; Fogg, D. E. *Inorg. Chem.* **2000**, *39*, 5412-5414.
(16) Camm, K. D.; Castro, N. M.; Liu, Y.; Czechura, P.; Snelgrove, J. L.; Fogg, D. E. *J. Am. Chem. Soc.* **2007**, *129*, 4168-4169.
(17) Drouin, S. D.; Zamanian, F.; Fogg, D. E. *Organometallics* **2001**, *20*, 5495-5497.
(18) Miao, X.; Fischmeister, C.; Bruneau, C.; Dixneuf, P. H. *ChemSusChem* **2009**, *2*, 542-545.
(19) Malacea, R.; Fischmeister, C.; Bruneau, C.; Dubois, J.-L.; Couturier, J.-L.; Dixneuf, P. H. *Green Chem.* **2009**, *11*, 152-155.
(20) Schmidt, B. *Pure Appl. Chem.* **2006**, *78*, 469-476.
(21) Schmidt, B.; Pohler, M. *Org. Biomol. Chem.* **2003**, *1*, 2512-2517.
(22) Dinger, M. B.; Mol, J. C. *Eur. J. Inorg. Chem.* **2003**, 2827-2833.
(23) Bielawski, C. W.; Louie, J.; Grubbs, R. H. *J. Am. Chem. Soc.* **2000**, *122*, 12872-12873.
(24) Nishihara, Y.; Izawa, S.; Inoue, Y.; Nakayama, Y.; Shiono, T.; Takagi, K. *J. Polym. Sci., Part A* **2008**, *46*, 3314-3325.
(25) McLain, S. J.; McCord, E. F.; Arthur, S. D.; Hauptman, E.; Feldman, J.; Nugent, W. A.; Johnson, L. K.; Mecking, S.; Brookhart, M. *Polym. Mater. Sci. Eng.* **1997**, *76*, 246-247.
(26) Rowley, C. N.; Foucault, H. M.; Woo, T. K.; Fogg, D. E. *Organometallics* **2008**, *27*, 1661-1663.
(27) Beach, N. J.; Blacquiere, J. M.; Drouin, S. D.; Fogg, D. E. *Organometallics* **2009**, *28*, 441-447.

(28) Dinger, M. B.; Mol, J. C. *Organometallics* **2003**, *22*, 1089-1095.
(29) Banti, D.; Mol, J. C. *J. Organomet. Chem.* **2004**, *689*, 3113-3116.
(30) Trnka, T. M.; Morgan, J. P.; Sanford, M. S.; Wilhelm, T. E.; Scholl, M.; Choi, T.-L.; Ding, S.; Day, M. W.; Grubbs, R. H. *J. Am. Chem. Soc.* **2003**, *125*, 2546-2558.
(31) Schmidt, B. *Chem. Commun.* **2004**, 742-743.
(32) Arisawa, M.; Terada, Y.; Takahashi, K.; Nakagawa, M.; Nishida, A. *J. Org. Chem.* **2006**, *71*, 4255-4261.
(33) Louie, J.; Grubbs, R. H. *Organometallics* **2002**, *21*, 2153-2164.
(34) Hydrogenation reactions promoted by **Ru-1a** are likewise inhibited by addition of free PCy_3, and promoted by addition of HBF_4 as a phosphine scavenger. (a) S.D. Drouin, Ph.D. Thesis, University of Ottawa, 2003; p. 88. Protic acids have previously been shown to enhance the reactivity of **Ru-1a** in metathesis and of **Ru-7a** in hydrogenation catalysis. See: (b) Lynn, D. M.; Mohr, B.; Grubbs, R. H. *J. Am. Chem. Soc.* **1998**, *120*, 1627-1628. (c) Yi, C. S.; Lee, D. W.; He, Z. *Organometallics* **2000**, *19*, 2909-2915. (d) Lee, H. M.; Smith, D. C.; He, Z.; Stevens, E. D.; Yi, C. S.; Nolan, S. P. *Organometallics* **2001**, *20*, 794-797.
(35) Sanford, M. S.; Love, J. A.; Grubbs, R. H. *J. Am. Chem. Soc.* **2001**, *123*, 6543-6554.
(36) Arduengo, A. J.; Davidson, F.; Dias, H. V. R.; Goerlich, J. R.; Khasnis, D.; Marshall, W. J.; Prakasha, T. K. *J. Am. Chem. Soc.* **1997**, *119*, 12742-12749.
(37) Borowski, A. F.; Sabo-Etienne, S.; Christ, M. L.; Donnadieu, B.; Chaudret, B. *Organometallics* **1996**, *15*, 1427-1434.
(38) Amoroso, D.; Yap, G. P. A.; Fogg, D. E. *Can. J. Chem.* **2001**, *79*, 958-963.
(39) Indeed, IMes and related carbenes have been much used as organocatalysts to promote alcohol functionalization. See: (a) Raynaud, J.; Absalon, C.; Gnanou, Y.; Taton, D. *Macromolecules* **2010**, *43*, 2814-2823. (b) Zeng, T.; Song, G.; Li, C.-J. *Chem. Commun.* **2009**, 6249-6251. (c) Pignataro, L.; Papalia, T.; Slawin, A. M. Z.; Goldup, S. M. *Org. Lett.* **2009**, *11*, 1643-1646. (d) Enders, D.; Niemeier, O.; Henseler, A. *Chem. Rev.* **2007**, *107*, 5606-5655. (e) Marion, N.; Diez-Gonzalez, S.; Nolan, S. P. *Angew. Chem., Int. Ed.* **2007**, *46*, 2988-3000.
(40) Schmidt, M. A.; Muller, P.; Movassaghi, M. *Tet. Lett.* **2008**, *49*, 4316-4318.
(41) Movassaghi, M.; Schmidt, M. A. *Org. Lett.* **2005**, *7*, 2453-2456.
(42) While precedents exist for NHC dissociation in Ru-benzylidene complexes (see Ref. 30 and (a) Weskamp, T.; Schattenmann, W.C.; Spiegler, M.; Herrmann, W.A. *Angew. Chem., Int. Ed.* **1998**, *37*, 2490-2493. (b) Weskamp, T.; Kohl, F.J.; Herrmann, W.A. *J. Organomet. Chem.* **1999**, *582*, 362-365), no disproportionation is observed for **Ru-1b** during its synthesis or prolonged thermolysis. See (c) Huang, J.; Stevens, E.D.; Nolan, S.P.; Petersen, J.L. *J. Am. Chem. Soc.* **1999**, *121*, 2674-2678.
(43) Hong, S. H.; Day, M. W.; Grubbs, R. H. *J. Am. Chem. Soc.* **2004**, *126*, 7414-7415.
(44) Tan, K. L.; Vasudevan, A.; Bergman, R. G.; Ellman, J. A.; Souers, A. J. *Org. Lett.* **2003**, *5*, 2131-2134.
(45) Brustolan, M. G., E., *Electron Paramagnetic Resonance: A Practitioner's Toolkit*; Wiley-VCH: Hoboken, 2009.
(46) Malecki, J. G.; Jaworska, M.; Kruszynski, R.; Klak, J. *Polyhedron* **2005**, *24*, 3012-3021.
(47) Getty, K.; Delgado-Jaime, M. U.; Kennepohl, P. *J. Am. Chem. Soc.* **2007**, *129*, 15774-15776.
(48) Antonova, N. S.; Carbo, J. J.; Poblet, J. M. *Organometallics* **2009**, *28*, 4283-4287.

(49) Consistent with the thermal requirement for phosphine dissociation, this effect is not observed during the room-temperature reaction of **Ru-1b** with methanolic methoxide (Chapter 4).
(50) (a) Bautista, M. T.; Cappellani, E. P.; Drouin, S. D.; Morris, R. H.; Schweitzer, C. T.; Sella, A.; Zubkowski, J. *J. Am. Chem. Soc.* **1991**, *113*, 4876-4887. (b) Jessop, P. G.; Morris, R. H. *Coord. Chem. Rev.* **1992**, *121*, 155-284.
(51) Christ, M. L.; Sabo-Etienne, S.; Chaudret, B. *Organometallics* **1994**, *13*, 3800-3804.
(52) Chantler, V. L.; Chatwin, S. L.; Jazzar, R. F. R.; Mahon, M. F.; Saker, O.; Whittlesey, M. K. *Dalton Trans.* **2008**, 2603-2614.
(53) Lee, J. P.; Ke, Z.; Ramirez, M. A.; Gunnoe, T. B.; Cundari, T. R.; Boyle, P. D.; Petersen, J. L. *Organometallics* **2009**, *28*, 1758-1775.
(54) Schwab, P.; Grubbs, R. H.; Ziller, J. W. *J. Am. Chem. Soc.* **1996**, *118*, 100-110.

Chapter 4: Rapid Extinction of the Grubbs Catalysts with Methoxide Ion: Formation of Novel Methoxyhydride Complexes

4.1 Introduction

The Grubbs metathesis catalysts $RuCl_2(L)(PCy_3)(=CHPh)$ (e.g., **Ru-1a**: L = PCy_3; **Ru-1b**: L = IMes, *N*,*N*'-bis(mesityl)imidazol-2-ylidene) are now widely recognized as powerful agents for further, non-metathetical transformations.[1,2] In some cases, this expanded reactivity is due to the action of **Ru-1** and its alkylidene and/or methylidene derivatives: in others, it reflects the operation of further ruthenium catalysts generated in situ, whether by chance or design.[3] While a greater understanding of the underlying inorganic transformations of these important complexes would clearly be advantageous, overwhelming interest in their organic applications has tended to overshadow their inorganic reaction chemistry. Many of their fundamental reactivity patterns thus remain obscure, studies of the transformation of **Ru-1** into the catalytically important hydrides $RuHCl(CO)(L)(PCy_3)$ **Ru-7** (particularly **Ru-7a**; L = PCy_3) notwithstanding.[4,5]

A potentially important example of this obscurity is found in the reactions of the Grubbs catalysts with alkoxides. Schmidt has demonstrated that post-metathesis treatment of **Ru-1a** with isopropanol and NaOH (5-10 equiv vs. Ru) yields efficient catalysts for double-bond isomerization. Primary alcohols, however, were strikingly less effective.[6] While metal hydrides are formed in either case, one obvious difference lies in the resistance of *secondary* alkoxides to Ru-mediated decarbonylation. In contrast, Mol and co-workers[4a] have shown that treating **Ru-1a** with one equivalent of methoxide at 70-75 °C yields the carbonyl adduct **Ru-7a**, among other Ru species (ca. 50% **Ru-7a**; we suspected that the unidentified co-products might arise from thermolytic degradation of **Ru-1a**). Given that complexes **Ru-**

7a/b are high-productivity catalysts in the mechanistically-related context of olefin hydrogenation,[7] we hypothesized that the poor isomerization activity associated with primary alcohols might be due to formation of deactivated polycarbonyl species in the presence of excess alkoxide.

Within part of a broader program of study directed at evaluating the behaviour of Ru-alkylidene complexes with reactive $[ER]^-$ / HER species, we thus wished to clarify the reactivity of **Ru-1a** and **Ru-1b** toward *excess* methoxide (>2 equiv) in the presence of methanol. We chose to explore this chemistry at ambient temperatures, both to intercept the relevant Ru species (rather than "downstream" products arising from extraneous thermal decomposition pathways), and to gain a clearer picture of the minimum conditions required for loss of the benzylidene functionality. Here we report strikingly different outcomes for the first- and second-generation Grubbs catalysts. While **Ru-1a** is immediately converted into $RuH(OMe)(CO)_2(PCy_3)_2$ **Ru-18a** and $RuH(OMe)(CO)(H_2)(PCy_3)_2$ **Ru-17a** at 23 °C, complex **Ru-1b** undergoes much slower transformation into a rare, unexpectedly stable five-coordinate methoxyhydride species, $RuH(OMe)(CO)(IMes)(PCy_3)$ **Ru-16b**, with no sign of the expected **Ru-17b**/**Ru-18b**. Routes to the new complexes **Ru-16b** and **Ru-18a/b** from convenient hydride precursors were developed to confirm the identities of observed products (**Ru-16b**, **Ru-18a**), and the absence of expected products (**Ru-18b**).

4.2 Results and Discussion

4.2.1 Reactions of Grubbs catalysts with methoxide ion.

Addition of excess methanolic NaOMe to a solution of **Ru-1a** in CH_2Cl_2 (Scheme 4.1a) caused an instant color change from purple to pale yellow, evolution of small bubbles

presumed to be H_2, and complete loss of the NMR signals for **Ru-1a** within 5 minutes, without need for elevated temperatures. No evidence was seen of methoxyhydride RuH(OMe)(CO)$(PCy_3)_2$ **Ru-16a**, an intermediate inferred from the corresponding, slower reaction of **Ru-1b** discussed below (Scheme 4.1b). Instead, the sole Ru products observed were RuH(OMe)$(CO)_2(PCy_3)_2$ **Ru-18a** and RuH(OMe)(CO)$(H_2)(PCy_3)_2$ **Ru-17a**, formed in ca. 2:1 ratio. Formaldehyde and free PCy_3 were also detected (ca. 10% each), as well as toluene, although quantification of the latter was hampered by interfering signals from the cyclohexyl groups or the internal standard Ph_3PO. Co-formation of ca. 25% paramagnetic material is indicated by integration against Ph_3PO; vide infra.

The distribution of Ru products did not change on longer reaction (4 h), but stripping off the solvent and redissolving the residue in C_6D_6 effected transformation of **Ru-17a** into **Ru-18a**, via uptake of a further equivalent of methanol (see mechanistic section). Traces of known[8] dihydride $Ru(H)_2(CO)_2(PCy_3)_2$ **Ru-19a** (<5%) were also formed. The identity of **Ru-18a** was confirmed by independent synthesis from hydride precursors; dihydrogen adduct **Ru-17a** was characterized by in situ NMR analysis, including $T_{1(min)}$ measurements. Facile β-elimination from methoxide, discussed in more detail below, disfavors formation of stable bis(alkoxide) or deprotonated carbyne products, as formed in the corresponding reactions of **Ru-1a** with excess *tert*-butoxide[9] or phenoxides.[10-12]

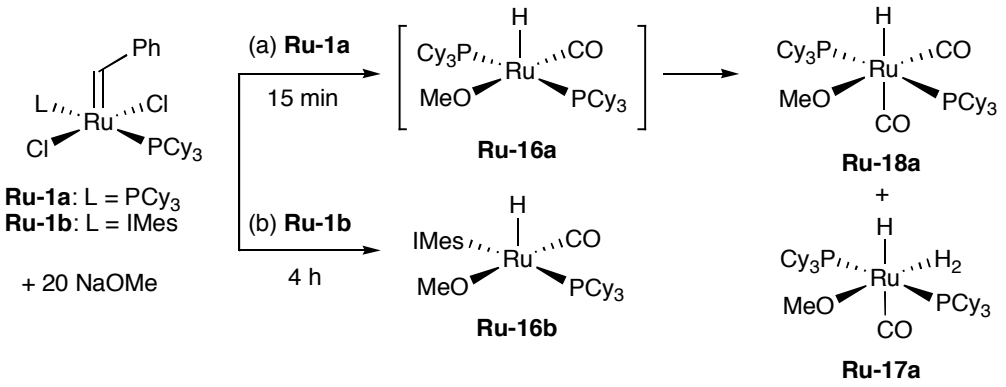

Scheme 4.1. Products observed following reaction of Grubbs catalysts with excess methoxide. Reactions at 23 ˚C in CH_2Cl_2-MeOH. PCy_3, toluene, and formaldehyde also observed; see text. The trans-disposition of the hydride and CO ligands in **Ru-17a** (favored by donor-acceptor push-pull interactions) is suggested by analogy to the structure of **Ru-18a**.

Consumption of **Ru-1b**, in comparison, required several hours even at relatively high proportions of methoxide (4 h at 20 equiv). As shown in Scheme 4.1b, reaction also halted at an earlier stage, yielding five-coordinate RuH(OMe)(CO)(IMes)(PCy_3) **Ru-16b** (a rare example of a coordinatively unsaturated alkoxyhydride complex),[13] rather than **Ru-18b** and/or **Ru-17b**. Addition of excess PCy_3 had no effect on the rate of transformation of **Ru-1b** into **Ru-16b**, although such treatment retarded consumption of the first-generation catalyst **Ru-1a**. We attribute the difference to the much higher lability of the PCy_3 ligand in **Ru-1a**, which gives equilibrium access to four-coordinate $RuCl_2(PCy_3)$(=CHPh) **Ru-1a'** in solution. Salt metathesis via this sterically accessible species (see Path II, Scheme 4.2) is sufficiently faster that the corresponding reaction of the parent **Ru-1a** (Path I) does not compete. The slow salt metathesis of **Ru-1b**, as well as the resistance of **Ru-16b** to further reaction, are consistent with the very low room-temperature lability of the PCy_3 ligand in these IMes complexes,[16] which significantly increases the steric impediment to reaction. The strong binding characteristic of phosphine ligands trans to an NHC ligand is known to retard

dissociative reaction pathways in catalysis, particularly at ambient temperatures. Such behaviour has been documented in hydrogenation and isomerization via the hydride complex **Ru-7b**,[14,15] and in metathesis via **Ru-1b**.[16,17]

A proposed mechanism for the transformation of **Ru-1** into **Ru-16** thus involves initial reaction of **Ru-1** via exchange of both chloride ligands, followed by proton transfer from bound methoxide to benzylidene (see **A**/**A'**; Scheme 4.2), and coordination of formaldehyde to give Ru-benzyl intermediate **B**/**B'**. Deinsertion of CO and liberation of the benzyl group as toluene (and recoordination of PCy_3, in the case of **Ru-16a'**) would then generate **Ru-16a/b**. Labeling evidence consistent with such a pathway was reported by Dinger and Mol[4a] in the transformation of **Ru-1a** into **Ru-7a** with a single equivalent of methoxide. For details (including the key CO deinsertion step), the reader is referred to the mechanism shown in Chapter 1 (Scheme 1.27). More recently, Leung and co-workers invoked the analogous attack by bound methoxide on benzylidene on treatment of $RuCl[N(^iPr_2PS)_2](PCy_3)(=CHPh)$ with NaOMe.[18] These reactions fall into a broader class of proton migrations onto benzylidene from E-R groups on an adjacent ligand[19] (notwithstanding the moderately electrophilic character inferred computationally for $Ru=CH_2$ systems).[20] Proton migration need not be restricted to β- or α-E-H groups: Owen and co-workers recently reported attack on benzylidene by a γ-dihydroborate moiety in a scorpionate derivative of **Ru-1a**,[21] underscoring the point that ligand flexibility, in conjunction with a reactive E-H bond, can expand the scope of this alkylidene transformation pathway. Ru-NHC derivatives[22,23] show substantially higher tolerance toward adjacent N-H functionalities than first-generation complexes,[24] perhaps indicating that migration proceeds via a dissociative pathway (vide infra).

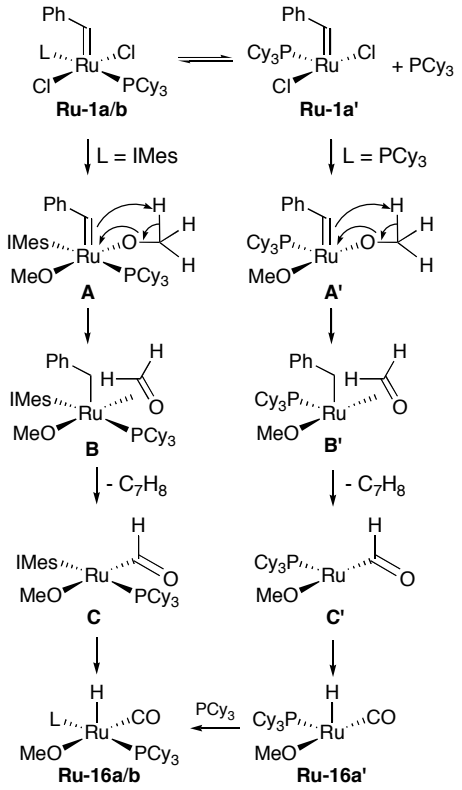

Scheme 4.2. Proposed pathways for transformation of **Ru-1a/b** into five-coordinate **Ru-16a/b**. Product is isolable only for **Ru-16b** (L = IMes). For ensuing reactions of **Ru-16a**/**Ru-16a'**, see text. For L = PCy_3, both of the pathways depicted are feasible, but Path II is kinetically dominant. For L = IMes, only Path I is available, and reaction is slow.

Conversion of the intermediate **Ru-16a** (or, more probably, **Ru-16a'**) into methoxydicarbonyl **Ru-18a** necessitates installation of a further equivalent of methoxide via reaction with methanol. The fact that **Ru-16b** does *not* evolve indicates that the associative pathway is not productive in this case. Scheme 4.3 depicts a plausible pathway for **Ru-16a**, involving coordination of methanol and σ-metathesis[25] of the O-H and Ru-hydride bonds, followed by β-hydride elimination and CO deinsertion as before. Scavenging of H_2 by unreacted **Ru-16a** would account for the competitive formation of dihydrogen adduct **Ru-17a**. Reversible binding of dihydrogen enables release and recycling of **Ru-16a**, as indicated

by the conversion of **Ru-17a** into **Ru-18a** on workup noted above. Transient signals assigned to **Ru-16a** are observed by in situ NMR analysis, at shifts very similar to those for **Ru-16b**, on freeze-pump-thaw degassing solutions of **Ru-17a**. Hydrogen-bonding interactions between incoming methanol and the hydride and/or methoxide ligands may account for the dramatically faster reaction of methanol with **Ru-16a**, vs. the benzylidene complex **Ru-1a** (the latter reaction requires hours even at 60 °C).[5]

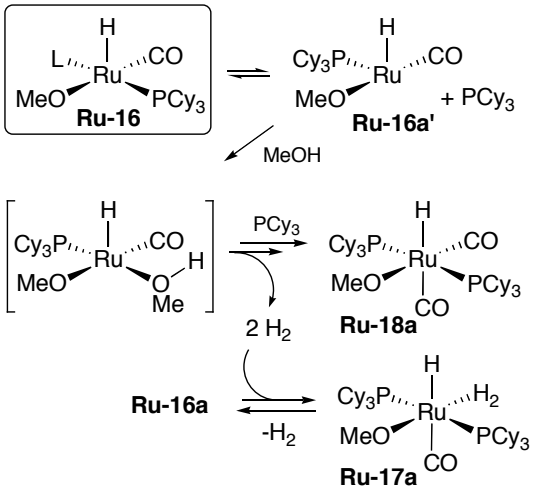

Scheme 4.3. Proposed pathway for transformation of **Ru-16a** into six-coordinate **Ru-18a** and **Ru-17a**.

An anticipated competing pathway involves direct *β*-elimination and deinsertion from **Ru-16a/b** to afford dihydrides $Ru(H)_2(CO)_2(L)(PCy_3)_2$ **Ru-19a/b**. While traces of **Ru-19a** and **Ru-19b** form on workup, this pathway is clearly a minor one. The minimal formation of **Ru-19a** is probably due to the rapid conversion of **Ru-16a** into **Ru-18a** and **Ru-17a**, reflecting the abundance and non-innocence of the methanol cosolvent. Importantly, however, the resistance of **Ru-16b** to transformation into **Ru-19b** implies that *β*-elimination again requires phosphine loss, despite the formal coordinative unsaturation of **Ru-16b**.

Finally, it may be noted that the inhibited methanolysis of **Ru-16b**, relative to **Ru-16a**, contrasts with the behaviour earlier established for the corresponding dihydrogen complexes $RuHCl(H_2)(L)(PCy_3)$ **Ru-6a/b**. The IMes derivative of the latter reacted only marginally more slowly with methanol and NEt_3 than did its PCy_3 analog.[5] The difference may be due to the lability of the H_2 ligand (although this will be attenuated by the cis-hydride effect),[26] which circumvents the requirement for phosphine loss found in the present chemistry. Alternatively, an associative pathway involving outer-sphere, σ-bond metathesis of methanol may be enabled by the acidity of bound H_2.[27] Either is consistent with the reported $[PCy_3]$-independence of the reaction.[5]

4.2.2 Paramagnetic byproducts.

A common challenge in organometallic chemistry is the formation of paramagnetic products that go undetected by direct NMR methods. In the work above, observation of free PCy_3 led us to suspect the presence of such co-products. We quantified the proportion of paramagnetic Ru by integration against Ph_3PO as an internal standard. A ca. 25% decrease in total integration was evident for the reactions of both **Ru-1a** and **Ru-1b**: we attribute this to the formation of paramagnetic species, rather than fluxional diamagnetic products, as low-temperature $^{31}P\{^1H\}$ NMR analysis revealed no additional signals. Notably, however, **Ru-18a** can be prepared in 85% isolated yield from a non-benzylidene precursor (see below), tending to implicate the benzylidene functionality in the Ru(II) to Ru(III) oxidation. It is unclear whether C-H activation of the PCy_3 and/or IMes ligands also contributes: both are well precedented.[28,29] The four-coordinate species generated by phosphine loss is almost certainly a key vector for decomposition, as suggested by parallel experiments with the labile, phosphine-free "third-generation" Grubbs catalyst $RuCl_2(IMes)(py)_2(=CHPh)$ **Ru-1d**.

This complex was completely consumed within 15 min of treating with methoxide, but only ca. 15% of a hydride product was observed, which itself disappears within 1 h.

4.2.3 Preparation of Five-Coordinate Methoxyhydride RuH(OMe)(CO)(IMes)(PCy_3) ***Ru-16b***.

To confirm the identity of **Ru-16b**, we undertook its synthesis on preparative scale from the well-behaved hydride precursors **Ru-7b**. Addition of methanolic NaOMe (20 equiv; Scheme 4.4) to a solution of **Ru-7b** in CH_2Cl_2 at 23 ˚C caused an immediate color change from orange-yellow to red-orange. NMR analysis revealed complete conversion to the new methoxyhydride species RuH(OMe)(CO)(IMes)(PCy_3) **Ru-16b** within 15 minutes. Quantitative conversion was confirmed in separate NMR-scale experiments by integration against Ph_3PO as internal standard, as noted above. Isolation of **Ru-16b** was frustrated by formation of traces of **Ru-18b** and **Ru-19b** on concentrating to dryness, but detailed NMR analysis supports the proposed structure. In particular, the upfield location and doublet multiplicity of the hydride signal (-23.61 ppm; $^2J_{HP}$ = 22 Hz; Table 4.1; cf. the very similar data for chloride analogue **Ru-7b**) provide unequivocal evidence for a square-pyramidal complex in which an apical hydride ligand lies cis to a single basal phosphine. The latter gives rise to a $^{31}P\{^1H\}$ singlet at 50.2 ppm. The hydride signal correlates (HMBC) with the IMes carbene carbon (δ_C 193.9 ppm, d, $^2J_{CP}$ = 103.2 Hz) and a single carbonyl ligand (δ_C 204.7 ppm, d, $^2J_{CP}$ = 8.7 Hz), although not with the broad O*C*H_3 signal (63.5 ppm, $\omega_{0.5}$ 25 Hz). Assignment of the latter was confirmed by a DEPT-135 experiment (–30 ˚C, C_7D_8) and HMQC correlation with the methoxy proton singlet (4.22 ppm). ^1H NOESY-NMR analysis reveals a through-space interaction between the methoxy protons and hydride. Rapid rotation about the Ru-C_{IMes} bond in **Ru-16b** is indicated by the equivalence of the IMes

"backbone" protons, as well as the mesityl *p*-Me nuclei, despite the difference in environment above and below the basal plane of the square pyramid.[30]

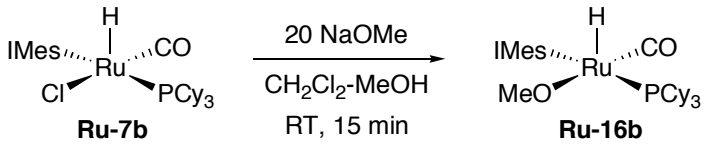

Scheme 4.4. Synthesis of five-coordinate methoxyhydride complex **Ru-16b**.

4.2.4 Synthesis of six-coordinate RuH(OMe)(CO)$_2$(L)(PCy$_3$) ***Ru-18a/b*** *and Ru(H)$_2$(CO)$_2$(IMes)(PCy$_3$)* ***Ru-19b*** *from RuH(OTf)(CO)$_2$(L)(PCy$_3$)* ***Ru-21a/b****.*

High-yield routes to **Ru-18a/b** and **Ru-19b** were devised to support characterization of these previously unreported complexes (Scheme 4.5). We initially envisaged synthesis of **Ru-18** from the known[8] bis(carbonyl) complex RuHCl(CO)$_2$(PCy$_3$)$_2$ **Ru-20a** and its IMes analogue **Ru-20b**. Complexes **Ru-20** were conveniently prepared in ca. 85% isolated yield via reaction of **Ru-7a/b** with CO. Reactions of **Ru-20a** with methanolic NaOMe in THF proved slow (<20% in 4 h), however. We therefore converted **Ru-20a/b** into their more reactive triflates RuH(OTf)(CO)$_2$(L)(PCy$_3$) **Ru-21a/b** by reaction with AgOTf in THF (**Ru-21a**: 70%; **Ru-21b**: 83%). Treatment of **Ru-21a/b** with NaOMe/MeOH in THF effected complete conversion to yellow RuH(OMe)(CO)$_2$(L)(PCy$_3$) **Ru-18a/b** within 30 min.[31] Sodium triflate was removed by stripping the reaction mixture to dryness, extracting with CH_2Cl_2, and filtering through Celite. Reprecipitation with hexanes afforded **Ru-18a/b** as light yellow powders in excellent yields (ca. 85% each).

A convenient route to Ru(H)$_2$(CO)$_2$(IMes)(PCy$_3$) **Ru-19b** from **Ru-21b** was also developed, via reaction with excess NaH at 50 °C in THF. Reaction was complete within 45 min. While high solubility in hexanes and diethyl ether frustrated reprecipitation, crude **Ru-**

19b exhibits spectroscopic features closely similar to those reported for **Ru-19a** (originally prepared by the Chaudret group by treating $Ru(H)_2(H_2)_2(PCy_3)_2$ with CO; data are provided in Table 4.1).[8]

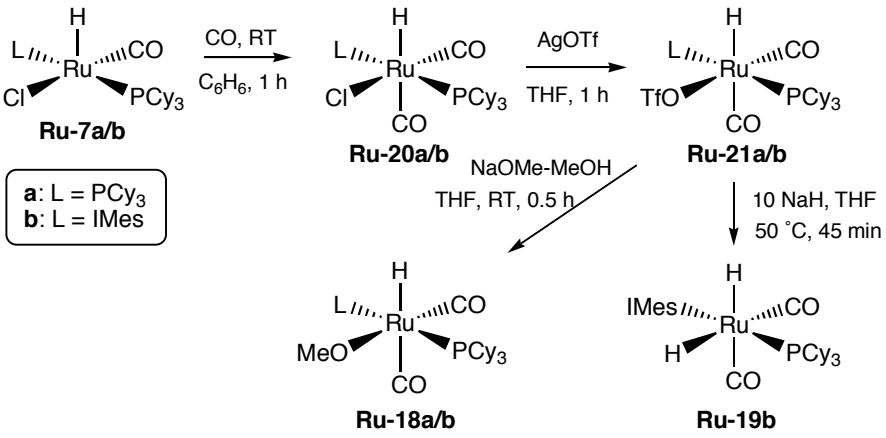

Scheme 4.5. Synthetic routes to **Ru-18a/b** and **Ru-19b** from **Ru-7a/b**.

The structures of the new complexes **Ru-18a/b**, **Ru-19b**, **Ru-20b**, and **Ru-21a/b** were established by one- and two-dimensional NMR experiments, supported by IR spectroscopy,[32] and by elemental analysis for all but **Ru-19b**, which proved highly sensitive toward decomposition even in the solid state. Coordinative saturation in each is indicated by the downfield location of the hydride signal (between –4 and –8 ppm; Table 4.1), the triplet or doublet multiplicities of which indicate retention of the PCy_3 ligand(s) originally present. Trans-disposition of the two PCy_3 groups, or of the PCy_3 and IMes groups, is confirmed from the singlet multiplicity of the ^{31}P NMR signal (for **Ru-18a**, **Ru-21a**), or from the magnitude of $^2J_{CP}$ coupling to the carbene carbon (**Ru-18b**: 96 Hz; **Ru-19b**: 70 Hz; **Ru-20b**: 88 Hz; **Ru-21b**: 84 Hz). In contrast with **Ru-19b**, the symmetry of which results in equivalent carbonyl carbon (and hydride) signals, complexes **Ru-18a/b**, **Ru-20a/b**, and **Ru-21a/b** contain inequivalent carbonyl groups. Each appears as a $^{13}C\{^1H\}$ NMR doublet or

triplet, the $^{2}J_{CP}$ values for which (6-15 Hz) confirm cis-disposition relative to the PCy_3 ligand(s). The expected HMBC correlations are seen between the hydride and the carbonyl and carbene ligands. For methoxides **Ru-18a/b**, assignment of the methoxy carbons (ca. 67 ppm) is confirmed by DEPT-135 analysis and HMQC correlation with the methoxy methyl singlet at ca. 4.0 ppm. A NOESY correlation between the latter and the hydride signal confirms the cis-disposition of these ligands. Finally, the triflate CF_3 groups in **Ru-21a/b** exhibit essentially identical NMR values (a $^{13}C\{^{1}H\}$ quartet at ca. 120 ppm ($^{1}J_{CF}$ = 319 Hz), and a $^{19}F\{^{1}H\}$ singlet at -77 ppm).

Table 4.1. Key NMR chemical shifts (ppm), coupling constants (Hz), and IR bands (cm^{-1}) for hydride complexes discussed in this Chapter.[a]

Complex	NMR solvent	δ_P	δ_H (Ru-X)		δ_{CO} ($^2J_{CP}$)	IR (ν)	
			H ($^2J_{HP}$)	OC*H*$_3$		CO	Ru-H
RuHCl(CO)(L)(PCy_3)							
L = PCy_3, **Ru-7a**[32]	C_6D_6	46.9	–24.21 (t, 18)	–	202.1 (t, 14)	1905	1862
L = IMes, **Ru-7b**[16, 32]	C_6D_6	47.8	–24.82 (d, 21)	–	202.3 (d, 14)	1894	1881
RuH(OMe)(CO)(L)(PCy_3)							
L = IMes, **Ru-16b**[b,c]	C_6D_6	50.2[b]	–23.61 (d, 22)	4.22	204.7 (d, 9)[b]	1875	1890
RuH(OMe)(CO)$_2$(L)(PCy_3)							
L = PCy_3, **Ru-18a**[b]	C_6D_6	53.8	–4.25 (t, 20)	4.10	203.7 (t, 7) 201.4 (t, 12)	2006 1891	1939
L = IMes, **Ru-18b**[b]	C_6D_6	54.0	–4.18 (d, 25)	3.96	202.9 (d, 12) 199.5 (d, 7)	2013 1896	1948
RuH(OMe)(CO)(H$_2$)(L)(PCy_3)							
L = PCy_3, **Ru-17a**[b]	CH_2Cl_2 MeOH	72.0	–7.45 (br s)	n.d.[d]	n.d.[d]	n.d.[d]	n.d.[d]
Ru(H)$_2$(CO)$_2$(L)(PCy_3)							
L = PCy_3, **Ru-19a**[8]	C_6D_6	68.3	–7.9 (t, 23)	–	206.2	2004 1994	n.d.
L = IMes, **Ru-19b**[b]	C_6D_6	68.9	–7.37 (d, 25)	–	204.7 (d, 8)	1995 1951	1898
RuHCl(CO)$_2$(L)(PCy_3)							
L = PCy_3, **Ru-20a**[8]	C_6D_6	49.8	–4.9 (t, 20)	–	201.6 (t, 7) 200.7 (t, 12)	2016[c] 1942[c]	1869[c]
L = IMes, **Ru-20b**[b]	C_6D_6	48.2	–4.77 (d, 23)	–	202.3 (d, 13) 197.2 (d, 7)	2035 1913	1954
RuH(OTf)(CO)$_2$(L)(PCy_3)							
L = PCy_3, **Ru-21a**[b]	C_6D_6	53.7	–4.02 (t, 19)	–	202.7 (t, 14) 201.7 (t, 7)	2046 1966	1917
L = IMes, **Ru-21b**[b]	C_6D_6	51.3	–4.07 (d, 23)	–	204.4 (d, 14) 196.7 (d, 6)	2049 1935	1972

[a]NMR chemical shifts in ppm; coupling constants in Hz; IR bands in cm^{-1}. Values at 23 °C unless otherwise noted. NMR samples in 10:1 CH_2Cl_2-MeOH were spiked with C_6D_6 as a deuterium lock. References are given to literature values in the solvents indicated. [b] This work. [c] Cf. values for transient species **Ru-16a** at –30 °C in C_7D_8: δ_P 47.8 ppm (s); δ_H –22.94 (d, 19 Hz). At 23 °C in C_6D_6, δ_H –22.81 (br t, $^2J_{HP}$ = 17.4 Hz). [d] Measurement of IR and ^{13}C NMR data was hampered by the low proportion of these species.

4.3 Conclusions

The foregoing describes the rapid reaction of the first-generation Grubbs catalyst **Ru-1a** with excess methoxide and methanol at room temperature. Major products are the coordinatively saturated methoxyhydride complexes $RuH(OMe)(CO)_2(PCy_3)_2$ **Ru-18a** and $RuH(OMe)(CO)(H_2)(PCy_3)_2$ **Ru-17a**. Formation of such species may account for the poor isomerization activity found when an excess of primary alkoxides is used to trigger C=C isomerization following **Ru-1a**-mediated metathesis. Reaction of the second-generation catalyst **Ru-1b** with methanolic methoxide is much slower, and terminates at the five-coordinate methoxyhydride complex $RuH(OMe)(CO)(IMes)(PCy_3)$ **Ru-16b**. The identities of the new complexes **Ru-16b** and **Ru-18a/b** were confirmed by independent synthesis from $RuHCl(CO)(IMes)(PCy_3)$ **Ru-7b** or hydridotriflates $RuH(OTf)(CO)_2(L)(PCy_3)$ **Ru-21a/b**, respectively; isolation of $RuH(OMe)(CO)(PCy_3)_2$ **Ru-16a** is hampered by its much higher reactivity. The slower rate of formation of **Ru-16b** at room temperature, and its stability once formed, reflect the low lability characteristic of phosphine ligands trans to an *N*-heterocyclic carbene. This constrains salt metathesis to a non-dissociative pathway for **Ru-1b**, rather than (as with **Ru-1a**) proceeding via a sterically accessible four-coordinate species formed by equilibrium loss of PCy_3. The stability of **Ru-16b** toward reaction with methanol indicates that for this subsequent reaction, the associative pathway is either inaccessible or prohibitively slow. Precipitation of NaCl from solution (in which the proportion of CH_2Cl_2 dominates by 10:1 over MeOH) contributes to the greater driving force of the initial salt metathesis reaction.

Notable in this chemistry is the facility with which these "robust" benzylidene complexes decompose into hydride species under exceptionally mild conditions. Consumption of **Ru-**

1a by alkoxide occurs within minutes at room temperature; loss of **Ru-1b** – while slower – is complete within a few hours. Reaction conditions that can give rise to adventitious alkoxides, particularly in the presence of methanol co-solvent (a favored reaction medium for olefin metathesis reactions of biologically relevant substrates)[34] should thus be recognized as profoundly detrimental to catalytic performance.

4.4 Experimental

4.4.1 General Procedures.

Reactions were carried out at room temperature (23 ˚C) under argon using standard Schlenk or glovebox techniques, unless otherwise stated. Dry, oxygen-free solvents were obtained using a Glass Contour solvent purification system, and stored over Linde 4Å molecular sieves. C_6D_6 was degassed by consecutive freeze/pump/thaw cycles and dried over molecular sieves (Linde 4Å). Methanol was distilled from $Mg(OMe)_2$ under Ar and stored over molecular sieves (Linde 3Å). Sodium methoxide solutions were prepared by digesting Na metal in methanol immediately before use. $RuCl_2(PCy_3)_2(=CHPh)$ **Ru-1a**,[35] $RuCl_2(IMes)(PCy_3)(=CHPh)$ **Ru-1b**,[36,37] and $RuHCl(CO)(L)(PCy_3)$ (**Ru-7a**: L = PCy_3, **Ru-7b**: L = IMes)[33] were prepared according to literature procedures. NMR spectra were recorded on a Bruker Avance 300 or Avance 500 spectrometer, at 298 K unless otherwise specified. Chemical shifts are reported relative to TMS (^{13}C, ^{1}H), 85% external H_3PO_4 (^{31}P), or $CFCl_3$ (^{19}F) at 0 ppm. ^{1}H and ^{13}C NMR spectra were referenced to the carbon or residual proton signal of the deuterated solvent, ^{19}F spectra to CF_3CO_2H at -76.55 ppm. In the NMR assignments of IMes derivatives given below, *a/b* labels indicate corresponding, inequivalent nuclei on the same mesityl ring, as indicated by HMQC or HMBC correlations. IR spectra were measured as Nujol mulls between NaCl plates using a Bomem MB100

spectrometer, or as powders using a Varian 640-IR reflectance IR spectrometer. Microanalyses were carried out by Guelph Chemical Laboratories Ltd., Guelph, Ontario.

4.4.2 NMR-scale reactions of Grubbs catalysts with methoxide.

In a representative reaction, a solution of **Ru-1a** (10 mg, 0.012 mmol) was dissolved in CH_2Cl_2 (0.7 mL, with a 50 μL spike of C_6D_6) in a J. Young NMR tube. To this was added NaOMe as a solution in MeOH (9.7 μL of a 3.75 M solution, 3 equiv), and the reactions were monitored by NMR analysis (in some cases with Ph_3PO added as an internal standard for integration). No solvent suppression was used for the ^1H NMR spectra, as the alkylidene and hydride regions (10 to 30 ppm and 0 to -30 ppm, respectively) could be viewed without interference.

4.4.3 $RuCl_2(PCy_3)_2$(=CHPh) ***Ru-1a*** *+ methoxide: observation of* ***Ru-18a*** *and* ***Ru-17a****.*

The solution changed color from deep purple to pale yellow over 5 min. $^{31}P\{^1H\}$ NMR (CH_2Cl_2-MeOH-C_6D_6): 52.1 (s, **Ru-18a**, 48%), 72.0 (s, **Ru-17a**, 19%); 11.1 (s, PCy_3, 13%); the deficit is attributed to paramagnetic material (see text). ^1H NMR (CH_2Cl_2-MeOH-C_6D_6; hydride region): -4.59 (**Ru-18a**), -7.45 (**Ru-17a**). For the synthesis and full characterization of **Ru-18a**, see below.

4.4.4 $RuCl_2$(IMes)(PCy_3)(=CHPh) ***Ru-1b*** *+ methoxide: observation of* ***Ru-16b****.*

A color change from red to pale orange-yellow occurred over 4 h. $^{31}P\{^1H\}$ NMR (CH_2Cl_2-MeOH-C_6D_6): 49.6 (**Ru-16b**, 73%), 11.1 (s, PCy_3, 10%); the deficit is attributed to paramagnetic material (see text). ^1H NMR (CH_2Cl_2-MeOH-C_6D_6; hydride region): -25.02 ppm (**Ru-16b**). For the synthesis of **Ru-16b** using 20 equiv NaOMe, with full details of NMR characterization, see below.

4.4.5 In Situ Observation of RuH(OMe)(CO)(H_2)(PCy_3)$_2$ ***Ru-17a***.

Complex **Ru-17a** was generated in situ (as a 2:1 mixture of **Ru-18a** and **Ru-17a**) as described above. Sweeping the atmosphere with Ar resulted in partial transformation of **Ru-17a** into **Ru-16a** (ca. 15% vs. the original **Ru-1a**). This was readily reversed by freeze-pump-thaw degassing (3×) and backfilling with H_2. NMR data for **Ru-17a**: $^{31}P\{^1H\}$ NMR (121.5 MHz, 10:1 CH_2Cl_2-MeOH): δ 72.0 (s). ^1H NMR (300.1 MHz, 10:1 CH_2Cl_2-MeOH): -7.45 (br s). Hydride $T_{1(min)}$ (C_7D_8, H_2, 263 K, 500.1 MHz): 37.5 ms (d_{H-H} = 0.95 Å for fast-spinning H_2).[26,38] Decoalescence was not observed down to -90 °C in C_7D_8.

4.4.6 Synthesis of RuH(OCH_3)(CO)(IMes)(PCy_3) ***Ru-16b***.

Adding a solution of NaOMe in methanol (300 μL, 2.75 M, 0.83 mmol, 20 equiv) to a vigorously-stirred solution of RuHCl(CO)(IMes)(PCy_3) **Ru-7b** (31 mg, 0.041 mmol) in 3 mL CH_2Cl_2 caused a color change from orange-yellow to red-orange over 15 min. In situ $^{31}P\{^1H\}$ NMR analysis indicated solely **Ru-16b**. The solvent was stripped off, and the residue was redissolved in benzene, filtered through Celite, and stripped to dryness. Yield 24 mg (78%). $^{31}P\{^1H\}$ NMR analysis of the residue revealed, in addition to **Ru-16b**, small amounts of Ru$(H)_2$(CO)$_2$(IMes)(PCy_3) **Ru-19b** (5%), RuH(OMe)(CO)$_2$(IMes)(PCy_3) **Ru-18b** (2%), and free PCy_3 (5%), which impede microanalysis. Data for **Ru-16b**: $^{31}P\{^1H\}$ NMR (121.5 MHz, C_7D_8): δ 50.2 (s). ^1H NMR (300.1 MHz, C_6D_6): δ 6.85 (s, 2H, Mes *m*-C*H*^{b}) 6.83 (s, 2H, Mes *m*-C*H*^{a}), 6.26 (s, 2H, =C*H*N), 4.22 (s, 3H, OCH_3), 2.42-2.38 (two overlapping s, 12H, Mes *o*-CH_3), 2.14 (s, 6H, Mes *p*-CH_3), 2.2-1.1 (m, Cy; accurate integration impeded by overlap with Cy signals for **Ru-18b**, **Ru-19b**), -23.61 (d, $^2J_{HP}$ = 22.2 Hz, 1H, Ru*H*). $^{13}C\{^1H\}$ NMR (125.8 MHz, C_7D_8, 243 K): δ 204.7 (d, $^2J_{CP}$ = 8.7 Hz, *C*O), 193.9 (d, $^2J_{CP}$ = 103.2 Hz, N*C*N), 138.3 (s, Mes *p*-*C*), 138.0 (br, Mes *o*-*C*), 137.3 (br, Mes *o*-

C), 136.4 (s, Mes *i-C*), 129.0 (s, Mes *m-C*H), 122.1 (s, =*C*HN), 63.5 (br s, $\omega_{0.5}$ 25 Hz, O*C*H_3), 34.2 (d, $^1J_{CP}$ = 16.6 Hz, C1 of Cy), 31.1 (s, Cy), 30.2 (s, Cy) 28.6 (m, Cy), 27.4 (s, Cy), 21.5 (s, Mes *p-C*H_3), 19.3 (s, Mes *o-C*H_3). IR (Nujol, cm^{-1}): ν(CO) 1875 (s); ν(Ru-H) 1890 (w).

4.4.7 Preparation of RuH(OMe)(CO)$_2$(L)(PCy$_3$) ***Ru-18a/b****. L = PCy$_3$,* ***Ru-18a****.*

Addition of NaOMe as a solution in methanol (49 μL, 3.58 M, 0.18 mmol) to RuH(OSO_2CF_3)$(CO)_2(PCy_3)_2$ **Ru-21a** (150 mg, 0.173 mmol) in THF (5 mL), with stirring, caused a color change from pale brown to yellow over 30 min, and deposition of a white precipitate. The reaction mixture was stripped to dryness, and the residue was taken up in CH_2Cl_2 (15 mL). The mixture was filtered through Celite, concentrated to ca. 0.5 mL, treated with hexanes (5 mL), and chilled to -35 ˚C. A light yellow powder deposited, which was filtered off, washed with cold hexanes (3 × 2 mL) and dried under vacuum. Yield: 110 mg (85%). $^{31}P\{^1H\}$ (121.5 MHz, C_6D_6): δ 53.8 (s). ^1H NMR (300.1 MHz, C_6D_6): δ 4.10 (s, 3H, O*CH$_3$*), 2.3–1.2 (m, 66H, Cy), –4.25 (t, $^2J_{HP}$ = 20.2 Hz, 1H, Ru*H*). $^{13}C\{^1H\}$ (125.8 MHz, C_6D_6): δ 203.7 (t, $^2J_{CP}$ = 6.6 Hz, *C*O), 201.4 (t, $^2J_{CP}$ = 11.6 Hz, *C*O), 66.4 (s, O*C*H_3), 34.4 (vt, $^1J_{CP}$ = 10 Hz, C1 of Cy), 29.8 (d, J_{CP} = 2.6 Hz (or two overlapping s), Cy), 28.3 (overlapping m, Cy), 27.1 (s, C4 of Cy). IR (Nujol, cm^{-1}): ν(CO) 2006 (s), 1891 (s); ν(Ru-H) 1939 (w). Anal. Calcd. for $C_{39}H_{70}O_3P_2Ru$: C, 62.46; H, 9.41. Found: C, 62.07; H, 9.77.

L = IMes, ***Ru-18b****.*

The light yellow powder was prepared as for **Ru-18a**, from RuH(OSO_2CF_3)$(CO)_2$(IMes)(PCy_3) **Ru-21b** (154 mg, 0.173 mmol). Yield: 115 mg (86%). $^{31}P\{^1H\}$ NMR (121.5 MHz, C_6D_6): δ 54.0 (s). ^1H NMR (300.1 MHz, C_6D_6): δ 6.91 (s, 2H,

Mes *m*-C*H*^{a}), 6.89 (s, 2H, Mes *m*-C*H*^{b}), 6.32 (s, 2H, =C*H*N), 3.96 (s, 3H, OCH_3), 2.37 (s, 6H, Mes *o*-CH_3^{b}), 2.30 (s, 6H, Mes *o*-CH_3^{a}), 2.20 (s, 6H, Mes *p*-CH_3), 2.2-1.0 (m, 33H, Cy), -4.18 (d, $^2J_{HP}$ = 25.3 Hz, 1H, Ru*H*). $^{13}C\{^1H\}$ NMR (125.8 MHz, C_6D_6): δ 202.9 (d, $^2J_{CP}$ = 12.4 Hz, *C*O), 199.5 (d, $^2J_{CP}$ = 6.9 Hz, *C*O), 187.5 (d, $^2J_{CP}$ = 95.6 Hz, N*C*N), 139.4 (s, Mes *i*-*C*), 138.2 (s, Mes *p*-*C*), 137.4 (s, Mes *o*-*C*^{a}), 136.2 (s, Mes *o*-*C*^{b}), 129.2 (s, Mes *m*-*C*H^{b}), 128.9 (s, Mes *m*-*C*H^{a}), 122.3 (m, =*C*HN), 67.4 (s, O*C*H$_3$), 34.1 (d, $^1J_{CP}$ = 18.8 Hz, C1 of Cy), 29.4 (d, J_{CP} = 6.9 Hz (or two overlapping s), Cy), 28.3 (d, $^3J_{CP}$ = 9.9 Hz, Cy), 28.3 (d, $^3J_{CP}$ = 10.1 Hz, Cy), 27.0 (s, C4 of Cy), 21.2 (s, Mes *p*-*C*H$_3$), 18.4 (overlapping s, Mes *o*-*C*H$_3$). IR (powder, cm^{-1}): ν(CO) 2013 (s), 1896 (s); ν(Ru-H) 1948 (w). Anal. Calcd. for $C_{42}H_{62}N_2O_3PRu$: C, 65.09; H, 8.06; N, 3.61. Found: C, 64.76; H, 7.96; N, 3.67.

4.4.8 Preparation of Ru(H)$_2$(CO)$_2$(IMes)(PCy$_3$) ***Ru-19b***.

Solid NaH (30 mg, 1.3 mmol) was added to a solution of RuH(OSO$_2$CF$_3$)(CO)$_2$(IMes)(PCy$_3$) **Ru-21b** (110 mg, 0.123 mmol) in THF (1.0 mL), and the reaction mixture was heated to 50 ˚C. A color change from pale brown to light yellow occurred over 45 min, accompanied by complete transformation to **Ru-19b**. The solvent was stripped off, and the residue taken up in benzene (5 mL) and filtered through Celite. Additional, unassigned NMR signals (<5% total integration) were observed when the filtrate was stripped to dryness and redissolved in C_6D_6. Attempts to obtain pure **Ru-19b** by reprecipitation from benzene-hexanes, benzene-diethyl ether, or neat hexanes were frustrated by high solubility, and satisfactory microanalysis could not be obtained. $^{31}P\{^1H\}$ NMR (121.5 MHz, C_6D_6): δ 68.9 (s). ^1H NMR (300.1 MHz, C_6D_6): δ 6.88 (s, 4H, Mes *m*-C*H*), 6.28 (s, 2H, =C*H*N), 2.24 (s, 12H, Mes *o*-CH_3), 2.19 (s, 6H, Mes *p*-CH_3), 2.0-1.1 (m, 33H, Cy), -7.37 (d, $^2J_{HP}$ = 24.9 Hz, 2H, Ru*H*). $^{13}C\{^1H\}$ NMR (125.8 MHz, C_6D_6): δ 204.7 (d,

$^2J_{CP}$ = 7.7 Hz, *C*O), 190.1 (d, $^2J_{CP}$ = 69.8 Hz, NCN), 139.6 (s, Mes *i-C*), 138.0 (s, Mes *p-C*), 136.1 (s, Mes *o-C*), 129.2 (s, Mes *m-C*H), 121.5 (s, =*C*HN), 37.9 (d, $^1J_{CP}$ = 20.9 Hz, C1 of Cy), 30.1 (s, Cy), 28.1 (d, J_{CP} = 10.1 Hz, Cy), 27.0 (s, C4 of Cy), 21.2 (s, Mes *p-C*H_3), 18.6 (s, Mes *o-C*H_3). IR (Nujol, cm^{-1}): ν(CO) 1995 (s), 1951 (s); ν(Ru-H) 1898 (w).

4.4.9 Preparation of RuHCl(CO)$_2$(IMes)(PCy$_3$) ***Ru-20b***.

(Known[8] **Ru-20a** was prepared similarly, in 84% yield). An orange-yellow solution of RuHCl(CO)(IMes)(PCy$_3$) **Ru-7b** (320 mg, 0.546 mmol) in benzene (5 mL) was stirred under 1 atm CO for 1 h, after which the colorless solution was concentrated (ca. 0.5 mL) and hexanes added to precipitate the white product. This was reprecipitated from benzene-hexanes, filtered off, washed with cold hexanes (3 × 2 mL) and dried under vacuum. Yield: 270 mg (81%). $^{31}P\{^1H\}$ NMR (121.5 MHz, C_6D_6): δ 48.2 (s). ^1H NMR (300.1 MHz, C_6D_6): δ 6.87 (s, 2H, Mes *m*-C*H*), 6.84 (s, 2H, Mes *m*-C*H*), 6.28 (s, 2H, =C*H*N), 2.36 (s, 6H, Mes *o*-CH_3), 2.34 (s, 6H, Mes *o*-CH_3), 2.21 (s, 6H, Mes *p*-CH_3), 2.3-1.1 (m, 33H, Cy), -4.77 (d, $^2J_{HP}$ = 22.8 Hz, 1H, Ru*H*). $^{13}C\{^1H\}$ NMR (125.8 MHz, C_6D_6): δ 202.3 (d, $^2J_{CP}$ = 12.6 Hz, *C*O), 197.2 (d, $^2J_{CP}$ = 6.6 Hz, *C*O), 184.6 (d, $^2J_{CP}$ = 88.4 Hz, NCN), 139.4 (m, Mes *i-C*), 138.5 (s, Mes *p-C*), 136.9 (m, Mes *o-C*), 136.6 (m, Mes *o-C*), 129.4 (m, Mes *m-C*H), 122.7 (overlapping s, =*C*HN), 34.5 (d, $^1J_{CP}$ = 20.0 Hz, C1 of Cy), 29.3 (d, *J* = 12.4 Hz (or overlapping s), Cy), 28.0 (d, J_{CP} = 9.0 Hz, Cy), 27.9 (d, J_{CP} = 9.0 Hz, Cy), 26.8 (s, C4 of Cy), 21.2 (s, Mes *p-C*H_3), 18.8 (s, Mes *o-C*H_3), 18.7 (s, Mes *o-C*H_3). IR (powder, cm^{-1}): ν(CO) 2035 (s), 1913 (s); ν(Ru-H) 1954 (w). Anal. Calcd. for $C_{41}H_{59}ClN_2O_2PRu$: C, 63.18; H, 7.63; N, 3.59. Found: C, 63.09; H, 7.53; N, 3.63.

4.4.10 Preparation of $RuH(OSO_2CF_3)(CO)_2(L)(PCy_3)$ ***Ru-21a/b****. L = PCy_3,* ***Ru-21a****.*

Solid $AgOSO_2CF_3$ (90 mg, 0.35 mmol) was added to $RuHCl(CO)_2(PCy_3)_2$ **Ru-20a** (250 mg, 0.35 mmol) in THF (15 mL) in a foil-wrapped vessel, and stirred for 1 h. The solvent was stripped off under vacuum, and the residue extracted with CH_2Cl_2 (3 × 5 mL). The combined extracts were filtered through Celite, concentrated (ca. 0.5 mL), and treated with hexanes to precipitate the pale beige powder. This was chilled (-35 °C), filtered off, washed with cold hexanes (3 × 2 mL), and dried under vacuum. Yield: 200 mg (70%). $^{31}P\{^1H\}$ NMR (121.5 MHz, C_6D_6): δ 53.7 (s). ^1H NMR (300.1 MHz, C_6D_6): δ 2.4-1.0 (m, 66H, Cy), -4.02 (t, $^2J_{HP}$ = 18.8 Hz, 1H, Ru*H*). $^{13}C\{^1H\}$ NMR (125.8 MHz, C_6D_6): δ 202.7 (t, $^2J_{CP}$ = 13.5 Hz, *C*O), 201.7 (t, $^2J_{CP}$ = 7.0 Hz, *C*O), 119.8 (q, $^1J_{CF}$ = 319.2 Hz, OSO_2CF_3), 34.7 (br s, C1 of Cy), 29.7 (d, J_{CP} = 12.2 Hz (or overlapping s), Cy), 27.7 (m, Cy), 26.8 (s, C4 of Cy). $^{19}F\{^1H\}$ NMR (282.4 MHz, C_6D_6): δ -77.2 (s, CF_3). IR (powder, cm^{-1}): ν(CO) 2046 (s), 1966 (s); ν(Ru-H) 1917 (w). Anal. Calcd. for. $C_{39}H_{67}F_3O_5P_2RuS$: C, 53.96; H, 7.78 Found: C, 54.22; H, 8.20.

L = IMes, ***Ru-21b****.*

Reaction as for **Ru-21a**, using $RuHCl(CO)_2(IMes)(PCy_3)$ **Ru-20b** (250 mg, 0.321 mmol) as precursor. Yield of the pale beige powder: 190 mg (83%). In the NMR assignments, *a/b* labels indicate corresponding, inequivalent nuclei on the same mesityl ring, as indicated by HMQC or HMBC correlations; a prime label is used to differentiate the two Mes rings. $^{31}P\{^1H\}$ NMR (121.5 MHz, C_6D_6): δ 51.3 (s). ^1H NMR (300.1 MHz, C_6D_6): δ 6.94 (s, 1H, Mes *m*-CH^{a}'), 6.89 (s, 1H, Mes *m*-CH^{a}), 6.84 (s, 1H, Mes *m*-CH^{b}), 6.73 (s, 1H, Mes *m*-CH^{b}'), 6.32 (s, 1H, =C*H*N), 6.22 (s, 1H, =C*H*N), 2.57 (s, 3H, Mes *o*-CH_3^{a}'), 2.34 (s, 3H, Mes *o*-CH_3^{a}), 2.19 (s, 3H, Mes *p*-CH_3), 2.12 (s, 3H, Mes *p*-CH_3'), 2.02 (overlapping s; 6H,

Mes *o*-CH_3^b, *o*-C$H_3^{b'}$), 2.2-1.0 (m, 33H, Cy), -4.07 (d, $^2J_{HP}$ = 23.1 Hz, 1H, Ru*H*). $^{13}C\{^1H\}$ NMR (125.8 MHz, C_6D_6): δ 204.4 (d, $^2J_{CP}$ = 13.9 Hz, *C*O), 196.7 (d, $^2J_{CP}$ = 5.5 Hz, *C*O), 182.3 (d, $^2J_{CP}$ = 83.8 Hz, N*C*N), 139.9 (s, Mes *i*-*C*), 139.7 (s, Mes *p*-*C'*), 138.3 (s, Mes *p*-*C*), 138.1 (s, Mes *o*-$C^{a'}$), 137.5 (s, Mes *o*-C^a), 137.3 (s, Mes *i*-*C*'), 135.3-135.2 (overlapping s, Mes *o*-C^b, *o*-$C^{b'}$), 130.4 (s, Mes *m*-C$H^{a'}$), 129.4 (s, Mes *m*-CH^a), 129.1 (s, Mes *m*-C$H^{b'}$), 128.5 (s, Mes *m*-CH^b), 123.5 (s, =*C*HN), 119.9 (q, $^1J_{CF}$ = 320.4 Hz, OSO_2CF_3), 34.2 (d, $^1J_{CP}$ = 15.7 Hz, C1 of Cy), 29.3 (overlapping s, Cy), 27.8 (d, J_{CP} = 10.2 Hz, Cy), 27.7 (d, J_{CP} = 10.4 Hz, Cy), 26.7 (s, C4 of Cy), 21.0 (coincident s, Mes *p*-CH_3, *p*-CH_3'), 19.1 (s, Mes *o*-CH_3), 18.4-18.3 (overlapping s, Mes *o*-CH_3). $^{19}F\{^1H\}$ NMR (282.4 MHz, C_6D_6): δ –77.1 (s, CF_3). IR (powder, cm^{-1}): ν(CO) 2049 (s), 1935 (s); ν(Ru-H) 1972 (w). Anal. Calcd. for $C_{42}H_{59}F_3N_2O_5PRuS$: C, 56.49; H, 6.66; N, 3.14. Found: C, 56.65; H, 6.68; N, 3.10.

4.5 References.

(1) Alcaide, B.; Almendros, P.; Luna, A. *Chem. Rev.* **2009**, *109*, 3817-3858.
(2) Alcaide, B.; Almendros, P. *Chem. Eur. J.* **2003**, *9*, 1259-1262.
(3) Tandem catalysis originating in the Grubbs complexes has been reviewed: (a) Shindoh, N.; Takemoto, Y.; Takasu, K. *Chem. Eur. J.* **2009**, *15*, 12168-12179. (b) Wasilke, J.-C.; Obrey, S. J.; Baker, R. T.; Bazan, G. C. *Chem. Rev.* **2005**, *105*, 1001-1020. (c) Fogg, D. E.; dos Santos, E. N. *Coord. Chem. Rev.* **2004**, *248*, 2365-2379.
(4) Heating the Grubbs catalysts with primary alkoxides, or alcohols and base, generated RuHCl(CO)(L)(PCy_3) (**Ru-7a**: L = PCy_3; **Ru-7b'**: L = H_2IMes) in 30-50% yield. See: (a) Dinger, M.B.; Mol, J.C. *Organometallics* **2003**, *22*, 1089-1095. (b) Dinger, M.B.; Mol, J.C. *Eur. J. Inorg. Chem.* **2003**, 2827-2833. Trace **Ru-7b'** also forms on washing **Ru-1a** with methanol (see: (c) Trnka, T.M.; Morgan, J.P.; Sanford, M.S.; Wilhelm, T.E.; Scholl, M.; Choi, T.-L.; Ding, S.; Day, M.W.; Grubbs, R.H. *J. Am. Chem. Soc.* **2003**, *125*, 2546-2558). Thermolysis of Fischer carbenes permits isolation of **Ru-7a** in 69% yield ((d) Louie, J.; Grubbs, R. H. *Organometallics* **2002**, *21*, 2153-2164) or **Ru-7b'** in quantitative yield ((e) Arisawa, M.; Terada, Y.; Takahashi, K.; Nakagawa, M.; Nishida, A. *J. Org. Chem.* **2006**, *71*, 4255-4261). In tandem ROMP-hydrogenation by various Grubbs catalysts, hydrogenation is catalyzed by **Ru-7a/b** generated in the presence of H_2, amine base and methanol. See: (f) Camm, K.D.; Castro, N.M.; Liu, Y.; Czechura, P.; Snelgrove, J.L.; Fogg, D.E. *J. Am. Chem. Soc.* **2007**, *129*, 4168-4169. (g) Drouin, S.D.; Zamanian, F.; Fogg, D.E. *Organometallics* **2001**, *20*, 5495-5497. Catalyst-specific protocols give improved yields of **Ru-7**: see ref. 5. Thus, sequential hydrogenolysis and methanolysis of **Ru-1a** maximizes formation of **Ru-7a** (72% net yield); in contrast, reaction with methanol and NEt_3 maximizes conversion of **Ru-1b** into **Ru-7b** (83%).
(5) Beach, N. J.; Camm, K. D.; Fogg, D. E. *Organometallics* **2010**, *29*, 5450-5455.
(6) Schmidt, B. *J. Org. Chem.* **2004**, *69*, 7672-7687.
(7) Beach, N. J.; Blacquiere, J. M.; Drouin, S. D.; Fogg, D. E. *Organometallics* **2009**, *28*, 441-447.
(8) Christ, M. L.; Sabo-Etienne, S.; Chaudret, B. *Organometallics* **1994**, *13*, 3800-3804.
(9) Sanford, M. S.; Henling, L. M.; Day, M. W.; Grubbs, R. H. *Angew. Chem., Int. Ed.* **2000**, *39*, 3451-3453.
(10) Conrad, J. C.; Amoroso, D.; Czechura, P.; Yap, G. P. A.; Fogg, D. E. *Organometallics* **2003**, *22*, 3634-3636.
(11) Coalter, J. N.; Bollinger, J. C.; Eisenstein, O.; Caulton, K. G. *New J. Chem.* **2000**, *24*, 925-927.
(12) Caskey, S. R.; Stewart, M. H.; Ahn, Y. J.; Johnson, M. J. A.; Kampf, J. W. *Organometallics* **2005**, *24*, 6074-6076.
(13) A prior example of a five-coordinate Ru-alkoxyhydride complex, RuH(OEt)(CO)(P^tBu_2Me)$_2$, was found to decompose rapidly in solution. See (a) Poulton, J.T.; Sigalas, M.P.; Felting, K.; Streib, W.E.; Eisenstein, O.; Caulton, K. G. *Inorg. Chem.* **1994**, *33*, 1476-1485. Several coordinatively saturated methoxyhydrides have been isolated: (b) FeH(OMe)[κ^4−P($CH_2CH_2PMe_2$)$_3$]; Field, L. D.; Messerle, B. A.; Smernik, R. J. *Inorg. Chem.* **1997**, *36*, 5984-5990. (c) *mer-cis*-IrHCl(OMe)(PEt_3)$_3$; Blum, O.; Milstein, D. *Angew. Chem., Int. Ed. Engl.* **1995**, *34*, 229-231. (d) OsHCl(NO)(OMe)(P^iPr_3)$_2$; Werner, H.; Michenfelder, A.; Schulz, M. *Angew. Chem., Int. Ed. Engl.* **1991**, *30*, 596-598. (e) cis-

[IrH(OMe)(PMe_3)$_4$]PF_6; Milstein, D.; Calabrese, J. C.; Williams, I. D. *J. Am. Chem. Soc.* **1986**, *108*, 6387-6389. (f) $Cp^*_2ZrH(OMe)$; Manriquez, J. M.; McAlister, D. R.; Sanner, R. D.; Bercaw, J. E. *J. Am. Chem. Soc.* **1976**, *98*, 6733-6735. For polynuclear examples, see: (g) Buil, M. L.; Esteruelas, M. A.; Modrego, J.; Onate, E. *New J. Chem.* **1999**, *23*, 403-406. (h) Lee, K. K. H.; Wong, W. T. *J. Chem. Soc., Dalton Trans.* **1996**, 1707-1720.
(14) Dharmasena, U. L.; Foucault, H. M.; dos Santos, E. N.; Fogg, D. E.; Nolan, S. P. *Organometallics* **2005**, *24*, 1056-1058.
(15) Lee, H. M.; Smith, D. C., Jr.; He, Z.; Stevens, E. D.; Yi, C. S.; Nolan, S. P. *Organometallics* **2001**, *20*, 794-797.
(16) Sanford, M. S.; Love, J. A.; Grubbs, R. H. *J. Am. Chem. Soc.* **2001**, *123*, 6543-6554.
(17) Fogg, D. E.; Foucault, H. M., Ring-Opening Metathesis Polymerization. In *Comprehensive Organometallic Chemistry III*, Crabtree, R. H.; Mingos, D. M. P., Eds. Elsevier: Oxford, 2007; Vol. 11, pp 623-652.
(18) Cheung, W.-M.; Chiu, W.-H.; Yi, X.-Y.; Zhang, Q.-F.; Williams, I. D.; Leung, W.-H. *Organometallics* **2010**, *29*, 1981-1984.
(19) In striking contrast, attack of bound phenoxide on the alkylidene proton results in α-elimination of phenol and formation of a ruthenium carbyne (see above, and refs. 10-12).
(20) Occhipinti, G.; Jensen, V. R. *Organometallics* **2011**, *30*, 3522–3529.
(21) Rudolf, G. C.; Hamilton, A.; Orpen, A. G.; Owen, G. R. *Chem. Commun.* **2009**, 553-555.
(22) Wilson, G. O.; Porter, K. A.; Weissman, H.; White, S. R.; Sottos, N. R.; Moore, J. S. *Adv. Synth. Catal.* **2009**, *351*, 1817-1825.
(23) Jong, H.; Patrick, B. O.; Fryzuk, M. D. *Organometallics* **2011**, *30*, 2333-2341.
(24) Occhipinti, G.; Bjorsvik, H.-R.; Toernroos, K. W.; Jensen, V. R. *Organometallics* **2007**, *26*, 5803-5814.
(25) Both σ-bond metathesis and σ-complex-assisted metathesis are plausible: we favor the latter, given the evidence for a dissociative pathway. See: Perutz, R. N.; Sabo-Etienne, S. *Angew. Chem., Int. Ed.* **2007**, *46*, 2578-2592.
(26) (a) Jessop, P.G.; Morris, R.H. *Coord. Chem. Rev.* **1992**, *121*, 155-284. (b) Kubas, G.J., *Metal Dihydrogen and σ-Bond Complexes*. Kluwer/Plenum: Dordrecht, 2001.
(27) Clapham, S. E.; Hadzovic, A.; Morris, R. H. *Coord. Chem. Rev.* **2004**, *248*, 2201-2237.
(28) For leading early examples of C-H activation of cyclohexylphosphine ligands at Ru centres, see: (a) Christ, M. L.; Sabo-Etienne, S.; Chaudret, B. *Organometallics* **1995**, *14*, 1082-1084. (b) Borowski, A.; Sabo-Etienne, S.; Christ, M. L.; Donnadieu, B.; Chaudret, B. *Organometallics* **1996**, *15*, 1427-1434. (c) Leitner, W.; Six, C. *Chem. Ber.* **1997**, *130*, 555-558. (d) Six, C.; Gabor, B.; Gorls, H.; Mynott, R; Philipps, P. *Organometallics*, **1999**, *18*, 3316-3326. Exhaustive dehydrogenation of the cyclohexyl rings affords paramagnetic products. See (e) Amoroso, D.; Yap, G. P. A.; Fogg, D. E. *Can. J. Chem.* **2001**, *79*, 958-963.
(29) For selected examples of activation of IMes ligands at electron-rich Ru centres, see: (a) Abdur-Rashid, K.; Fedorkiw, T.; Lough, A. J.; Morris, R. H. *Organometallics* **2004**, *23*, 86-94. (b) Chilvers, M. J.; Jazzar, R. F. R.; Mahon, M. F.; Whittlesey, M. K. *Adv. Synth. Catal.* **2003**, *345*, 1111-1114. (c) Jazzar, R. F. R.; Macgregor, S. A.; Mahon, M. F.; Richards, S. P.; Whittlesey, M. K. *J. Am. Chem. Soc.* **2002**, *124*, 4944-4945. For an early review of bond activation within NHC ligands, see: Crudden, C. M.; Allen, D. P. *Coord. Chem. Rev.* **2004**, *248*, 2247-2273.

(30) Rotation about the metal-C_{NHC} bond at room temperature is commonly observed for aryl-NHC complexes. See, for example: (a) Dible, B.R.; Sigman, M.S. *Inorg. Chem.* **2006**, *45*, 8430-8441; (b) Ritleng, V.; Barth, C.; Brenner, E.; Milosevic, S.; Chetcuti, M.J. *Organometallics* **2008**, *27*, 4223-4228; (c) Lee, J.P.; Ke, Z.; Ramirez, M.A.; Gunnoe, T.B.; Cundari, T.R.; Boyle, P.D.; Petersen, J.L. *Organometallics* **2009**, *28*, 1758-1775. (d) Kotyk, M. W.; Gorelsky, S. I.; Conrad, J. C.; Carra, C.; Fogg, D. E. *Organometallics* **2009**, 5424–5431.
(31) Related chemistry was suggested by a referee as an alternative route to **Ru-16a/b**, via reaction of **Ru-7a/b** with AgOTf, then NaOMe. This was explored for **Ru-7b**, but is thwarted by the rapid decomposition of **Ru-7b** in the presence of AgOTf.
(32) Two strong ν(CO) bands, and one weak ν(Ru-H) band, were observed in the IR spectrum for each of **Ru-18a/b**, **Ru-20a/b**, and **Ru-21a/b**.
(33) Beach, N. J.; Dharmasena, U. L.; Drouin, S. D.; Fogg, D. E. *Adv. Synth. Catal.* **2008**, *350*, 773-777.
(34) Camm, K. D.; Fogg, D. E., From Drug Cocktails to Tissue Engineering: Synthesis of ROMP Polymers for Biological Applications. In *NATO Sci. Ser. II*, Imamoglu, Y.; Dragutan, V., Eds. Springer Verlag: Berlin, 2007; Vol. 243, pp 285-303.
(35) Schwab, P.; Grubbs, R. H.; Ziller, J. W. *J. Am. Chem. Soc.* **1996**, *118*, 100-110.
(36) Scholl, M.; Ding, S.; Lee, C. W.; Grubbs, R. H. *Org. Lett.* **1999**, *1*, 953-956.
(37) Huang, J.; Stevens, E. D.; Nolan, S. P.; Petersen, J. L. *J. Am. Chem. Soc.* **1999**, *121*, 2674-2678.
(38) See ref. 26a and: (a) Bautista, M.T.; Cappellani, E.P.; Drouin, S.D.; Morris, R.H.; Schweitzer, C.T.; Sella, A.; Zubkowski, J. *J. Am. Chem. Soc.* **1991**, *113*, 4876-4687. (b) Maltby, P. A.; Schlaf, M.; Steinbeck, M.; Lough, A. J.; Morris, R. H.; Klooster, W. T.; Koetzle, T. F.; Srivastava, R. C. *J. Am. Chem. Soc.* **1996**, *118*, 5396-5407.

Chapter 5. Generating $RuHCl(CO)(L)(PCy_3)$ from the Initiating, Resting, and Quenched States of First- and Second-Generation Grubbs Catalysts

5.1 Introduction.

Recent advances in tandem catalysis involving (R)CM-functionalization were discussed in Chapter 1. Because these approaches are typically product-oriented, the identity of the second catalyst species is often a matter of conjecture. By extension, so are the optimal reaction protocols used to generate it from the metathesis catalyst. Our group has demonstrated the advantages of a mechanistic approach to optimization in ROMP-hydrogenation (see Chapter 1).[1,2] The protocols developed to efficiently transform Ru-alkylidenes into hydridocarbonyl **Ru-7** may hold unexploited promise for other tandem catalysis methodologies, of which tandem (R)CM-isomerization is one obvious candidate.

In Ru-catalyzed RCM and CM, however, the resting state is normally a methylidene species such as $RuCl_2(L)(PCy_3)(=CH_2)$ **Ru-2**. A key question thus centers on whether the $[Ru]=CH_2$ entity differs in its reaction chemistry from its better-studied [Ru]=CHPh parent. Despite the central importance of methylidene complexes in RCM[3] and CM[4] reactions, their organometallic chemistry remains almost wholly unexamined. While one report suggests that the behaviour of **Ru-2a** parallels that of its benzylidene parent, at least for hydrogenolysis at ambient temperatures,[5] we suspected that thermal stability might emerge as an important distinction. Methylidene complexes are notoriously fragile. The first-generation complex **Ru-2a**, for example, has a half-life of 40 min in C_6D_6 at 55 °C,[6] vs. 8 days for the benzylidene parent. Further, fundamental differences between the benzylidene and methylidene functionalities are suggested by the report that **Ru-2a** decomposes via a unimolecular pathway, but **Ru-1a** via a bimolecular pathway.[7] A clearer understanding of

the conditions under which such species can be efficiently transformed into other catalysts could greatly benefit tandem metathesis methodologies that begin with RCM or CM.

Of corresponding interest is the behaviour of the Fischer carbene products formed by the common practice of quenching Ru metathesis catalysts with ethyl vinyl ether.[8] Such heteroatom-functionalized alkylidenes (as well as [Ru]=CHC(O)R analogues), are less robust than their benzylidene parents: in some cases, they undergo decomposition faster than metathesis. The [Ru]=$CHCO_2Me$ entity, for example, is too unstable to detect at room temperature.[9,10] Similarly, Renata Nunes of this research group[11] noted that the [Ru]=CHC(O)Me moiety formed from **Ru-2a** or the "third-generation" Grubbs catalyst **Ru-1d** is readily displaced by pyridine at 50 ˚C. One product identified in the latter reaction is shown in Scheme 5.1. Several groups have reported that Fischer carbenes readily decompose to liberate **Ru-7** (Scheme 5.2, path (a)); indeed, Arisawa and co-workers report that the TMS derivative **Ru-23b'** affords **Ru-7b'** quantitatively.[12] The latter finding is particularly promising from the perspective of tandem catalysis, provided that the Fischer carbene can be efficiently generated from the methylidene resting-state species.

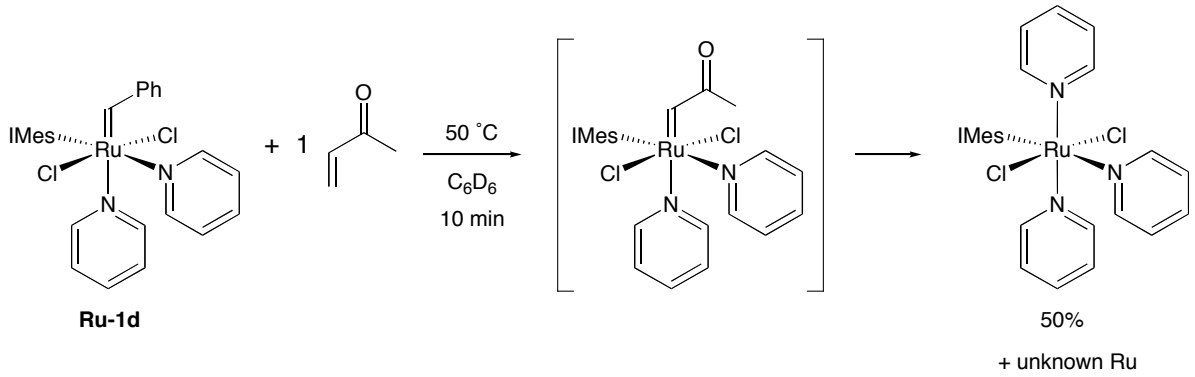

Scheme 5.1. Facile displacement of the keto-alkylidene moiety by pyridine.[11]

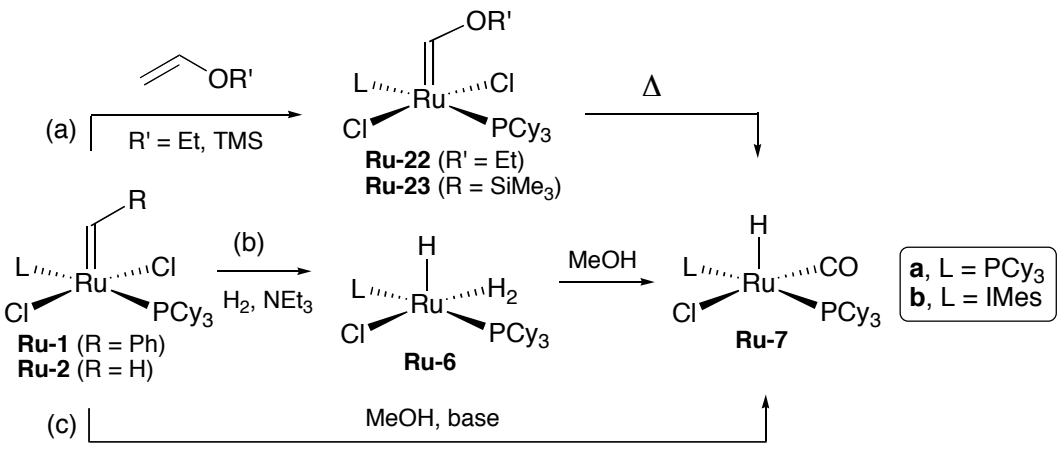

Scheme 5.2. Methods studied for transforming Ru metathesis catalysts into hydride **Ru-7**: (a) CM-thermolysis;[8,12] (b) hydrogenolysis,[5,13,14] followed by carbonylation;[13,15] (c) base-assisted methanolysis.[16-18]

This Chapter evaluates the efficiency with which first- and second-generation Grubbs methylidenes can be transformed into the versatile catalyst **Ru-7**, either directly or via in situ formation of their Fischer carbenes by cross-metathesis (Scheme 5.2). The behaviour of the benzylidene complexes, some of which was described in Chapter 3, is included here for comparison. Three of the most promising methodologies are selected for examination: CM-thermolysis, hydrogenolysis-carbonylation, or methanolysis. A question of added fundamental interest is whether the behaviour of **Ru-2** and **Ru-22** would replicate the "generation gap" observed for **Ru-1** in Chapter 3: that is, whether the protocol of Path (b) would prove superior for transformation of the first-generation catalyst into its hydridocarbonyl derivative **Ru-7a**, vs. that of Path (c) for the second-generation analogue. In situ NMR chemical shifts for all compounds surveyed are tabulated at the end of the Experimental section.

5.2 Results and Discussion.

*5.2.1 Preparation of $RuCl_2(IMes)(PCy_3)(=CH_2)$ **Ru-2b**.*

The literature route to first-generation methylidene **Ru-2a** involves CM of benzylidene **Ru-1a** with ethylene (1 atm C_2H_4, 15 min, CH_2Cl_2).[4] While quantitative yields were reported, we found that this procedure resulted in persistent contamination by small amounts of **Ru-1a** (as indeed expected from the equilibrium formation of **Ru-2a**; Eqn 5.1. Justin Lummiss of this research group improved the synthesis by isolating the **Ru-2a** product and washing it with pentane to remove styrene, then resubjecting the clean material to ethylene. This afforded **Ru-2a** free of **Ru-1a** in 85% yield. From clean **Ru-2a**, he developed a high-yield, high-purity route to the second-generation analogue **Ru-2b'**, previously accessible in <40% yield with limited purity,[19] via ligand exchange of **Ru-2a** with free H_2IMes.

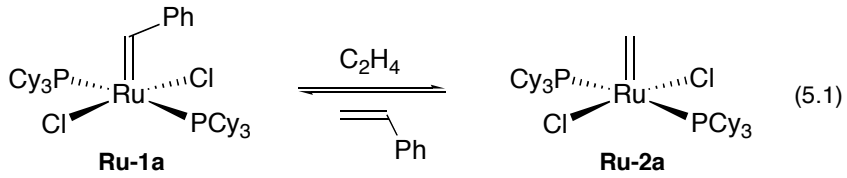

(5.1)

The same method was used to prepare IMes analogue **Ru-2b**. Thus, on stirring methylidene **Ru-2a** with 1 equiv IMes at 60 ˚C in C_6H_6 (Eqn. 5.2), complete conversion was observed at 1 h by $^{31}P\{^1H\}$ NMR analysis, accompanied by a color change from red to orange. Reprecipitation from C_6H_6-hexanes afforded **Ru-2b** as an orange powder in 78% yield. (Future experiments should be undertaken to determine whether the reaction is complete in shorter time, as this could potentially improve the yield). The identity of **Ru-2a** is supported by NMR and elemental analysis. The methylidene protons appear as a singlet at 18.74 ppm (2H, cf. **Ru-2b'**: δ_H 18.41), and the corresponding carbon as a $^{13}C\{^1H\}$ NMR doublet at 295.3 ppm ($^2J_{CP}$ = 7.9 Hz; cf. **Ru-2b'**: δ_C 294.8, $^2J_{CP}$ = 10 Hz). The $^{31}P\{^1H\}$ NMR

singlet is likewise very near that for **Ru-2b'** (δ_P 41.1, vs. 38.6 ppm). As with related complexes,[20] restricted rotation about the N–C_{Mes} bond is evident from the inequivalent mesityl C–H and ortho-methyl groups.

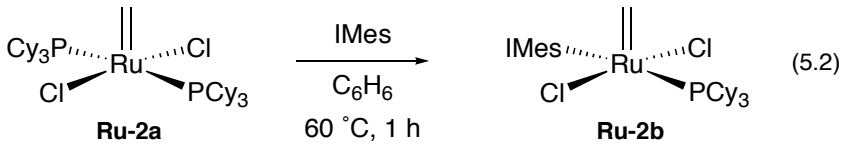

(5.2)

5.2.2 Thermolysis of Fischer carbenes $RuCl_2(L)(PCy_3)(=CHOR)$ ***Ru-22/23***.

As noted in the Introduction, ethyl vinyl ether is potentially attractive as a vector for transformation of metathesis catalysts into **Ru-7**, provided that formation *and* deinsertion of the Fischer carbenes (Scheme 5.3) is rapid and efficient. We also explored use of CH_2=CHOTMS, which appeared highly promising from Arisawa's work[12] (see above).

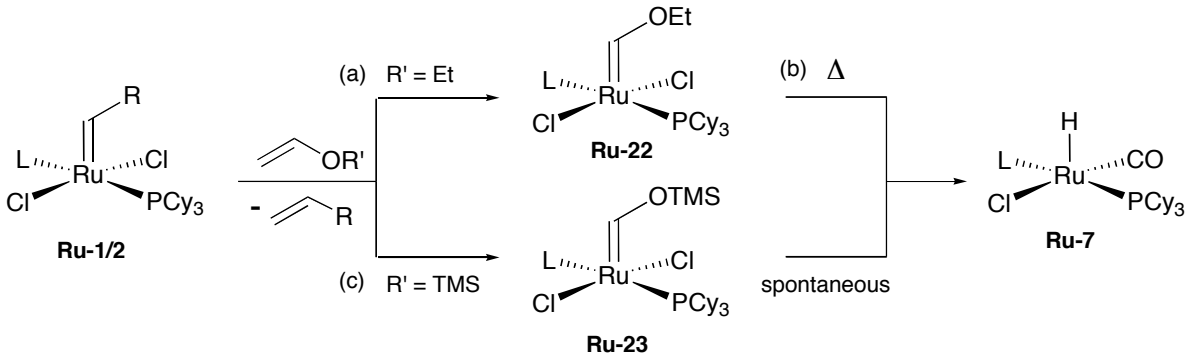

Scheme 5.3. CM-thermolysis of **Ru-2** (R = H) and **Ru-1** (R = Ph) with (a) CH_2=CHOEt and (c) CH_2=CHOTMS (**a**, L = PCy_3; **b**, L = IMes).

5.2.2.1 Optimizing formation of Fischer carbenes by CM with CH_2=CHOEt (EVE)

Reactions of methylidenes **Ru-2a/b** with a tenfold excess of ethyl vinyl ether (EVE) in CH_2Cl_2 or C_6H_6 were assessed at ambient and elevated temperatures (Table 5.1). At these proportions of EVE, formation of the Fischer carbene is slow at RT even for the first-generation methylidene **Ru-2a** (91% conversion only after 13 h in CH_2Cl_2, with 83% net

yield of **Ru-22a** and the ultimate target **Ru-7a**; cf. complete CM of benzylidene **Ru-1a** within 0.5 h). In refluxing C_6H_6, 20% **Ru-7a** is observed once loss of **Ru-2a** is complete, indicating that deinsertion competes with CM at 80 ˚C. At 40 ˚C, consumption of **Ru-2a** requires 3 h (in CH_2Cl_2 or C_6H_6); at 60 ˚C in C_6H_6, the reaction time can be reduced to 0.5 h, but yields drop to ca. 50%. Justin Lummiss of this research group has observed a sharp onset of thermal decomposition for **Ru-2a** at 50 ˚C ($t_{1/2}$ ca. 40 min) in C_6D_6.

For **Ru-2b**, methylidene exchange with EVE is much slower at 23 ˚C (again as expected from the trend in PCy_3 lability),[19] with no change after 24 h. Even for the benzylidene analogue **Ru-1b**, reaction is slow at RT (5% conversion at 1 h: in quenching of metathesis reactions, this may be overcome by use of larger excesses of EVE). High temperatures are evidently essential to overcome the low lability of the PCy_3 ligand in these second-generation complexes. In refluxing C_6H_6, CM of **Ru-2b** is complete in 8 h, vs. three days at 60 ˚C (cf. 15 min for benzylidene **Ru-1b**). At this temperature, benzylidene **Ru-1b** yields **Ru-22b** quantitatively. In contrast, the greater fragility of the methylidene complex results in substantial decomposition to unknown byproducts,[6,21] with just 55% of the Ru targets (30% **Ru-22b**, 24% **Ru-7b**). Also observed is 22% $MePCy_3Cl$, a marker for methylidene decomposition (the methyl group of this phosphonium salt originates in the methylidene ligand). This species emerges in both methylene chloride and benzene. This salt was observed by Piers and co-workers during thermal decomposition (70 ˚C, CH_3CHCl_2) of his phosphonium-alkylidene complexes,[22] and by the Grubbs group during thermal decomposition (55 ˚C, C_6D_6) of **Ru-2a**[21] and its H_2IMes analogue **Ru-2b'**.[23]

Table 5.1. Ligand exchange by reaction of **Ru-2** or **Ru-1** with CH_2=CHOEt (10 equiv).[a]

Starting complex	Solvent	T (˚C)	Time	Conv. (%)	**Ru-22** (%)	**Ru-7** (%)	$MePCy_3Cl$ (%)
Ru-2a	CH_2Cl_2	23	13 h	91	80	3	5
	CH_2Cl_2	**40**	**3 h**	**100**	**79**	**4**	**10**
	C_6H_6	**40**	**3 h**	**100**	**79**	**3**	**5**
	C_6H_6	60	0.5 h	100	43	8	8
Ru-1a	CH_2Cl_2	23	20 min	100	100	0	–
	C_6H_6	23	0.5 h	100	100	0	–
	CH_2Cl_2	40	5 min	100	100	0	–
	C_6H_6	80	5 min	100	80	20	–
Ru-2b	CH_2Cl_2	23	24 h	0	0	0	0
	C_6H_6	60	3 d	96	43	10	15
	C_6H_6	**80**	**8 h**	**100**	**31**	**24**	**22**
Ru-1b	CH_2Cl_2	23	1 h	5	5	0	–
	C_6H_6	23	1 h	5	5	0	–
	CH_2Cl_2	40	8 h	100	100	0	–
	C_6H_6	80	15 min	100	100	0	–

[a] Conditions: [Ru] = 17 mM. Reaction subjected to NMR analysis at 30 min intervals. Time is that required to consume the proportion of starting complex indicated, as determined from kinetic profiles for all reactions except those complete at 5 min. Optimal conditions for the key methylidene complexes indicated in bold face.

*5.2.2.2 Optimizing yields of **Ru-7** from thermolysis of **Ru-22**.*

Data for thermolysis of **Ru-22a/b** are summarized in Table 5.2. In refluxing CH_2Cl_2, reaction is slow for first-generation **Ru-22a** (45% unreacted after 16 h), but is complete within 6 h at 60 ˚C, with 96% selectivity for **Ru-7a**. More forcing conditions are required for **Ru-22b** (2 days at 60 ˚C in CH_2Cl_2), but selectivity for **Ru-7b** is again nearly 95%. Thermolysis is much slower in C_6H_6, requiring over a month for consumption of **Ru-22b** at 60 ˚C, though this is reduced to 2 days at reflux.

These data indicate that thermolysis is highly selective for the hydridocarbonyls **Ru-7**, and can be completed in <2 h for the first-generation ethoxylidene **Ru-22a** in refluxing C_6H_6. In contrast, the second-generation complex **Ru-22b** shows high thermal stability, and its decomposition into **Ru-7b** is inconveniently slow.

Table 5.2. Yields of **Ru-7** from thermolysis of **Ru-22**.[a]

Starting complex	Solvent	T (°C)	Time	Conv. (%)	**Ru-7** (%)
Ru-22a	CH_2Cl_2	40	16 h	55	55
	CH_2Cl_2	60	6 h	100	96[b]
	C_6H_6	80	1.5 h	100	92[b]
Ru-22b	CH_2Cl_2	60	51 h	100	86[c]
	C_6H_6	60	35 d	100	78
	C_6H_6	80	46 h	100	93[b]

[a] Conditions: [Ru] = 17 mM. Time is that required for complete consumption of **Ru-22a/b**, unless otherwise stated. Byproducts observed: [b] 5% $RuCl_2(CO)(PCy_3)_2$ **Ru-27a**. [c] 12% **Ru-27b**.

A minor side-product (ca. 5%) in these reactions is dichloride $RuCl_2(CO)(L)(PCy_3)$ **Ru-27** (**a**: L = PCy_3, 35.7 ppm in CH_2Cl_2; 36.7 ppm in C_6D_6; **b**: L = IMes, 34.6 ppm in CH_2Cl_2; 34.2 ppm in C_6D_6). The bis-PCy_3 species is known;[24,25] the identity of the IMes analogue was confirmed by its independent synthesis (Scheme 5.4). These species are formed in C_6H_6, as well as chlorinated solvents. They may arise from elimination of ethane from a Ru(IV)-formyl intermediate $RuCl_2(Et)[C(O)H](L)$. This does not appear to significantly compete with reductive elimination of EtCl, however (cf. thermolysis of $Ru(OC(O)CF_3)_2(PPh_3)_2(=CHOBn)$ **Ru-24**).[26] An unknown byproduct (δ_P 46.3 ppm) is also observed for the IMes derivatives.

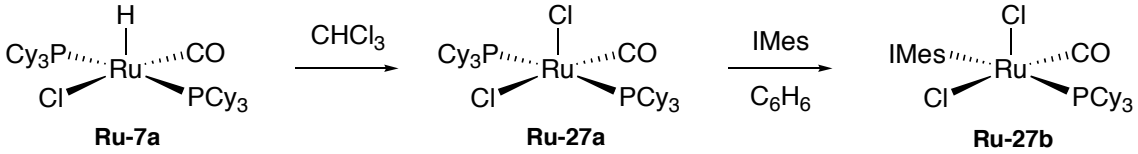

Scheme 5.4. Formation of **Ru-27a/b** from **Ru-7a** at 23 °C.

*5.2.2.3 CM-thermolysis of **Ru-2** and **Ru-1** with CH_2=CHOEt.*

The conditions optimized above for the individual CM and thermolysis steps were combined (Table 5.3). Thus, CM was carried out in C_6H_6 with 10 CH_2=CHOEt. The thermal

sensitivity of the first-generation methylidene **Ru-2a**[21,23] necessitated CM at 40 ˚C, then thermolysis at 80 ˚C; for **Ru-2b** and **Ru-1a/b**, both reactions were performed at 80 ˚C.

For the first-generation methylidene **Ru-2a**, CM-thermolysis afforded **Ru-7a** in 69% overall yield, with 10% of a PCy_3 byproduct. (In comparison, benzylidene **Ru-1a** affords **Ru-7a** in 80% yield after 2 h). For second-generation methylidene **Ru-2b**, conversion of **Ru-22b** into **Ru-7b** was complete after 28 h (faster than the 8 + 46 h period expected from the independent reactions), but proceeded in only 45% overall yield. Trace amounts (5%) of the dichloride **Ru-27b** were also observed.

In comparison, CM of benzylidene **Ru-1b** is rapid (15 min) but, somewhat unexpectedly, thermolysis of the **Ru-22b** product is even slower, requiring 80 h to reach completion (cf. half that for isolated **Ru-22b**). Selectivity for **Ru-7b** was also lower than that observed during thermolysis of isolated **Ru-22b** (70%, vs. 100%). The excess CH_2=CHOEt present may inhibit deinsertion by binding to ruthenium. Relevant in this context is the high affinity of second-generation complexes for olefins.[19]

Despite the reasonable selectivities for **Ru-7a/b** found on CM-thermolysis of **Ru-1** and **Ru-2** with CH_2=CHOEt, the lengthy thermolysis required is inconvenient. An alternative is suggested by Arisawa's report of the fast formation and decomposition of vinylsiloxy species described in the Introduction. Of particular interest was the rapid reaction of **Ru-1b'** with CH_2=CHOTMS at 50 ˚C (toluene), and the quantitative formation of **Ru-7b'** within 1 h.[12] The utility of the vinylsiloxy route to **Ru-7a/b** from **Ru-2a/b** and **Ru-1a/b** was therefore examined.

Table 5.3. Formation of **Ru-7** by CM-thermolysis of **Ru-2** and **Ru-1** with CH_2=CHOEt.[a]

Starting complex	Time		**Ru-7** (%)
	CM	Thermolysis	
Ru-2a	3 h (40 ˚C)	2 h	69[b]
Ru-1a	5 min	2 h	80
Ru-2b	8 h	20 h	46[c]
Ru-1b	15 min	80 h	70

[a] General conditions: [Ru] = 17 mM, C_6H_6, 10 equiv CH_2=CHOEt, 80 ˚C bath temperature unless otherwise stated. Time is that required for complete loss of starting **Ru-1** or **Ru-22**. Byproducts observed: [b] 10% $MePCy_3Cl$. [c] 20% $MePCy_3Cl$, 5% **Ru-27b**.

*5.2.2.4 CM-thermolysis of **Ru-2** and **Ru-1** with CH_2=CHOTMS.*

Decomposition of [Ru]=CHOR is much faster for R = $SiMe_3$ than R = Et. We find that $RuCl_2(PCy_3)_2$(=CHOTMS) **Ru-23a** converts to **Ru-7a** almost immediately once formed. At room temperature, no more than 5% **Ru-23a** was evident at any time. Even at 0 ˚C, no remaining **Ru-23a** was observed by the time that **Ru-1a** was completely consumed (12 h; 50 equiv CH_2=CHOTMS). The TMSCl co-product was observed as a ^{1}H NMR singlet at δ_H 0.15 ppm.

Rates of CM between methylidenes **Ru-2a/b** and benzylidenes **Ru-1a/b** and 10 equiv CH_2=CHOTMS (Table 5.3) are similar to those observed with CH_2=CHOEt. That is, CM requires hours for methylidenes **Ru-2a** and **Ru-2b** (3 or 8 h, respectively), vs. minutes for benzylidenes **Ru-1a** and **Ru-1b** (5 or 15 min). For **Ru-23a/b**, rapid deinsertion eliminates the need for thermolysis. While enabling much faster formation of **Ru-7**, in comparison to the EVE route, selectivities for **Ru-7** were lower by ca. 10% for the first-generation systems, though only by 5% for the IMes analogue (Table 5.4 vs. 5.3). This is probably due to liberation of TMSCl during deinsertion,[26] and attack of the silyl chloride on the hydride ligand in **Ru-7a/b** to form dichlorides **Ru-27a/b**. This is particularly problematic during the

lengthy CM-thermolysis of **Ru-2b**, which results in 30% **Ru-27b**. Addition of base may be advantageous in preventing consumption of this catalyst species by liberated TMSCl.

Table 5.4. Yields of **Ru-7** from CM-thermolysis with CH_2=CHOTMS (10 equiv).[a] For duration of CM, see Table 5.3.

Starting complex	Time	Solvent	T (˚C)	**Ru-7** (%)	Key byproducts
Ru-2a	3 h	C_6H_6	40	60	10% $MePCy_3Cl$, 5% PCy_3
Ru-1a	5 min	C_6H_6	80	90	5% **Ru-27a**
Ru-2b	8 h	C_6H_6	80	40	30% **Ru-27b**, 25% $MePCy_3Cl$
Ru-1b	15 min	C_6H_6	80	75	5% **Ru-27a**

[a] General conditions: [Ru] = 17 mM. Time shown is that required for complete consumption of starting complex.

The diminished metathesis activity of the methylidenes **Ru-2a/b** means that these key resting-state species undergo slower, less selective formation of **Ru-7a/b** during CM-thermolysis than is suggested by model studies of benzylidenes **Ru-1a/b**. Use of CH_2=CHOTMS (and base, to take up the TMSCl co-product) is likely to aid in reducing the timescale required for transformation into **Ru-7**.

*5.2.3 Hydrogenolysis of **Ru-2** and **Ru-22**.*

While hydrogenolysis offers a less versatile entry point to **Ru-7** for tandem metathesis-functionalization, it may be useful where competing olefin hydrogenation is slow. We were also curious to see if the "generation gap" noted for benzylidenes **Ru-1a/b** in Chapter 3[13] would carry over to the methylidenes **Ru-2a/b** and ethoxylidenes **Ru-22a/b**. Reactions with H_2 were therefore carried out under the same conditions (at 60 ˚C in CH_2Cl_2 in the presence of NEt_3; 1000 psi H_2; Table 5.5). Data from the analogous reactions of benzylidenes **Ru-1a/b** are included for comparison.

Hydrogenolysis of **Ru-2a** generated hydride **Ru-6a** in near-quantitative yield within 30

min (Scheme 5.5), accompanied by a color change from pale red to bright orange. Selectivity for **Ru-6a** is substantially higher than was the case for benzylidene **Ru-1a**, perhaps due to the greater steric accessibility of **Ru-2a**. An intriguing alternative possibility, however, is that the methylidene ligand of **Ru-2a** is *displaced* by incoming H_2, as it is by pyridine.[21] We were unable to confirm formation of the hydrogenolysis product CH_4 under these conditions, as any of this volatile species was lost when the autoclave is opened.

The first-generation ethoxylidene $RuCl_2(PCy_3)_2$(=CHOEt) **Ru-22a** is likewise converted within 30 min. Selectivity for **Ru-6a** is only 83%, in part due to competing deinsertion of **Ru-22a** to afford **Ru-7a** (10%). The total yield of catalytically-relevant hydrides is again impressive, however, approaching 95%. As discussed in Chapter 3, **Ru-6a** can be converted into **Ru-7a** in 96% yield by treatment with methanol and NEt_3 at 60 ˚C in CH_2Cl_2.

Table 5.5. Proportion of **Ru-6** present after complete hydrogenolysis of **Ru-2** and **Ru-22**.[a]

Starting complex	Time (h)	**Ru-6** (%)	Byproducts
Ru-2a	0.5	95	
Ru-22a	0.5	83	10% **Ru-7a**
Ru-1a[b]	0.5	80	
Ru-2b	66	0	
Ru-22b	12	0	
Ru-1b[b]	1	60	10% **Ru-6a**, 7% **Ru-6c**

[a] Conditions: [Ru] = 17 mM, CH_2Cl_2, H_2 (1000 psi), 3 equiv NEt_3, 60 ˚C bath temperature. Time corresponds to that required for complete consumption of starting complex. [b] Data from Section 3.2.1.

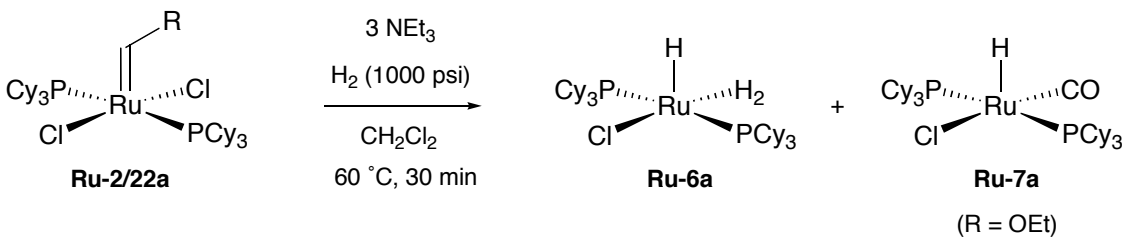

Scheme 5.5. Hydrogenolysis of first-generation **Ru-2a** (R = H) and **Ru-22a** (R = OEt).

The second-generation methylidene **Ru-2b** and ethoxylidene **Ru-22b** underwent extremely slow hydrogenolysis, with complete consumption of starting material requiring 66 h and 12 h, respectively (vs. 1 h for benzylidene **Ru-1b**). In remarkable contrast with its first-generation counterpart, methylidene **Ru-2b** undergoes substantial decomposition (27% $MePCy_3Cl$), yielding low proportions of four unidentified species (ca. 5% each; $^{31}P\{^1H\}$ NMR singlets between 70 and 65 ppm).

Identical Ru species form in hydrogenolysis of **Ru-22b**, with larger amounts of a fifth species (δ_P 70.0 ppm, br; 25%). Only traces of **Ru-6b** form (ca. 5% after 8 h). None is observed once reaction is complete (12 h), owing to its low thermal stability (Section 2.2.3).[27] No **Ru-7b** is observed, indicating that reaction with H_2 is rapid compared to β-ethyl elimination. Broad, overlapping hydride multiplets centered around -11.5 ppm integrate to 25% (**Ru-2b**) and 80% (**Ru-22b**) relative to the starting material, although their breadth ($\omega_{0.5}$ >100 Hz) limits the reliability of integration, and prevents correlation with $^{31}P\{^1H\}$ NMR signals. The high proportion of "missing" (i.e. NMR-invisible) material during these reactions indicates formation of paramagnetic byproducts, as for thermolysis and carbonylation of **Ru-6b** (Sections 2.2.3 and 3.2.2).

Clearly, these second-generation systems exhibit the same vulnerability during hydrogenolysis observed for benzylidene **Ru-1b** (Section 3.2.1),[13] and are indeed even more susceptible. This reflects their lower lability, which retards hydrogenolysis, enabling decomposition of **Ru-6b** to compete with its formation. Thus, the "generation gap" is maintained: while hydrogenolysis-carbonylation is a viable route to hydridocarbonyl **Ru-7a**

from the first-generation methylidene and ethoxylidene, this transformation is incompatible with second-generation systems.

*5.2.4 Methanolysis of **Ru-2**, **Ru-22**, and **Ru-1**.*

Reactions of **Ru-2b** and **Ru-22b** with methanolic methoxide were considered promising, given the rapidity of these reactions with **Ru-1a** (cf. Section 4.2.1). Use of methanol and NEt_3 was also explored for its potential relevance to state-of-the-art ROMP-hydrogenation protocols (cf. Section 3.2.3).[1,28]

*5.2.4.1 Reactions of **Ru-2**, **Ru-22** and **Ru-1** with methoxide and methanol.*

Solutions of the Ru species in CH_2Cl_2 were treated with equimolar amounts of NaOMe, as a ca. 0.2 M solution in MeOH, and heated to 60 ˚C (Scheme 5.6; Table 5.6). Under these conditions, the first-generation methylidene **Ru-2a** was consumed in 30 min, but **Ru-7a** is obtained in only 30% yield, while decomposition is significant. Transformation of ethoxylidene **Ru-22a** is slower (3 h), but generates **Ru-7a** product in 80% yield. Formation of the six-coordinate methoxyhydride complex $RuH(OMe)(CO)_2(PCy_3)_2$ **Ru-18a** (5%) indicates abstraction of the second chloride ligand. Unexpectedly, **Ru-1a** is only 80% converted at the same stage. Abstraction of the second chloride ligand results in coordinatively saturated dihydride and methoxyhydride species (Chapter 4). An unidentified $RuHCl(PCy_3)L_3$ product was also formed (5% yield), as noted in Section 3.2.3.[13]

The corresponding reaction of second-generation methylidene **Ru-2b** is complete in 2 h, and likewise gives **Ru-7b** in low (25%) yield. Competing decomposition and disproportionation are observed, behaviour not seen for **Ru-22b**. The latter complex generates 78% **Ru-7b** in 1 h, with small amounts of coordinatively saturated

methoxyhydride **Ru-18b** (11%) and dihydride **Ru-19b** (5%). Benzylidene **Ru-1b** was also efficiently transformed into **Ru-7b** (83%; 30 min) under these conditions. The absence of disproportionation or dihydrides renders this treatment the most efficient route to hydridocarbonyl **Ru-7b** for this benzylidene species. For the key methylidene species **Ru-2a/b**, however, competing decomposition undermines yields of **Ru-7a/b**. Use of the weaker base Cs_2CO_3 was explored in the hope of circumventing the side-reactions found with NaOMe.

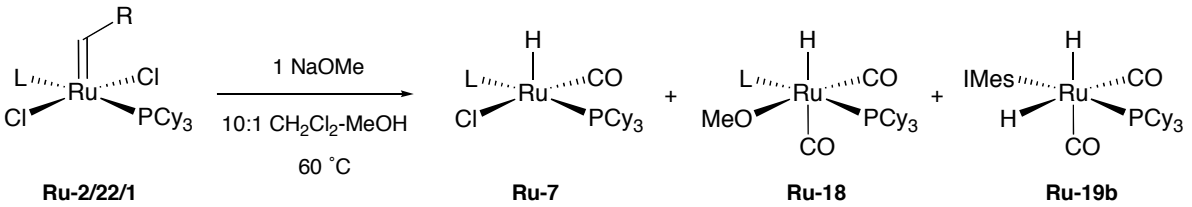

Scheme 5.6. Reactions of Ru complexes (**Ru-2**, **Ru-22**, **Ru-1**) with methanolic methoxide.

Table 5.6. Formation of **Ru-7** during NaOMe-assisted methanolysis of **Ru-2**, **Ru-22** and **Ru-1**.[a]

Starting complex	Time (h)	**Ru-7** (%)	Key byproducts
Ru-2a	0.75	30	25% $MePCy_3Cl$
Ru-22a	3	80	5% **Ru-18a**
Ru-1a	0.5	40	
Ru-2b	2	25	20% $MePCy_3Cl$ 12% **Ru-7a** 3% **Ru-7c**
Ru-22b	1	78	11% **Ru-18b** 5% **Ru-19b**
Ru-1b	0.5	83	

[a] Conditions: [Ru] = 17 mM, 10 CH_2Cl_2 : 1 MeOH, 1 equiv NaOMe (0.20 M in MeOH), 60 °C bath temperature. Time corresponds to that required for complete consumption of starting complex, except for **Ru-1a**, which remains 20% unreacted.

*5.2.4.2 Cs_2CO_3-assisted methanolysis of **Ru-2**, **Ru-22** and **Ru-1**.*

Mol and coworkers reported formation of **Ru-7a** via reaction of **Ru-1a** with 0.5 equiv K_2CO_3 and methanol.[16] In reactions of **Ru-2a/b**, **Ru-22a/b** and **Ru-1a/b** with Cs_2CO_3 and methanol (Scheme 5.7; Table 5.7), THF solvent was used to maximize the solubility of Cs_2CO_3. Given the diprotic nature of the conjugate acid H_2CO_3, initial reactions employed 0.5 equiv of Cs_2CO_3.

Methanolysis was complete in 0.5 h for **Ru-2a**, but yields of **Ru-7a** were limited to 30%. A similar proportion of methylcarbonatohydride **Ru-28a** was formed (for characterization data, see next Section). For **Ru-22a** and **Ru-1a**, reaction was slower (3 or 6 h, respectively) but gave ca. 55% **Ru-7a** with 10% **Ru-28a**.

The second-generation complexes are consumed within 1.5-3 h, and afford ca. 60% **Ru-7b**, with 10% **Ru-28b**. On doubling the proportion of Cs_2CO_3 (1 equiv per Ru), thermolysis is complete in 15 min, probably owing to the higher basicity of carbonate, vs. bicarbonate

(pK_a 6.35, vs. 10.33)[29] and the efficiency with which chloride is abstracted by the twofold excess of Cs^+ (2 equiv per Ru). The hydridocarbonyls **Ru-7a/b** were not observed, presumably due to abstraction of both chloride ligands by Cs^+, and subsequent coordination of CO_3^{2-}; the methylcarbonatohydrides **Ru-28a/b** were formed in moderate yield (45%). A common byproduct (5% from **Ru-1a**; 20% from **Ru-1b**) is tentatively identified as the bicarbonatohydride RuH(κ^2-OC(O)OH)(CO)(L)(PCy_3) **Ru-29a/b** based on the similarity of its NMR shifts to **Ru-28a/b**, respectively (see next Section).

As with NaOMe, Cs_2CO_3 effects rapid methanolysis of methylidenes and ethoxylidenes (as well as benzylidenes), but results in poor selectivity for **Ru-7a/b**. Neither of these methodologies is thus useful in the present context.

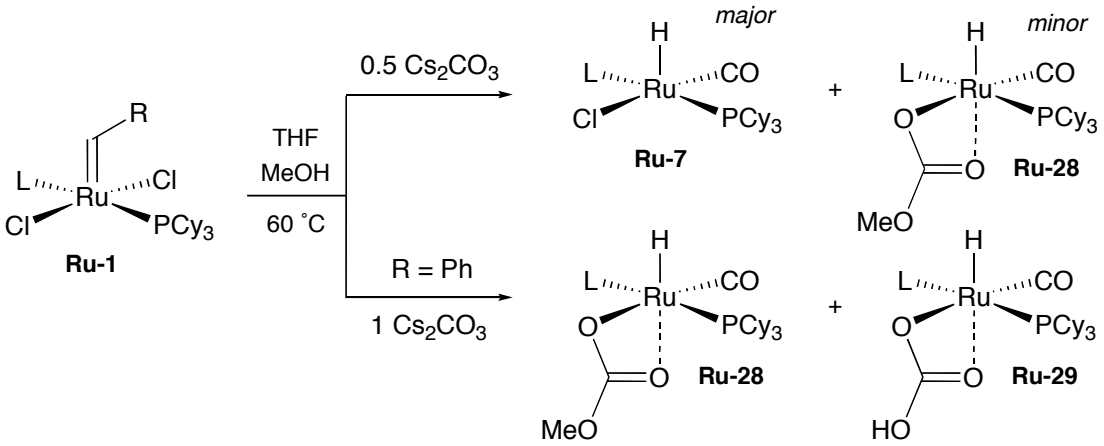

Scheme 5.7. Cs_2CO_3-assisted methanolysis of **Ru-1**.

Table 5.7. Yield of hydrides following reactions of **Ru-2**, **Ru-22** and **Ru-1** with methanol and Cs_2CO_3. [a]

Starting complex	Equiv. Cs_2CO_3 [b]	Time (h)	**Ru-7** (%)	**Ru-28** (%)	**Ru-29** (%)
Ru-2a	0.5	0.5	30	30	-
Ru-22a	0.5	3	52	10	-
Ru-1a	0.5	6	55	10	-
	1	0.25	0	45	5
Ru-2b	0.5	1.5	62	10	-
Ru-22b	0.5	2	55	15	-
Ru-1b	0.5	3	57	10	-
	1	0.25	0	45	20

[a] Conditions: [Ru] = 17 mM, 10 THF : 1 MeOH, 60 ˚C bath temperature. Time is that required for complete consumption of starting complex [b] [Cs_2CO_3] = 8.5 mM (0.5 equiv), 17 mM (1.0 equiv).

Salt metathesis of **Ru-7** with the $CsHCO_3$ byproduct is presumed to form **Ru-29** (Scheme 5.8). In turn, this methoxycarbonatohydride species may be converted into **Ru-28** by nucleophilic attack at the bicarbonate carbon by MeOH, followed by proton transfer and elimination of water.

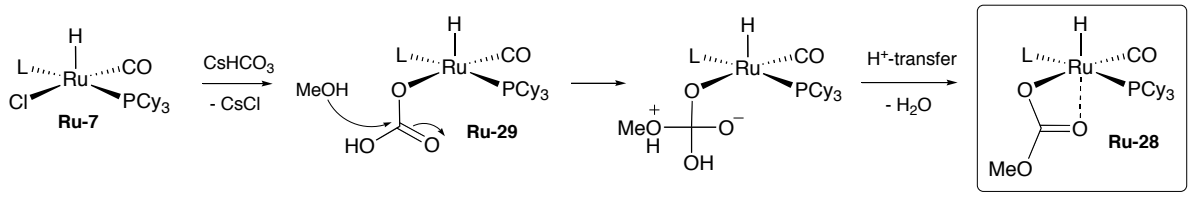

Scheme 5.8. Proposed mechanism of formation of **Ru-28** from **Ru-7**.

*5.2.4.3 Preparation of RuH(κ^2-OC(O)OMe)(CO)(L)(PCy_3) **Ru-28**.*

Stirring the hydridocarbonyl complexes **Ru-7a/b** with equimolar methanolic Cs_2CO_3 in THF resulted in their complete consumption within 15 min at 23 ˚C (NMR analysis). The solvent was stripped off and the residue redissolved in C_6H_6, and filtered through Celite. The crude product was contaminated by 5% of side-products tentatively identified as the

bicarbonatohydrides **Ru-29a/b**. The major products are suggested to be **Ru-28a/b** on the basis of NMR analysis (Scheme 5.9).

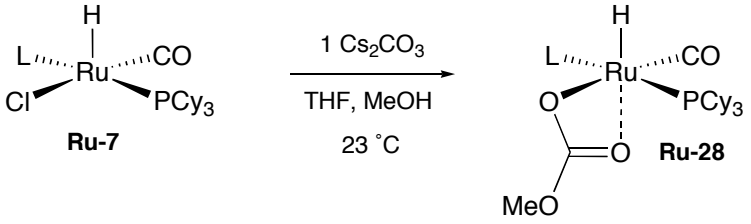

Scheme 5.9. Formation of **Ru-28** via reaction of **Ru-7** with methanolic Cs_2CO_3 (**a**, L = PCy_3; **b**, L = IMes).

The hydride signals for **Ru-28a/b** appear at –17.58 (t, $^2J_{HP}$ = 19.2 Hz) and –17.96 ppm (d, $^2J_{HP}$ = 22.3 Hz), which correlate (HMBC) to $^{31}P\{^1H\}$ singlets at 45.7 and 46.8 ppm, respectively. These multiplicities, and the $^2J_{HP}$ values, indicate the presence of two or one cis-PCy_3 ligands, respectively. The hydride shifts suggest coordinative unsaturation; a nearly identical shift (δ_H –18.49; C_6D_6) was reported for RuH(κ^2-OC(O)C_5H_4N)(CO)$(IMes)_2$ **Ru-30**, in which κ^2-*O,O*-coordination mode of the isonicotinate ligand was indicated by X-ray analysis.[30] (κ^2-*O,O*-coordination of the methylcarbonato ligands in **Ru-28a/b** is consistent with the small frequency difference between the symmetric (1608 and 1607 cm^{-1}) and asymmetric OCO stretching bands (1445 and 1448 cm^{-1}), respectively).[31-33] The methoxy protons of **Ru-28a/b** appear as sharp ^1H NMR singlets at 3.64 and 3.50 ppm, respectively, which integrate 3:1 relative to hydride and exhibit HMQC correlations to $^{13}C\{^1H\}$ NMR singlets at 53.1 and 52.6 ppm, respectively. The latter are assigned to methyl groups by ^{13}C DEPT analysis. The methoxy ^1H signals also correlate (HMBC) to $^{13}C\{^1H\}$ singlets for the carbonate carbons at 159.1 and 158.9 ppm, respectively (cf. δ_C 160.3 for RuH(κ^2-OC(O)OH)(CO)$(IMes)_2$ **Ru-29c**).[30] An HMBC correlation was also observed between the hydride ^1H doublet and the singlet for the carbonate carbon for **Ru-28b**. Finally, the

presence of single carbonyl ligands is confirmed for **Ru-28a** and **Ru-28b** by HMBC correlations between the hydride multiplets and $^{13}C\{^1H\}$ signals at 202.2 (t, $^2J_{CP}$ = 12.8 Hz) and 208.0 ppm (d, $^2J_{CP}$ = 5.7 Hz), respectively.

Other byproducts noted above were tentatively identified as the bicarbonatohydride complexes RuH(κ^2-OC(O)OH)(CO)(L)(PCy_3) **Ru-29a/b** based on NMR analysis. These give rise to hydride multiplets at -16.54 (t, $^2J_{HP}$ = 19.8 Hz) and -16.73 ppm (d, $^2J_{HP}$ = 23.9 Hz), which correlate (HMBC) with $^{31}P\{^1H\}$ NMR singlets at 46.0 and 47.1 ppm, respectively. Broad ^1H NMR singlets at 7.98 and 8.51 ppm (integrating 1:1 vs. hydride) are assigned to the carbonate O*H* proton; cf. 8.80 ppm for RuH(κ^2-OC(O)OH)(CO)$(IMes)_2$ **Ru-29c**.[30] Low yield and rapid decomposition impeded more detailed analysis.

*5.2.4.4 Reaction of **Ru-2** and **Ru-22** with methanol and NEt_3*

The relatively efficient conversion of **Ru-1b** into **Ru-7b** on treatment with methanol and NEt_3 (83% in 4 h in CH_2Cl_2-MeOH at 60 ˚C; Section 3.2.3) led us to hope that similar behaviour might apply to **Ru-2b** and **Ru-22b**. As well, we wished to see if the behaviour of the benzylidene complexes accurately modeled that of the methylidene or Fischer carbene derivatives. These reactions are summarized in Scheme 5.10 and Table 5.8.

Methylidenes **Ru-2a/b** are converted more rapidly than the benzylidenes **Ru-1a/b**.[13] Their NMR signals disappear within 15 min or 1.5 h, respectively, accompanied by a color change from pale red (**Ru-2a**) or dark orange (**Ru-2b**) to yellow-orange. A ^1H NMR singlet at 0.24 ppm[5] confirms reduction of the methylidene ligand to CH_4 in both cases. For **Ru-2a**, the yield of **Ru-7a** was 65%; for **Ru-2b**, unexpectedly, it dropped below 50%, owing to

competing disproportionation and decomposition (the latter being indicated by the formation of substantial $MePCy_3Cl$; **Ru-2a**: 25%; **Ru-2b**: 15%).

Methanolysis of ethoxylidenes required hours (4 h for **Ru-22a**; 1.5 h for **Ru-22b**) but afforded hydridocarbonyls **Ru-7a/b** in 91% and 80% yield, respectively. No disproportionation of **Ru-22b** is evident. The faster reaction of **Ru-2b** relative to **Ru-1b** (1.5 vs. 4 h) is consistent with the mechanism discussed in Chapter 3: that is, stronger binding of MeOH to the more electropositive NHC-bound Ru center. Computational work suggests a more positive Ru center for methylidenes **Ru-2a** and **Ru-2b'**[34] than benzylidene analogues **Ru-1a** and **Ru-1b'**[35] (Δq_{Ru} = ca. 0.30 e^- for the non-truncated complexes).

Thus, while methanolysis of the first-generation methylidene **Ru-2a** is fast and moderately selective for **Ru-7a**, the second-generation **Ru-2b** suffers from disproportionation. The quenched Fischer carbenes **Ru-22a/b** exhibited excellent to good selectivity for **Ru-7a/b**, and hence may offer the most useful route, albeit offset by slow formation of **Ru-22** from the [Ru]=CH_2 resting states.

Table 5.8. Formation of **Ru-7** by treating **Ru-2**, **Ru-22** and **Ru-1** with methanol and NEt_3.[a]

Starting complex	Time (h)	**Ru-7** (%)	Key byproducts
Ru-2a	0.25	65	$MePCy_3Cl$ (25%)
Ru-22a	4	91	**Ru-27a** (<2%)
Ru-1a	8	60[b]	
Ru-2b	1.5	47[d]	**Ru-7a** (15%)
			Ru-7c (3%)
			$MePCy_3Cl$ (15%)
Ru-22b	1.5	80	-
Ru-1b	4	85[b]	-

[a] Conditions: [Ru] = 17 mM, 4:1 CH_2Cl_2-MeOH, 3 equiv NEt_3, 60 °C. Time corresponds to that required for complete consumption of starting complex. [b] Data from Section 3.2.3.

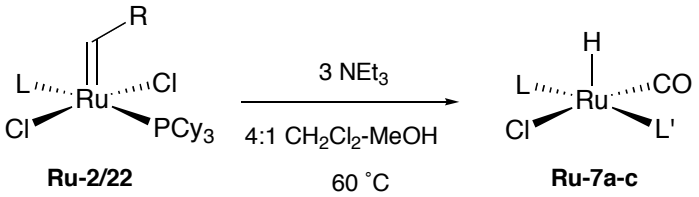

Ru-2/22 **Ru-7a-c**

Scheme 5.10. Reactions of [Ru]=CHR species with methanol and NEt_3. **Ru-2** (R = H) and **Ru-22** (R = OEt): L, L' = **a**, $(PCy_3)_2$; **b**, (IMes)(PCy_3); **c**, $(IMes)_2$.

5.3 Conclusions.

This chapter explored methods by which first- and second-generation Grubbs metathesis catalysts can be converted into the versatile hydridocarbonyl catalyst **Ru-7**. The reaction chemistry of benzylidenes, methylidene, and selected Fischer carbenes is compared. Table 5.9 summarizes the routes that give efficient access to **Ru-7** (arbitrarily defined as yields ≥60%, within 8 h). For the first-generation catalysts **Ru-1a** and **Ru-2a**, the most attractive route involves CM with ethyl vinyl ether or vinyloxytrimethylsilane, followed by thermolytic degradation. Hydrogenolysis, followed by reaction with methanol and NEt_3, is efficient for both these complexes and for the Fischer carbene **Ru-22a**. However, the high H_2 pressures are problematic if tandem (R)CM-functionalization is the goal, as competing olefin hydrogenation may occur.

Transformation of the second-generation methylidene **Ru-2b** into **Ru-7b** is of particular interest, given the central importance of Ru-NHC catalysts in RCM and CM. Few methods work well, however. Hydrogenolysis is generally problematic for the second-generation systems, because the dihydrogen adducts formed are susceptible to ligand disproportionation. The Fischer carbene route is slow: the CM step alone requires 8 h, and yields significant byproducts. The reaction with vinyloxytrimethylsilane is more promising: it offers fast conversion, and the yield of **Ru-7b** can reach 70% where formation of the

byproduct $RuCl_2(CO)(IMes)(PCy_3)$ **27b** is inhibited by (e.g.) carrying out the reaction in the presence of a sacrificial base such as NEt_3. Otherwise, the best route involves reaction with methanol in the presence of Cs_2CO_3.

Table 5.9. Efficient[a] routes to **Ru-7** from Grubbs benzylidenes, methylidenes and ethoxylidenes.

Triggers	Complex	time (h)	**Ru-7** (%)	Comments
(i) CH_2=CHOEt (ii) heat (Table 5.3)	**Ru-1a**	2	80	Compatible with first-generation catalysts only
	Ru-2a	5	69	
CH_2=CHOTMS (Table 5.4)	**Ru-1a**	5 min	90	Compatible with first-generation catalysts and second-generation precatalyst
	Ru-2a	3	60	
	Ru-1b	0.25	75	
(i) H_2, NEt_3 (ii) MeOH, NEt_3 (Table 5.5)	**Ru-1a**	3	77	Compatible with first-generation catalysts (but requires high H_2 pressures; risk of competing hydrogenation)
	Ru-2a	3	90	
	Ru-22a	3	90	
MeOH, NaOMe (Table 5.6)	**Ru-22a**	3	80	Compatible with quenched Fischer carbenes and second-generation precatalyst. Poor stoichiometric control; may yield byproducts.
	Ru-22b	1	78	
	Ru-1b	0.5	83	
MeOH, Cs_2CO_3 (Table 5.7)	**Ru-2b**	1.5	62	**Compatible with second-generation methylidene**
MeOH, NEt_3 (Table 5.8)	**Ru-1a**	8	60	Broad compatibility, except for second-generation methylidene **Ru-2b**
	Ru-2a	0.25	65	
	Ru-22a	4	91	
	Ru-1b	4	85	
	Ru-22b	1.5	80	

[a] Defined as methods that generate **Ru-7** in ≥60% yield within 8 h.

Table 5.10. Optimal methods for production of **Ru-7** from Ru metathesis catalysts for various tandem catalysis procedures.

Targeted procedure	First-generation	Second-generation
ROMP, RCM, or CM-hydrogenation	(i) H_2 + 3 NEt_3, (ii) MeOH	1 NaOMe + MeOH or 0.5 Cs_2CO_3 + MeOH
ROMP-functionalization	10 CH_2=CHOTMS	10 CH_2=CHOTMS
RCM/CM-functionalization	3 NEt_3 + MeOH	0.5 Cs_2CO_3 + MeOH or 1 NaOMe + MeOH

5.4 Experimental.

5.4.1 General Procedures:

See Chapter 2; other aspects are given here. In situ NMR chemical shifts for all compounds surveyed are presented in Table 5.11 below. Triethylamine was distilled from CaH_2 and stored under Ar. Methanol was distilled from $Mg(OCH_3)_2$ under Ar and stored over molecular sieves (Linde 3Å). Literature procedures were used to prepare **Ru-1a**,[4] **Ru-1b**,[36,37] **Ru-2a**,[4] **Ru-22a/b**[8], and **Ru-27a**.[24,25] In NMR assignments of IMes derivatives, *a*/*b* labels indicate nuclei that correlate via HMQC or HMBC experiments. IR spectra of powdered compounds were measured on a Varian 640-IR reflectance FTIR spectrometer. NMR-scale reactions were performed in protio solvents with C_6D_6 (5% v/v) added as a deuterium source for locking and shimming. Conversions were quantified by integration against Ph_3P=O (^{31}P) and 1,3,5-trimethoxybenzene (TMB, ^1H) as internal standards. Reactions at 60 ˚C in CH_2Cl_2 were carried out in thick-walled J Young NMR tubes. The anticipated vapor pressure of the solvent at this temperature is 28.4 psi (see: Chemical Engineering Research Information Center (CERIC)).

5.4.2 Synthesis of $RuCl_2(IMes)(PCy_3)(=CH_2)$ ***Ru-2b***.

In the glovebox, solid white IMes (62 mg, 0.203 mmol) was added to a stirred solution of **Ru-2a** (150 mg, 0.200 mmol) in C_6H_6 (15 mL). The Schlenk tube was removed to a vacuum line and heated to 60 °C for 45 min under Ar. Over 1 h at 60 ˚C, a color change from red to orange was observed. The solution was concentrated to ca. 1 mL, treated with hexanes (10 mL), and chilled to -35 ˚C. The resulting orange powder was filtered off, washed with cold hexanes (3×2 mL), and dried under vacuum. Yield: 120 mg (78%). Spectroscopic data are in good agreement with those obtained for **Ru-2b'**. $^{31}P\{^1H\}$ NMR (202.5 MHz, C_6D_6): δ 40.9 ppm (s, *P*Cy_3). ^1H NMR (500.1 MHz, C_6D_6): δ 18.77 (s, 2H, Ru=CH_2), 6.90 (s, 2H, Mes *m*-C*H*), 6.72 (s, 2H, Mes *m*-C*H*), 6.22 (d, $^3J_{HH}$ = 2 Hz, 1H, NC*H*=), 6.13 (dd, $^3J_{HH}$ = 2 Hz, $^5J_{PH}$ = 1 Hz, 1H, NC*H*=), 2.60 (s, 6H, *o*-CH_3), 2.37 (s, 6H *o*-CH_3), 2.44-2.30 (m, 3H, Cy), 2.19 (s, 3H, *p*-CH_3), 2.12 (s, 3H, *p*-CH_3), 1.77-1.47 (m, 15H, Cy), 1.30-1.01 (m, 15H, Cy). $^{13}C\{^1H\}$ NMR (125.8 MHz, C_6D_6): δ 294.5 (d, $^2J_{PC}$ = 12 Hz, Ru=*C*H_2), 191.6 (d, $^2J_{PC}$ = 79 Hz, N*C*N), 139.4, 139.0, 138.4, 137.4, 137.0, 135.6, 129.8, 129.4, 124.1 (d, $^4J_{PC}$ = 3 Hz, N*C*H=), 123.6 (s, N*C*H=), 30.9 (d, J_{PC} = 19 Hz, Cy), 29.4 (Cy), 28.2 (d, J_{PC} = 10 Hz, Cy), 26.8 (Cy), 21.34 (*p*-*C*H_3), 21.32 (*p*-*C*H_3), 19.8 (*o*-*C*H_3), 18.9 (*o*-*C*H_3). Anal. Calcd. for $C_{40}H_{61}Cl_2N_2PRu$: C, 62.16%; H, 7.96%; N, 3.62%. Found: C, 62.46%; H, 7.59%; N, 3.62%.

5.4.3 NMR-Scale Observation of $RuCl_2(CO)(IMes)(PCy_3)$ ***Ru-27b***.

Solid IMes (5 mg, 0.016 mmol) was added to a solution of $RuCl_2(CO)(PCy_3)_2$ (8.6 mg, 0.011 mmol) in C_6D_6 (0.75 mL) and stirred at 23 ˚C for 2 h. $^{31}P\{^1H\}$ NMR analysis revealed **Ru-27b** (δ_P 34.6) and **Ru-27a** (δ_P 36.6); integration 2:1; molar ratio 1:1. Also present was free PCy_3 (δ_P 11.1; 1:1 vs. **Ru-27b**. An unknown signal at δ_P 46.3 was also present, which

grew as the reaction continued. Consumption of **Ru-27a** was complete after 6 h, with **Ru-27b** (85%), free PCy_3 (100%), and δ_P 46.3 (ca. 10%).

5.4.4 NMR-Scale Preparation of RuH(κ^2-OC(O)OMe)(CO)(L)(PCy_3) ***Ru-28****.*

L = PCy_3, ***Ru-28a****.*

A solution of Cs_2CO_3 in MeOH (86 μL, 0.16 M, 0.014 mmol) to an orange solution of RuHCl(CO)(PCy_3)$_2$ **Ru-7a** (10 mg, 0.014 mmol) in THF (0.6 mL) and C_6D_6 (50 μL). After stirring for 15 min at 23 ˚C, a colour change from orange-yellow to pale yellow was observed and a white precipitate formed. NMR analysis confirmed conversion of **Ru-7a** to **Ru-28a** (with ca. 5% of bicarbonatohydride **Ru-29a** at δ_H –16.54 (t, $^2J_{HP}$ = 19.8) and δ_P 45.8 (s)). The reaction mixture was stripped of solvent, taken up in C_6H_6, filtered through Celite, and stripped again, then redissolved in C_6D_6 for NMR analysis. ^{1}H NMR (300.1 MHz, C_6D_6): δ 3.64 (s, 3H, OC(O)OC*H*$_3$), 2.6–1.1 (m, Cy), –17.58 (t, $^2J_{HP}$ = 19.2 Hz, 1H, Ru*H*). ^{31}P{^{1}H} NMR (121.5 MHz, C_6D_6): δ 45.7 (s, PCy_3). ^{13}C{^{1}H} NMR (75.5 MHz, C_6D_6): δ 202.2 (t, $^2J_{CP}$ = 12.8 Hz, *C*O), 159.1 (s, O*C*(O)OCH$_3$), 53.1 (s, OC(O)O*C*H$_3$), 34.9 (t, $^2J_{CP}$ = 9.6 Hz, Cy), 31.2 (s, Cy), 30.3 (s, Cy), 28.1 (m, Cy), 27.0 (s, Cy). IR (cm^{-1}): ν(Ru–H) 2037, ν(CO) 1897, ν(OCO) 1608, ν(OCO) 1445, ν(COC) 1323.

L = IMes, ***Ru-28b****.*

Preparation as for **Ru-28a**, from RuHCl(CO)(L)(PCy_3) **Ru-7b** (10 mg, 0.014 mmol). A small amount (ca. 5%) of bicarbonatohydride **Ru-29b**, appearing at δ_H –16.73 (d, $^2J_{HP}$ = 23.9) and δ_P 47.1 (s) is also formed. ^{1}H NMR (500.1 MHz, C_6D_6): δ 6.85 (s, 1H, Mes *m*-CH^a), 6.83 (s, 1H, Mes *m*-CH^a), 6.66 (s, 2H, Mes *m*-CH^b), 6.23 (s, 2H, *H*C=C*H*), 3.50 (s, 3H, OC(O)OC*H*$_3$), 2.33 (s, 6H, Mes *o*-C*H*$_3^a$), 2.27 (s, 6H, Mes *o*-C*H*$_3^b$), 2.13 (s, 6H, Mes *p*-

C*H*$_3$), 2.6–1.1 (m, Cy), –17.96 (d, $^2J_{HP}$ = 22.3 Hz, 1H, Ru*H*). $^{31}P\{^1H\}$ NMR (121.5 MHz, C_6D_6): δ 46.8 (s, PCy_3). $^{13}C\{^1H\}$ NMR (75.5 MHz, C_6D_6): δ 208.0 (d, $^2J_{CP}$ = 5.7 Hz, *C*O), 190.8 (d, $^2J_{CP}$ = 92.0 Hz, N*C*N), 158.9 (s, O*C*(O)OCH$_3$), 138.1 (s, Mes *i*-*C*), 137.8 (s, Mes *p*-*C*), 136.7 (s, Mes *o*-*C*^{a}), 136.0 (s, Mes *o*-*C*^{b}), 129.2 (s, Mes *m*-*C*H^a), 129.0 (s, Mes *m*-*C*H^b), 122.5 (m, N*C*=*C*N), 52.6 (s, OC(O)O*C*H$_3$), 34.6 (d, J_{PC} = 16.7 Hz, Cy), 30.2 (s, Cy), 29.4 (s, Cy), 28.3 (d, J_{CP} = 9.0 Hz, Cy), 28.2 (d, J_{CP} = 10.2 Hz, Cy), 27.0 (s, Cy), 21.1 (s, Mes *p*-*C*H$_3$), 18.5 (s, Mes *o*-*C*H$_3^a$), 18.4 (s, Mes *o*-*C*H$_3^b$). IR (cm^{-1}): ν(Ru–H) 2031, ν(CO) 1908, ν(OCO) 1607, ν(OCO) 1448, ν(COC) 1324.

5.4.5 General protocol for in situ NMR monitoring of methanolysis, thermolysis, and hydrogenolysis reactions.

In a representative procedure, a solid mixture of **Ru-2a** (9.0 mg, 0.012 mmol), 1,3,5-trimethoxybenzene (1 mg, 0.01 mmol) and Ph_3P=O (6 mg, 0.02 mmol) was dissolved in CH_2Cl_2 (520 μL), MeOH (130 μL), and C_6D_6 (50 μL, added as deuterium source for shimming) in a J. Young NMR tube. Initial ^1H and $^{31}P\{^1H\}$ NMR spectra were acquired to establish the **Ru-2a**:Ph_3P=O integration ratio at t_o. NEt_3 (5.0 μL, 0.036 mmol) was then added to the sample and the tube heated in an oil bath (60 ˚C). At various times, the sample tube was cooled and subjected to ^1H and $^{31}P\{^1H\}$ NMR analysis in order to assess the reaction progress. MeO / MeOH made use of methanolic solutions of NaOMe, prepared by digestion of Na metal in MeOH (64 μL, 0.20 M). Cs_2CO_3-assisted methanolyses were performed in THF using methanolic solutions of Cs_2CO_3 (64 μL, 0.10 M).

Thermolysis and CM-thermolysis reactions were performed as above using CH_2Cl_2 or C_6H_6 (0.65 mL) and C_6D_6 (50 μL) as reaction solvent. Vinyl ethers CH_2=CHOEt (1.2 μL,

0.013 mmol) or CH_2=CHOTMS (1.9 μL, 0.013 mmol) were added following acquisition of t_0 NMR spectra, and the ensuing reaction monitored by ^{1}H and ^{31}P{^{1}H} NMR analysis.

Hydrogenolysis reactions utilized stock solutions of Ru starting material with internal standards. Thus, **Ru-22a** (18 mg, 0.023 mmol), 1,3,5-trimethoxybenzene (2 mg, 0.01 mmol) and Ph_3P=O (12 mg, 0.043 mmol) were dissolved in CH_2Cl_2 (1.340 mL). A 670 μL aliquot of this stock solution was transferred to a J Young NMR tube, and t_0 data were acquired as above. Another 670 μL aliquot was transferred to a screw-cap vial equipped with a stirbar, and NEt_3 (4.5 μL, 0.033 mmol) was added. The vial was then loosely capped and transferred to a Parr autoclave, which was purged with H_2 (3 × 250 psi), pressurized to 1000 psi, and heated to 60 ˚C (oil bath). After 30 min, the reactor was vented (ca. 50 psi), cooled in an ice bath, purged with Ar (3 × 250 psi) and brought into a glovebox to transfer the reaction mixture to a J Young NMR tube. A C_6D_6 spike (50 μL) was added for NMR analysis.

Table 5.11. In situ NMR chemical shifts of key complexes discussed in this chapter.[a]

Complex	solvent	δ_P (ppm)	δ_H (ppm)	$^2J_{HP}$ (Hz)
$RuCl_2(PCy_3)_2(=CH_2)$ **Ru-2a**	C_6H_6	43.6 (s)	19.40 (s)	–
	CH_2Cl_2	43.9 (s)	19.02 (s)	–
$RuCl_2(PCy_3)_2(=CHOEt)$ **Ru-22a**	C_6H_6	35.1 (s)	14.76 (s)	–
	CH_2Cl_2	35.0 (s)	14.58 (s)	–
$RuCl_2(PCy_3)_2(=CHPh)$ **Ru-1a**	C_6H_6	37.1 (s)	20.61 (s)	–
	CH_2Cl_2	36.8 (s)	20.12 (s)	–
$RuCl_2(PCy_3)_2(=CHOTMS)$ **Ru-23a**[d]	C_6H_6	33.9 (s)	15.58 (s)	–
	CH_2Cl_2	34.2 (s)	15.16 (s)	–
$RuCl_2(IMes)(PCy_3)(=CHPh)$ **Ru-1b**	C_6H_6	31.9 (s)	19.45 (s)	–
	CH_2Cl_2	32.0 (s)	19.46 (s)	–
$RuCl_2(IMes)(PCy_3)(=CH_2)$ **Ru-2b**	C_6H_6	41.1 (s)	19.02 (s)	–
	CH_2Cl_2	40.0 (s)	18.17 (s)	–
$RuCl_2(IMes)(PCy_3)(=CHOEt)$ **Ru-22b**	C_6H_6	33.3 (s)	14.23 (s)	–
	CH_2Cl_2	32.6 (s)	13.89 (s)	–
$RuCl_2(IMes)(PCy_3)(=CHOTMS)$ **Ru-23b**[b]	C_6H_6	34.6 (s)	14.95 (d)	3
	CH_2Cl_2	–	–	–
$RuHCl(H_2)(PCy_3)_2$ **Ru-6a**	CH_2Cl_2	53.2 (s)	–16.91 (br)	–
$RuHCl(H_2)(IMes)(PCy_3)$ **Ru-6b**	CH_2Cl_2	55.1 (s)	–16.91 (br)	–
$RuHCl(CO)(PCy_3)_2$ **Ru-7a**	C_6H_6	47.3 (s)	–24.22 (t)	18
	CH_2Cl_2	46.9 (s)	–24.63 (t)	18
$RuHCl(CO)(IMes)(PCy_3)$ **Ru-7b**	C_6H_6	47.8 (s)	–24.82 (d)	21
	CH_2Cl_2	47.5 (s)	–25.26 (d)	21
$RuH(OMe)(CO)_2(PCy_3)_2$ **Ru-18a**	10:1 CH_2Cl_2-MeOH	50.5 (s)	–5.30 (t)	20
$RuH(OMe)(CO)_2(IMes)(PCy_3)$ **Ru-18b**	10:1 CH_2Cl_2-MeOH	55.9 (s)	–4.99 (d)	23
$Ru(H)_2(CO)_2(IMes)(PCy_3)$ **Ru-19b**	10:1 CH_2Cl_2-MeOH	68.2 (s)	–7.68 (d)	25
$RuH(\kappa^2\text{-}OC(O)OMe)(CO)(PCy_3)_2$ **Ru-28a**	10:1 THF-MeOH	45.5 (s)	–18.07 (t)	19
$RuH(\kappa^2\text{-}OC(O)OMe)(CO)(IMes)(PCy_3)$ **Ru-28b**	10:1 THF-MeOH	46.4 (s)	–18.38 (d)	22
$RuH(\kappa^2\text{-}OC(O)OH)(CO)(PCy_3)_2$ **Ru-29a**	10:1 THF-MeOH	45.8 (s)	–16.54 (t)	20
$RuH(\kappa^2\text{-}OC(O)OH)(CO)(IMes)(PCy_3)$ **Ru-29b**	10:1 THF-MeOH	47.1 (s)	–16.73 (d)	24

[a] C_6D_6 added as deuterium source for locking and shimming. ^1H NMR values given for alkylidene or hydride signals observed on solvent suppression. All reactions of methylidenes **Ru-2a/b** displayed the methylphosphonium salt $MePCy_3Cl$ (s, δ_P 34.5 in C_6D_6, 34.6 in CH_2Cl_2). [b] Formed in situ from **Ru-1** + 10 CH_2=CHOTMS at 23 °C.

5.5 References

(1) Camm, K. D.; Castro, N. M.; Liu, Y.; Czechura, P.; Snelgrove, J. L.; Fogg, D. E. *J. Am. Chem. Soc.* **2007**, *129*, 4168-4169.
(2) Fogg, D. E. *Can. J. Chem.* **2008**, *86*, 931-941.
(3) Dias, E. L.; Nguyen, S. T.; Grubbs, R. H. *J. Am. Chem. Soc.* **1997**, *119*, 3887-3897.
(4) Schwab, P.; Grubbs, R. H.; Ziller, J. W. *J. Am. Chem. Soc.* **1996**, *118*, 100-110.
(5) Oliván, M.; Caulton, K. G. *Inorg. Chem.* **1999**, *38*, 566-570.
(6) Ulman, M.; Grubbs, R. H. *J. Org. Chem.* **1999**, *64*, 7202-7207.
(7) Ulman, M.; Grubbs, R. H. *Organometallics* **1998**, *17*, 2484-2489.
(8) Louie, J.; Grubbs, R. H. *Organometallics* **2002**, *21*, 2153-2164.
(9) Ulman, M.; Belderrain, T. R.; Grubbs, R. H. *Tetrahedron Lett.* **2000**, *41*, 4689-4693.
(10) Choi, T.-L.; Lee, C. W.; Chatterjee, A. K.; Grubbs, R. H. *J. Am. Chem. Soc.* **2001**, *123*, 10417-10418.
(11) Nunes, R.; dos Santos, E. N.; Fogg, D. E., unpublished work.
(12) Arisawa, M.; Terada, Y.; Takahashi, K.; Nakagawa, M.; Nishida, A. *J. Org. Chem.* **2006**, *71*, 4255-4261.
(13) Beach, N. J.; Camm, K. D.; Fogg, D. E. *Organometallics* **2010**, *29*, 5450-5455.
(14) Drouin, S. D.; Yap, G. P. A.; Fogg, D. E. *Inorg. Chem.* **2000**, *39*, 5412-5414.
(15) Chaudret, B. N.; Cole-Hamilton, D. J.; Nohr, R. S.; Wilkinson, G. *J. Chem. Soc., Dalton Trans.* **1977**, 1546-1557.
(16) Dinger, M. B.; Mol, J. C. *Organometallics* **2003**, *22*, 1089-1095.
(17) Dinger, M. B.; Mol, J. C. *Eur. J. Inorg. Chem.* **2003**, 2827-2833.
(18) Banti, D.; Mol, J. C. *J. Organomet. Chem.* **2004**, *689*, 3113-3116.
(19) Sanford, M. S.; Love, J. A.; Grubbs, R. H. *J. Am. Chem. Soc.* **2001**, *123*, 6543-6554.
(20) Kotyk, M. W.; Gorelsky, S. I.; Conrad, J. C.; Carra, C.; Fogg, D. E. *Organometallics* **2009**, 5424–5431.
(21) Hong, S. H.; Wenzel, A. G.; Salguero, T. T.; Day, M. W.; Grubbs, R. H. *J. Am. Chem. Soc.* **2007**, *129*, 7961-7968.
(22) Leitao, E. M.; Dubberley, S. R.; Piers, W. E.; Wu, Q.; McDonald, R. *Chem. Eur. J.* **2008**, *14*, 11565-11572.
(23) Hong, S. H.; Day, M. W.; Grubbs, R. H. *J. Am. Chem. Soc.* **2004**, *126*, 7414-7415.
(24) S.D. Drouin, Ph.D. Thesis, University of Ottawa, 2003; p. 29.
(25) Moers, F. G.; ten Hoedt, R. W. M.; Langhout, J. P. *J. Organomet. Chem.* **1974**, *65*, 93-98.
(26) Wu, Z.; Nguyen, S. T.; Grubbs, R. H.; Ziller, J. W. *J. Am. Chem. Soc.* **1995**, *117*, 5503-5511.
(27) Beach, N. J.; Blacquiere, J. M.; Drouin, S. D.; Fogg, D. E. *Organometallics* **2009**, *28*, 441-447.
(28) Merrett, K.; Liu, W.; Mitra, D.; Camm, K. D.; McLaughlin, C. R.; Liu, Y.; Watsky, M. A.; Li, F.; Griffith, M.; Fogg, D. E. *Biomaterials* **2009**, *30*, 5403–5408.
(29) Lide, D. R., Eds. CRC Handbook of Chemistry and Physics, Internet Version 2005. CRC Press: Boca Raton, Florida, 2005.
(30) Jazzar, R. F. R.; Bhatia, P. H.; Mahon, M. F.; Whittlesey, M. K. *Organometallics* **2003**, *22*, 670-683.

(31) Edwards, A. J.; Elipe, S.; Esteruelas, M. A.; Lahoz, F. J.; Oro, L. A.; Valero, C. *Organometallics* **1997**, *16*, 3828-3836.
(32) Yoshida, T.; Thorn, D. L.; Okano, T.; Ibers, J. A.; Otsuka, S. *J. Am. Chem. Soc.* **1979**, *101*, 4212-4221.
(33) Flynn, B. R.; Vaska, L. *J. Am. Chem. Soc.* **1973**, *95*, 5081-5083.
(34) Antonova, N. S.; Carbo, J. J.; Poblet, J. M. *Organometallics* **2009**, *28*, 4283-4287.
(35) Getty, K.; Delgado-Jaime, M. U.; Kennepohl, P. *J. Am. Chem. Soc.* **2007**, *129*, 15774-15776.
(36) Scholl, M.; Ding, S.; Lee, C. W.; Grubbs, R. H. *Org. Lett.* **1999**, *1*, 953-956.
(37) Huang, J.; Stevens, E. D.; Nolan, S. P.; Petersen, J. L. *J. Am. Chem. Soc.* **1999**, *121*, 2674-2678.

6 Conclusions and Future Work

The focus of this thesis work was the potential opportunities presented by tandem catalysis within the context of olefin metathesis. Coupling of metathesis manifolds with olefin hydrogenation or functionalization was reviewed in Chapter 1. The key step involves transformation of the spent, uninitiated, or resting-state metathesis catalyst into a second catalyst species. To maximize the efficiency of this transformation – and hence to maximize the efficiency with which the second catalytic cycle can operate – a clearer mechanistic and practical understanding of the chemistry is essential. Similarly desirable is identification of the most appropriate structure for catalysis in the second cycle.

Chapter 2 of this thesis presents a comparative study of the hydrogenation activity and lifetime of hydride catalysts accessible from benzylidene complexes. Specifically, hydridodihydrogen complexes were compared to their hydridocarbonyl analogues: the superior hydrogenation performance of the latter was demonstrated, and was related to their exceptionally long lifetime under typical hydrogenation conditions.

A mechanistic study follows (Chapter 3), which gives insight into the factors controlling the efficiency with which the catalytically most productive hydridocarbonyl complexes can be generated via state-of-the-art procedures for tandem ROMP-hydrogenation. The Grubbs benzylidene precatalysts were used as proxies for the alkylidene complexes that represent the propagating species in ROMP. A "generation gap" was observed, in which the first-generation catalyst was found to be most efficiently transformed into the $RuHCl(CO)(L)(PCy_3)$ target **Ru-7** by a two-step reaction with H_2 and base, then methanol and base, but the second-generation catalyst was much more efficiently transformed via the H_2-free reaction with methanol and base. This study demonstrates that catalyst-specific

tailoring is essential, even for such closely related catalyst species, and thus carries profound implications for the design of successful tandem catalysis protocols.

A cautionary study follows (Chapter 4), in which use of excess methoxide in methanol to trigger formation of the target hydride has unexpected consequences. Reactions of this promiscuous reagent with the benzylidene precatalysts (used as a proxy for the alkylidene resting state) yields unanticipated methoxyhydride derivatives, rather than **Ru-7**. The implications are clear: knowledge of the fundamental inorganic reaction pathways is essential to the development of efficient tandem catalysis protocols.

Finally, Chapter 5 examines the validity of using [Ru]=CHPh precatalysts as a proxy for [Ru]=CH_2 and [Ru]=CHOR species. A specific question was the efficiency with which catalytically-versatile **Ru-7** could be obtained from methylidenes (resting-state species in RCM and CM), or from Fischer carbenes (such as those formed on quenching metathesis). Efficient routes for such transformations could improvement of established methodologies, and development of new methodologies for tandem (R)CM-functionalization. The first-generation benzylidene, methylidene and ethoxylidene complexes were found to be transformed into **Ru-7a** most efficiently via hydrogenolysis, followed by treatment with methanol and NEt_3. In cases where olefin saturation is not wanted, CM with vinyloxytrimethylsilane, followed by degradation of the resulting trimethylsiloxylidene, gives yields of **Ru-7a** from benzylidene **Ru-1a**, while methylidene **Ru-2a** and ethoxylidene are most compatible with H_2-free methanolysis. Hydrogenolysis cannot be used for the second-generation systems, because it triggers disproportionation and decomposition. Instead, H_2-free methanolysis proved optimal, as with the benzylidene complex described in Chapter 3. Thus, while the second-generation benzylidene serves as an excellent proxy for

its methylidene and ethoxylidene analogues, the first-generation benzylidene exhibits an optimal H_2-free pathway to **Ru-7a** that is dissimilar to that of its methylidene and ethoxylidene analogues.

The latter studies, in particular, set the stage for tandem (R)CM-functionalization processes based on **Ru-7**. Future studies should include examination of the activity of first- and second-generation **Ru-7a/b** for olefin functionalization. Attractive candidates for preliminary catalytic studies include hydroamination and alkene-amine coupling, given the proliferation of nitrogenous compounds in natural products and pharmaceuticals.

Structural characterization and isolation of the paramagnetic byproducts, formed during all reactions of Grubbs-type complexes described in this thesis, would enable elucidation of their olefin functionalization activity. Use of optimized olefin functionalization protocols could then be matched to appropriate metathesis transformations, using the optimized trigger protocols outlined in this thesis, thereby providing a versatile toolkit for the efficient, economical synthesis of challenging organic targets via tandem metathesis-functionalization.

The relative thermal stability of the IMes- and H_2IMes-substituted catalyst systems should be examined, in hopes of explaining our observation of lower post-ROMP hydrogenation activity of the H_2IMes systems. Of particular interest is the possibility that saturation of the imidazole backbond leads to fundamental differences in reactivity.

Appendices:

A.1: NMR Spectra

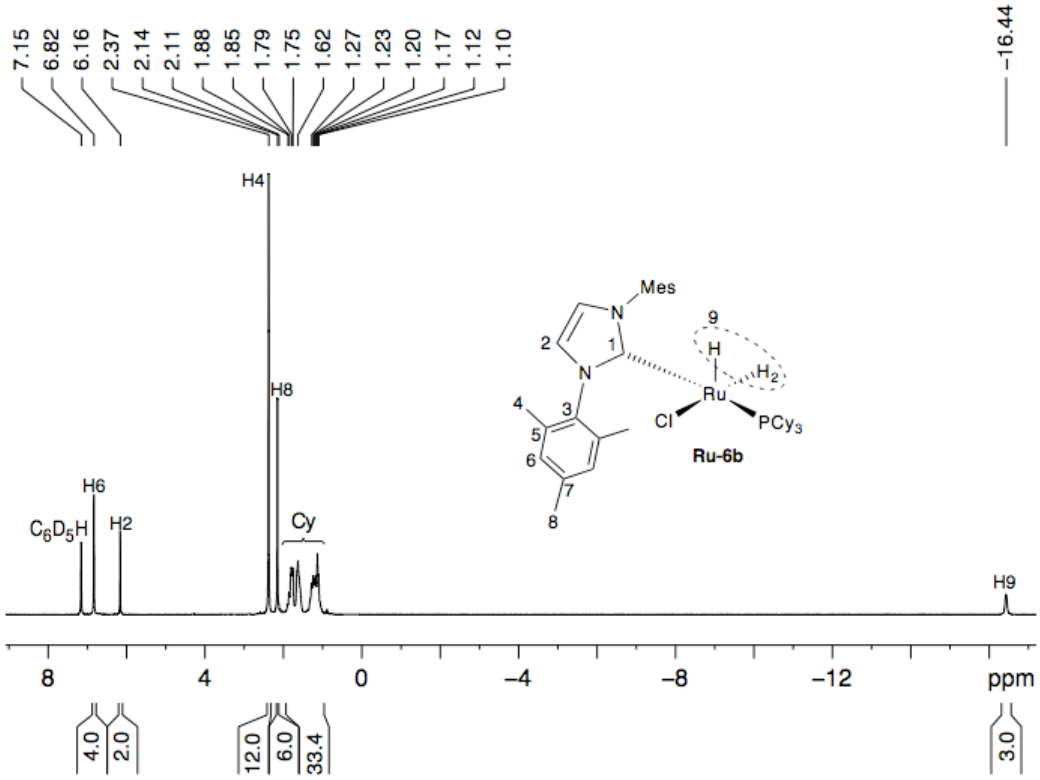

Figure A.1.1. ^{1}H spectrum of **Ru-6b** (C_6D_6).

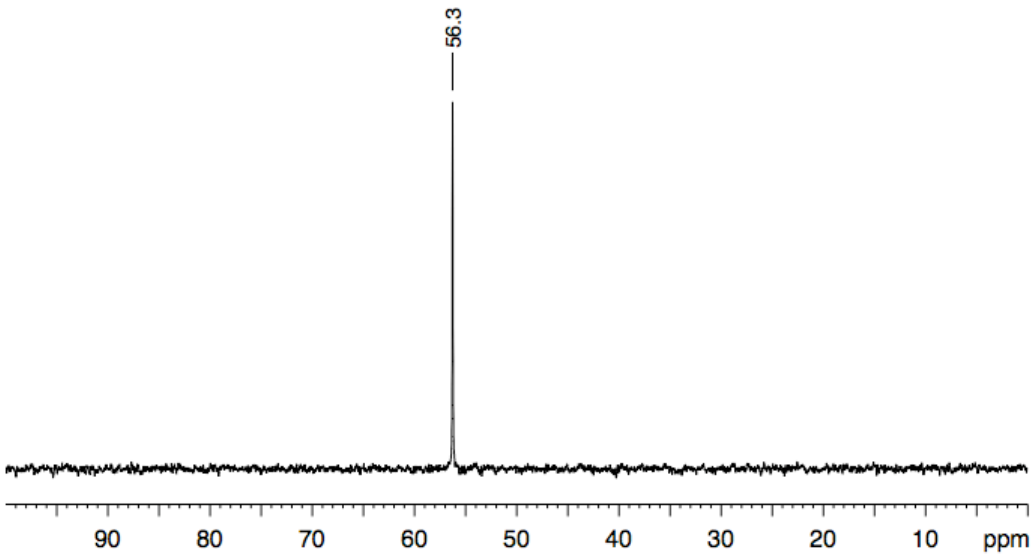

Figure A.1.2. $^{31}P\{^{1}H\}$ spectrum of **Ru-6b** (C_6D_6).

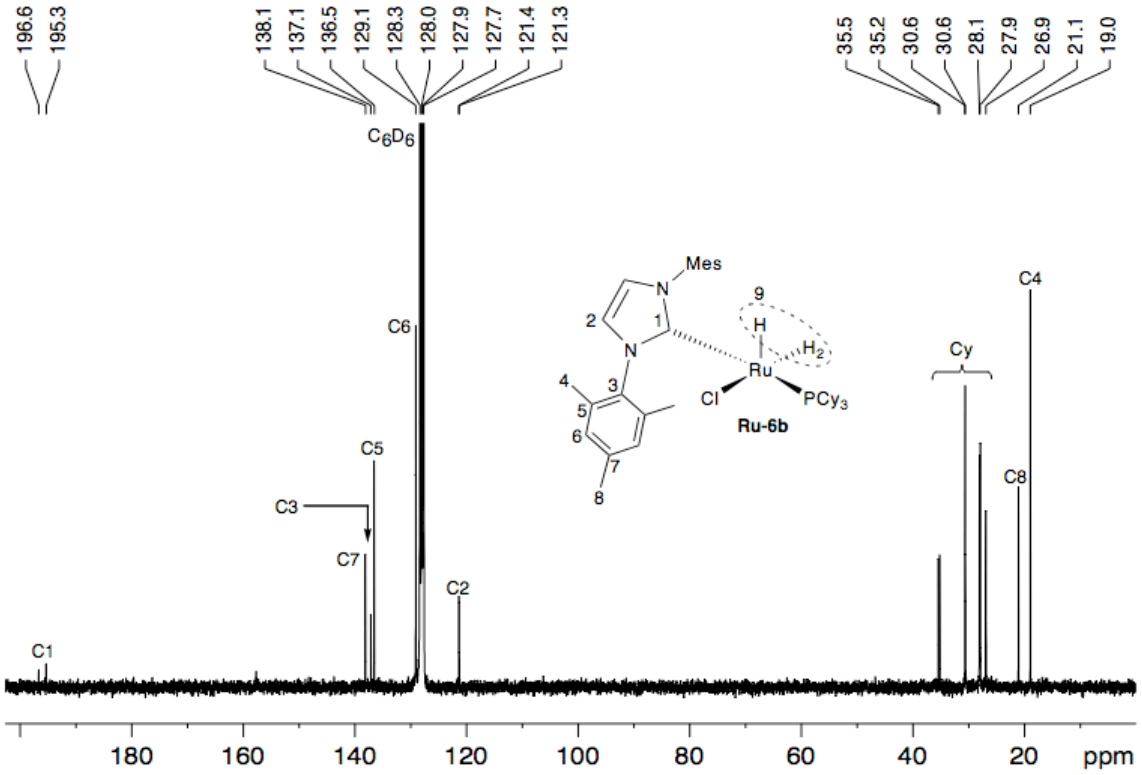

Figure A.1.3. $^{13}C\{^{1}H\}$ spectrum of **Ru-6b** (C_6D_6).

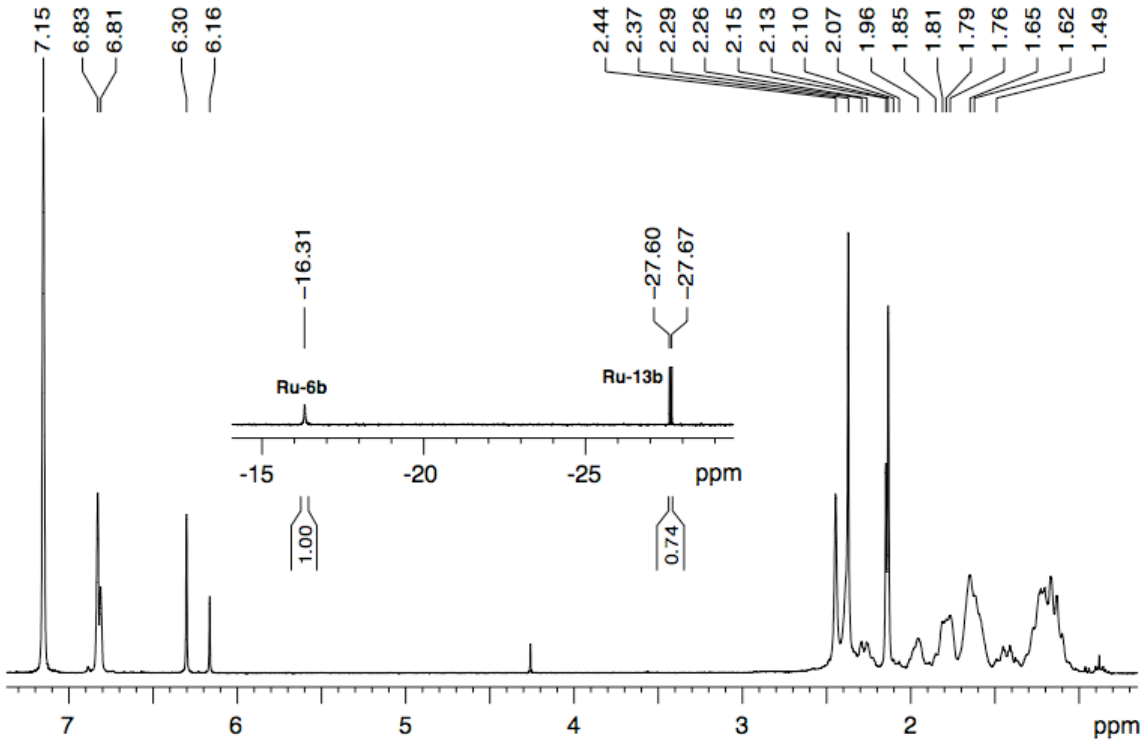

Figure A.1.4. ^{1}H spectrum for **Ru-6b** under N_2, 24 h (C_6D_6).

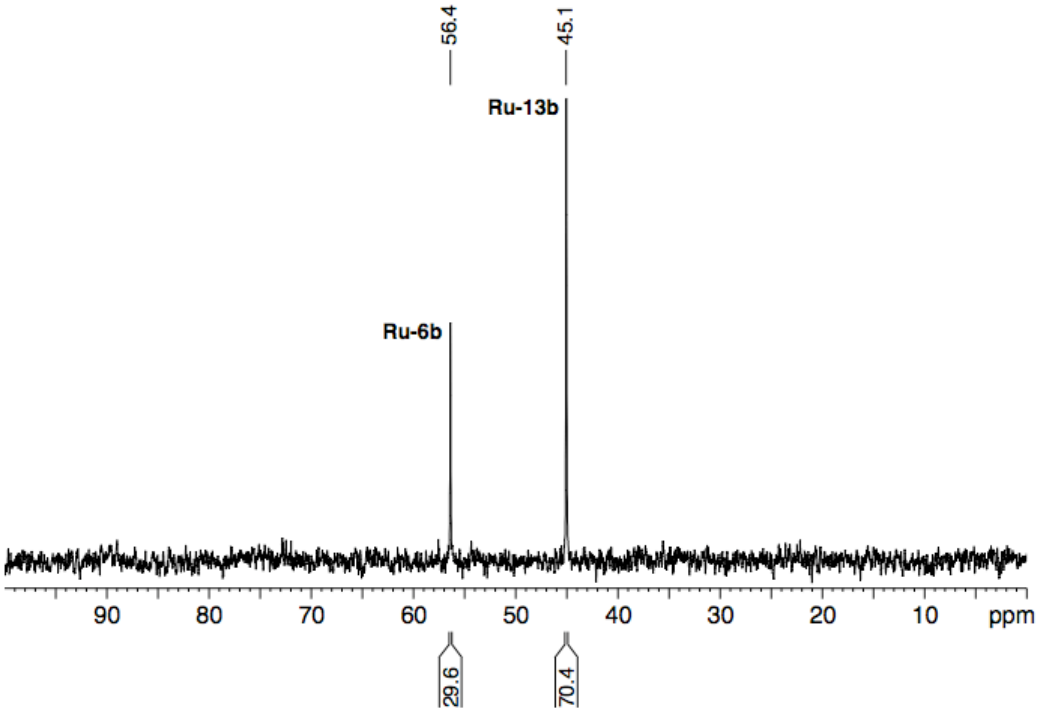

Figure A.1.5. $^{31}P\{^{1}H\}$ spectrum for **Ru-6b** under N_2, 24 h (C_6D_6).

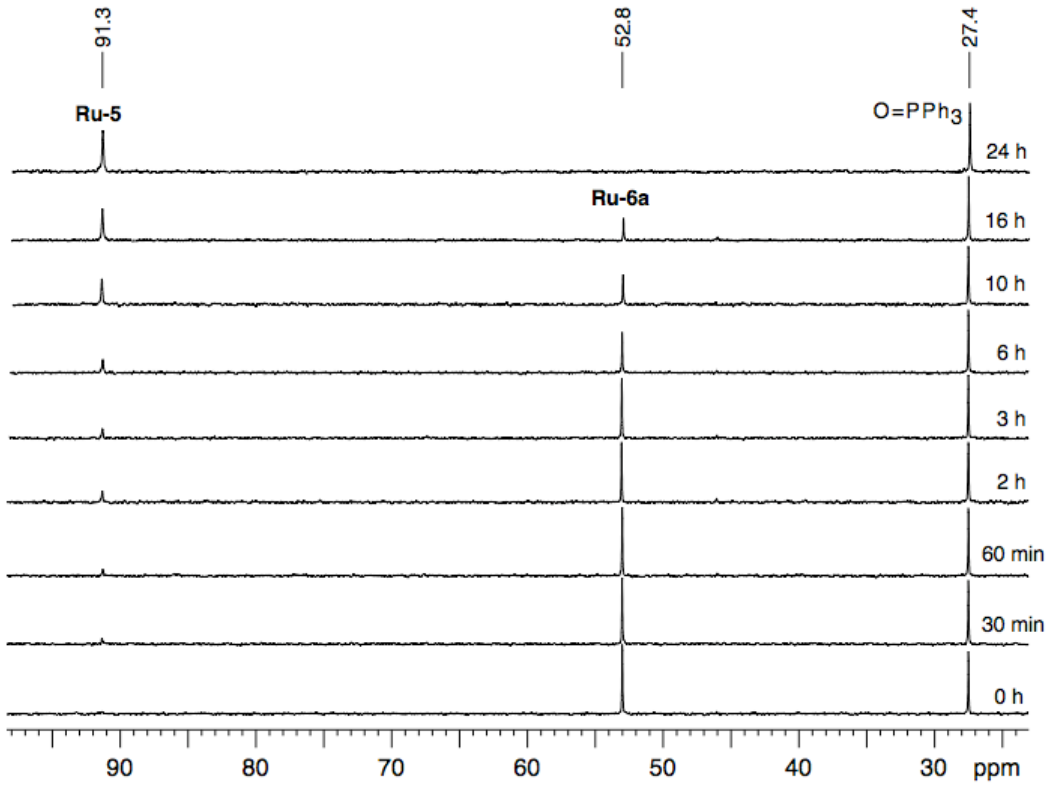

Figure A.1.6. $^{31}P\{^{1}H\}$ spectra for **Ru-6a** thermolysis. [**Ru-6a**] = 14 mM, CH_2Cl_2, H_2 (1 atm), 55 ˚C.

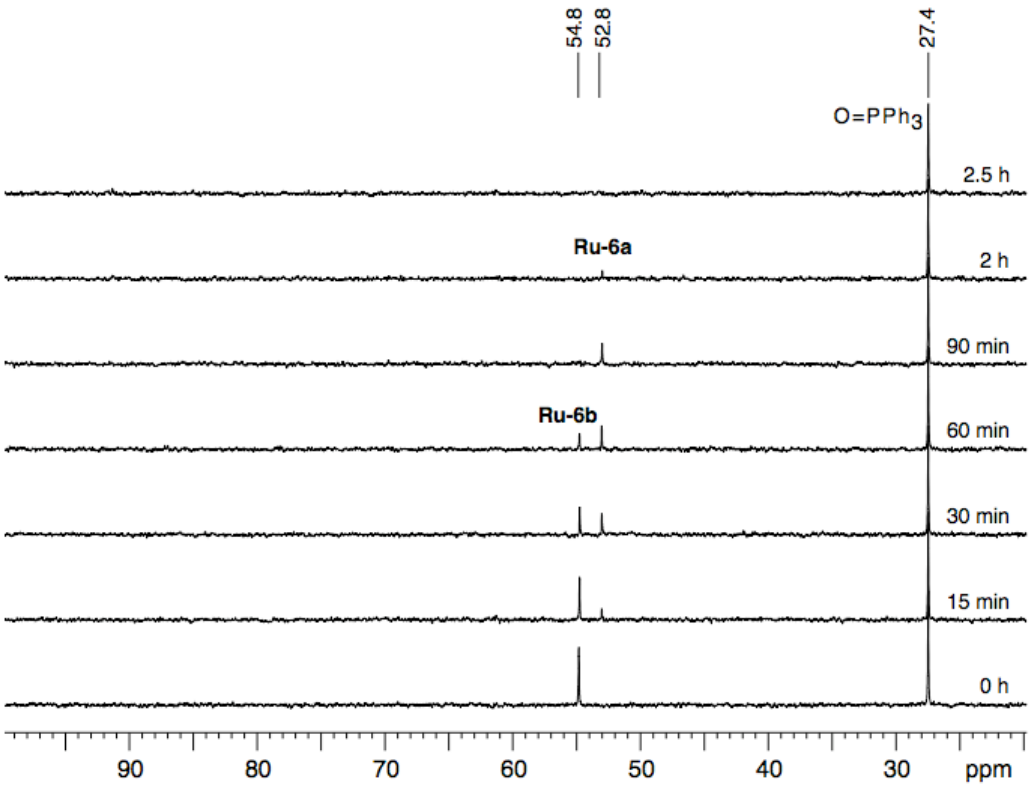

Figure A.1.7. $^{31}P\{^{1}H\}$ spectra for **Ru-6b** thermolysis. [**Ru-6b**] = 14 mM, CH_2Cl_2, H_2 (1 atm), 55 ˚C.

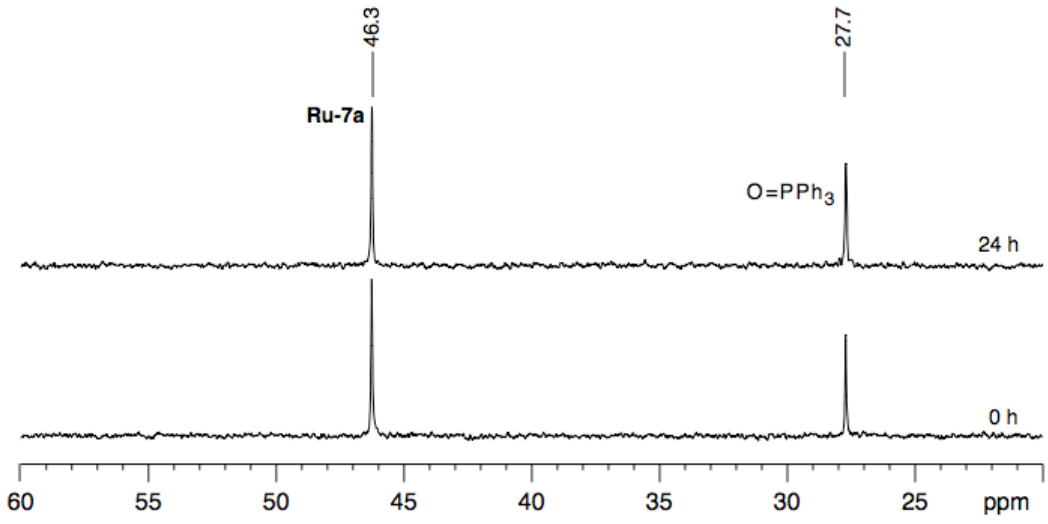

Figure A.1.8. $^{31}P\{^{1}H\}$ spectra for **Ru-7a** thermolysis. [**Ru-7a**] = 14 mM, CH_2Cl_2, H_2 (1 atm), 55 ˚C.

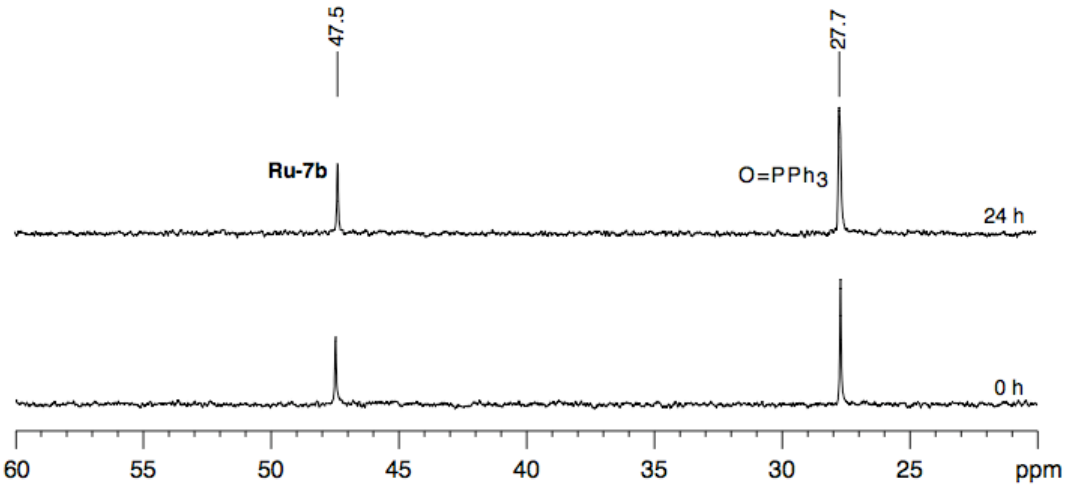

Figure A.1.9. $^{31}P\{^{1}H\}$ spectra for **Ru-7b** thermolysis. [**Ru-7b**] = 14 mM, CH_2Cl_2, H_2 (1 atm), 55 ˚C.

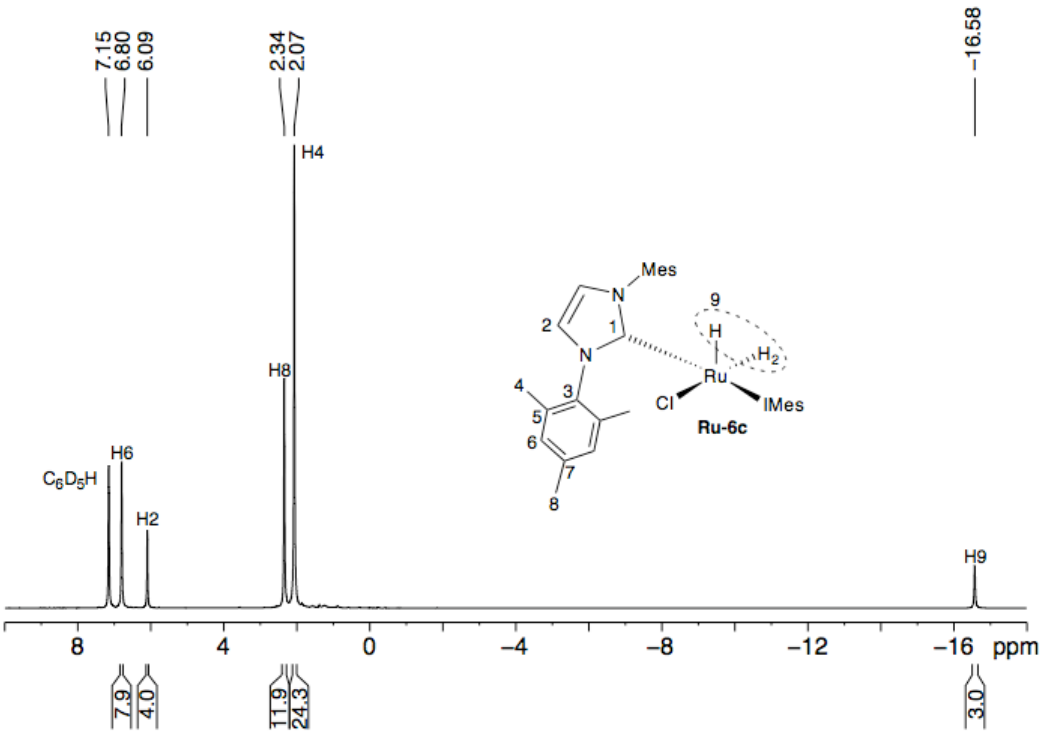

Figure A.1.10. ^{1}H spectrum of isolated **Ru-6c** (C_6D_6).

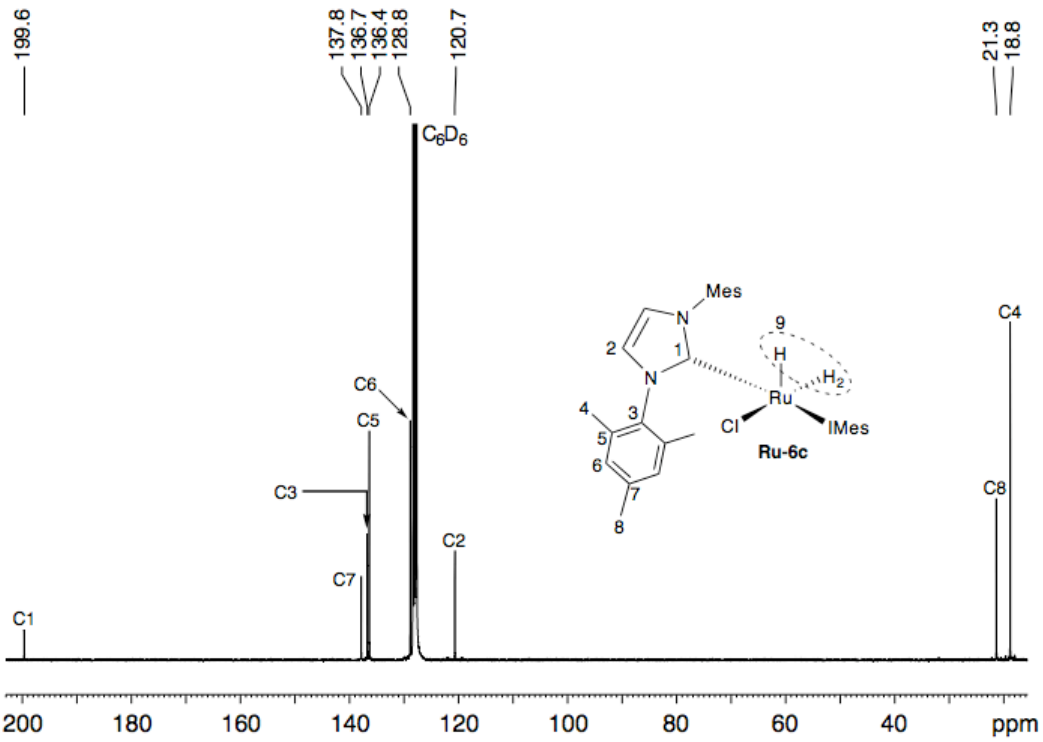

Figure A.1.11. $^{13}C\{^{1}H\}$ spectrum of isolated **Ru-6c** (C_6D_6).

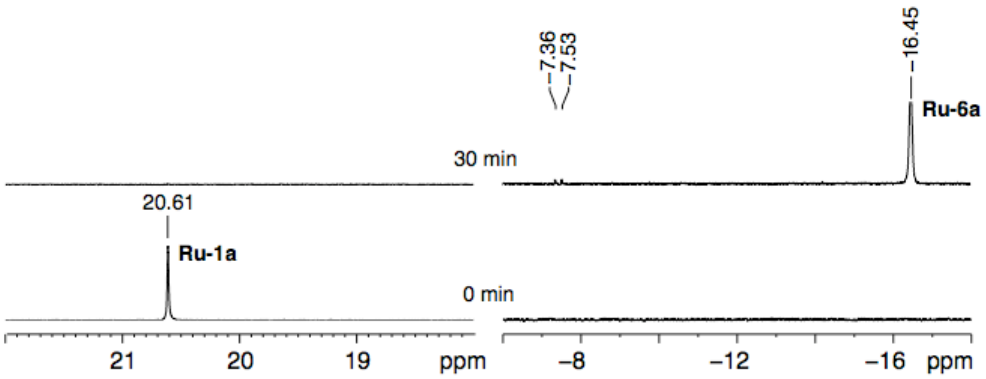

Figure A.1.12. ^{1}H spectra for **Ru-1a** hydrogenolysis (C_6D_6). Left: alkylidene region; right: hydride region.

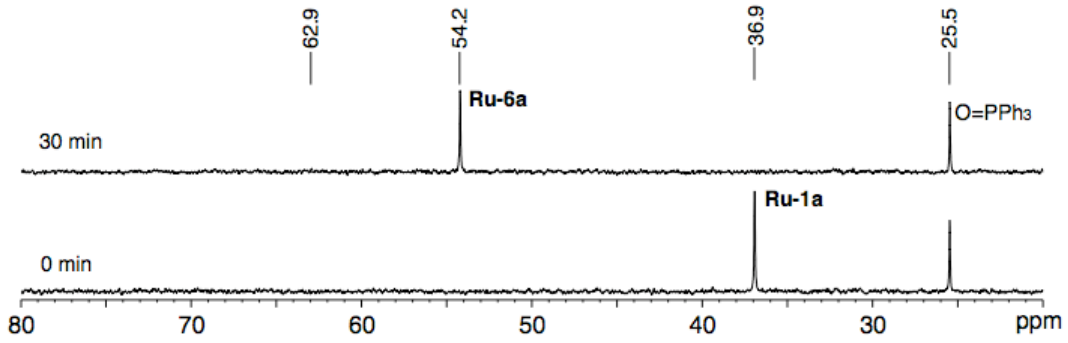

Figure A.1.13. $^{31}P\{^{1}H\}$ spectra for **Ru-1a** hydrogenolysis (C_6D_6).

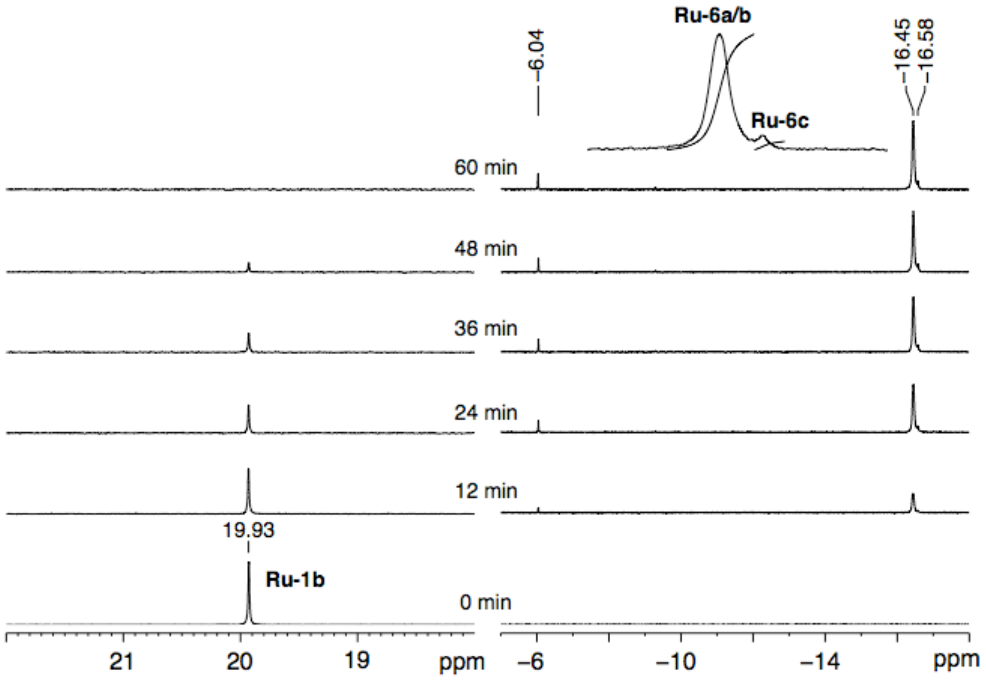

Figure A.1.14. ^{1}H spectra for **Ru-1b** hydrogenolysis (C_6D_6). Left: alkylidene region; right: hydride region.

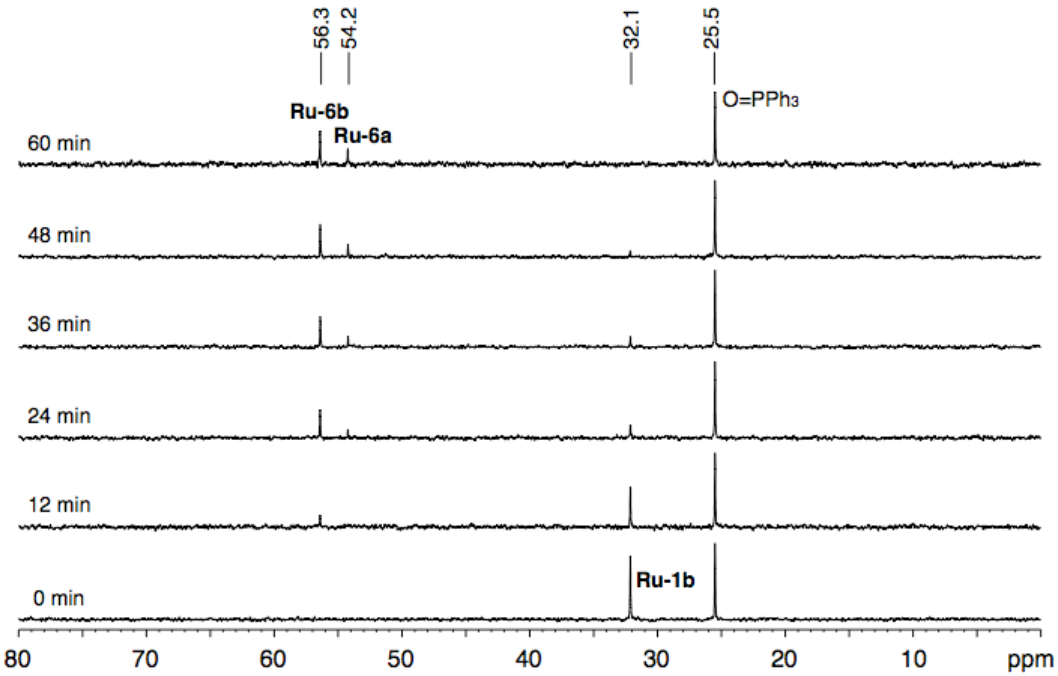

Figure A.1.15. $^{31}P\{^{1}H\}$ spectra for **Ru-1b** hydrogenolysis (C_6D_6).

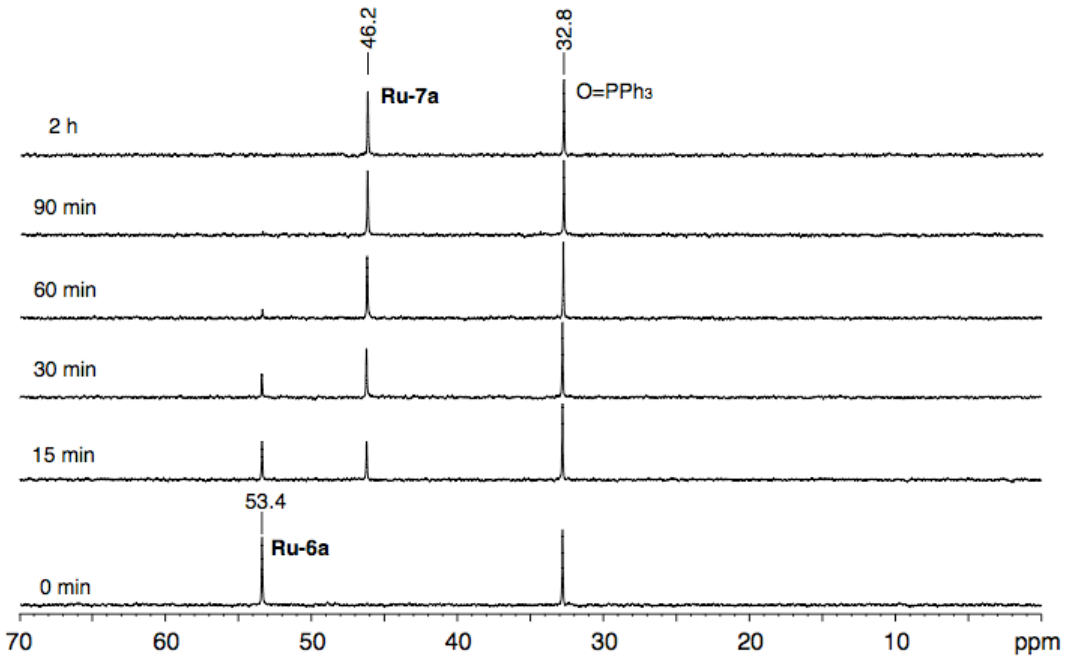

Figure A.1.16. $^{31}P\{^{1}H\}$ spectra for **Ru-6a** carbonylation (4:1 CH_2Cl_2-MeOH, C_6D_6 lock).

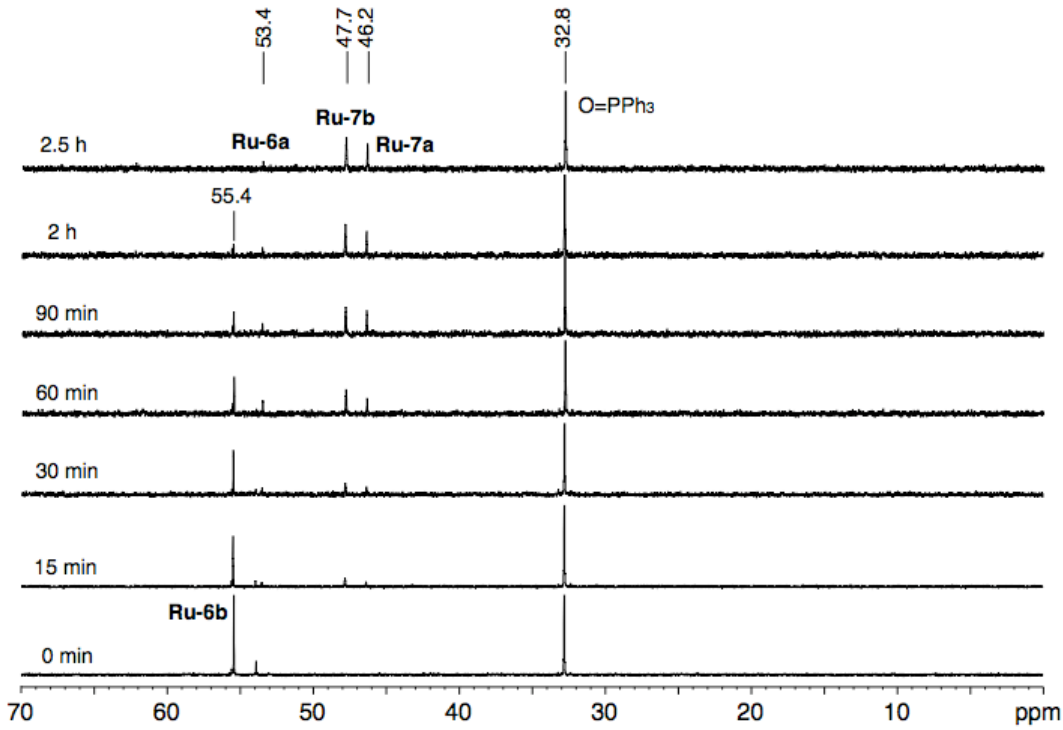

Figure A.1.17. $^{31}P\{^{1}H\}$ spectra for **Ru-6b** carbonylation (4:1 CH_2Cl_2-MeOH, C_6D_6 lock).

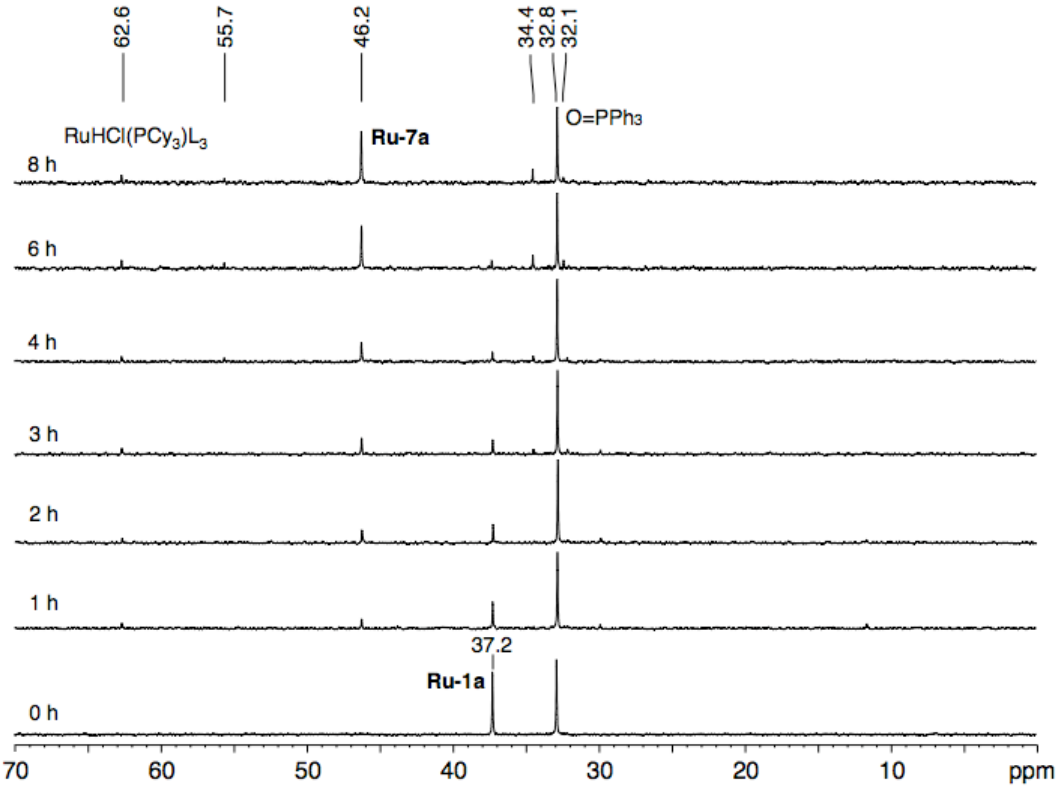

Figure A.1.18. $^{31}P\{^{1}H\}$ spectra for **Ru-1a** methanolysis (4:1 CH_2Cl_2-MeOH, C_6D_6 lock).

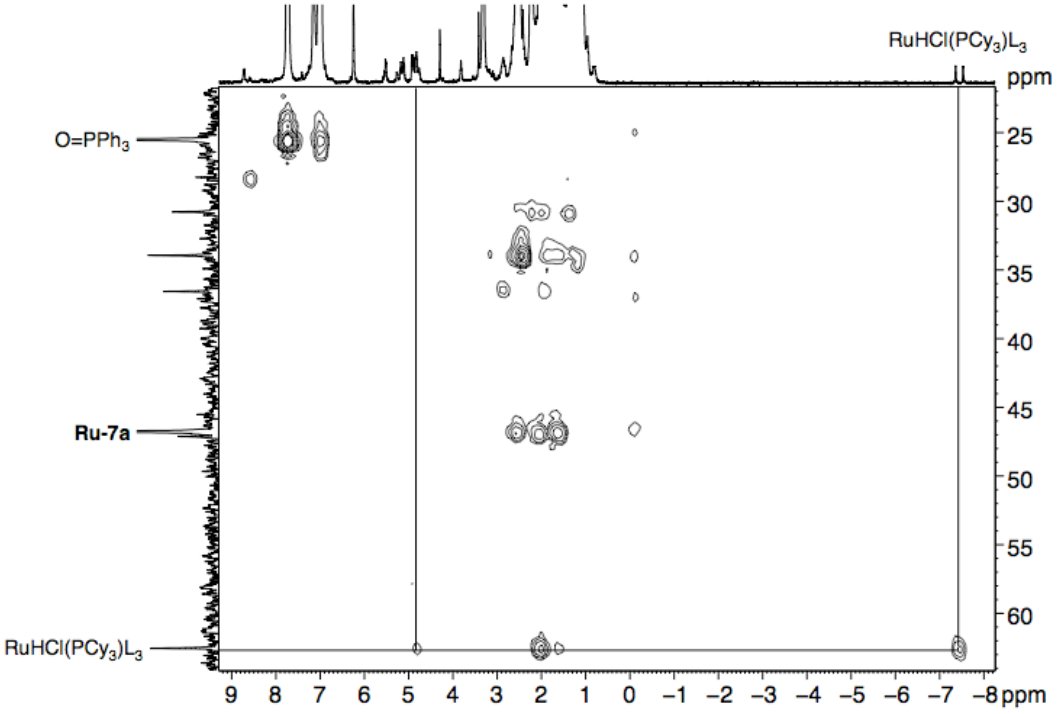

Figure A.1.19. ^{1}H-^{31}P HMBC spectrum of **Ru-1a** methanolysis reaction mixture (C_6D_6).

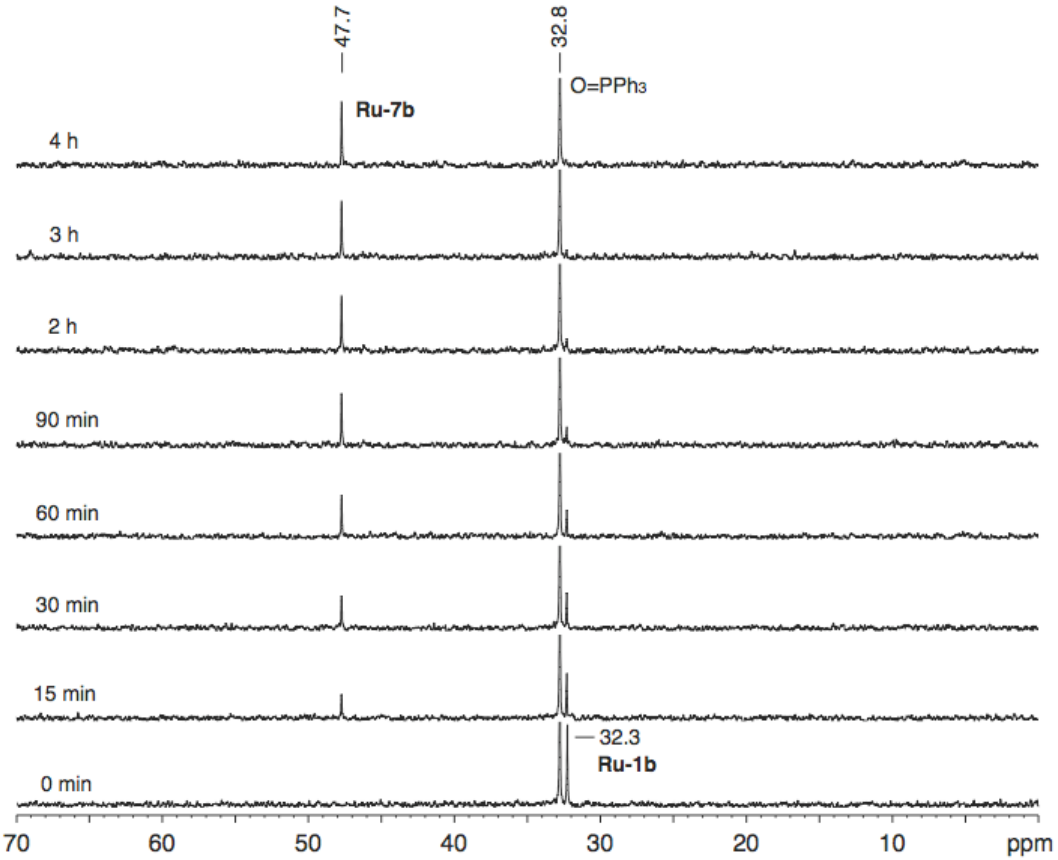

Figure A.1.20. $^{31}P\{^{1}H\}$ spectra for **Ru-1b** methanolysis (4:1 CH_2Cl_2-MeOH, C_6D_6 lock).

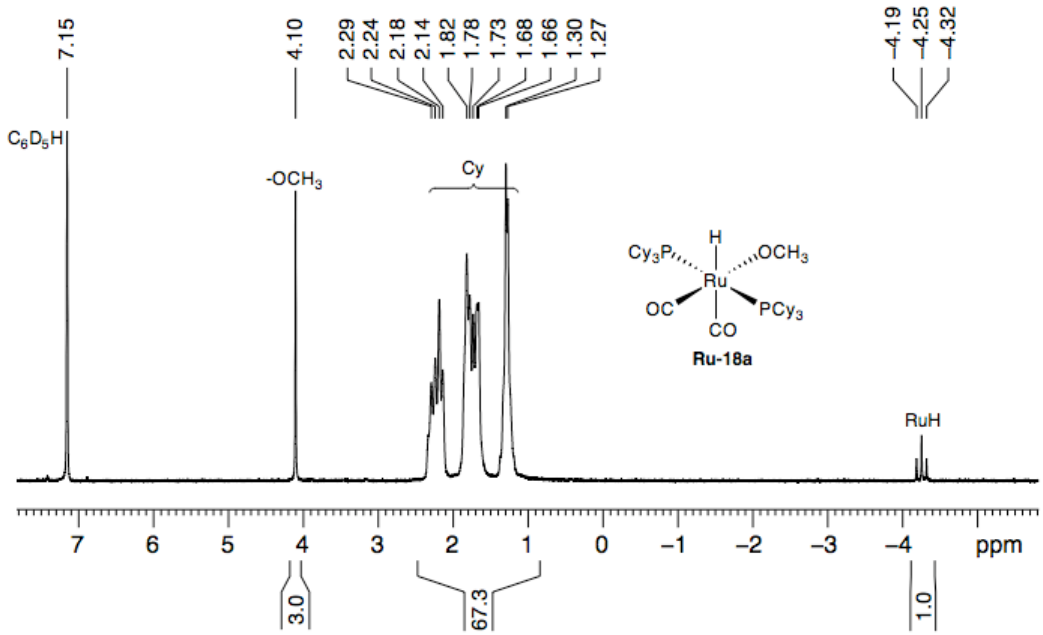

Figure A.1.21. ^{1}H spectrum of **Ru-18a** (C_6D_6).

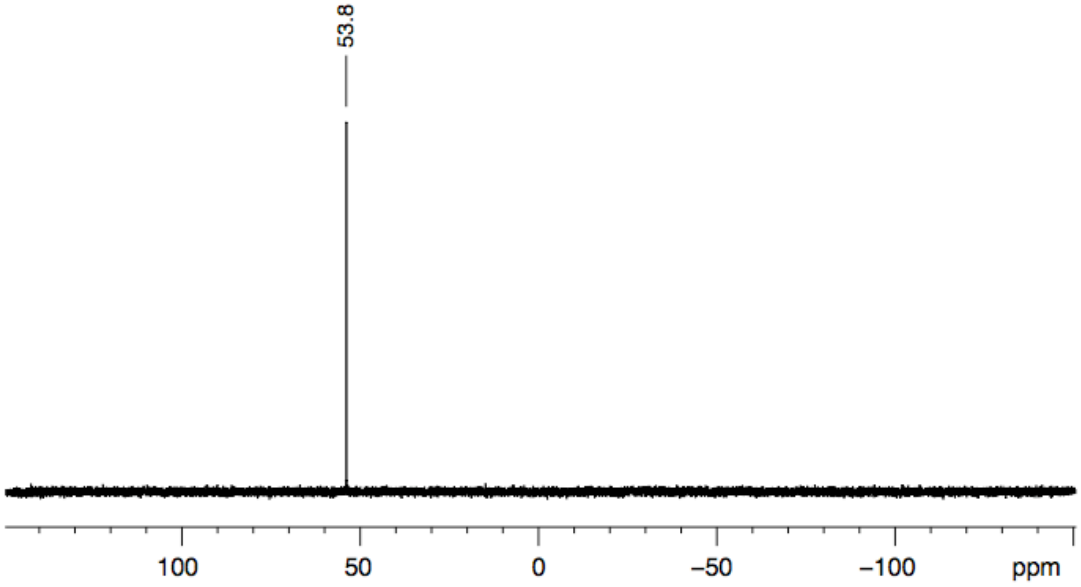

Figure A.1.22. $^{31}P\{^{1}H\}$ spectrum of **Ru-18a** (C_6D_6).

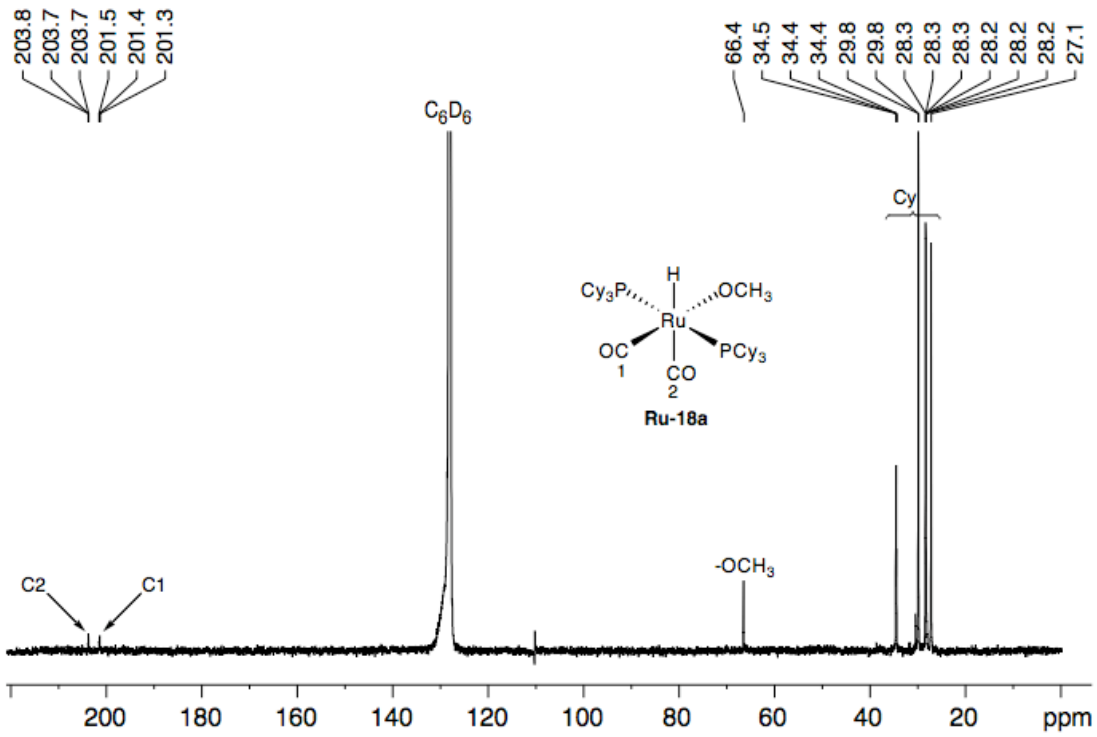

Figure A.1.23. $^{13}C\{^{1}H\}$ spectrum of **Ru-18a** (C_6D_6).

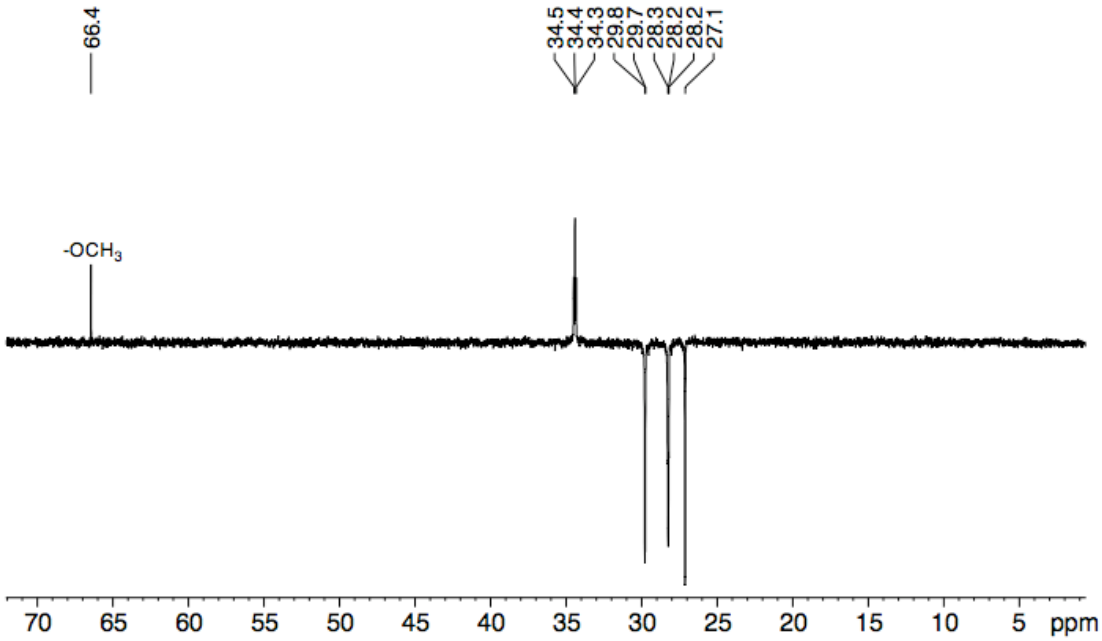

Figure A.1.24. ^{13}C DEPT spectrum of **Ru-18a** (C_6D_6).

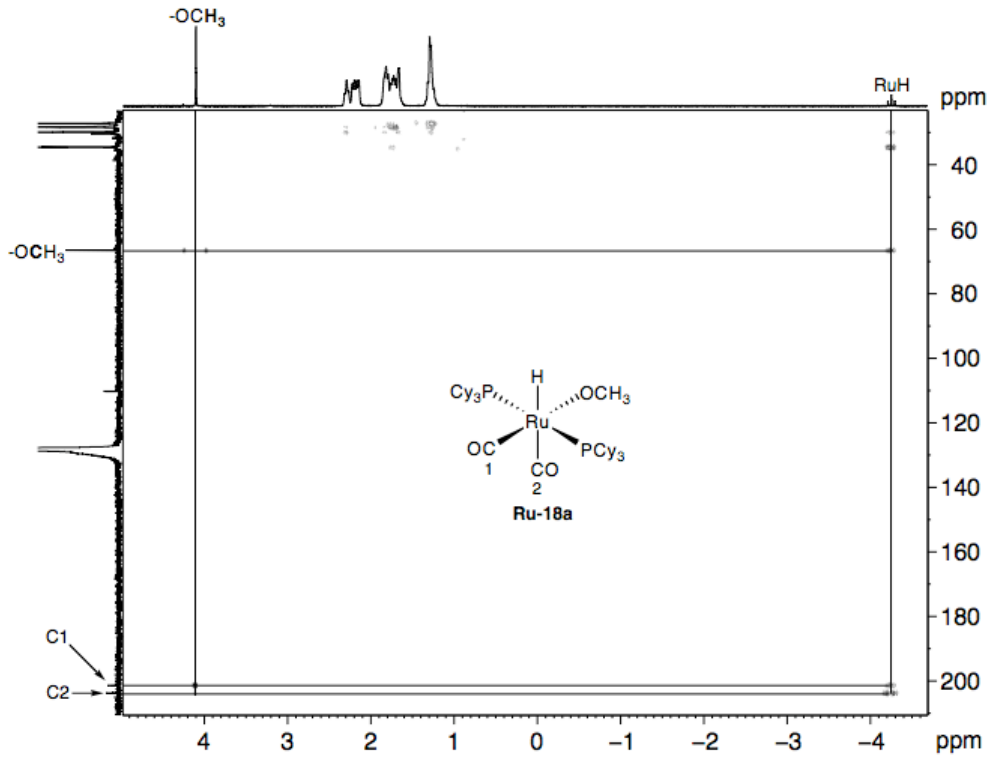

Figure A.1.25. ^{1}H-^{13}C HMBC spectrum of **Ru-18a** (C_6D_6).

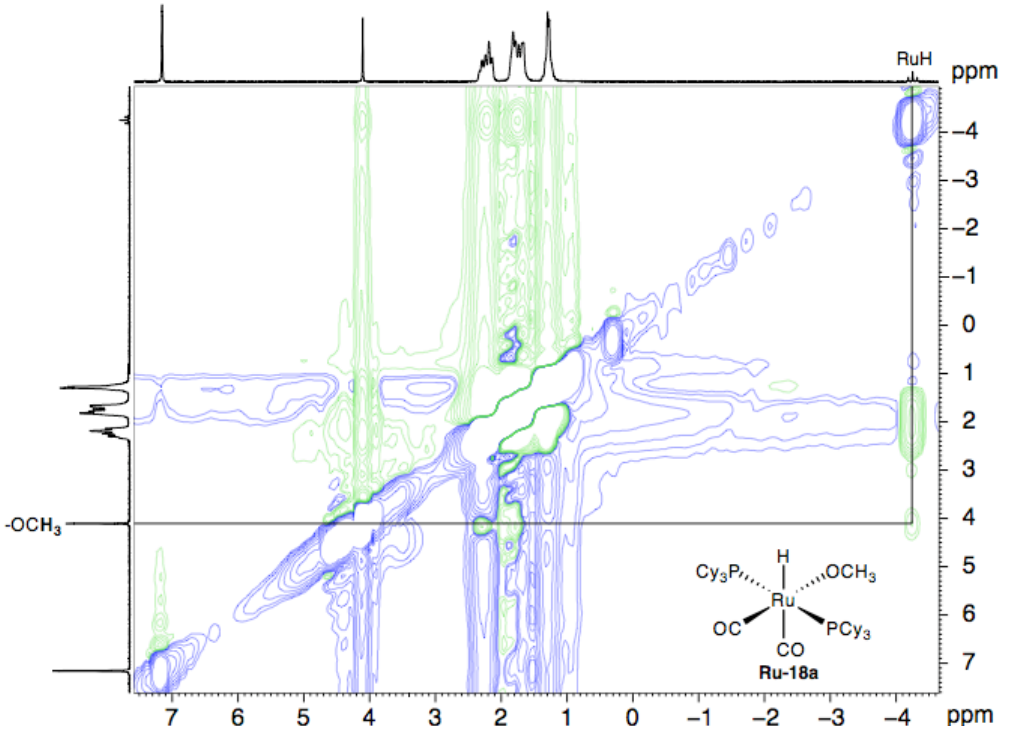

Figure A.1.26. ^{1}H NOESY spectrum of **Ru-18a** (τ_{mix} = 345 ms).

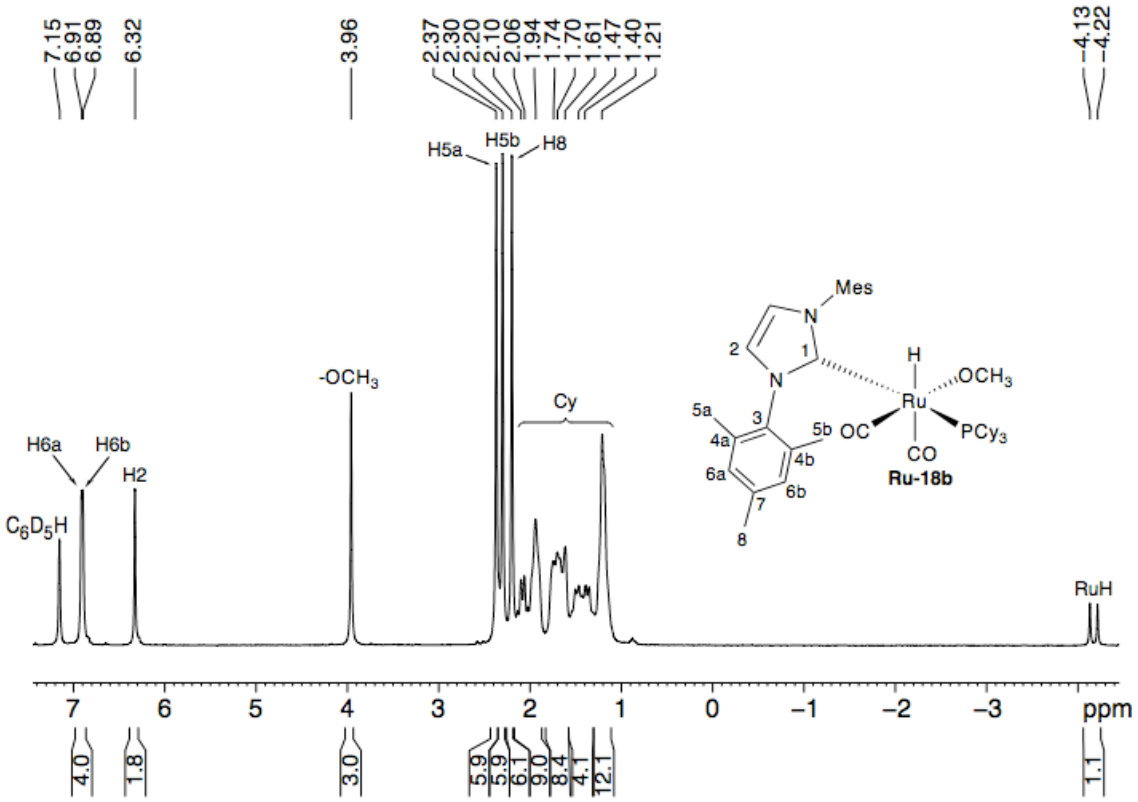

Figure A.1.27. ^{1}H spectrum of **Ru-18b** (C_6D_6).

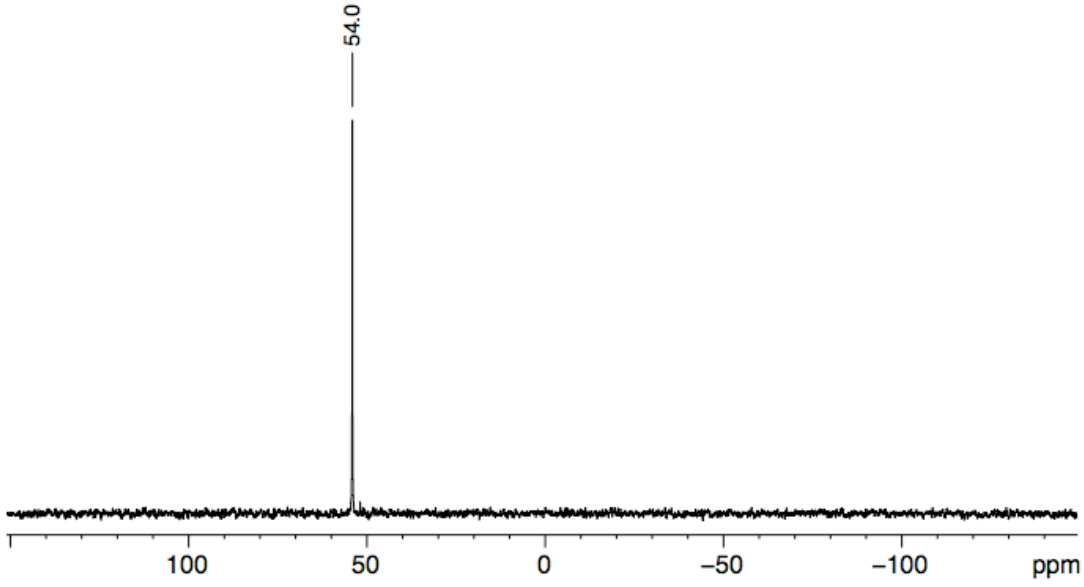

Figure A.1.28. $^{31}P\{^{1}H\}$ spectrum of **Ru-18b** (C_6D_6).

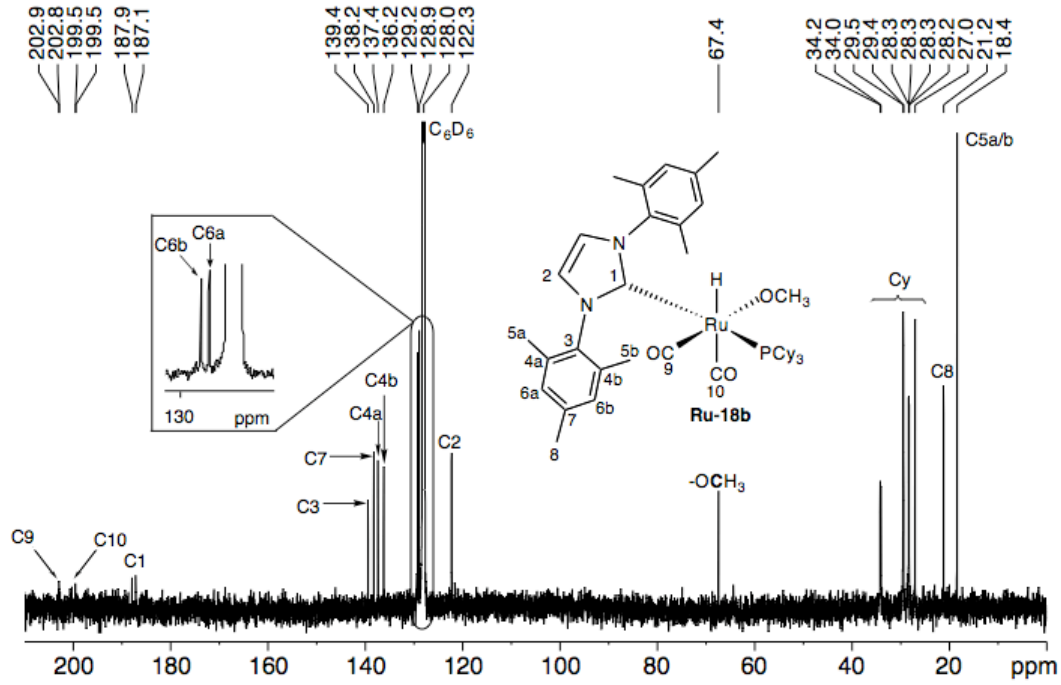

Figure A.1.29. $^{13}C\{^{1}H\}$ spectrum of **Ru-18b** (C_6D_6).

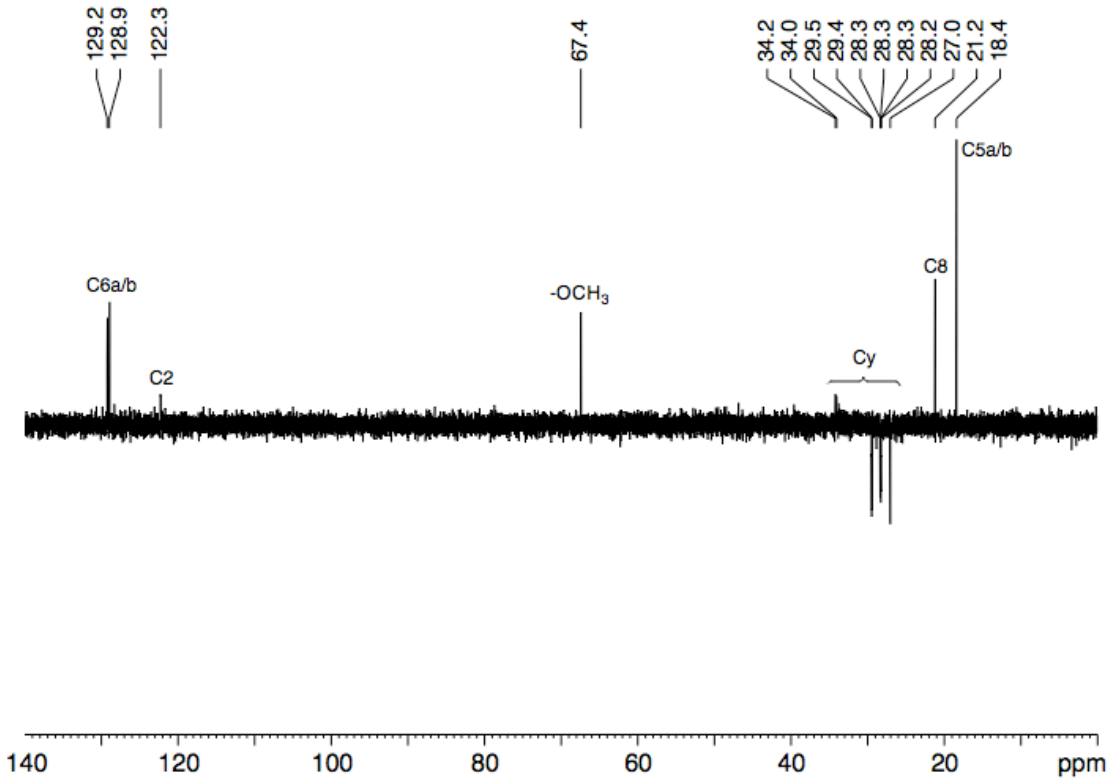

Figure A.1.30. ^{13}C DEPT spectrum of **Ru-18b** (C_6D_6).

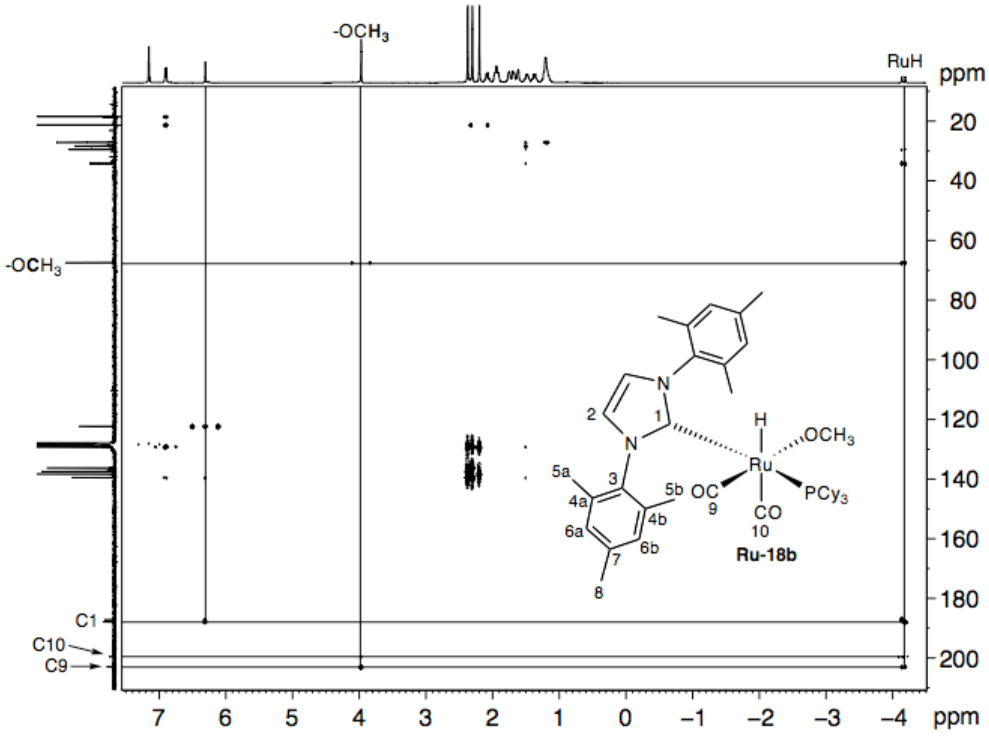

Figure A.1.31. ^{1}H-^{13}C HMBC spectrum of **Ru-18b** (C_6D_6).

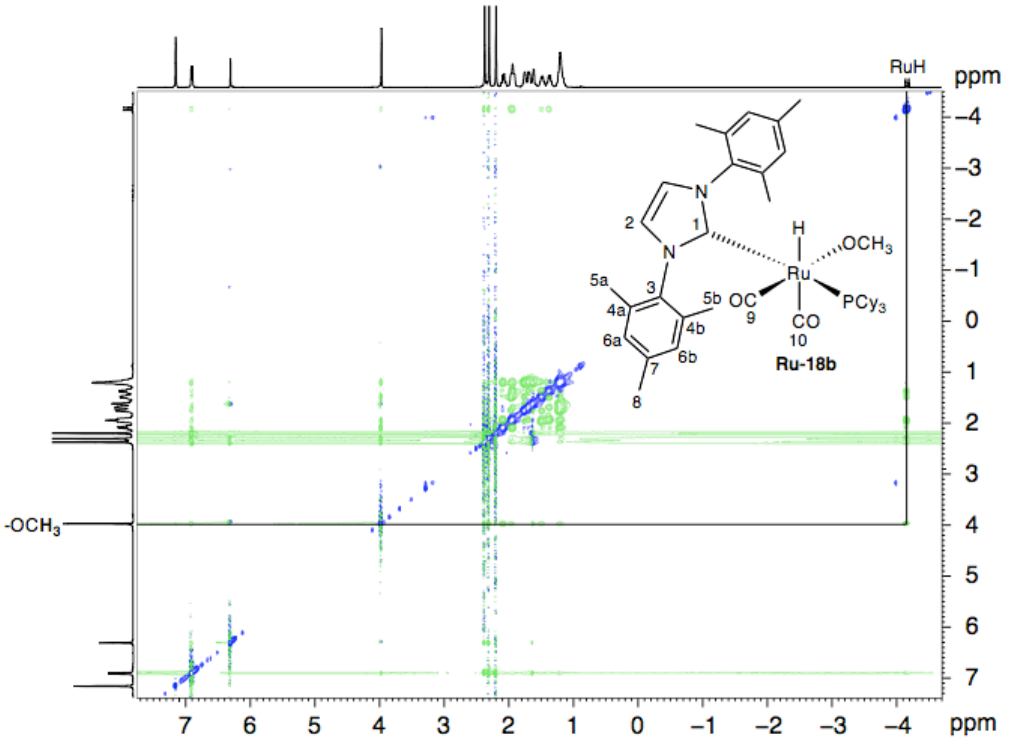

Figure A.1.32. ^{1}H NOESY spectrum of **Ru-18b** (C_6D_6, τ_{mix} = 1 s).

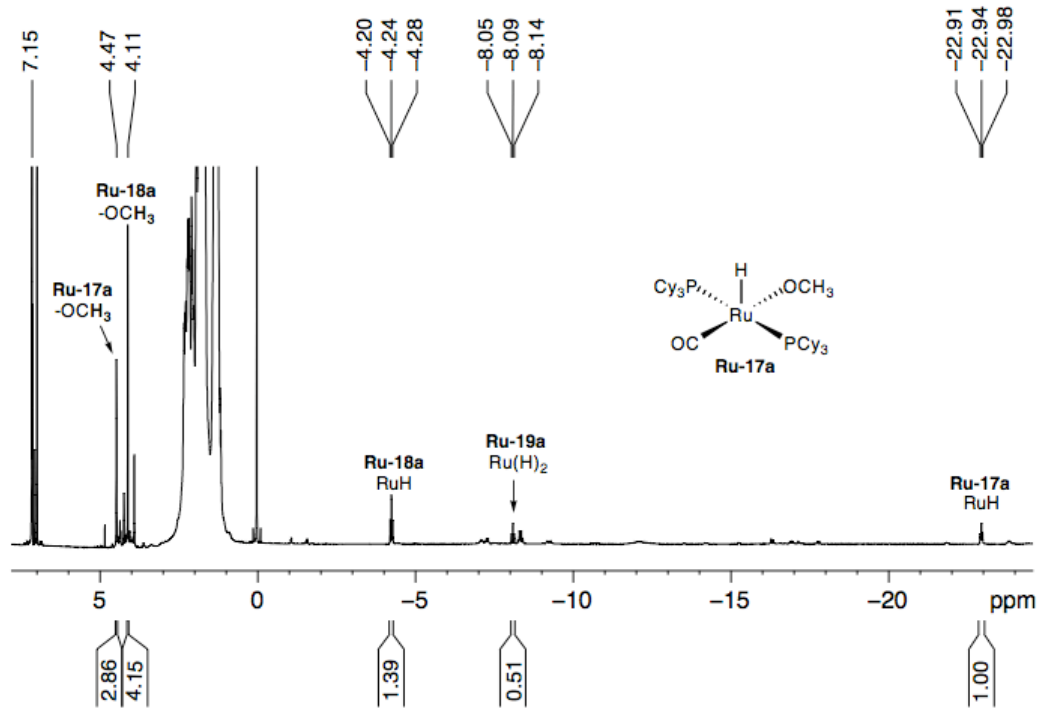

Figure A.1.33. ^{1}H spectrum of crude **Ru-17a** (C_7D_8, 243 K).

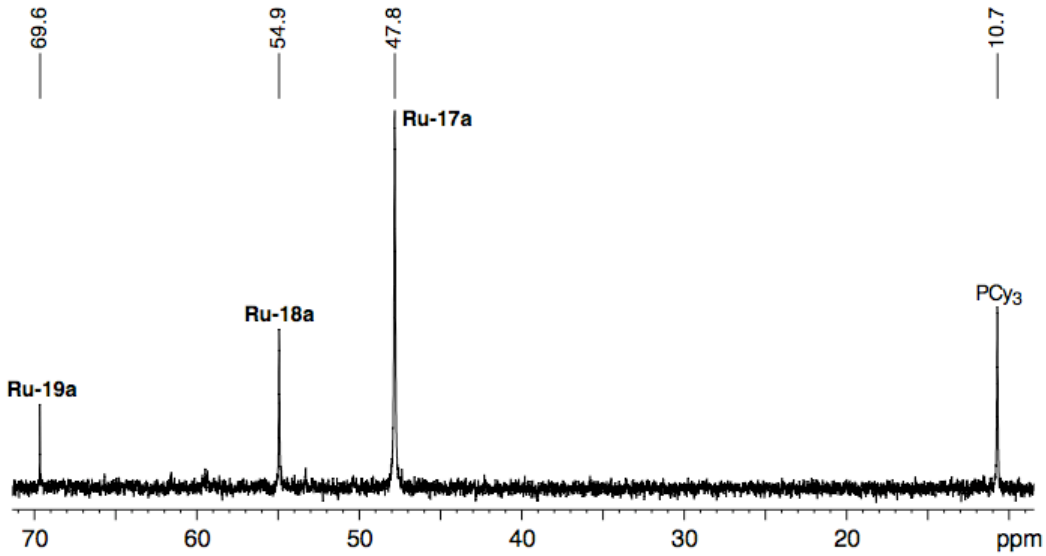

Figure A.1.34. $^{31}P\{^{1}H\}$ spectrum of crude **Ru-17a** (C_6D_6).

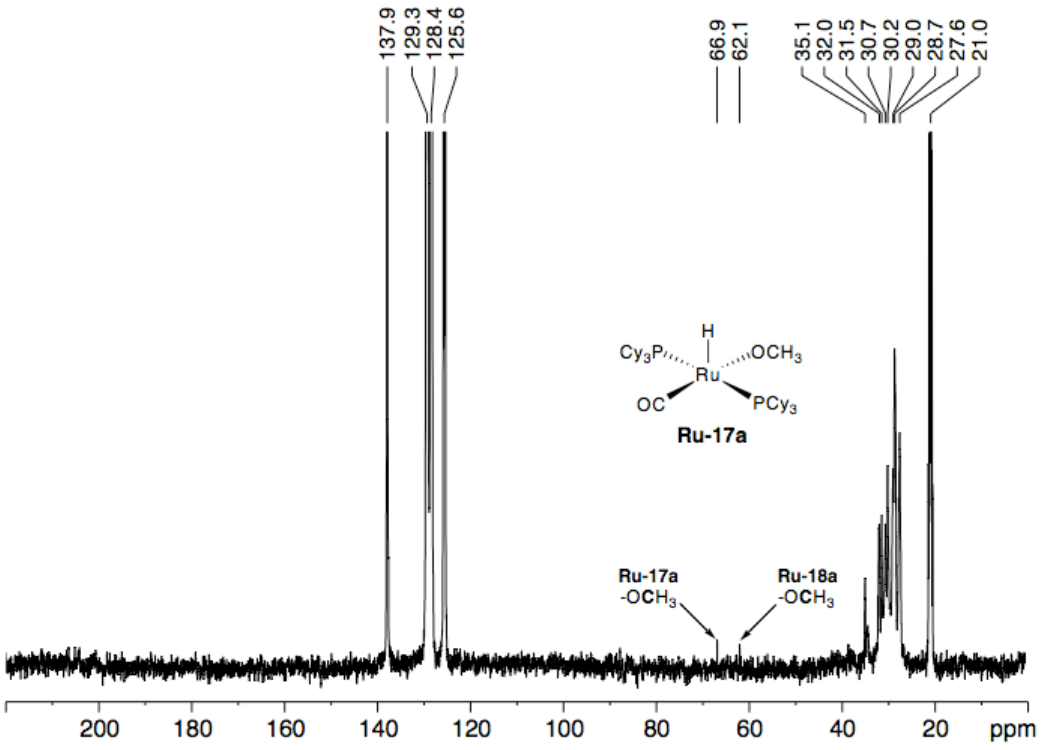

Figure A.1.35. $^{13}C\{^{1}H\}$ spectrum of crude **Ru-17a** (C_7D_8, 243 K).

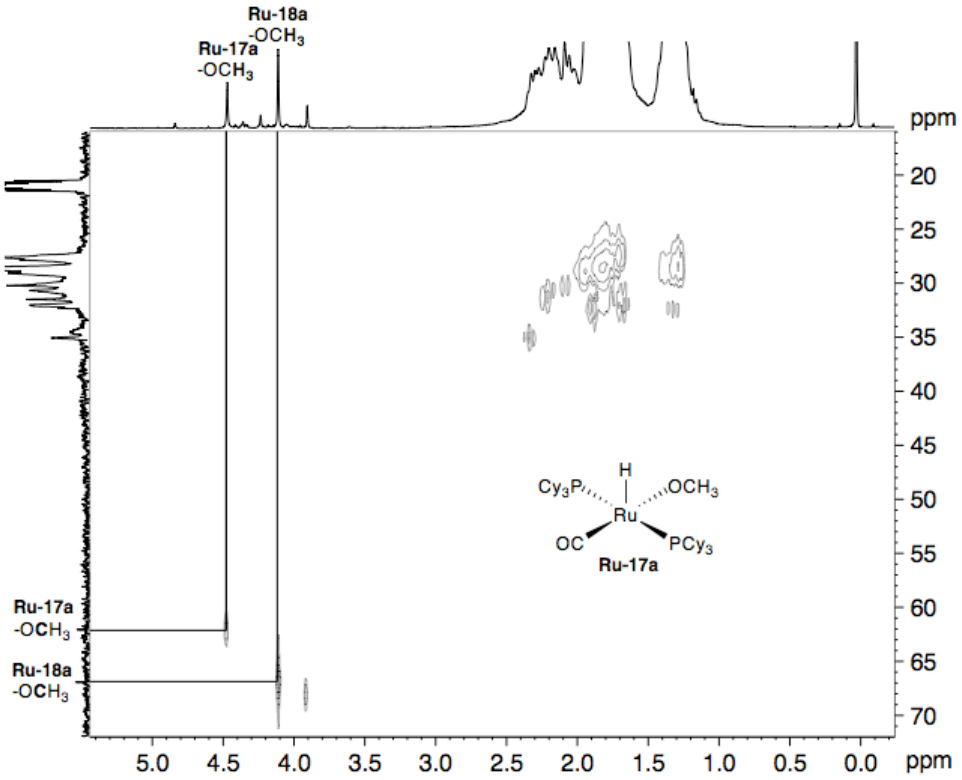

Figure A.1.36. ^{1}H-^{13}C HMQC of crude **Ru-17a** (C_7D_8, 243 K).

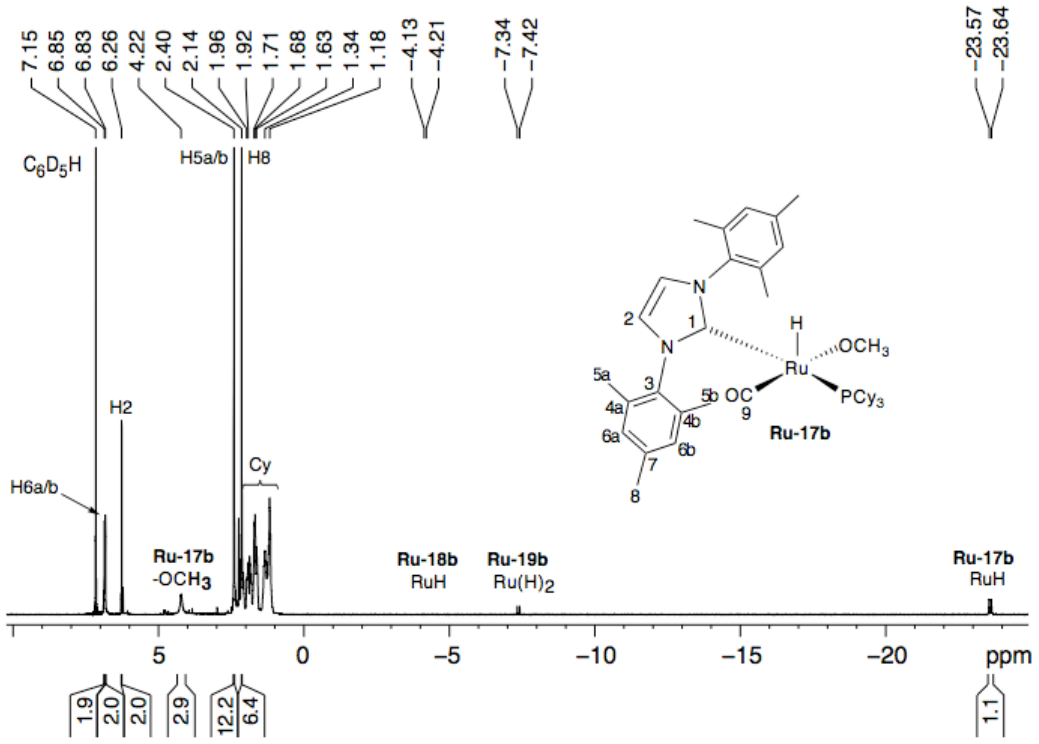

Figure A.1.37. ^{1}H spectrum of crude **Ru-17b** (C_6D_6).

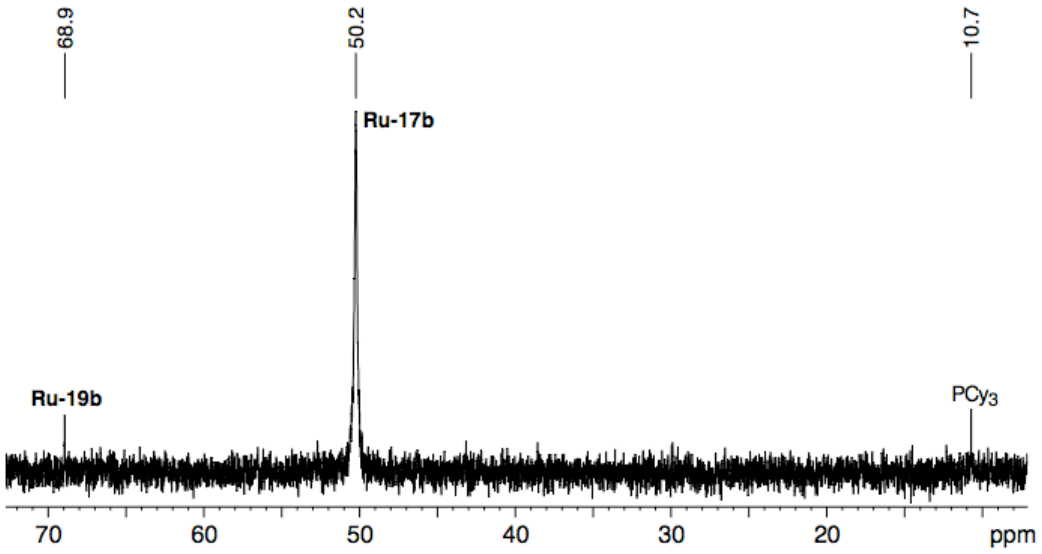

Figure A.1.38. $^{31}P\{^{1}H\}$ spectrum of crude **Ru-17b** (C_7D_8).

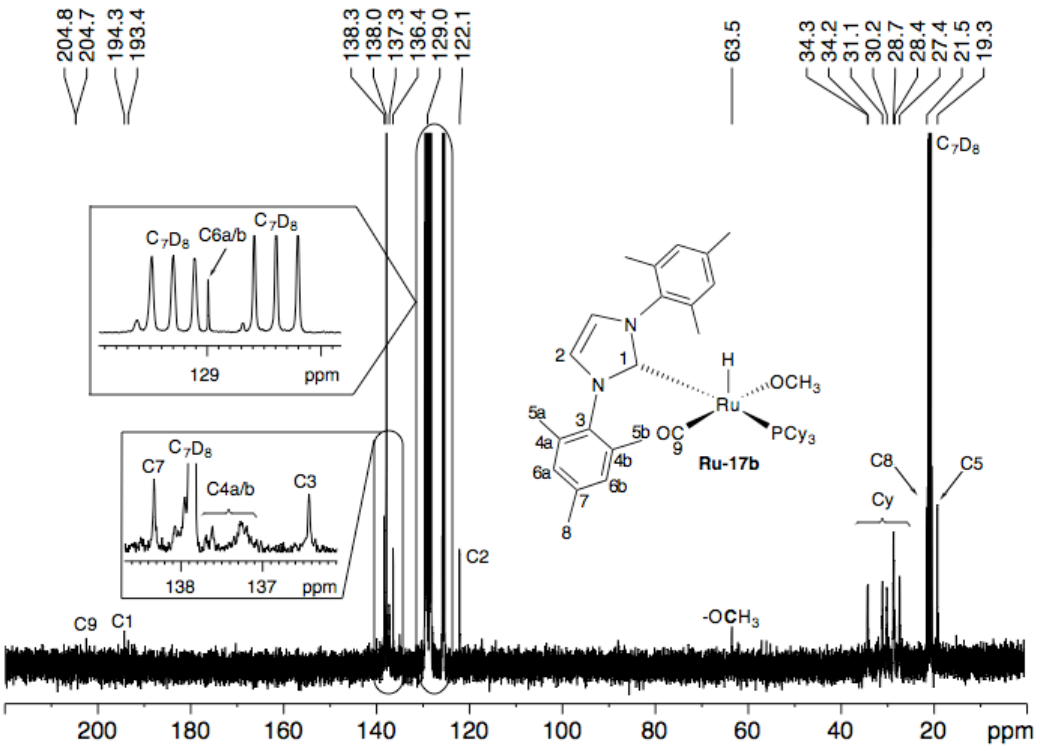

Figure A.1.39. $^{13}C\{^{1}H\}$ spectrum of crude **Ru-17b** (C_7D_8, 243 K).

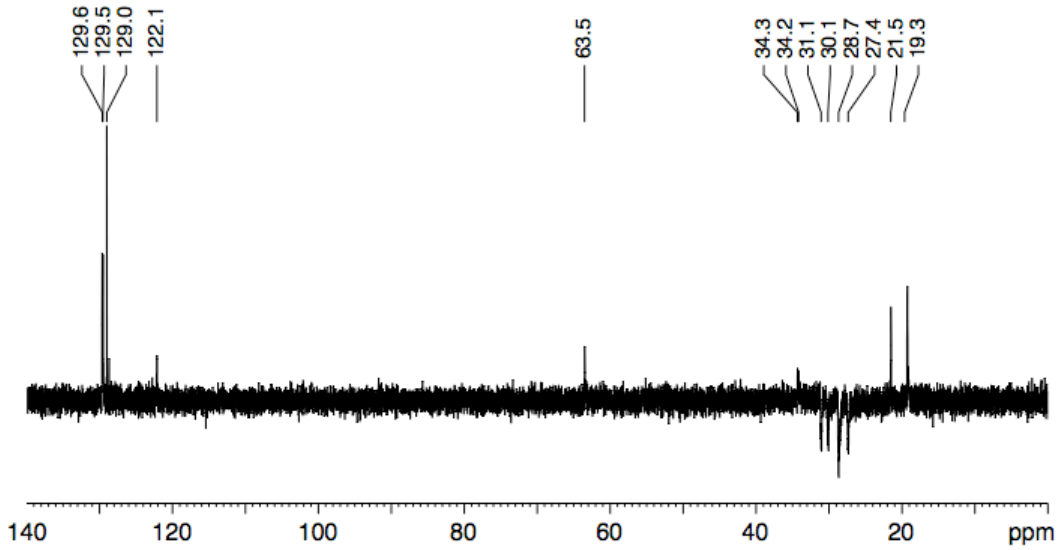

Figure A.1.40. ^{13}C-DEPT spectrum of crude **Ru-17b** (C_7D_8, 243 K).

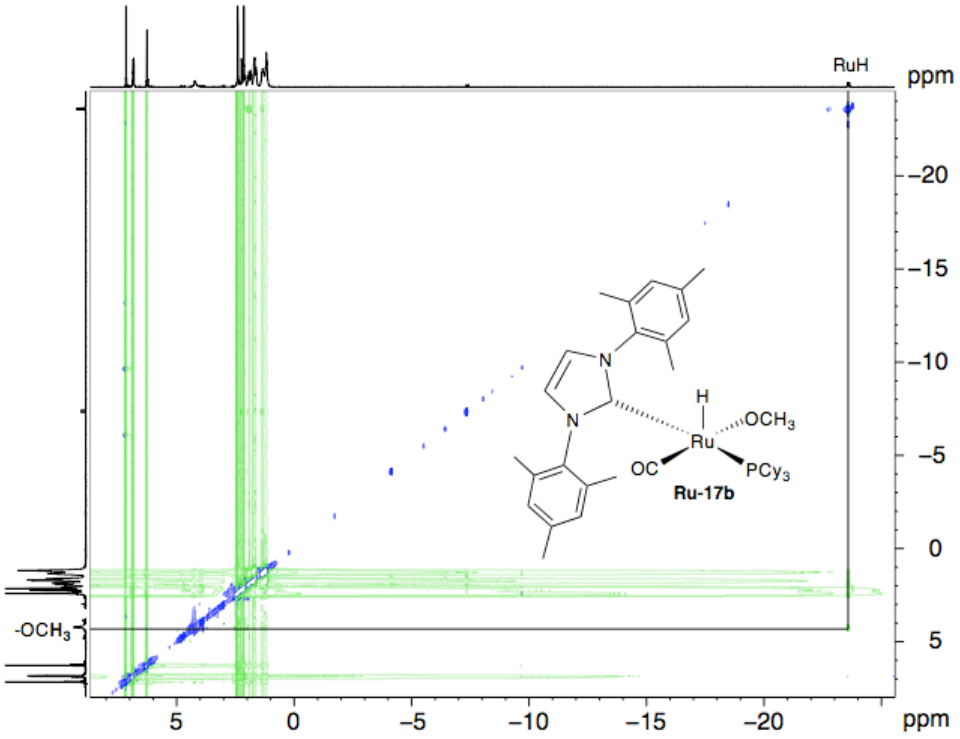

Figure A.1.41. ^{1}H NOESY of crude **Ru-17b** (C_6D_6, τ_{mix} = 1 s).

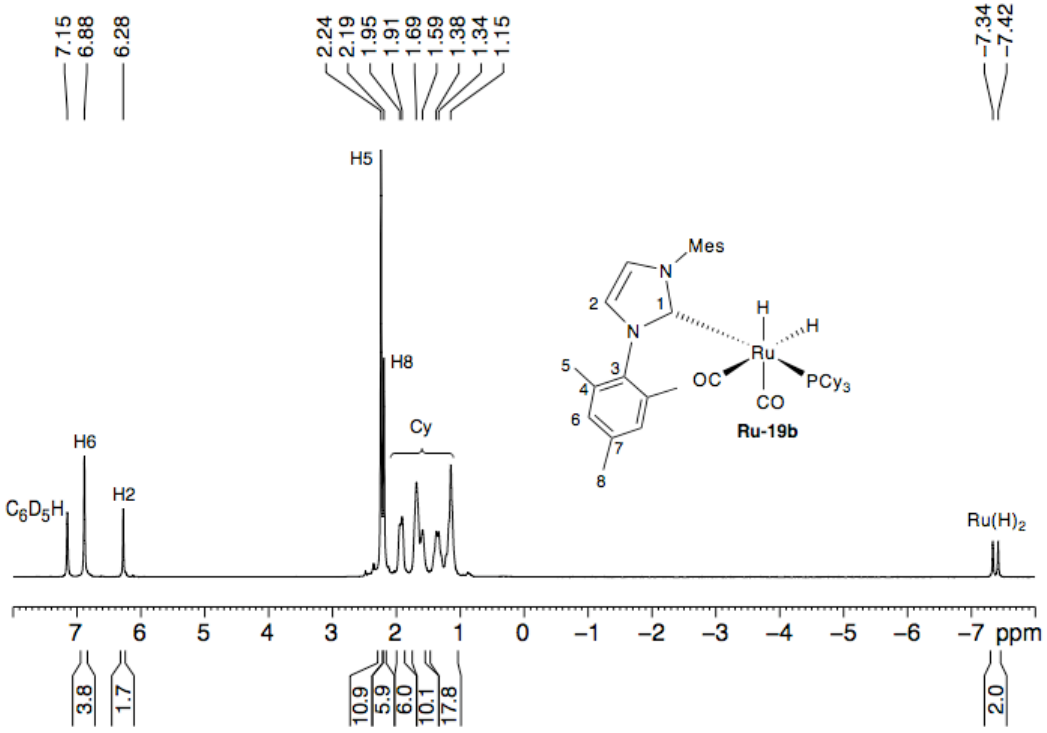

Figure A.1.42. ^{1}H spectrum of crude $Ru(H)_2(CO)_2(IMes)(PCy_3)$ **Ru-19b** (C_6D_6).

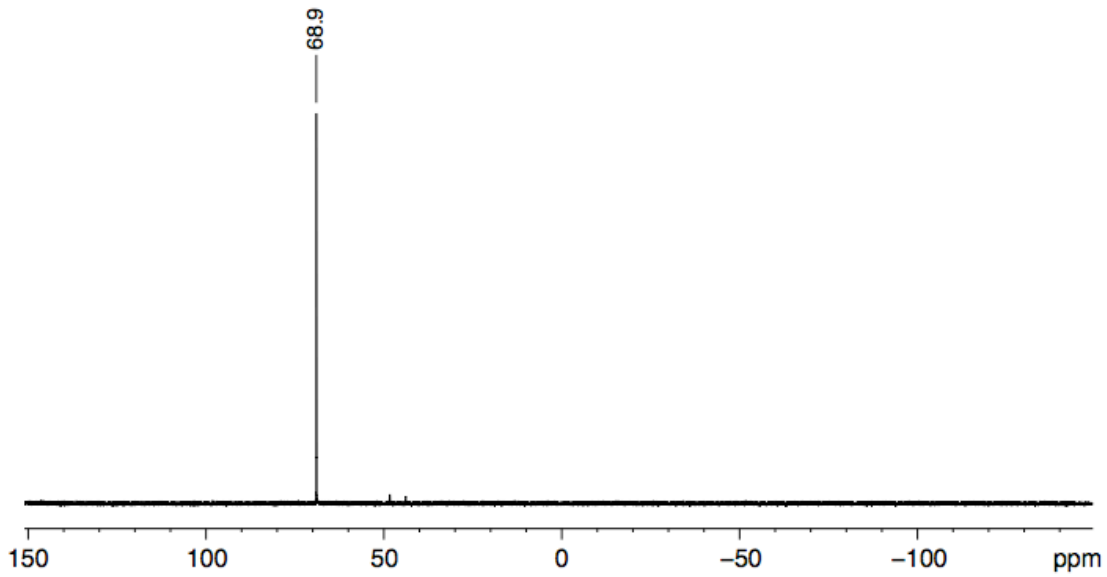

Figure A.1.43. $^{31}P\{^{1}H\}$ spectrum of crude $Ru(H)_2(CO)_2(IMes)(PCy_3)$ **Ru-19b** (C_6D_6).

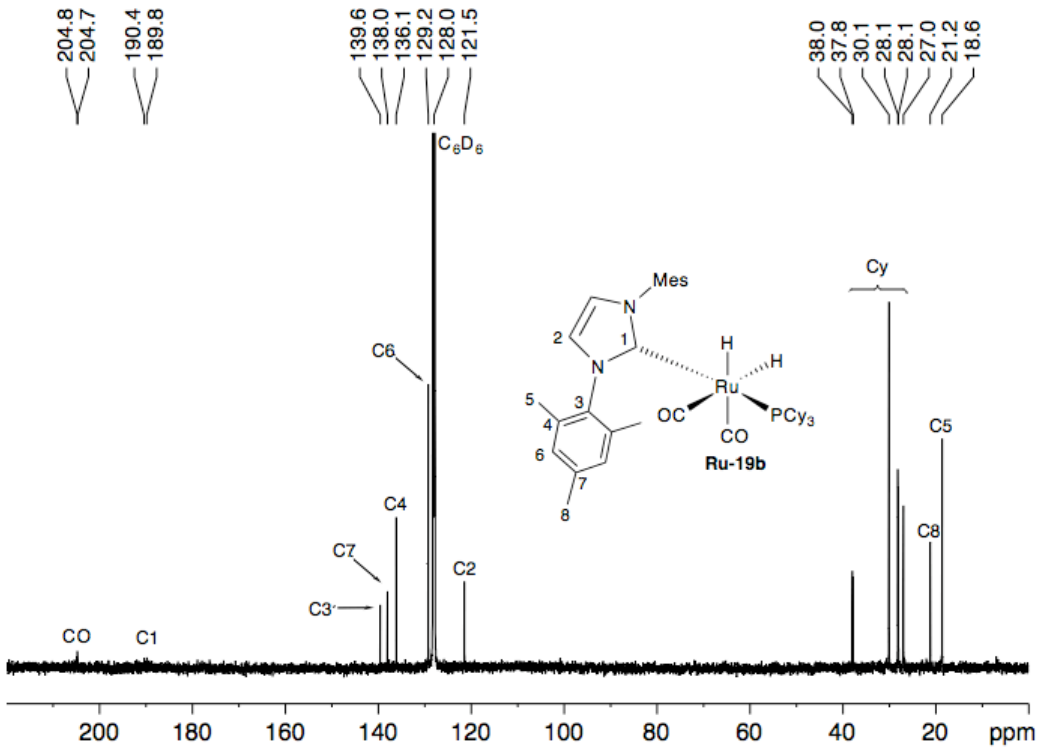

Figure A.1.44. $^{13}C\{^{1}H\}$ spectrum of crude $Ru(H)_2(CO)_2(IMes)(PCy_3)$ **Ru-19b** (C_6D_6).

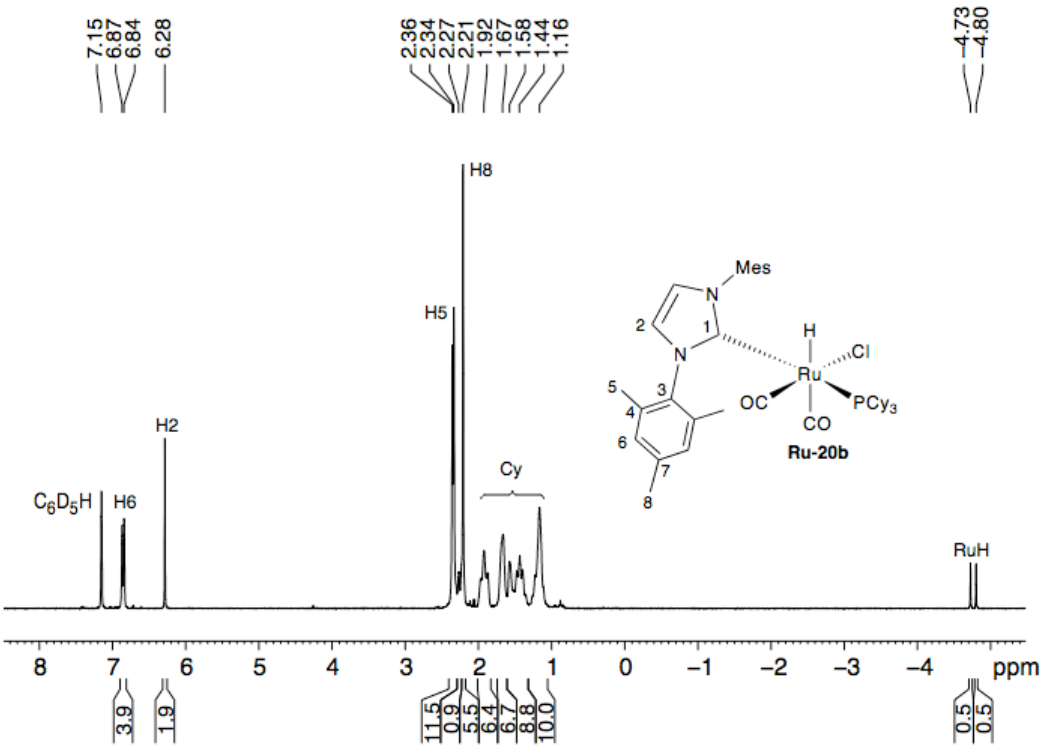

Figure A.1.45. ^{1}H spectrum of $RuHCl(CO)_2(IMes)(PCy_3)$ **Ru-20b** (C_6D_6).

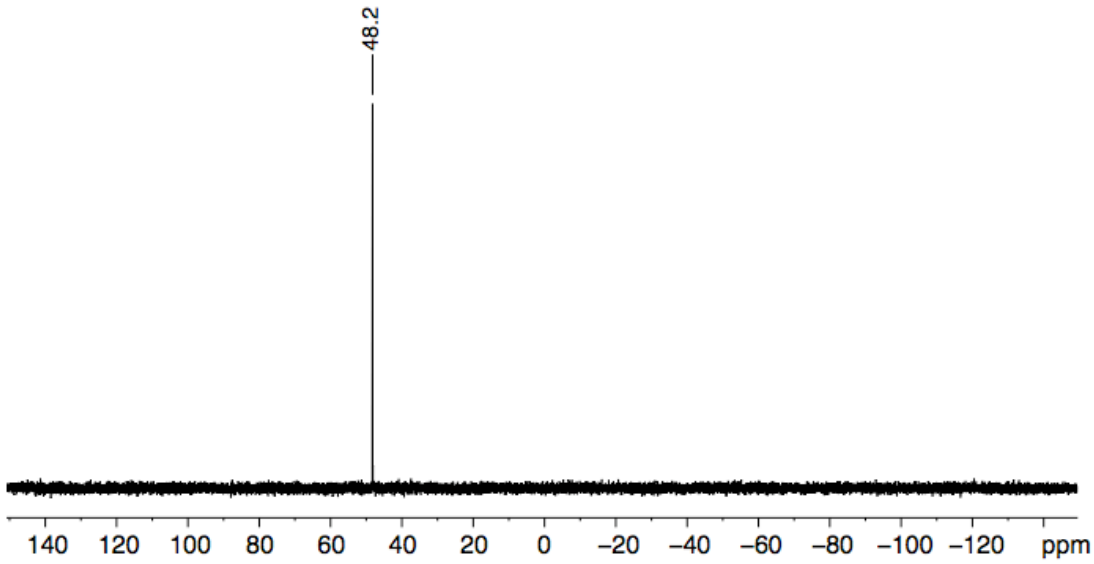

Figure A.1.46. $^{31}P\{^{1}H\}$ spectrum of $RuHCl(CO)_2(IMes)(PCy_3)$ **Ru-20b** (C_6D_6).

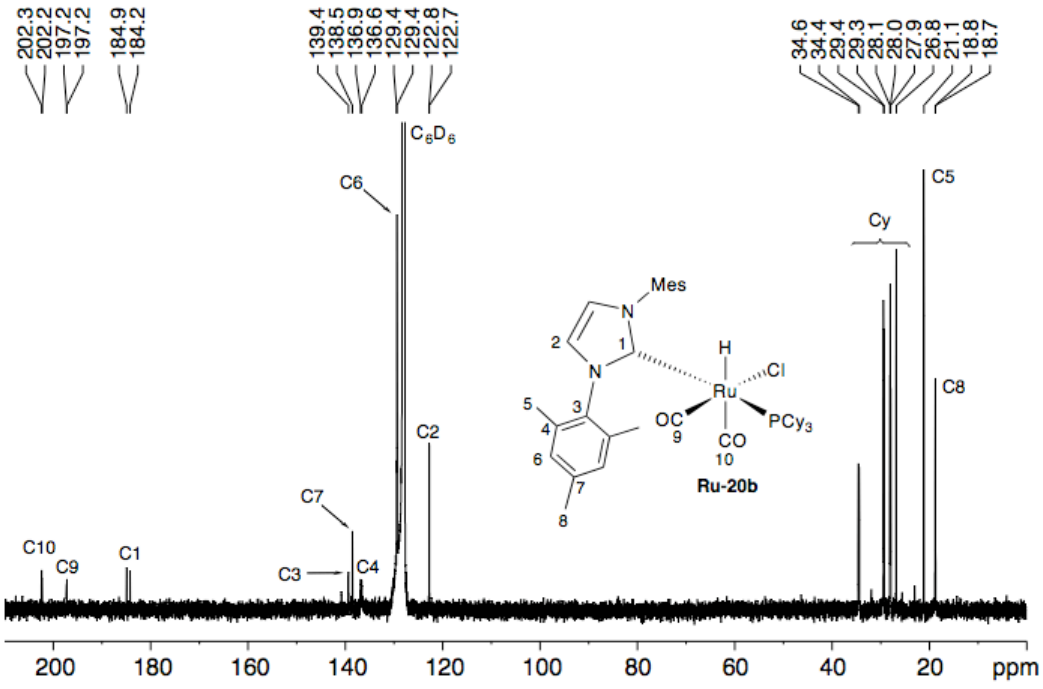

Figure A.1.47. $^{13}C\{^{1}H\}$ spectrum of $RuHCl(CO)_2(IMes)(PCy_3)$ **Ru-20b** (C_6D_6).

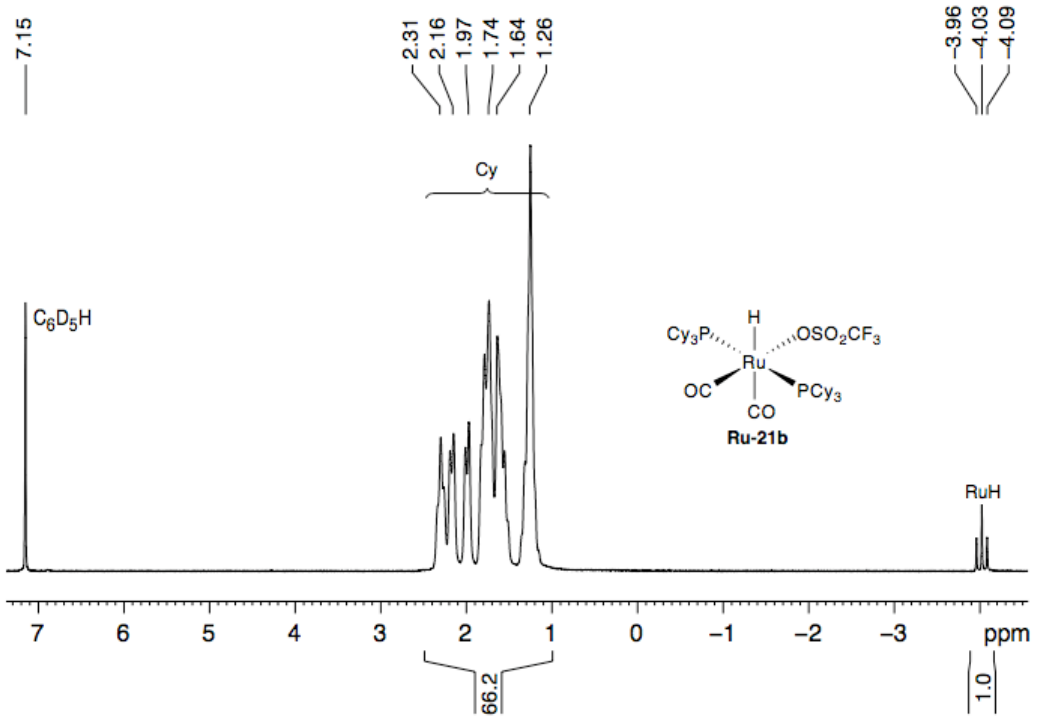

Figure A.1.48. ^{1}H spectrum of $RuH(OSO_2CF_3)(CO)_2(PCy_3)_2$ **Ru-21a** (C_6D_6).

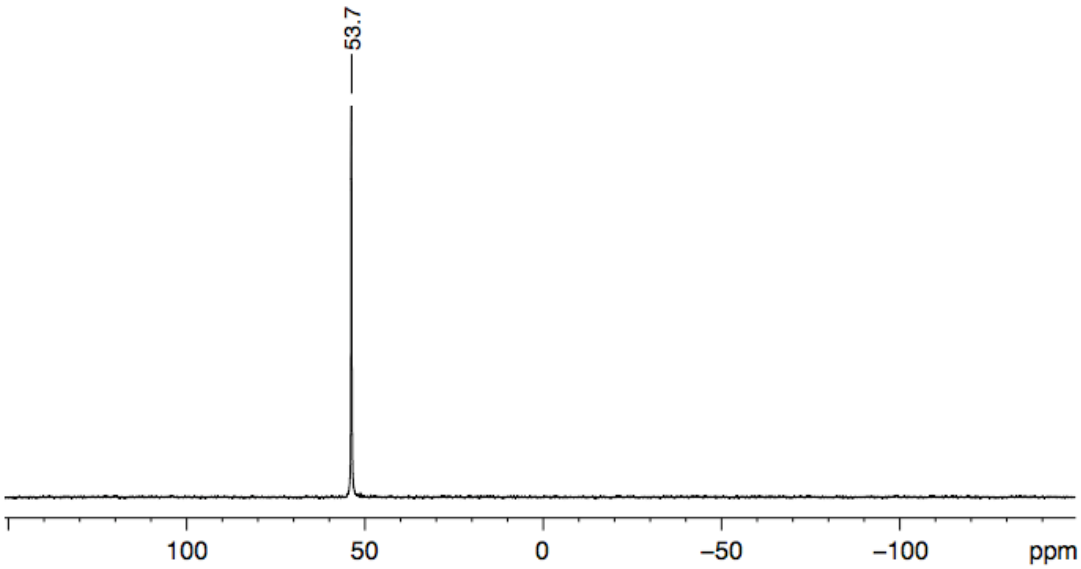

Figure A.1.49. $^{31}P\{^{1}H\}$ spectrum of $RuH(OSO_2CF_3)(CO)_2(PCy_3)_2$ **Ru-21a** (C_6D_6).

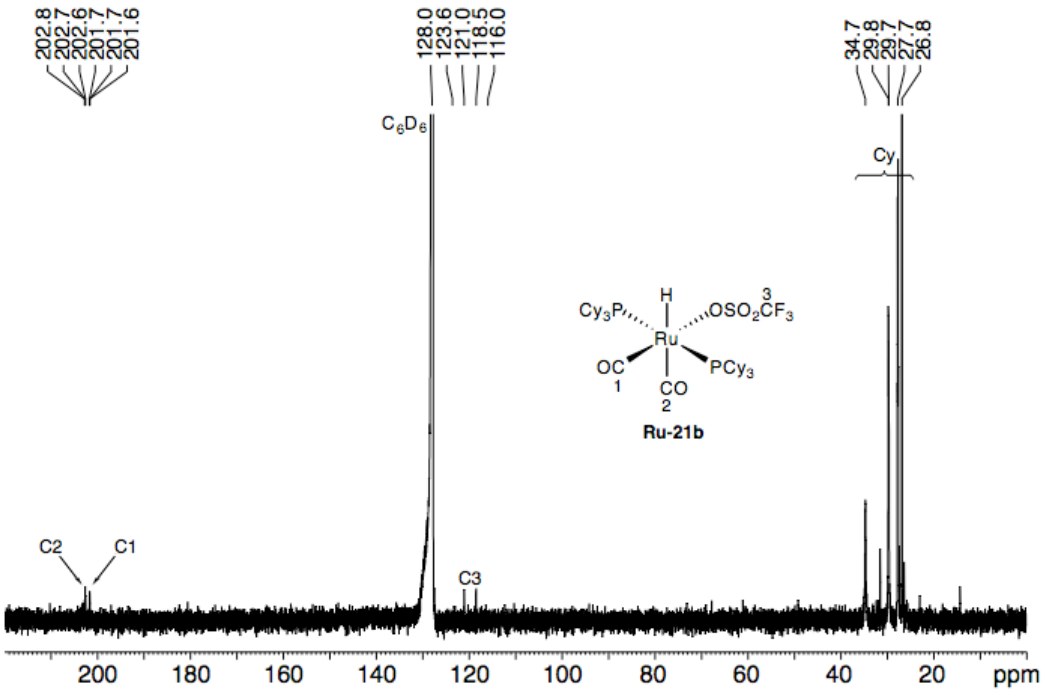

Figure A.1.50. $^{13}C\{^{1}H\}$ spectrum of $RuH(OSO_2CF_3)(CO)_2(PCy_3)_2$ **Ru-21a** (C_6D_6).

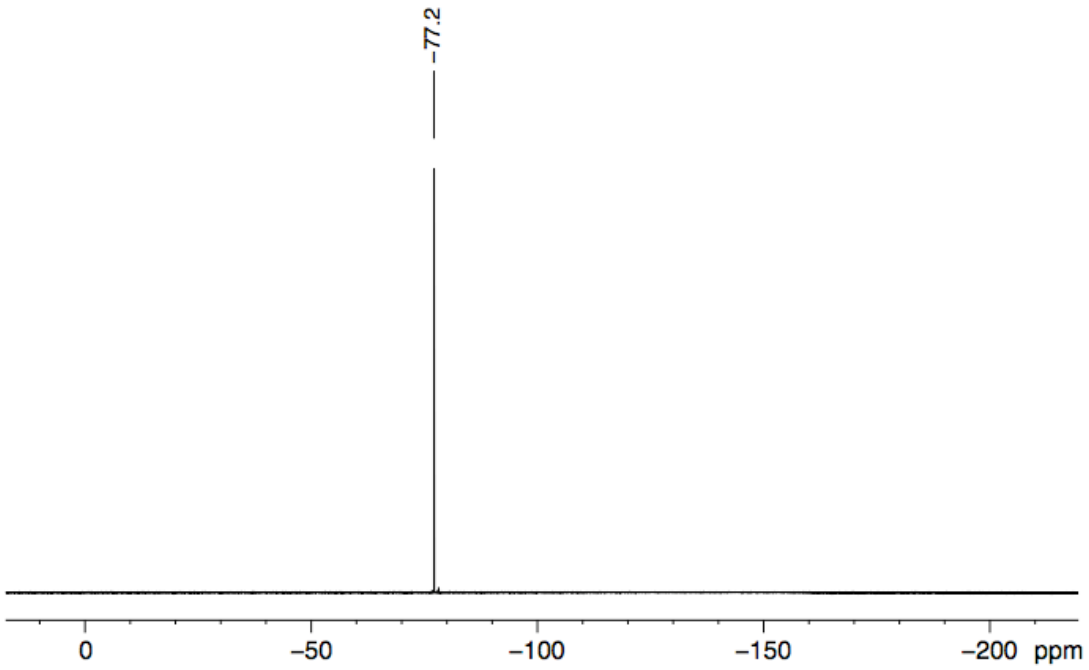

Figure A.1.51. $^{19}F\{^{1}H\}$ spectrum of $RuH(OSO_2CF_3)(CO)_2(PCy_3)_2$ **Ru-21a** (C_6D_6).

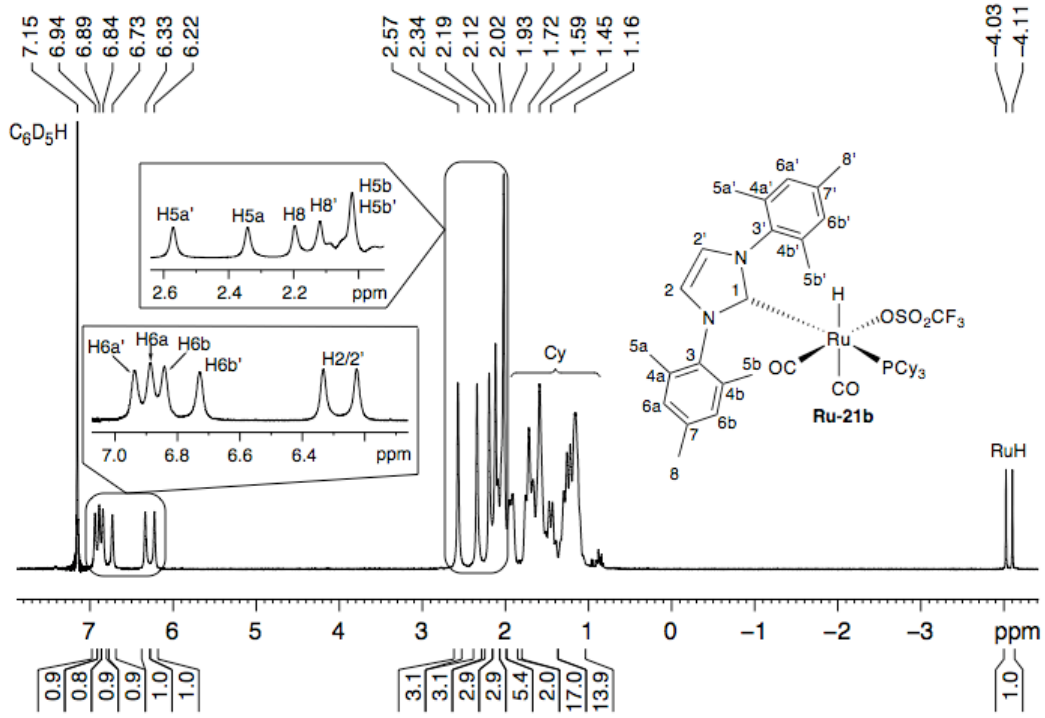

Figure A.1.52. ^{1}H spectrum for $RuH(OSO_2CF_3)(CO)_2(IMes)(PCy_3)$ **Ru-21b** (C_6D_6).

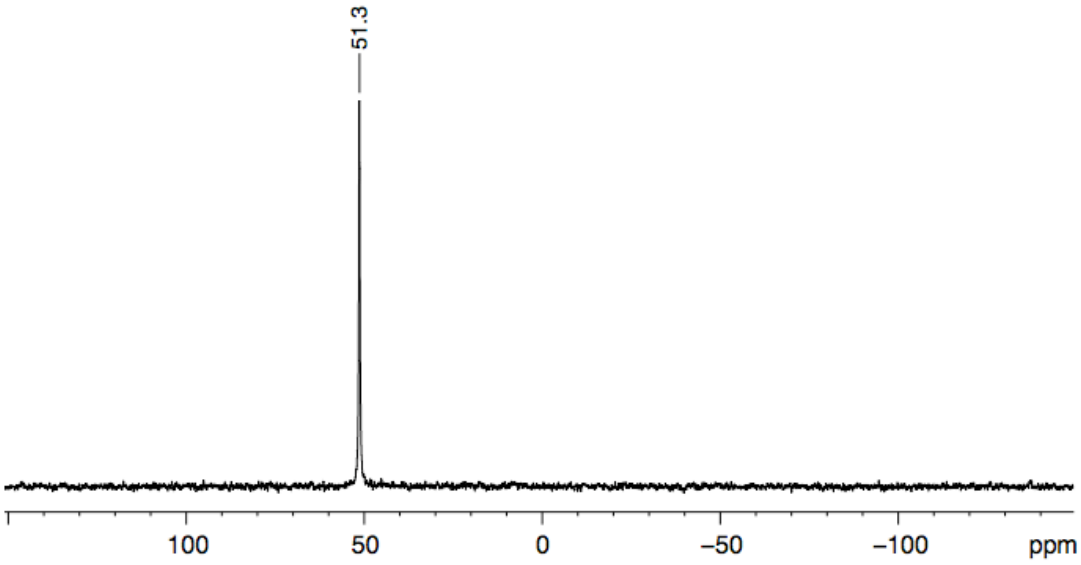

Figure A.1.53. $^{31}P\{^{1}H\}$ spectrum for $RuH(OSO_2CF_3)(CO)_2(IMes)(PCy_3)$ **Ru-21b** (C_6D_6).

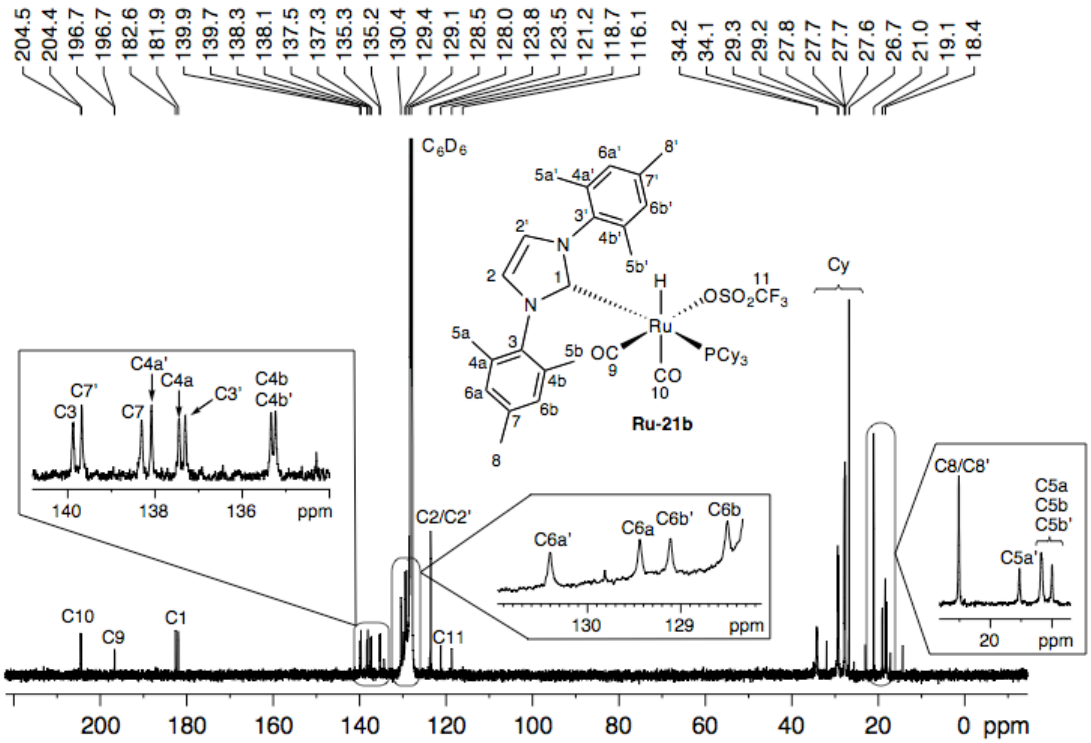

Figure A.1.54. $^{13}C\{^{1}H\}$ spectrum of $RuH(OSO_2CF_3)(CO)_2(IMes)(PCy_3)$ **Ru-21b** (C_6D_6).

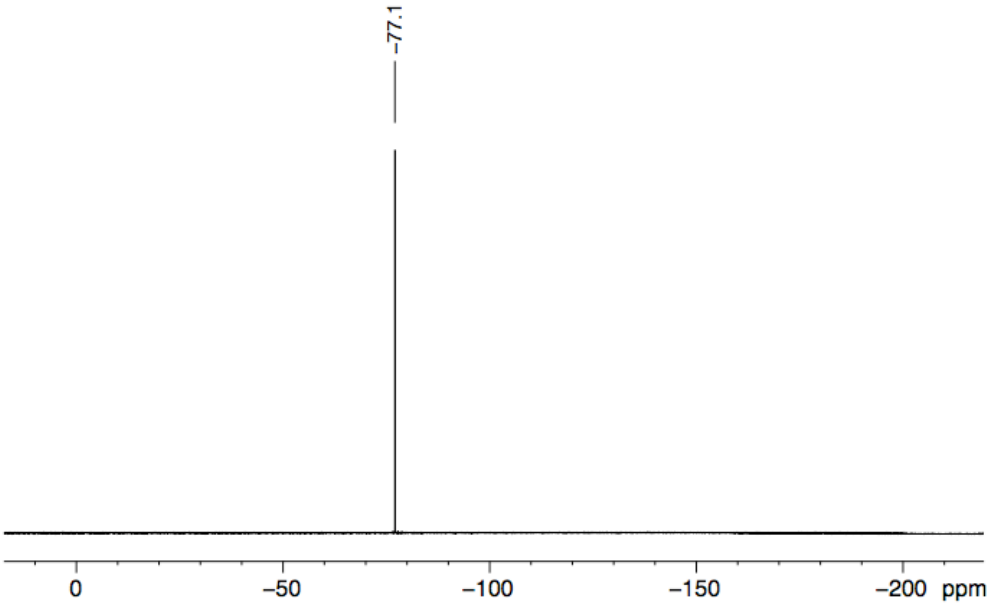

Figure A.1.55. $^{19}F\{^{1}H\}$ spectrum for $RuH(OSO_2CF_3)(CO)_2(IMes)(PCy_3)$ **Ru-21b** (C_6D_6).

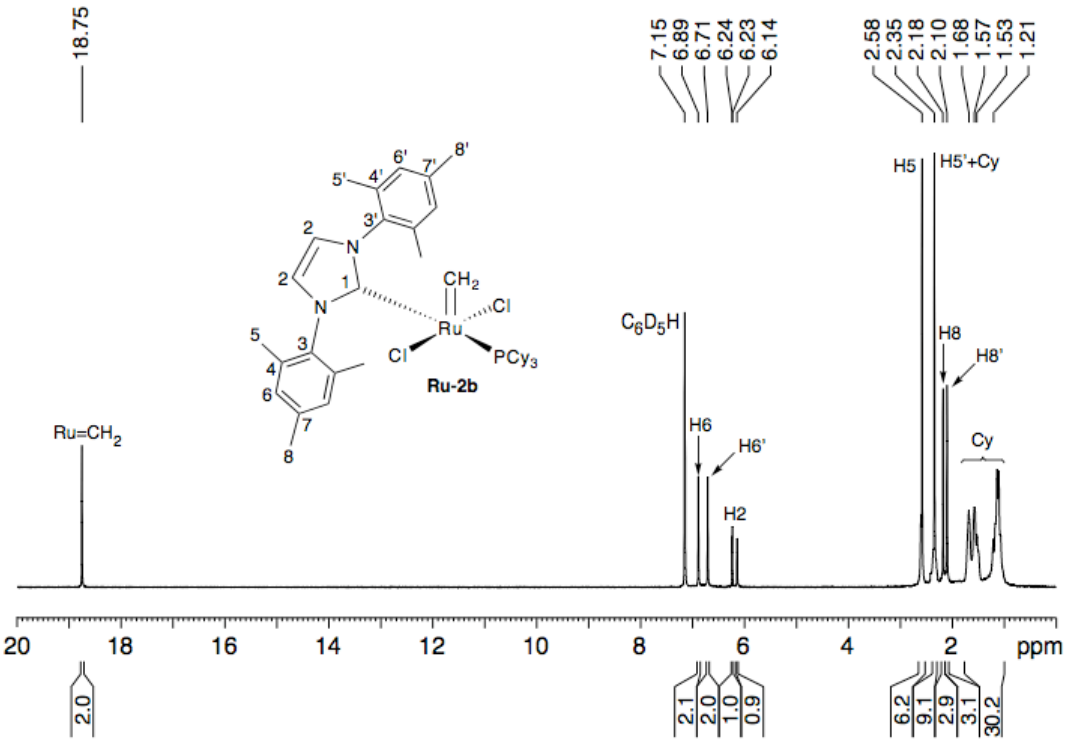

Figure A.1.56. ^{1}H spectrum for $RuCl_2(IMes)(PCy_3)(=CH_2)$ **Ru-2b** (C_6D_6).

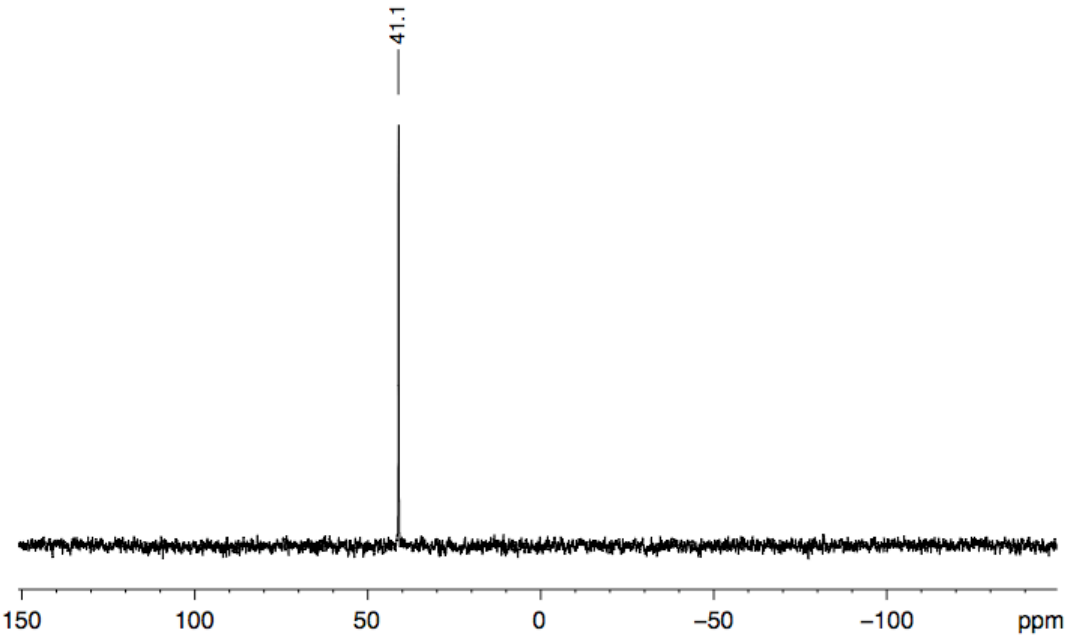

Figure A.1.57. $^{31}P\{^{1}H\}$ spectrum for $RuCl_2(IMes)(PCy_3)(=CH_2)$ **Ru-2b** (C_6D_6).

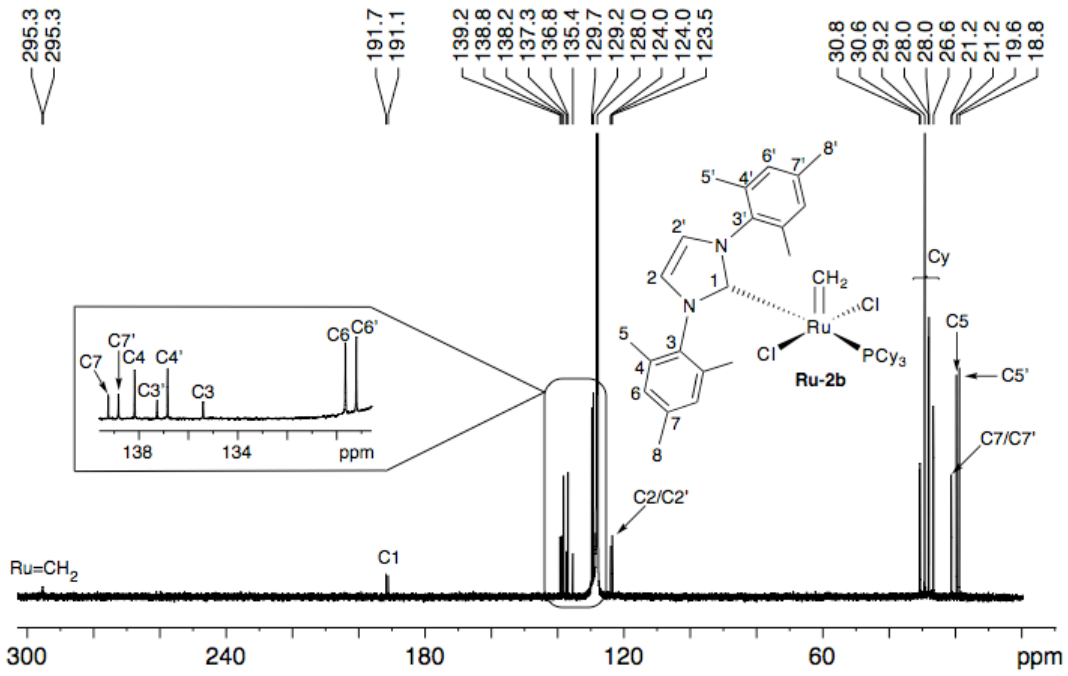

Figure A.1.58. $^{13}C\{^{1}H\}$ spectrum for $RuCl_2(IMes)(PCy_3)(=CH_2)$ **Ru-2b** (C_6D_6).

A.2: Reaction plots illustrating PCy_3-dependence of Ru-1 consumption during Ru hydride production processes.

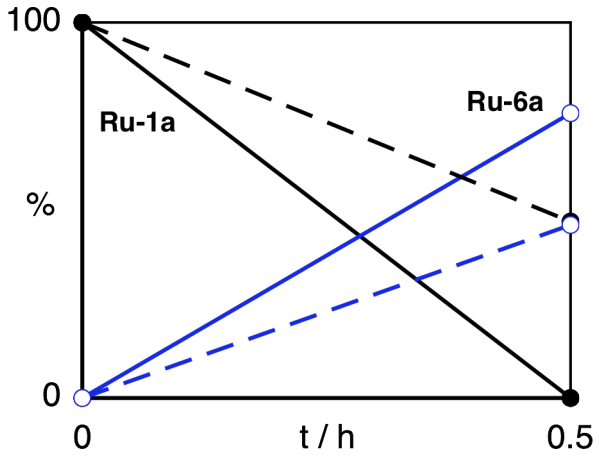

Figure A.2.1. Inhibition of NEt-assisted **Ru-1a** hydrogenolysis by added PCy_3. Solid lines: no PCy_3 added. Dashed lines: 3 equiv PCy_3 added. Conditions: CH_2Cl_2, 60 ˚C; 3 equiv NEt_3, 1000 psi H_2, [Ru]= 15 mM.

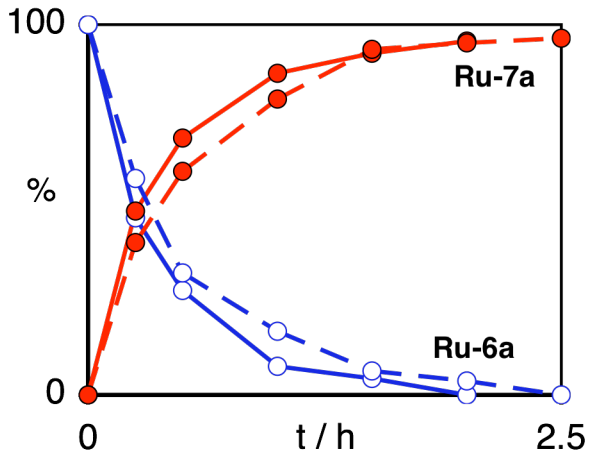

Figure A.2.2. Inhibition of NEt_3-assisted **Ru-6a** carbonylation by PCy_3. Solid lines: no PCy_3 added. Dashed lines: 3 equiv PCy_3 added. Conditions: 10:1 CH_2Cl_2-MeOH, 60 ˚C; 3 equiv NEt_3, [Ru]= 15 mM.

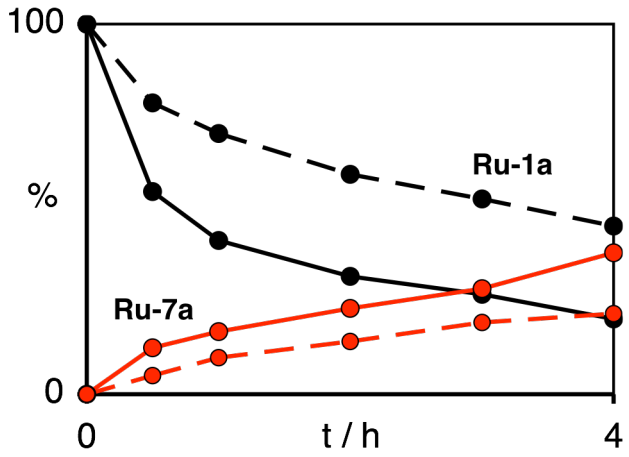

Figure A.2.3. Inhibition of NEt_3-assisted **Ru-1a** methanolysis by PCy_3. Solid lines: no PCy_3 added. Dashed lines: 3 equiv PCy_3 added. Conditions: 10:1 CH_2Cl_2-MeOH, 60 ˚C; 3 equiv NEt_3, [Ru]= 15 mM.

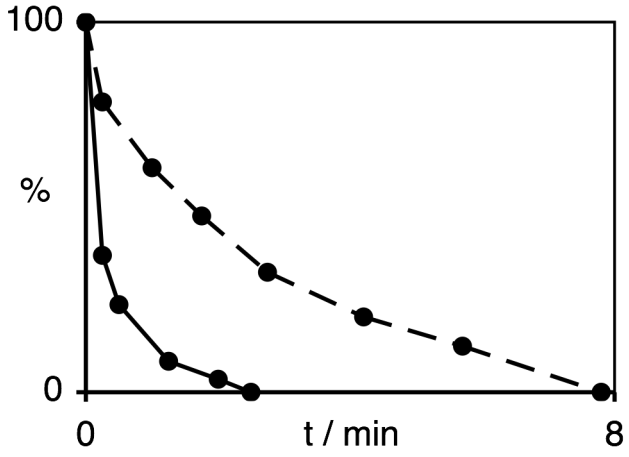

Figure A.2.4. Inhibition of NaOMe-assisted **Ru-1a** methanolysis by PCy_3. Solid lines: no PCy_3 added. Dashed lines: 5 equiv PCy_3 added. Conditions: 10:1 CH_2Cl_2-MeOH, 60 ˚C; 3 equiv NaOMe, [Ru]= 15 mM.

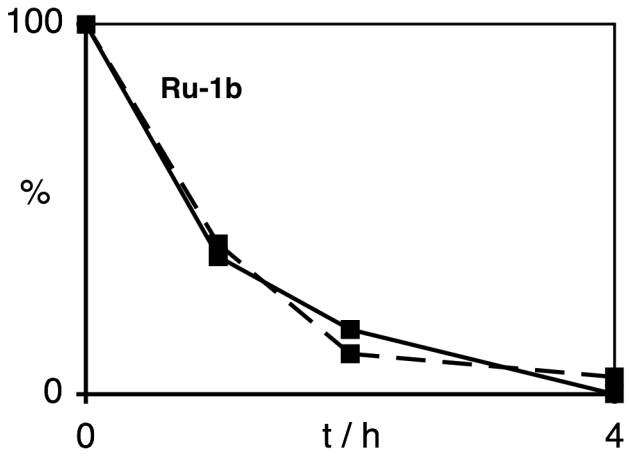

Figure A.2.5. Tolerance of NaOMe-assisted **Ru-1b** methanolysis towards added PCy_3. Solid lines: no PCy_3 added. Dashed lines: 5 equiv PCy_3 added. Conditions: 10:1 CH_2Cl_2-MeOH, 60 ˚C; 20 equiv NaOMe, [Ru]= 15 mM.